Ludmila V. Yakushevich

WILEY-VCH

Nonlinear Physics of DNA

Second, Revised Edition

Ludmila V. Yakushevich

Nonlinear Physics of DNA

Ludmila V. Yakushevich

Nonlinear Physics of DNA

Second, Revised Edition

WILEY-VCH Verlag GmbH & Co. KGaA

Ludmila V. Yakushevich
Russian Academy of Sciences

Cover picture
The illustration is a drawing made by Nicolas Bouvier for Geneviève Almouzni, UMR 218 CNRS – Institut Curie

Library of Congress Card No.: applied for

British Library Cataloguing-in-Publication Data:
A catalogue record for this book is available from the British Library.

Bibliographic information published by Die Deutsche Bibliothek
Die Deutsche Bibliothek lists this publication in the Deutsche Nationalbibliografie; detailed bibliographic data is available in the Internet at <http://dnb.ddb.de>.

printed in the Federal Republic of Germany
printed on acid-free paper.

Composition Kühn & Weyh, Freiburg
Printing Strauss GmbH, Mörlenbach
Bookbinding Litges & Dopf Buchbinderei GmbH, Heppenheim

ISBN 3-527-40417-1

Contents

Preface to the First Edition

This book is devoted to a new and rapidly developing field of science, which I call here the nonlinear physics of DNA. This is the first monograph on the subject, where various theoretical and experimental data on the nonlinear properties of DNA published in different journals on mathematics, physics and biology are gathered, systematized and analyzed. I will only point out a few reviews which preceded the book: by Scott [1], Zhou and Zhang [2], Yakushevich [3], and Gaeta and coauthors [4]. A collection of lectures given by participants at the International workshop in Les Hauches (France, 1994) [5], and selected sections in the monographs of Davydov [6] and Yakushevich [7] can also be mentioned.

Three events can be considered as having stimulated the appearance and rapid development of nonlinear DNA science. The first was the success of nonlinear mathematics and its application to many physical phenomena [8–10]. The second was the emergence of new results in studies of the dynamics of biopolymers leading to an understanding of the important role of the dynamics in the biological functioning of biopolymers [11–13]. The third event was the publication of a series of works of Davydov, where for the first time the achievements of nonlinear mathematics were applied to biology, and the hypothesis of the occurrence of solitons in biopolymers (namely, in alpha-helical proteins) was suggested [14].

The study of the nonlinear physics of DNA began in 1980 when Englander et al. [15] published the article 'Nature of the open state in long polynucleotide double helices: possibility of soliton excitations'. This was the first time the concept of nonlinear conformational excitations (or DNA solitons) imitating the local opening of base pairs was introduced. In the article the first nonlinear Hamiltonian of DNA was presented and this gave a powerful impulse for theoretical investigations. A large group of authors, including Yomosa [16, 17], Takeno and Homma [18, 19], Krumhansl and coauthors [20, 21], Fedyanin and coauthors [22–24], Yakushevich [25–27], Zhang [28], Prohofsky [29], Muto and coauthors [30–32], van Zandt [33], Peyrard [34, 35], Dauxois [36], Gaeta [37, 38], Salerno [39], Bogolubskaya and Bogolubsky [40], Hai [41], Gonzalez and Martin-Landrove [42] made contributions to the development of this field by improving the model Hamiltonian and its dynamical parameters, by investigating corresponding nonlinear differential equations and their soliton-like solutions, by consideration of statistical properties of DNA solitons and calculation of corresponding correlation functions. The results obtained by them formed a theoretical basis for the nonlinear physics of DNA.

The experimental basis of nonlinear DNA physics was formed by the results of experimental investigations on DNA dynamics and interpretations, some of them in the framework of the nonlinear concept. The most important results were obtained by Englander et al. [15] on hydrogen–tritium exchange in DNA, by Webb and Booth [43], Swicord and coauthors [44–46] on resonant microwave absorption (interpretations were made by Muto and coauthors [30] and by Zhang [47]), and by Baverstock and Cundall [48] on neutron scattering by DNA. All these results, however, admitted alternative interpretations (see the discussion in Ref. [3]), and only after publication of the work of Selvin et al. [49], where the torsional rigidity of positively and negatively supercoiled DNA was measured, was the reliable experimental basis for theoretical predictions given.

Besides theoretical results and experimental data an important contribution to the formation of the nonlinear physics of DNA was made by numerous applications where the nonlinear concept was used to explain the dynamical mechanisms of DNA function such as transitions between different DNA forms [50–52], long-range effects [53–55], regulation of transcription [56], DNA denaturation [34], protein synthesis (namely, insulin production) [57], and carcinogenesis [58].

Taking into account the interests of a wide range of readers who are mostly physicists, I began the monograph with a brief excursion into molecular biology, and presented in the first three chapters the main elements of the DNA structure, dynamics and function.

To enable comparison of linear and nonlinear approximations I have included a chapter devoted to the linear theory of DNA and described briefly therein the main results of theoretical and experimental studies in this field.

The nonlinear theory of DNA is presented in the monograph in detail. The main ideal and non-ideal nonlinear models are described in the framework of the approach based on the hierarchy of the DNA models. To enable comparison of the results of theory and of experiment, and especially of experiments on scattering by DNA, the chapter devoted to the statistics of nonlinear excitations in DNA is also included. In the final two chapters several examples of interpretations of experimental data on DNA dynamics and function in terms of the nonlinear concept are presented.

The material of the book is given in a fairly complete form. However, the reader is assumed to be familiar with the elements of physical theory, including classical mechanics and statistical physics.

In this monograph I have tried to give a description of the main theoretical and experimental data on the nonlinear physics of DNA.

I have tried to organize the material in such a way as to give a complete picture which is why the chapters on DNA structure, dynamics and functioning are included. But I should note that because of the very young 'age' of this field of science, many gaps still remain. As a consequence, some of the chapters which I think should be traditionally included in monographs on physics are absent. For example, I could not present any data on nonlinear quantum mechanical properties of DNA or on DNA nonlinear electrical properties because these questions have not been studied at all. One more example is the interaction of DNA with the environment. I could present here only rather limited information about this because until now only a few very simple approaches have been proposed.

In spite of the absence of some chapters, I decided, for two reasons, to conserve the rather general form of the title of the book. First, I am sure that these problems will be actively developed in the very near future and many gaps will disappear, and secondly I hope to involve physicists in this very promising field of science.

The most promising directions I think are associated with the study of inhomogeneous nonlinear models of DNA, because this will lead to new interesting relations between the physical nonlinear properties of DNA and its biological functioning. Another very promising direction is associated with the study of the interaction of DNA and external fields. Both studies can lead to the discovery of new mechanisms of regulation of fundamental biological processes such as transcription or replication. So, in future we shall have a chance to 'bridge' the nonlinear physics of DNA and medicine.

Many sections of the book are part of a course of lectures delivered to students of the Physical and Biological Departments of the Moscow State University and Pushchino State University (Russia). Selected chapters of the book were discussed widely during my travel with lectures at the Universities of Durham, Loughborough, Warwick, Surrey (England), at the Ecole Normale Superieure de Lyon (France), at the Universities of Salerno, Roma, Firenze and the Institute of Health (Italy).

I would like to express my gratitude to my colleagues Kamzolova S.G., Karnaukhov V.N., Komarov V.M., Sidorova S.G, Kun'eva L.F. and Mitkovskaya L.I. for their constant support and help in preparing the manuscript for publication. I would like also to thank my parents for the warmth and patience they have shown me during the whole period of writing the monograph.

Preface to the Second Edition

I am very much obliged to Dr. Michael Baer, a Senior Publishing Editor of Wiley, for the invitation to prepare the second edition of my book. This gave me an opportunity to add new interesting results that have been intensively discussed in recent years [59–65].

In the second edition of the book I have included new data on the distribution of electrostatic potential around DNA, on charge transfer along the double helix, on computer modeling propagation of nonlinear conformational waves along the DNA and the effects of thermal bath, random and real (native) sequence of bases and asymmetry on the propagation. I have also included a short description of supercoiling DNA as one of the possible types of internal motion in DNA and new impressive data on single molecule experiments which were the theme of a special workshop of CECAM in Lyon (France) in 2001 [66].

Moscow, October 2003 Ludmila V. Yakushevich

Dedication

The author dedicates this book to the memory of the pioneer in nonlinear biophysics, Professor Alexandr Sergeevich Davydov.

1
DNA Structure

DNA is one of the most interesting and mysterious biological molecules. It belongs to the class of biopolymers and has a very important biological function consisting of the ability to conserve and transfer genetic information. In this book, we shall try to look at the DNA molecule from the physical point of view, that is we shall consider it as a complex dynamical system consisting of many atoms and having a quasi-one-dimensional structure with unusual symmetry, many degrees of freedoms, many types of internal motions, and specific distribution of internal forces.

In this chapter we describe briefly the main features of the DNA structure.

1.1
Chemical Composition and Primary Structure

Deoxyribonucleic acid or DNA is assembled from two linear polymers. The basic formula of each of the polymers is now well established. It consists of monomeric units called nucleotides (Figure 1.1). Each nucleotide consists of three components: sugar (furanose-derivative deoxyribose), heterocyclic (5-carbonic) base and phosphate (PO_4^-). The bases are of four different types. Two of them, adenine (A) and guanine (G), are purines, and the other two, thymine (T) and cytosine (C), are pyrimidines (Figure 1.2). The sugar is connected by a beta-glycoside bond to one of the four bases and forms one of four natural nucleosides: adenosine, guanosine, cytidine and thymidine. The nucleotide is formed by phosphorylation of the 3′- and 5′-hydroxyl groups of the sugar which is a component of the nucleoside.

Each of the polymers described above (they are often named 'strand') is characterized by its polarity (there is a 3′-end and a 5′-end) and the polarity-specified sequence of the bases borne by consecutive deoxyriboses, which is the carrier of the genetic information. Two strands associate to form DNA, the strands being arranged so that

1. they run parallel to each other but have opposite polarities (Figure 1.3);
2. the bases are inside and connected to one another by weak hydrogen bonds;
3. two bases connected by hydrogen bonds form the base pair and according to the rule of Chargaff [67] there are only two types of base pairs in DNA: A-T pairs and G-C pairs (Figure 1.4).

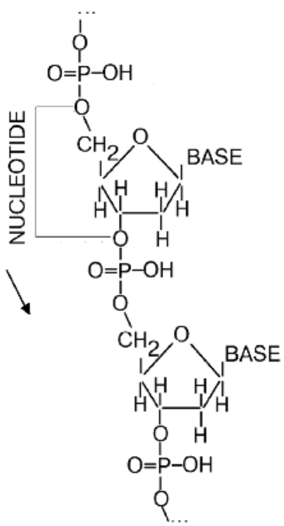

Figure 1.1 A fragment of polynucleotide chain. The direction of the chain is shown by the arrow.

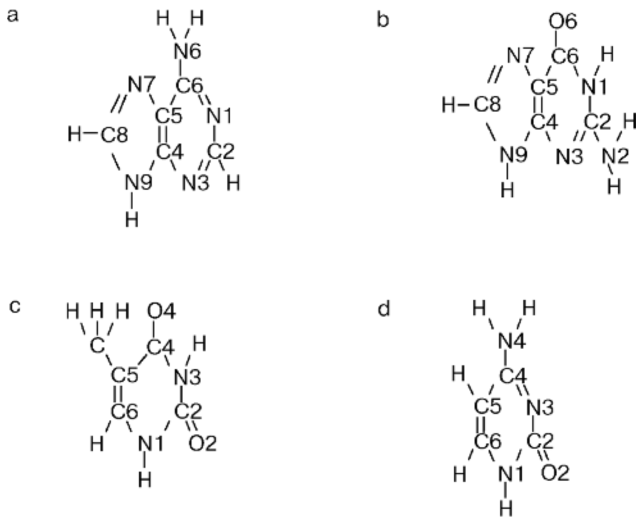

Figure 1.2 DNA bases: (a) adenine, (b) guanine, (c) thymine and (d) cytosine.

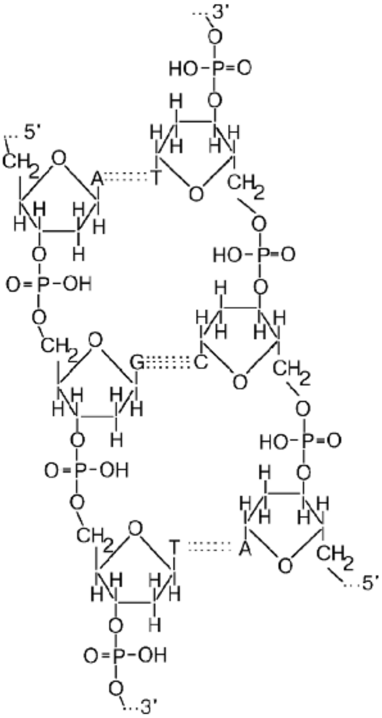

Figure 1.3 Two strands of the DNA molecule. Hydrogen bonds between bases A, T, G and C are shown by dotted lines.

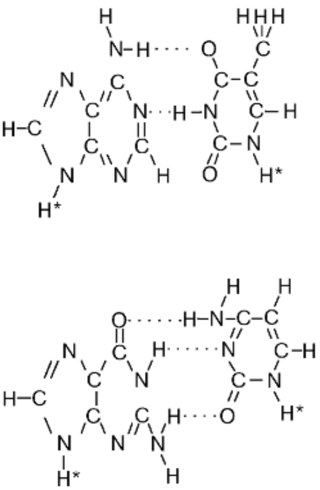

a

b

Figure 1.4 Base-pairs: (a) A-T and (b) G-C. Hydrogen atoms which are substituted in DNA for carbon atoms of sugar rings are marked by asterisks.

Thus, the DNA molecule has a quasi-regular chemical structure. The regular part (backbone) is formed by regularly alternating sugar and phosphate groups, joined together in regular, 3′, 5′-phosphate-di-ester linkages, and the irregular part (side groups) is formed by bases bonding to sugar groups and forming a sequence along the chain. It is this sequence that determines the so-called primary structure of DNA. The sequence of bases in the polynucleotide chain is unique for every organism, and changes in the sequence can lead to crucial changes in the properties of the organisms and in its function.

1.2 Spatial Geometry and Secondary Structure

The way in which two polynucleotide chains are held together, i.e. the principles of formation of the secondary structure of the DNA molecule, was found by Watson and Crick [68, 69], Franklin and Gosling [70], and Wilkins et al. [71] in 1953. The main features of the structure can be formulated briefly in the following way.

1. Two polynucleotide chains are wound around a common axis to produce a double helix (Figure 1.5).
2. The diameter of the helix is 20 Å. The adjacent bases are 3.4 Å apart along the axis and rotated 36° with respect to one another. So, we have 10 nucleotides per one full turn of the helix which corresponds to a length of 3.4 Å.
3. Bases are located inside and phosphates and sugars outside the double helix.
4. The two polynucleotide chains are held together by hydrogen bonds between the bases, as shown schematically in Figure 1.3. The bases are joined together in pairs (Figure 1.4), a single base from one chain being hydrogen-bonded to a single base from the other.
5. Only certain pairs of bases are possible: one member of the pair must be a purine and the other a pyrimidine (Figure 1.4). Due to specific pairing, polynucleotide chains complement each other.

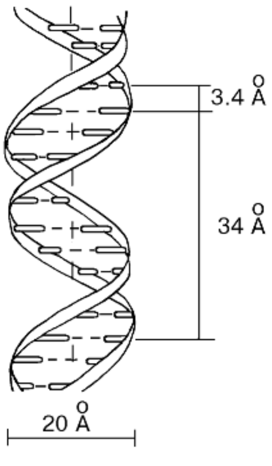

Figure 1.5 Sketch of double helix. The sugar–phosphate backbone is shown by ribbons. The bases are shown by short transverse rods.

This 'classical' description of the secondary DNA structure was later added to and specified [72]. Moreover, several alternative DNA structures have been proposed and widely discussed [73–76].

In the next two sections we shall consider two important problems which can be considered as a further development of the theme: the forces stabilizing the secondary structure and the polymorphism of DNA.

1.3 Forces Stabilizing the Secondary DNA Structure

To understand the physical properties of the DNA molecule it is very important to have a clear idea about the distribution of the interactions between the main atomic groups. The most important interactions are those stabilizing the secondary DNA structure: the so-called horizontal or hydrogen interactions between bases in pairs, vertical or stacking interactions between neighbor bases along the DNA axis, and long-range intra- and inter-backbone forces.

1.3.1 Hydrogen Interactions

In general, hydrogen interactions have the form

$$\mathrm{X{-}H} \cdots \mathrm{Y}, \tag{1-1}$$

where the atom of hydrogen H is connected to two electronegative atoms X and Y. The strength of the bond, and hence its length, depends on the charge of the atoms X, H, and Y.

In the mean plane of a DNA base pair, protons are exchanged between the NH donor groups of one base and the N or H acceptors of the other. So, in DNA the hydrogen bonds are of two types

$$\mathrm{N{-}H} \cdots \mathrm{N}, \tag{1-2}$$

and

$$\mathrm{N{-}H} \cdots \mathrm{O}. \tag{1-3}$$

The A-T pair contains two hydrogen bonds and the G-C pair contains three hydrogen bonds (Figure 1.4). Although, these hydrogen bonds are weak and not highly directional [77], they contribute to the stability of the Watson–Crick-type pairing, and hence have a crucial role in coding the genetic information, its transcription and replication.

Note, however, that in addition to the Watson–Crick pairing described above there is the Hoogsteen pairing: in the former, the H-bonds involve atoms or groups borne by six-membered rings of the purines only, whereas in the latter, N7 of the five-membered ring can be an acceptor.

The nature of hydrogen interactions is mainly (~80%) electrostatic. The results of quantum-chemical calculations show that three types of forces: dispersion, polarization and electrostatic forces, contribute to them. Calculations of the total energy of the hydrogen bonds give the following results for an A-T pair [78]

$$E_{\text{A-T}} = 7.00 \text{ kcal mol}^{-1}; \tag{1-4}$$

and for a G-C pair

$$E_{\text{G-C}} = 16.79 \text{ kcal mol}^{-1}. \tag{1-5}$$

Let us now compare these energies with those of covalent bonds. Usually, the energy of hydrogen bonds is 20 or 30 times weaker than the energy of covalent bonds. As an example confirming this statement, we present here the energies of the covalent bonds C–C and C–H [79]

$$E_{\text{C-C}} = 83.1 \text{ kcal mol}^{-1}; \qquad E_{\text{C-H}} = 98.8 \text{ kcal mol}^{-1}; \tag{1-6}$$

and the energy of the O–H···O bond [80]

$$E_{\text{O-H...O}} = 3\text{–}6 \text{ kcal mol}^{-1}, \tag{1-7}$$

so, the difference between them is rather large.

There is also a marked difference in the rigidities of the bonds. To illustrate this, we can compare the energy, e, which is required to lengthen the bonds by 0.1 Å. For covalent bonds we have [80]

$$e_{\text{C-C}} = 3.25 \text{ kcal mol}^{-1}; \qquad e_{\text{C-H}} = 3.60 \text{ kcal mol}^{-1}; \tag{1-8}$$

and for the O–H···O bond we have [80]

$$e_{\text{O-H...O}} = 0.1 \text{ kcal mol}^{-1}. \tag{1-9}$$

So, the covalent bonds are much more rigid. On the other hand, intrabase paired H-bonds are easily disrupted at physiological temperatures by a variety of chemical agents and physical parameters at concentrations and values commonly encountered in a living system.

1.3.2 Stacking Interactions

Stacking interactions are the other type of forces which stabilize the DNA structure [81, 82]. They hold one base over the next one, and form a stack of bases. According to quantum-chemical analysis, stacking interactions are contributed to by dipole–dipole interactions, π-electron systems, London's dispersion forces and (in water solutions) hydrophobic forces. These forces result in a complex interaction pattern between overlapping base pairs, with a minimum energy distance close to 3.4 Å in the normal DNA double helix.

Like H-bonds, base pair stacking depends on temperature, the state of protonation of the bases, the local dielectric constant and other parameters external to the nucleic acid, summarized as 'environmental' parameters.

Stacking interactions depend on the sequence of bases [83–87]. The results of quantum-chemical calculations show that the total energies of stacking interactions between different types of base pairs are [88]

$$\begin{aligned}
&E_{\substack{\text{C-G}\\\text{G-C}}} = 14.59\ \text{kcal mol}^{-1}; && E_{\substack{\text{T-A}\\\text{A-T}}} = 6.57\ \text{kcal mol}^{-1};\\
&E_{\substack{\text{C-G}\\\text{A-T}}} = E_{\substack{\text{T-A}\\\text{G-C}}} = 10.51\ \text{kcal mol}^{-1}; && E_{\substack{\text{C-G}\\\text{T-A}}} = E_{\substack{\text{A-T}\\\text{C-G}}} = 6.57\ \text{kcal mol}^{-1};\\
&E_{\substack{\text{A-T}\\\text{G-C}}} = E_{\substack{\text{C-G}\\\text{T-C}}} = 9.81\ \text{kcal mol}^{-1}; && E_{\substack{\text{G-C}\\\text{A-T}}} = E_{\substack{\text{T-A}\\\text{C-G}}} = 6.78\ \text{kcal mol}^{-1};\\
&E_{\substack{\text{T-A}\\\text{C-G}}} = 9.69\ \text{kcal mol}^{-1}; && E_{\substack{\text{A-T}\\\text{A-T}}} = E_{\substack{\text{T-A}\\\text{T-A}}} = 5.37\ \text{kcal mol}^{-1};\\
&E_{\substack{\text{G-C}\\\text{G-C}}} = E_{\substack{\text{C-G}\\\text{C-G}}} = 8.26\ \text{kcal mol}^{-1}; && E_{\substack{\text{A-T}\\\text{T-A}}} = 3.82\ \text{kcal mol}^{-1}.
\end{aligned} \tag{1-10}$$

So, the stacks with a high concentration of G-C pairs are more stable than those with a high concentration of A-T pairs. If we now compare the energies of stacking interactions with those of hydrogen bonds we note that they are of the same order of value. If we then compare the energies of stacking interactions with those of covalent bonds we note that the stacking interactions are weaker.

1.3.3 Long-range Intra- and Inter-backbone Forces

Long-range intra- and inter-backbone forces depend mainly on the presence of the phosphate groups. The distance between the phosphates on the two strands is about 20 Å, hence their interactions are weak. In contrast, along the same strand, the distance between phosphates can be about 5 Å, meaning that mutual repulsion could be rather strong. But in its double-helical native form, DNA must be kept in a medium having a minimal ionic strength. The phosphate groups are then shielded by the counter-ions supplied by the medium. The shielding is very stable; as the NaCl concentration of the media is changed from 0.5 mM to 0.5 M, the number of Na^+ ions shielding the phosphates remains constant, since, on average, 0.88Na^+ shield each phosphate group of the backbones, throughout this ion-concentration range. Again, environmental parameters in the physiological range can alter the shielding (type of counter-ion element and valency, pH) and structural transitions of the double helix can significantly modify the inter-phosphate distances.

1.3.4
Electrostatic Field of DNA

The distribution of electrostatic potential around the molecule is an important physical characteristic of DNA. It is especially important in studies of condensed counterions around DNA [89–93], as well as in studies of DNA–DNA [94, 95] and protein–DNA [96, 97] interactions. Clustering of positive and negative charges on the macromolecule surfaces determines not only their attraction or repulsion but also their proper orientation and positioning with respect to each other which, in turn, may trigger mutual conformational fit leading to formation of more extensive contacts.

An *ab initio* calculation of the electrostatic potential still remains an intractable problem. For many years even approximate modeling of the electrostatic field around DNA has been hampered by the difficulty in calculating the electrostatic potentials for long DNA fragments (> 100 base pairs). However, in recent years a simple method of calculation of electrostatic potential distribution for long (~ 1000 base pairs) double chains has been proposed [98,99], and investigators have come close to the solution of the problem of finding the relationship between the nucleotide sequence and the electrostatic potential distribution [100].

1.4
Polymorphism

As we mentioned before, the DNA molecule has a double helix structure. In general, any helix can be described by the following parameters: (1) the pitch P which is determined by the formula

$$P = nh, \tag{1-11}$$

where n is the number of nucleotides per one turn and h is the distance between the adjacent nucleotides along the helix axis; (2) the angle of helix rotation which is determined by the formula

$$t = 360°/n. \tag{1-12}$$

In addition, every helix is characterized by the direction of the helix rotation, so the helixes can be right-handed and left-handed.

The DNA helix described above is right-handed, and its parameters are

$$n = 10,\ h = 3.4\ \text{Å}. \tag{1-13}$$

So, for the helix pitch we have

$$P = 34\ \text{Å}, \tag{1-14}$$

and for the angle of helix rotation we have

$$t = 36°. \tag{1-15}$$

In addition to the helix parameters described above, the double helix can be characterized by the handedness and the depth of its grooves. Looking down the helix axis in either direction, in a right (or left)-handed helix each strand winds clockwise (or counter-clockwise) as it moves away from the observer. The helix has small and large grooves, found respectively on the side of the base-pair turned towards the small or large angle made between the two C1–′N (base) bonds of the base-pair.

The double helix parameters described above are not, however, constant. As was shown by X-ray data [101, 102] they depend on the ambient relative humidity, the cation species present and the amount of retained salt. So, one can expect that many different types (or forms) of the stable DNA double helix structures are possible. They have been classified into three main families: the B family, with base-pairs almost perpendicular to the helix axis, a shallow wide groove and a deep small groove; the A family having a deep large groove, a shallow minor groove and base-pairs markedly non-perpendicular to the helix axis; and the Z family having a left-handed helix, in contrast to the right-handed helices of the A and B families. The structure of the DNA double helix described in the previous section has the B-form or the B-DNA. It is right-handed. Examples of the stable right-handed B-, A-forms and left-handed Z-form are shown in Figure 1.6. In addition the C-, D-forms of the double-strand DNA and the forms consisting of three strands (for example, poly(dA) · 2poly(dT)) are known. Structural parameters of all these forms are described in detail in Ref. [72]; we note here only that the existence of different DNA forms and the ability of the molecule to transfer from one form to another when the environmental parameters are changed contribute some of the most important evidence for the high internal mobility of the DNA molecule.

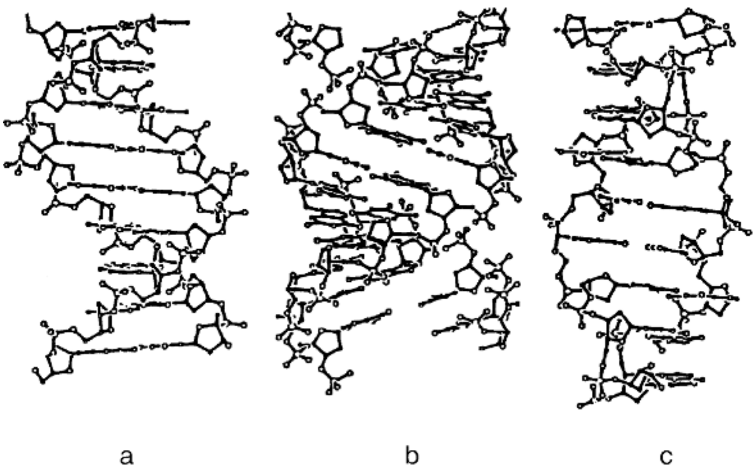

Figure 1.6 Skeleton drawing of (a) B-, (b) A- and (c) Z-DNA.

1.5
Tertiary Structure

Above we described the structure of a linear double strand DNA (in solution or in fiber) which is in a relaxed state. Due to its conformational flexibility, the DNA double helix can form various tertiary structures. We describe here two of them. The first is a supercoil, and the second illustrates how the molecule can be organized in living organisms.

1.5.1
Superhelicity

When in the relaxed state the DNA molecule is usually inactive or weakly active in the processes of replication, transcription or recombination. To provide the normal velocity of the processes, the DNA molecule should be under some stress or, in other words, it should be in the superhelical state [103–107]. It is known that most DNAs so far have been observed to form supercoils, at least in one stage of their biological life cycle. A superhelical state can be created by joining the 3′- and 5′-ends of the molecule and forming a coil, or by simple fixation of the ends, or by restriction of the rotations of the ends. But if we form a coil by using the usual relaxed B-form DNA we do not obtain a superhelical DNA. To obtain it we need to first slightly rewind the double helix or unwind it, and only after that form a coil by connecting the 3′- and 5′-ends. In the first case we obtain a so-called positive superhelicity and in the second case a negative one.

It is assumed that there are two reasons why the superhelicity is required: (1) to make the conformation needed to pack the DNA molecule or to make it more active, and (2) for energy accumulation [108].

Mathematical models of superhelical DNA have been developed in the papers of Frank-Kamenetskii et al. [109–113], Schlick [114] and Benham [115–117].

1.5.2
Structural Organization in Cells

The length of the DNA molecule of different organisms varies from several μm to several cm. It can be localized in viruses, in procaryote cells and in the nucleus of eycaryote cells. The sizes of some different DNA molecules are given in Table 1.1. In human cells there are 46 chromosomes and each of them contains one double-chain DNA molecule with the length being approximately equal to 4 cm. If we connected all these DNA molecules with one another, we could obtain a double chain with length about 2 m. With the help of small proteins named histones, this long double chain is packed into a nucleus having diameter 0.5 μm. There are four types of histones and they form a globular octamer consisting of eight histones (with two histones of each type). Fragments of DNA molecule with length about 146 base pairs are wound around this octamer. This structure is called a nucleosoma core. There is also one additional histon H_1 which strengthens the core, and the whole structure is called a nucleosome. So, the DNA molecule in a cell looks like a chain of nucleosomes connected to one another by fragments of DNA of length 40–100 base pairs. This structure is called chromatine. The chain of nucleosomes has a solenoidal form with 3–6 nucleosomes per turn, and this solenoid forms a more condensed and helical structure which is known as a chromosome. The human chromosomes contain double-chain DNA with total length about 2 m.

Table 1.1 Sizes of different DNA molecules.

Organism	Number of Bases	Length (Å)	Diameter (Å)
Viruses:			
Polyoma or SV-40	5.1×10^3	1.7×10^4	20
λ-phage	4.86×10^4	1.7×10^5	20
T2-phage	1.66×10^5	5.6×10^5	20
Viruses of cow-pox	1.9×10^5	6.5×10^5	20
Bacteria:			
Mycoplasma	7.6×10^5	2.6×10^6	20
E.coli	4.0×10^6	1.36×10^6	20
Eukaryotes:			
Yeast	1.35×10^7	4.6×10^7	20
Drosophila	1.65×10^8	5.6×10^8	20
Human	2.9×10^9	9.9×10^9	20

1.6 Approximate Models of DNA Structure

As is seen from the previous sections, the structure of the DNA molecule is rather complex, but in many cases it is sufficient and more convenient to use some simplified (approximate) versions of the structure. Let us consider in this section the problem of constructing approximate structural models of DNA.

1.6.1 General Comments

When constructing approximate models it is usually assumed that they must not include all details of the DNA structure but only the most important (or dominant) structural properties of DNA. What are these properties?

1. Reading the previous sections one can notice at least two general characteristics of the DNA structure. The first is that the DNA molecule consists of long chains of atoms. The second is that these chains have nearly regular structure, that is the DNA molecule has a ‘skeleton’ (sugar-phosphate chain) with an accurately repeating pattern of atoms along the chain. Due to these properties DNA is to a certain extent similar to the one-dimensional periodical structure which is known in physics as a quasi-one-dimensional crystal. This

is why Charles Bunn gave to biomolecules of this type the poetical name: 'crystals of chains of life' [118].

2. However, in some aspects the DNA molecule is more similar to a polymer than to a crystal because, in addition to the properties mentioned above, DNA is not a rigid system, but a flexible one. So, if we want to construct a more accurate model, we must take into account the flexible nature of DNA, that is its ability to bend, to twist, to form superstructures and so on.
3. Besides a 'skeleton' with a regular alteration of atoms or atomic groups, DNA has elements of irregular structure. So, if we want to improve the model, we must take into account the irregularity of the base sequence. We can consider this irregularity as a small disturbance of the regular pattern of the 'skeleton' and use perturbation theory for the mathematical treatment.

And so on. The list of properties could be continued by inserting more and more details of the internal structure. When constructing the model we can restrict ourselves by taking into account only the first property in the list, or the first two properties, and so on. Thus, many different approximate models may be constructed describing DNA with different degrees of accuracy. The choice of the approximation depends on the conditions and the aim of the investigation. For example, if we are interested in the mobility of the DNA molecule as a whole in the solution, or the penetration of the molecule through some channel, or the mechanism of forming a superhelical DNA structure, it is sufficient to consider the DNA molecule as an elastic filament. If, however, we are interested in the problem of protein–DNA recognition or transcription we need to take into account some more details of the internal structure such as the helicity or the inhomogeneity due to the sequence of bases.

1.6.2
Hierarchy of Structural Models

To describe different structural models of the DNA molecule it is convenient to use another approach. In this approach the DNA structural models are arranged in order of increasing complexity. In this case the models look like the elements of a hierarchy. Let us describe the main possible levels of the hierarchy.

1. *Models of the first level of the hierarchy.* The simplest structural model of DNA, which opens the hierarchy, is prompted by microphotos of the molecule where the DNA molecule looks like a thin elastic filament (Figure 1.7). So it can be suggested that the uniform elastic rod with a circular section (Figure 1.8a) can be considered as the simplest structural model of a fragment of DNA [119].

The discrete analog of the rod-like model consists of a chain of coupled disks (Figure 1.8b), each disk imitating a very small piece of the DNA molecule, which contains one base pair.

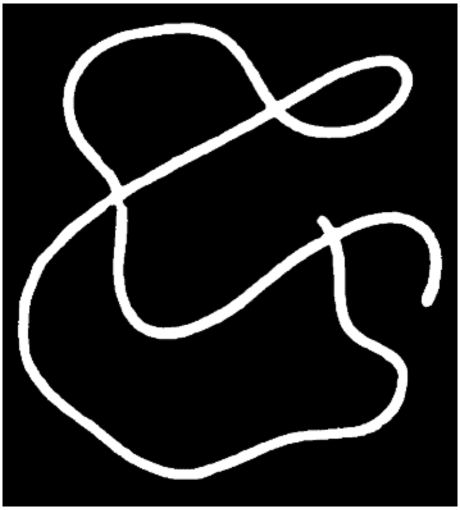

Figure 1.7 A schematic picture of a thin elastic filament.

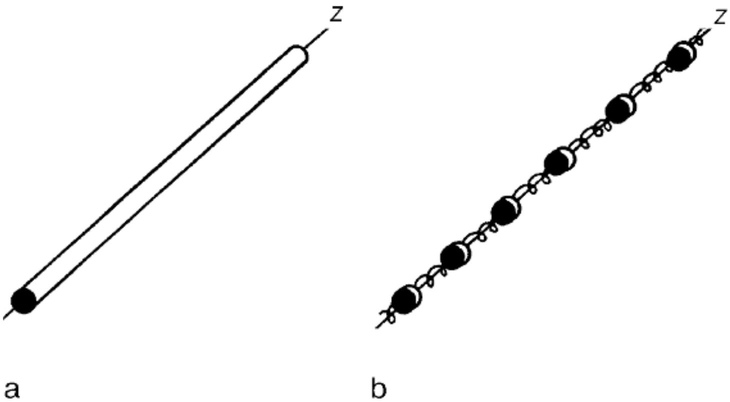

Figure 1.8 (a) The model of an elastic rod and (b) its discrete analog.

2. *Models of the second level of the hierarchy.* Some more complex structural models of the DNA molecule take into account that the molecule consists of two polynucleotide chains interacting with one another via hydrogen bonds and being wound around each other to produce the double helix. In this approximation, the internal structure of the chains is neglected, and each of the chains is simulated by an elastic uniform rod (in the continuous case) or by a chain of coupled disks (in the discrete case). So, the complete model consists of two elastic rods (or two chains of coupled disks) weakly interacting with one another and wound around each other as shown in Figure 1.9. In the discrete case each of the disks imitates a very small piece of one of two polynucleotide chains, which contains only one base.

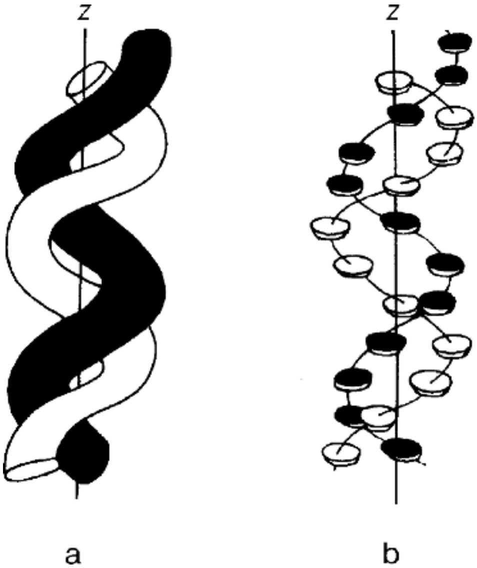

Figure 1.9 (a) A helical double rod-like model and (b) its discrete analog

To simplify calculations, a simpler version of the models described above is widely used. It consists of two straight uniform elastic rods weakly interacting with one another (Figure 1.10) and at least the discrete analog of the model has the form of two straight chains with disks connected to one another by longitudinal and transverse springs [26].

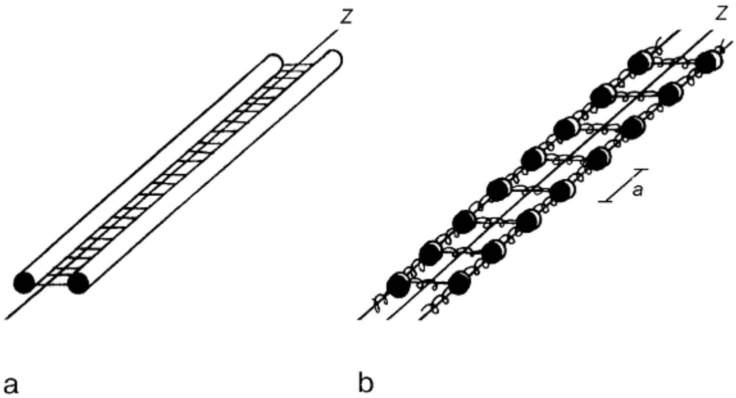

Figure 1.10 (a) A straight double rod-like model and (b) its discrete analog.

3. *Models of the third level of the hierarchy.* In the structural models of this group additional details of the internal DNA structure are taken into account. Every polynucleotide chain is considered here as consisting of mutually rigidly

bound atomic subgroups: the bases, the sugar rings and the phosphate–carbon pieces, with relatively weak, flexible bonds connecting them to each other [120]. A simple straight version of the model is shown in Figure 1.11.

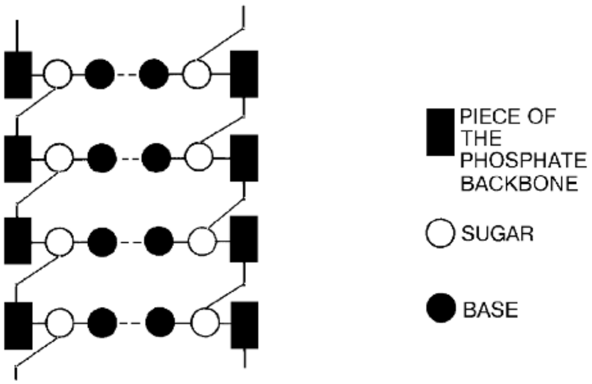

Figure 1.11 The third-level model of DNA.

4. *Models of the fourth level of the hierarchy.* The fourth group of the structural models comprises the so-called lattice models where a finite group of atoms (named nucleotide) forms a 'unit cell' quasi-periodically repeating along the DNA molecule [121]. A simple version of the lattice models is shown in Figure 1.12.

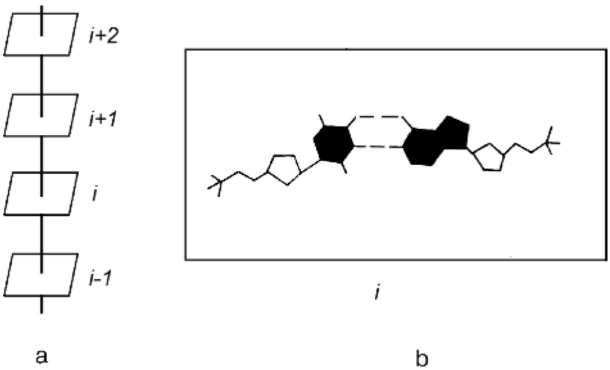

Figure 1.12 (a) One-dimensional lattice (b) with a unit cell (a pair of nucleotides) containing A-T base-pair. For simplicity, the screw symmetry of the model is not shown here.

5. *Models of the fifth level of the hierarchy.* The fifth group of the structural models is formed by the most accurate structural models taking into account the positions of every atom of the molecule (Figure 1.13).

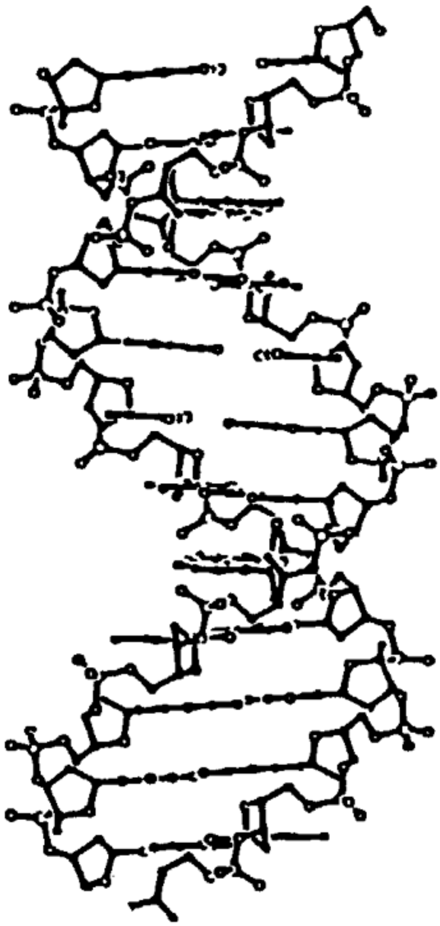

Figure 1.13 The most accurate model of the internal DNA structure.

1.7
Experimental Methods of Studying DNA Structure

To study the DNA molecule structure different mathematical, physical, chemical and biochemical methods and combinations of them are used. The history of the discovery of the structure of DNA gives an impressive illustration of this statement. The main events in the discovery were the following:

The suggestion that DNA exists in the form of thin rather rigid fibers approximately 20 Å in diameter and many thousands of Å in length was made after physical-chemical studies, involving sedimentation diffusion and light-scattering measurements [122,123]. These indirect inferences have been confirmed by electronic microphotographs [124,125].

The source of more detailed information about the configuration of atoms within the fibers was X-ray analysis. In 1951 Furberg published the first data on the crystal structure of cytidine [126]. His results were obtained by the X-ray method. The maps of the electron density were calculated at that time by hand. Now there are powerful computer calculation methods which, together with the spectroscopy data, enable the structures of different DNA fragments at the atomic level to be obtained.

Further investigations of the DNA structure were continued by Dekker, Michelson and Todd who showed by chemical methods that the linear polymer molecule of DNA consists of nucleotides, connected to one another by 3′,5′-phosphodietheric bonds [127]. Additional information was given in the work of Chargaff and coauthors [67] where it was shown that in different DNA molecules the relations A/T and G/C are equal to 1.

X-ray study of DNA fibers by Austbury [128] showed that the base pairs A-T or G-C are packed one over another and that the distance between them is equal to 3.4 Å. From the data on electrochemical titration Gulland [129] concluded that the bases in DNA are connected to one another by hydrogen bonds. Finally, additional X-ray data, obtained by Wilkins [101], showed that DNA has the helical structure which is able to change its conformation when environmental parameters such as hydration, temperature, or concentration of certain ions are changed.

All this information was gathered and analyzed by Watson and Crick [68,69]. As a result they proposed the double helical model of DNA, which explained all previous experimental data and, in addition, gave a simple explanation of the main features of DNA function. This discovery gave an impulse to intensive development of biochemistry, molecular biology and genetics. It was honored with the Nobel prize in 1962 and is described in detail in Watson's book *The Double Helix* [130].

Besides the methods mentioned above, many other methods, including well known physical methods such as NMR, infrared, Raman and neutron spectroscopy are now used to obtain detailed information about the DNA structure, DNA polymorphism, the dependence of the structure on the sequence of bases, the surroundings and so on. This information is also collected in the databases whose Internet addresses are described in a special issue of the journal *Nucleic Acids Research* [131].

2
DNA Dynamics

In Chapter 1, when describing the main features of the structure of the DNA molecule, we considered the molecule as being static. This approach has been widely used in the study of the DNA structure but, in reality, the DNA molecule is usually immersed in some thermal bath, and its structural elements such as individual atoms, groups of atoms (bases, sugar rings, phosphates), fragments of the double chain including several base pairs, are in constant motion, and this motion plays an important role in the function of the molecule. The thermal bath is not the only source of the DNA internal mobility. Collisions with molecules of the solution which surrounds DNA, local interactions with proteins, drugs or with some other ligands also lead to internal mobility. Thus, it is more correct to consider the DNA molecule as a dynamical system than as a static one.

In this chapter we describe the main features of the DNA molecule as a dynamical system.

2.1
General Picture of the DNA Internal Mobility

Because the structure of the DNA molecule is rather complex, one can expect that the general picture of its internal mobility will also be complex. In the first approximation, it can be described, however, by a few simple characteristics: the timescale, the amplitudes of the internal motions and the energies or frequencies associated with these motions. So, we can state that :

1. The dynamical events in DNA occur on a timescale ranging from femtoseconds to at least seconds.
2. The amplitudes of the internal motions can be both small (for example, small vibrations of individual atoms or atomic groups near their equilibrium positions with amplitudes no more than 0.1 Å) and large (for example, large amplitude motions of the fragments of polynucleotide chains associated with the local unwinding or opening of the double helix).
3. The frequencies associated with the internal motions are 1–100 cm^{-1} , much lower than the frequencies of internal vibrations in isolated small molecules.

Table 2.1 Classification of experimental and theoretical data on the internal DNA mobility.

The Timescale and the Main Intervals	Picosecond	Nanosecond	Microsecond	Millisecond	Second
The main types of internal motions and their amplitudes	Short-living motions and ($\tau = 10^{-12}$ s) oscillations of atoms with amplitudes $A = 10^{-1}$ Å	Limited motions; oscillations of small groups of atoms: sugars, phosphates, bases; bending and twisting motions of the double chain with amplitudes $A = 5 \div 7$ Å	Bending motions; winding and unwinding of the double helix; opening of base pairs	Dissociation (untwisting) of the double helix; change of superhelicity; overall rotation of the DNA molecule	Motions with amplitudes $A = 2 \div 3$ μu; writhing, isomerization, division of bacteria
Energy of activation possible; sources of energy	$E = 0.6$ kcal mol^{-1}; Source: external thermal reservoir	$E = 2 \div 5$ kcal mol^{-1}; Sources: collisions with hot molecules of solution	$E = 5 \div 20$ kcal mol^{-1}; Sources: change of PH, increasing temperature, action of denaturalization agents	$E = 10 \div 50$ kcal mol^{-1}; Sources: interactions with proteins and other ligands	
Experimental methods	NMR, IRS, Raman spectroscopy, X-ray	NMR, EPR, Raman spectroscopy, fluorescence	NMR, EPR, optical anisotropy reaction, with formaldehyde, hydrogen exchange	NMR, hydrogen exchange, reaction with formaldehyde, quasielastic scattering of light, hydrodynamical methods	
Theoretical methods	Harmonic analysis, lattice model, methods of molecular dynamics	Harmonic analysis, rod-like model, methods of molecular dynamics	Theory of helix–coil transition	Methods of conformational mechanics, topological models	

To describe the picture of the internal DNA mobility in more detail, it is convenient to classify DNA internal motions according to their forms (types), energies, amplitudes and characteristic times. Some of the classifications have been proposed in the works of Fritzsche [132], Keepers and James [133], McClure [134], McCammon and Harvey [13] and Yakushevich [3, 53]. As an example, we present in Table 2.1 one of these classifications proposed in Ref. [53]. It is based on the time characteristics of internal DNA motions. The timescale is divided into several intervals; for each interval, the main types of internal motions, the main structural elements involved in these motions, the energies of activation and the amplitudes of the motions are described. In addition, the main experimental and theoretical methods for studying the internal motions are given.

If we are interested, however, only in the part of the general picture which is assumed to be connected with the DNA function, we should restrict ourselves to consideration of the internal motions which belong to the nanosecond diapason and its neighborhood. This diapason includes, beside others, the so-called solid-like motions of sugars, phosphates and bases, which are known to be very important in many biophysical phenomena: conformational transitions, gene regulation, DNA–protein recognition, energy transmission, DNA denaturation, and other phenomena involving energies E of several kcal mol^{-1} and frequencies ν of several cm^{-1}.

In the following sections we shall describe the internal motions which belong to the nanosecond diapason and its neighborhood. When describing the motions we shall follow the traditional method used by biologists, which consists in simply listing the motions and their characteristics. However, where possible, and especially in Section 2.7, we shall use another approach to the problem based on the construction of models of the internal DNA dynamics.

2.2 Twisting and Bending Motions

Twisting (or torsional) and bending motions belong to the group of motions which imitate the internal dynamics of the DNA molecule in the so-called elastic rod approximation. In this approximation the DNA molecule is modeled by a thin, flexible rod of length L, circular cross section of radius b, and uniform elasticity along the helix axis. The rod is immersed in a viscous fluid at thermal equilibrium (Figure 2.1). This approach to DNA dynamics has been proposed by Barkley and Zimm [119] and Allison and Shurr [135], and was developed later in many works devoted to superhelical DNA (see, for example, Refs. [136,137]).

The model of an elastic rod is well known and studied in physics [138], so we can use the results obtained there to describe twisting and bending motions. Suppose the rod imitating a DNA molecule is divided into small elements bounded by adjacent cross sections. Take a coordinate system for the rod with the z axis along its long axis. We consider torsional deformations of the rod as its elements twist about the long axis and bending deformations as they rotate about their transverse axes. In the case of DNA, it is natural to assume that each of the elements contains only one base pair.

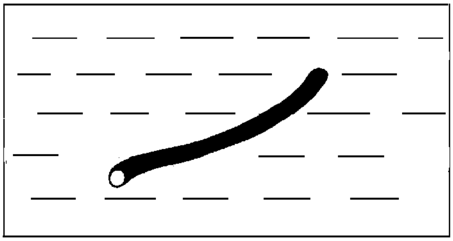

Figure 2.1 The rod immersed in a viscous fluid at thermal equilibrium.

Let $\varphi(z,t)$ be the relative rotation angle of two cross sections, so that $\partial\varphi/\partial z$ is the twist of the rod. The torque at z due to the twist is

$$M(z) = C\,\partial\varphi/\partial z. \tag{2-1}$$

where C is the torsional rigidity of the rod. Since the torque changes with z, an element of the rod between z and z+dz will have a net torque $(\mathrm{d}M/\mathrm{d}z)\mathrm{d}z$ which turns it in the fluid. Assuming the torque exerted by the element on the fluid to be proportional to its rate of turning. The equation of motion for twisting is

$$\partial\varphi/\partial t = (C/\rho)\,\partial^2\varphi/\partial z^2, \tag{2-2}$$

where ρ is the frictional coefficient per unit length.

Assuming that the torsional deformations obey Hook's law, we find the elastic energy of this twisted rod (or twisted DNA) to be [138]

$$E^{tw} = (C/2)\int_0^L (\partial^2\varphi/\partial^2 z)^2\,\mathrm{d}z \tag{2-3}$$

Suppose now that the z axis coincides with the center of the undeformed rod, and consider small bending deflections in a principal plane, which we take to be the xy plane. Let $y(z,t)$ denote the transverse displacement of the center line away from equilibrium. The net force per unit length on the rod due to the transverse motion is

$$F(z) = -EI\,\partial^4 y/\partial z^4, \tag{2-4}$$

where EI is the flexural rigidity of the rod (E is the Young's modulus and I the moment of inertia).

Assume again Hook's law deformations, so the elastic energy of the bent rod (or bent DNA) is [138]

$$E^b = (EI/2)\int_0^L (\partial^2 y/\partial^2 z)^2\,\mathrm{d}z. \tag{2-5}$$

A more accurate mathematical description of the torsional and bending motions and its relation to the description given above is presented in Appendix 1.

2.3
Dynamics of the Bases

To describe the dynamics of the bases, it is convenient to begin with a brief description of the equilibrium state of the bases and then to describe possible motions of the bases as deviations from their equilibrium positions.

2.3.1
Equilibrium State

The structures of the four DNA bases: adenine, thymine, guanine and cytosine, are shown in Figure 1.2. Because the deviations of the atoms of the bases from the plane are small (< 0.1–0.3 Å) and not regular, the base structure can be considered as planar. So, for simplicity, the bases can be shown in figures as rectangular plates and the pair of bases can be shown as pairs of plates (Figure 2.2). In the general case, the positions of the plates relative to the helix axis are different for different DNA conformational forms (see Figure 1.6). But in the first approximation, we can assume that for B-DNA the plates are perpendicular to the helix axis.

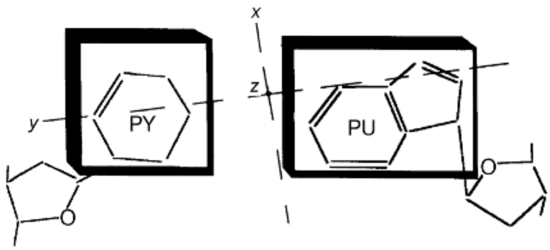

Figure 2.2 Purine and pyrimidine sketched as two rectangular plates.

2.3.2
Possible Motions of the Bases

A pair of bases is best visualized in the right-handed orthogonal axial set *Oxyz*, where *O* is chosen at the 'center' (close to N1 of the purine) of the pair under consideration (Figure 2.2). *Oz* is taken along the helix axis, *Oy* runs from C6 (pyrimidine) to C8 (purine), so that Ox intercepts the H-bonds of the pair.

When considering possible motions of the bases, we shall neglect the intrabase motions. In this case, a simple plate-like model of the bases can be used and possible solid-like motions of the plates can be considered.

The flexibility of the H-bonds enables rotational freedom between the bases (plates) of the pair, which are thus not necessarily coplanar. In Figure 2.3 three possible intra-pair rotation motions called 'opening', 'propeller-twist' and 'buckle' are shown. The amplitudes of the motions are characterized by the dihedral angles between the planes of individual bases (looking down the rotational axis, the angle being positive if the nearest base is rotated clockwise relative to the farthest one).

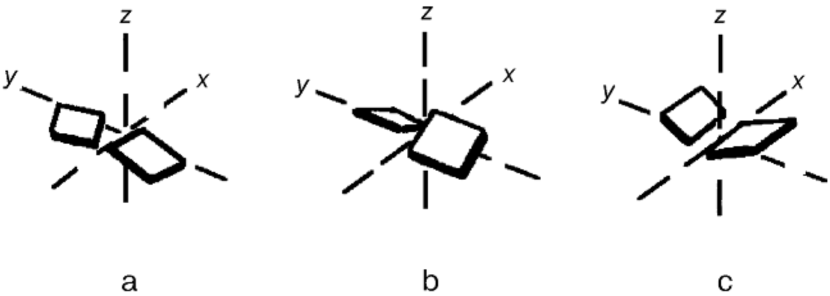

Figure 2.3 Intra-pair rotation: (a) opening, (b) propeller twist, and (c) buckle.

Another group of three intra-pair motions includes translation motions of bases (plates). They are called 'stagger', 'stretch' and 'shear' (Figure 2.4). Their amplitudes are characterized by the displacements of the planes from the corresponding equilibrium positions.

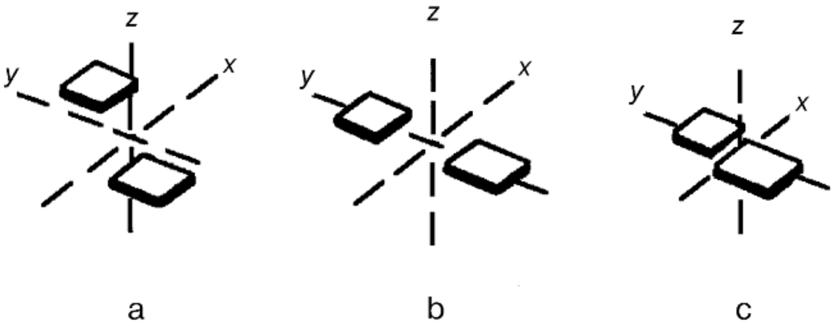

Figure 2.4 Intra-pair translation: (a) stagger, (b) stretch, and (c) shear.

In addition, the base pair as a whole also has rotational and translational degrees of freedom. We can consider three rotations of some mean plane of the base pair around *Oz*, *Oy* and *Ox* (Figure 2.5). They are called 'twist', 'roll' and 'tilt', respectively. And three translation motions along the axes should also be considered (Figure 2.6). They are called 'rise', 'slide' and 'shift', respectively.

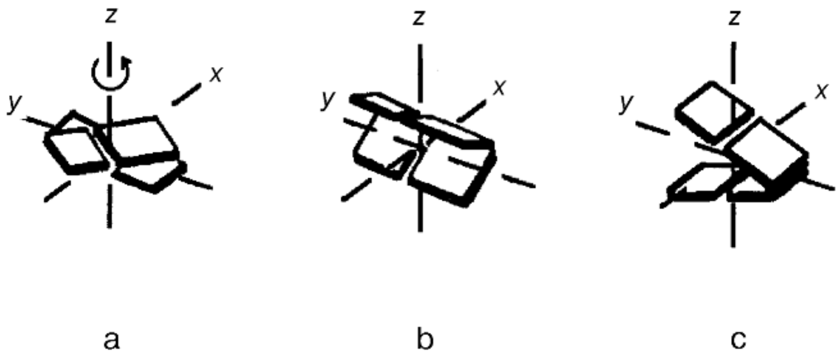

Figure 2.5 Inter-pair rotation: (a) twist, (b) roll, and (c) tilt.

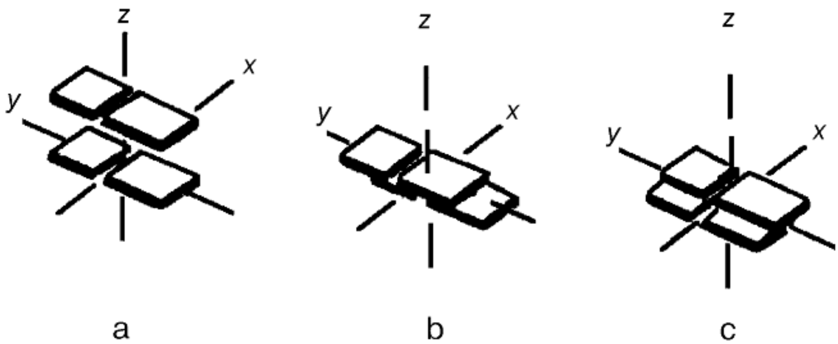

Figure 2.6 Inter-pair translation: (a) rise, (b) slide, and (c) shift.

It is necessary to note, however, that the bases or base pairs are not free to rotate or to translate according to the degrees described above as these movements may be opposed by hindrances. Two hindrances are predominant. The first results from the presence of nearest-neighbor base pairs, on both sides of the pair under consideration. The propeller twist, for example, can lead to steric clashes with the next base pairs, as could buckle, roll, tilt, etc. Conversely, however, the degrees of freedom of each neighboring pair can be instrumental in removing these steric hindrances, and so on for their next neighbors. Thus the clash can be handled and eased with the mutual help of a row of base pairs, each modifying its position in accordance with its degrees of freedom, following rules first proposed by Calladine [139]. The second hindrance is imposed by the glycosil bond linking the base to the sugar. Although this bond is covalent, and hence very strong, the glycosil ring to which it is attached has a rather flexible structure. Hence, the hindrance is rather weak and can be accommodated within rather large limits, but in this case mainly by intranucleotide rearrangements.

2.4
Dynamics of the Sugar–Phosphate Backbone

2.4.1
Equilibrium State

The backbone equilibrium structure between two consecutive phosphorus atoms is usually described by six torsional angles: α, β, γ, δ, ξ, ζ (Figure 2.7). The conformation of the sugar is characterized by four more torsional angles: ν_0, ν_1, ν_2, ν_3 (which is identical to δ), and ν_4. In addition, one more important structural parameter is the torsional angle of the glycosidic bond, χ.

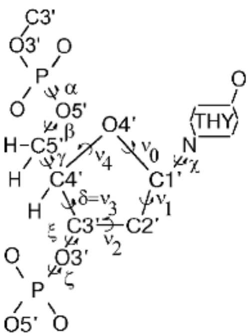

Figure 2.7 The rotational angles of the sugar–phosphate backbone with thymine attached.

2.4.2
Possible Motions of the Sugar–Phosphate Backbone

When considering the DNA molecule as a dynamical system, we suggest that all parameters described above can be changed.

The changes in the values of the torsional angles are in general restricted to the common steric ranges, syn (0°), anti (180°), synclinal (±60°) and anticlinal (±120°). In DNA, however, not all these ranges may be accessible; for example, the glycosil torsional angle χ is restricted to syn and anti ranges mainly. Furthermore, most of the motions associated with the changes in the torsional angles are correlated (only the changes in parameter are independent).

To describe possible changes of the structural parameters of sugars, we should take into account that the five-membered furanose ring is usually not planar but 'puckered', either in the 'envelope' form, when four atoms of the ring are approximately coplanar and the fifth is out of the plane by less than about 0.5 Å, or in the 'twisted' form, when two adjacent atoms are displaced on opposite sites of the plane defined by the other three atoms. Those being displaced on the side of C5′ are called 'endo' and those being displaced on the opposite side are called 'exo'; (Figure 2.8).

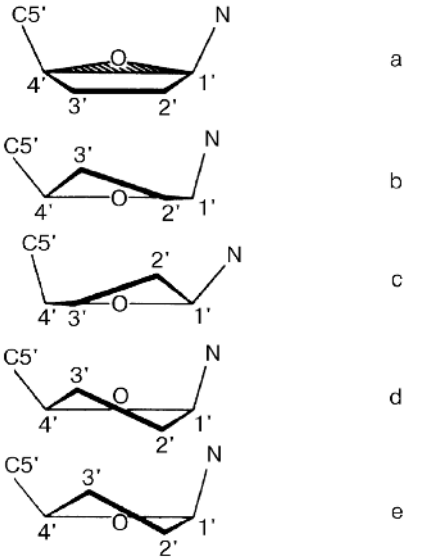

Figure 2.8 Different sugar conformations: (a) initial state (triangle C1′–O4′–C4′ is shaded; (b) C3′ endo; (c) C2′ endo; (d) symmetrical twist conformation; (e) asymmetrical twist conformation. In (b), (c), (d) and (e) the plane of triangle C1′–O4′–C4′ is perpendicular to the figure plane.

The conformational dynamics of sugars is usually described by the pseudo-rotation phase angle P, where

$$\tan P = ((\nu_1 + \nu_4) - (\nu_3 + \nu_0))/3.08\ \nu_2; \tag{2-6}$$

which allows computation of the five torsional angles ν_0, ν_1, ν_2, ν_3, ν_4 by

$$\nu_j = (\nu_0 \cos(P + j144°))/\cos P,\ j = 0,1,...4. \tag{2-7}$$

The case $P = 0°$ corresponds to ν_2 maximally positive, that is a symmetrically C2′ exo - C3′ endo twisted conformation, and the case $P = 180°$ corresponds to the mirror image of the latter. In DNA two ranges are preferred: $-1° < P < 34°$ (C3′ endo) and $137° < P < 194°$ (C2′ endo).

In Figure 2.9 the variation of the energy of furanose (in nucleosides) with P is shown. The preferred C3′ endo and C2′ endo are separated by a barrier of about 1.5 kcal and the highest barrier found over the whole range of P is about 5.5 kcal. Transitions between the various conformations are, therefore, easy: the sugar ring is indeed highly flexible. This flexibility can compensate to some degree the constraints imposed on the glycosil bond by the base (or base pair) and the constraints imposed by the backbone on the C5′–C4′–C3′ link, with minimal expenditure of energy.

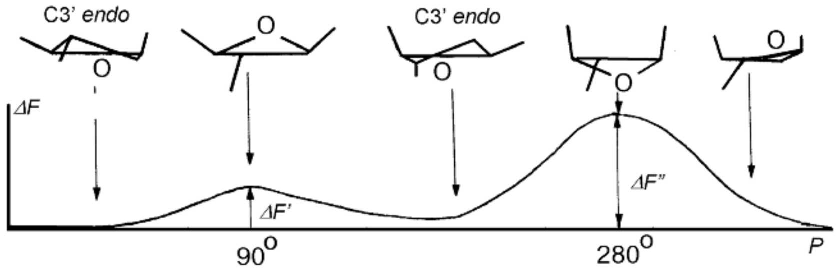

Figure 2.9 Nucleoside free energy difference (ΔF) as a function of the pseudorotational angle (P). $\Delta F' \cong 1.5\ kcal\ mol^{-1}$; $\Delta F'' \cong 5.5\ kcal\ mol^{-1}$.

2.5
Conformational Transitions

As we described in Section 1.4 the DNA double helix can take different conformational forms. It is widely accepted that transitions between the forms result mainly from the interplay between the conformational flexibilities of the sugars and the degrees of freedom corresponding to the base pairs and their mutual positioning.

The most important and widely studied transitions are the so-called B→A and B→Z transitions. Let us describe them briefly.

2.5.1
B→A Transition

Under physiological conditions DNA has the B-form. The B→A transitions may occur in some fragment of the DNA molecule with changes in the external conditions or with protein attachment. The transitions have a relatively small potential barrier and they are weakly dependent on nucleotide composition [9]. Nevertheless, there are some special examples of synthetic polynucleotides which cannot transform from the B-form to the A-form. For example, polynucleotide poly(dA-dG) • poly(dC-dT), one chain of which consists of purines and the other of pyrimidines, cannot transform from the B-form to the A-form [72]. In addition, it is known that in the DNA fragment containing less than 30% G-C base pairs the B→A transition is rather difficult, and if the proportion of the G-C pairs increases the transition becomes easier [140].

The main difference between the helixes of A- and B-types consists in the sugar conformations [72]. So, in B-DNA the sugar rings have C2′endo conformation and in the A-form they have C3′endo conformation. This difference leads to the change in the distances between the adjacent phosphates and this is the reason why the A- and B-helixes look very different.

The main changes in the helix parameters are the following:

- The number of nucleotides per one turn changes from $n_B = 10$ to $n_A = 11$.
- The distance between the adjacent nucleotides changes from $h_B = 3.38$ Å to $h_A = 2.56$ Å.

- The angle of helix rotation changes from $t_B = 36°$ to $t_A = 32.7°$.
- The direction of the helix rotation does not change.

From the analysis of the changes in the parameters of the double helix we can select the internal motions which make the main contribution to the transitions. These are usually named dominant motions. In B→A transitions dominant motions are those leading to the changes in the conformations of the sugar rings. So, to describe the transition mathematically it is necessary to consider, at the least, one group of motions associated with the changes in pseudo-rotational phase angle P.

2.5.2 B→Z Transition

In this transition the right-handed B-DNA transforms to the left-handed Z-DNA. The changes in the other parameters of the helix are the following:

- The number of nucleotides per one turn changes from n_B =10 to n_Z =12.
- The distance between the adjacent nucleotides changes from h_B = 3.38 Å to h_Z = 3.7 Å.
- The angle of helix rotation changes from $t_B = 36°$ to $t_Z = -30°$.

As in the previous case, the ability to transform from the B- to the Z-form depends on the base nucleotide composition. So, polynucleotide poly(dG-dC) • poly(dG-dC) can transform from the B-form to the Z-form but polynucleotide poly(dA-dT) • poly(dA-dT) cannot transform in this way.

It is rather difficult to select dominant motions contributing to the B→Z transitions. However, if we take into account that these motions should make a contribution to a local separation of the double chain in the range where the transition begins [52, 141–142], we can suggest that at the least the transverse displacements of nucleotides are one type of dominant motion which contributes to the transition.

2.6 Motions Associated with Local Strands Separation

The double helix can undergo local, partial or even total strand separations. They can be obtained in the test tube by adjusting various physical or chemical parameters, such as the temperature or the ionic strength of the buffer.

The double strand described above, is usually referred to as the 'native' state of DNA, and the process of separation is also called 'unwinding', 'opening', 'melting' or 'denaturation'. Recent single molecule experiments have permitted detailed study of the mechanical separation of the two strands of DNA sequences [66]. In general, the process is rather complex and many different types of simpler internal motions contribute to it. Below we describe briefly two of them.

2.6.1
Base-pair Opening Due to Rotations of Bases

The opening of base pairs is a complex motion leading to the disruption of the H-bonds joining the bases in pairs. It is usually assumed that the main contribution to the process of opening is made by rotation motions of bases near the sugar–phosphate chains. These motions are shown schematically in Figure 2.3a. Both, the opening of a single base pair and that of several base pairs which are neighbors and form a local range are possible. The opening can be monitored experimentally. A convenient parameter for this is the DNA absorbance in the near ultraviolet (more precisely between 240 and 280 nm), which increases by some 40% as the double helix melts, as a consequence of the disruption of stacking interaction between consecutive base pairs. The opening can be studied effectively by NMR [143,144] and hydrogen–tritium exchange methods [145–147].

2.6.2
Transverse Displacements in Strands

Another group of motions which is very important in the process of local separation is the transverse motions of nucleotides in both chains. To describe these motions it is convenient to consider a simplified model of the DNA molecule each strand of which is represented by a set of point masses corresponding to the nucleotides. Longitudinal displacements of the masses can be neglected because they are not dominant in the process of separation. In the framework of this model the main contribution will be made by the transverse motions leading to the stretching of the bonds connecting bases in pairs (Figure 2.4b).

2.7
Approximate Models of DNA Dynamics

When an investigator is interested in the dynamical mechanisms of some biological process involving DNA he must use some dynamical model of DNA. It could be a new model constructed by himself, or it could be a model proposed by some other investigators. In the first case, when constructing a new model, it is important to know the main principles of modeling DNA dynamics, and in the second case, when selecting one of the known models, it is important to know the limitations of the models used and the relations between them. We shall discuss both cases in this section.

2.7.1
The Main Principles of Modeling

Because of the complexity of the general picture of the DNA internal dynamics, mathematical modeling of the dynamics is also rather complex. It requires detailed information about physical parameters, such as the coordinates, mass and moment of inertia of the structural elements, and about interactions between the elements. In addition, we need to use a very powerful computer to imitate all possible internal motions. The problem, however, can be simplified if we construct approximate models which imitate only the internal motions which make the main contribution to the process considered. This approach is widely used in studying DNA internal dynamics. Let us describe briefly the main principles of constructing models in this way [148].

To construct an approximate model, first it is necessary to simplify the general picture of the DNA internal motions. This can be done by selection of a limited amount of internal motions which are dominant. Selection can be done in many ways, and this explains the large variety of the models proposed. Secondly, we need to describe these motions by mathematical equations. This can be done directly or through an intermediate stage consisting of finding some physical (very often mechanical) analog with the same type of internal motions and interactions. Thirdly, we need to solve the equations and to interpret their solutions in terms of the parameters of the DNA internal dynamics. These three stages of modeling DNA dynamics will be illustrated many times in the following chapters when different nonlinear models of the internal DNA dynamics will be constructed.

2.7.2
Hierarchy of Dynamical Models

If we do not plan to construct a new dynamical model and want only to choose an appropriate model from amongst those proposed earlier by some other authors, it is convenient to use a special approach where each of the models is considered as an element of a hierarchy. This approach automatically gives us information about possible restrictions of the models used and about the relations between them.

The hierarchy of dynamical models can be easily constructed in the following way. Let us assume that the structural models described in Section 1.6.2 are not static but dynamic ones. That is, all structural elements of the models are movable. Because the models have already been arranged in the order of increasing complexity, we obtain automatically the hierarchy of the dynamical models (Table 2.2). Let us briefly describe it.

The first level of the hierarchy is formed by the rod-like model (and by its discrete analog) having three types of internal motions: longitudinal and rotational motions of small elements of the rod bounded by adjacent cross sections, and bending motions.

The second level is formed by the model consisting of two elastic rods (or by their discrete analogs) weakly interacting with one another. In the helical version of the model the rods are assumed to be wound around each other to produce the double helix. In the straight version the helicity of the model is neglected. In both cases, the models have six types of internal motions: longitudinal, transverse and rotational motions in both rods.

The models of the third level take into account that each of the DNA strands consists of three types of atomic groups, sugars, phosphates and bases, and imitate

Table 2.2 Hierarchy of DNA dynamical models.

1	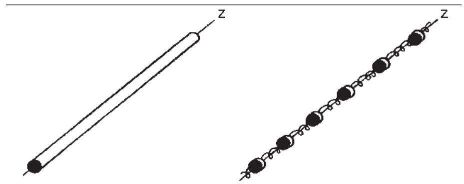
2	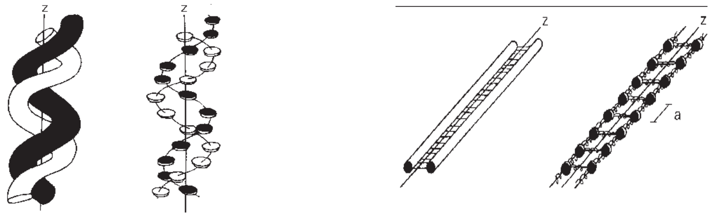
3	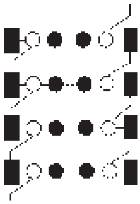
4	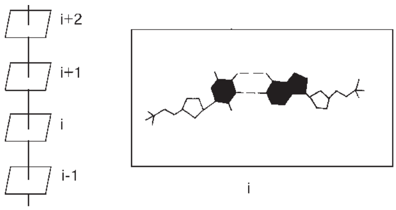
5	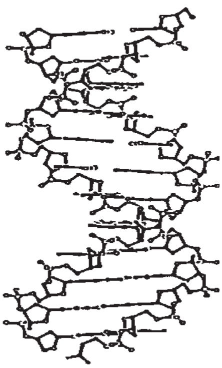

their motions as solid-like motions of the atomic groups weakly interacting with each other. To calculate how many types of internal motions are described in this model, we should take into account that, in the extreme case when the connecting bonds between the groups are absent, every group has six degrees of freedom, and that every chain has three types of groups. Thus, we obtain 36 degrees of freedom (instead of three for the first level models and six for the second level models). However, if we take into account the connecting bonds, the number of degrees of freedom will be decreased.

The models of the fourth level describe internal motions in a 'lattice' with a unit cell formed by a finite group of atoms (nucleotide) which periodically repeats along the DNA. In this approximation we consider all displacements of the nucleotide atoms but restrict ourselves to consideration of only homopolymer chains.

Finally, the fifth level comprises the most accurate models of the DNA molecule where all motions of all atoms are taken into account.

Because all internal motions mentioned above can be described by differential equations, we can obtain a set of mathematical models consisting of three (for the models of the first level), six (for the models of the second level) or more (for the third or higher level models) differential equations, these being arranged in the order of increasing complexity, that is forming the hierarchy.

In conclusion, let us consider one example illustrating how the hierarchy of the dynamical models can be applied. Assume, that we study the dynamical aspects of the process of local opening of the double helix. Which model should be chosen? We could begin with the simplest models of the first level. But these models are not appropriate because they do not take into account the DNA internal structure at all. The second level models are more appropriate and they can be used as the first approximation. The third level models are more accurate and their application permits description of the process in more detail. They can be considered for the second approximation, and so on.

2.8 Experimental Methods for Studying DNA Dynamics

There are many different experimental methods for studying DNA internal dynamics. The most important are Raman scattering [149–152], neutron scattering [153–155], infrared spectroscopy [156,157], hydrogen–deuterium (–tritium) exchange [15, 158], microwave absorption [159–161], NMR [162–165], charge-transfer [166–174] and single molecule [66, 175–178] experiments. In this section we describe each of them briefly.

2.8.1 Raman Scattering

Methods of inelastic light-scattering on oriented films are known as Raman scattering and have made a significant contribution to the understanding of the dynamics of DNA. The low-frequency range of Raman spectra is of much interest because its structure depends on internal motions of rigidly bound atomic groups (bases, for example) weakly connected with one another. The frequencies of most interest are in the range between 0.003 cm^{-1} and perhaps 100 cm^{-1} (1 GHz to 3 THz or time-scales of 1 ns to ~ 0.3 ps).

There are, however, some difficulties in obtaining and interpreting the spectral lines. There are also many difficulties in the theoretical calculation of Raman intensities. The predictions vary considerably, even for 'simple' molecules like benzene. Thus, for DNA we can expect that in many cases only qualitative assignments of the observed data will be possible. An example was given in the works of Urabe and Tominaga [179] and DeMarco et al. [180] where the softening of a Raman mode near 25 cm^{-1} in Na-DNA was observed. The softening increased substantially at the relative humidity where the X-ray fiber diffraction patterns indicate change from A to B conformation. So, it was concluded that low-lying Raman bands could be related to the A→B conformation shift in DNA.

A schematic layout of the experiment is shown in Figure 2.10. Wave vector conservation requires that an internal motion, for example, a vibration of small amplitude of an atomic group, which scatters the light through an angle α has a vector $\boldsymbol{k}$ equal to the change ($\boldsymbol{k}_i - \boldsymbol{k}_s$) in the light wave vector.

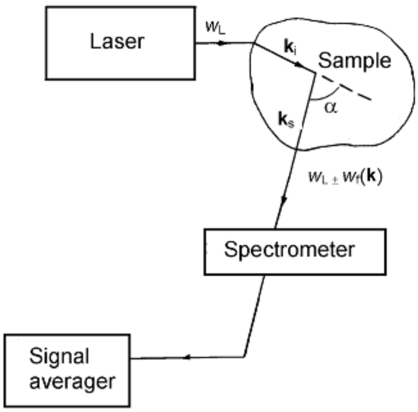

Figure 2.10 Schematic layout of inelastic laser light scattering experiment. The spectral components, w_L ($w_f(\boldsymbol{k})$, are separated by the spectrometer and recorded with a repetitive scan by a signal averaging computer. Here α is the scattering angle within the sample. $\boldsymbol{k} = \boldsymbol{k}_i - \boldsymbol{k}_s$.

Referring to Figure 2.10 the magnitude of k (k=|$\boldsymbol{k}$|) is given by

$$k = (4\pi n/\lambda_L)\,\sin(\alpha/2); \tag{2-8}$$

where n is the refractive index of the sample and λ_L is the laser wavelength. Energy conservation requires that the scattered light contains components at

$$w = w_L \pm w_f\,(\boldsymbol{k}); \tag{2-9}$$

where w_f ($\boldsymbol{k}$) are the eigenvalues of the so-called dynamical matrix of DNA, which will be discuss in detail in Chapter 4.

Even if k is well defined, these components appear as broadened peaks in the spectrum with a width that yields the lifetime of the vibration. The largest value of k is $4\pi/\lambda_L$, so scattering is confined to modes near a zone center. Thus the zone center of longitudinal and torsional acoustic mode shifts determine a speed of sound through $V = w_f/k$. The bending mode dispersion is quadratic, so the zone center shift is probably too small to be observed. Optic, resonant and local mode shifts are essentially independent of k.

Usually experimenters work with samples consisting of oriented fibers. In this case we can expect the lengthwise acoustic modes to be overdamped in solution. Fibers also allow the conformation to be monitored easily, and in principle, much is to be gained from knowing the orientation of $\boldsymbol{k}$ with respect to the fiber axis.

2.8.2
Neutron Scattering

Thermal (or slow) neutrons with de Broglie wavelengths between 2 and 20 Å are a versatile probe of the dynamics of DNA. They have energies between 20 and 0.2 meV, compared to ≈10 keV for X-ray quanta. Because of this, it is possible with neutrons to go beyond diffraction and do something that cannot be done with X-rays: to energy-analyze the intensity recorded at each scattering angle, in addition to measuring its variation with angle.

The geometry of the scattering problem is shown in Figure 2.11. The direction of propagation of the scattered neutron with respect to the incident neutron is defined by the polar angle θ and azimuthal angle φ. If the flux of incident neutrons, defined as the number per unit area per unit time, is N, then the number scattered per unit time into the element of solid angle $\Omega = \sin\theta \, d\theta \, d\varphi$ is

$$N(d\sigma/d\Omega)d\Omega; \tag{2-10}$$

where $(d\sigma/d\Omega)$ is the differential cross-section.

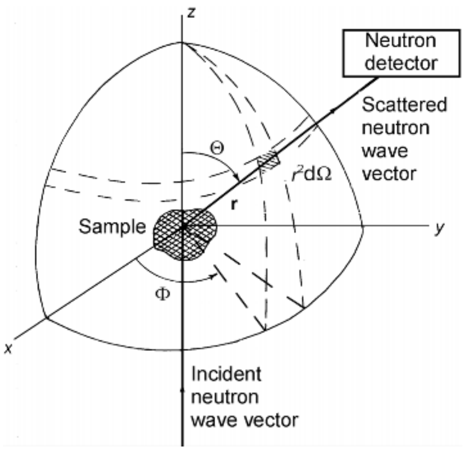

Figure 2.11 The geometry of the neutron scattering problem.

The basic conservation equations governing the interaction between a quantum of incident radiation and a scattering centre are given by

$$\hbar \boldsymbol{x} = \hbar(\boldsymbol{k}'\text{-}\boldsymbol{k}''), \text{ (momentum)} \tag{2-11}$$

$$\hbar \mathrm{w}' = E'\text{-}E'', \text{ (energy)} \tag{2-12}$$

where $\hbar\boldsymbol{x}$ and $\hbar w$ are the momentum and energy transfers, respectively ($\hbar$ = Planck's constant/2π). The initial and final wave vectors and energies are denoted by $\boldsymbol{k}'$, $\boldsymbol{k}''$ and E', E''.

Some fraction of radiation is usually scattered elastically. It is the so-called elastic scattering which is characterized by the relation $k' = k''$ ($k' = |\boldsymbol{k}'|$, $k'' = |\boldsymbol{k}''|$) and produces $\boldsymbol{x}$-dependent diffraction patterns related by Fourier transformation to the real-space structure.

The other fraction of the radiation, however, will be scattered inelastically, i.e. it will exchange energy with thermal vibrations and other excitations in the sample. Thus inelastic scattering carries information about internal motions in DNA.

With the exception of spin-echo instruments, all neutron spectrometers provide data in the form of a double differential cross-section, $\mathrm{d}^2\sigma/\mathrm{d}\Omega\mathrm{d}E'$. For the simplest case of a monoatomic assembly of target nuclei this is given by

$$\mathrm{d}^2\sigma/\mathrm{d}\Omega\mathrm{d}E' \sim N(k''/k')[\sigma_{\mathrm{inc}}\, S_{\mathrm{inc}}(\boldsymbol{x},w') + \sigma_{\mathrm{coh}}\, S_{\mathrm{coh}}(\boldsymbol{x},w')]; \tag{2-13}$$

where σ_{inc} and σ_{coh} are incoherent and coherent scattering cross-sections, respectively; and $S_{\mathrm{coh}}(\boldsymbol{x},w')$, $S_{\mathrm{inc}}(\boldsymbol{x},w')$ are the dynamical factors of coherent and incoherent scattering. In Chapters 4 and 7 we shall demonstrate several examples of calculation of dynamical factors for different DNA models.

In the thermal neutron experiments oriented DNA fibers are usually used [181]. This probe offers the advantage of a dominant incoherent cross-section for hydrogens and the simultaneous exploration of a wide range of frequency (w') and momentum ($\boldsymbol{x}$) space [182].

A major problem is the availability of sufficiently large oriented samples of DNA in order to exploit the discrimination of atomic displacements by means of the projection on $\boldsymbol{x}$. Existing thermal neutron sources require about 1 cm^3 DNA in order to reach the level of statistical significance for signals due to collective excitations within the practical limits of days measuring time. This problem has been partly overcome by the development and perfection of the wet-spinning method [183]. This method allows the controlled production of highly oriented (within a few degrees) thin films (1 to 100 μm) by winding up DNA fibers which are continuously stretched during precipitation into an aqueous alcohol solution. Films up to 45×275 mm^2 have been obtained in this way.

2.8.3
Infrared Spectroscopy

In order to study the structure of different molecules it is very important to know the length of the chemical bonds and the angles between them. Most of these data are obtained by the X-ray method and by the analysis of spectra of microwave absorption. To study the internal dynamics it is important to know the changes in the lengths and angles. Under physiological conditions oscillations of the atoms and atomic groups are accompanied by changes in the bond lengths of about ± 0.05 Å and changes in the angles about ±5°. Changes in the energies of these oscillations correspond to the energies of electromagnetic radiation in the infrared range.

The low frequency modes of infrared spectra between 40 and 240 cm^{-1} are of the most interest. For example, in the works of Beetz and Ascarelli [184] and Wittlin et al. [185] the hydration-dependent 45 cm^{-1} mode was observed. It was assigned to the complex internal vibration motion, the base pairs vibrating in phase and in countermotion to the two sugar–phosphate backbones along the helical axis.

2.8.4
Hydrogen–Deuterium (–Tritium) Exchange

Hydrogen–deuterium exchange is a very powerful tool for studying DNA internal dynamics and, especially, the dynamics of base-pair opening [10–12]. It is based on the observation that polar hydrogens of DNA bases can exchange with solvent hydrogens under conditions in which the DNA is far from any denaturation transition. High molecular weight DNA, for example, exchanges its hydrogens at 0 °C with a half-time of 5 min in solvent and salt conditions such that its thermal denaturation temperature is above 80 °C. Free bases are able to exchange their N-H with solvent much more rapidly. This behavior has led to the proposal that ordered helices contain small amounts of open states, in which bases are unpaired, and that these open states mediate the exchange of otherwise inaccessible hydrogen-bonded protons.

The scheme describing the conformationally limited exchange can be written in the following form

$$^2\mathrm{H}_{\mathrm{closed}} \underset{k_{\mathrm{cl}}}{\overset{k_{\mathrm{op}}}{\rightleftarrows}} {}^2\mathrm{H}_{\mathrm{open}} \xrightarrow{k_{\mathrm{chem}}} {}^1\mathrm{H}_{\mathrm{exchanged}}\,; \tag{2-14}$$

where k_{op} is the rate constant for conformational opening, k_{cl} is that for the reverse reaction (closing), and k_{chem} denotes the chemical transfer step. Equation (2.14) is written here in the form where a deuteron is exchanged for a proton. Since the exchange of nucleotide hydrogen for deuterium generates a special shift in the ultraviolet, it appears possible to follow hydrogen–deuterium exchange by a spectral difference method by using stopped-flow ultraviolet spectrophotometry. As a result, proton exchange rates can be measured over a broad range of temperatures.

2.8.5
Microwave Absorption

The method of microwave absorption is one more way of studying biopolymer dynamics. It was applied to DNA by Webb and Booth [43] and later by Swicord and Davis [44,45] and Edwards et al. [46]. The existence of longitudinal acoustic resonances in the low-gigahertz region was demonstrated in solutions of monodisperse DNA of finite length. Interpretation of the observations is, however, a rather complex problem, and many authors have tried to solve it by using rather different dynamical models of DNA including nonlinear ones [30, 47, 160, 186,187]. Their results are now under discussion.

2.8.6
NMR

Nuclear magnetic resonance (NMR) is a very advantageous technique for studying the dynamical properties of DNA. In order to understand the mechanism of DNA opening one has to be familiar with the exchange behavior of nucleotides/nucleosides. These processes are on the NMR timescale. Linewidth measurements of the imino protons have been studied by NMR [143,144, 147, 188]. In this way, the exchange rate was obtained. Studies of short fragments with 12, 43 and 69 base pairs have demonstrated the exchange of imino protons of the AT base pairs by a single base pair opening mechanism with an opening rate of 15–20 s^{-1} at 38 °C and activation energy of 15–17 kcal mol^{-1}. The data fit in very well with the poly(rA) • poly(rU) results with the activation energy of 15 kcal mol^{-1} and opening rate 1 s^{-1}.

The chemical shift of the hydrogen-bonded imino protons of nucleic acids is usually used for measuring the secondary and tertiary structure of nucleic acids. Broadening or disappearance of these resonances indicates fraying of the ends and/or melting of the double helix. Fraying is defined as the rapid opening and closing of base pairs at the end of a helix which results in proton exchange with water. Melting is an equilibrium process describing the fraction of opened and closed base pairs. The sequence of melting of different parts of nucleic acids can be followed by NMR.

The static structure of DNA is reflected in the NMR parameters of chemical shift (that is the position of the resonance signal on the frequency scale relative to a reference signal) and coupling constants (describing stereochemical relations between NMR active nuclei via chemical bonds). In special cases, the nuclear Overhauser effect (NOE) yields additional information on the through-space interactions of neighboring nuclei. The dynamical processes, on the other hand, are implied in the relaxation rates of NMR experiments (or the relaxation times, which are the reciprocals of the rates) and in the NOE. Indirectly, the relaxation rate $R_2 = 1/T_2$ describing the spin–spin relaxation is reflected in the linewidth of a conventional NMR spectrum. Generally, the overall relaxation rates $R_1 = 1/T_1$ (spin–lattice relaxation) and $R_2 = 1/T_2$ (spin–spin relaxation) are the sum of several relaxation processes. Problems arise in selecting a correct model for the interpretation of a relaxation experiment.

2.8.7
Charge-transfer Experiments

Electronic excitations and the motion of electronic charges are well known to play a significant role in a wide range of macromolecules of biological interest [189]. The double helical DNA has in its core a stacked array of base pairs. The bases possess an aromatic π-system in contact with those of neighboring residues and these linked π-systems represent a unique system which could serve as a wire to convey electrons through the DNA. In spite of this, for a long time many scientists believed that DNA molecules, like proteins, were insulators and could not facilitate long-range charge transfer. Others took a middle road and believed that DNA might serve as a semiconductor, relaying a charge only in certain situations. Only in 1986 to 1987 did the Barton group at California Institute publish a series of papers in Science [166–168] reporting that, in the DNA assemblies they constructed, damage could be promoted at a site some distance away from the site where a radical is injected into the DNA base pair stack. Barton believed that this damage was promoted through electron transfer mediated by the DNA double helix. Many other experimental works on charge transport along the DNA double helix have been published [169–174]. Various models have been proposed to describe charge transfer and charge transport along the DNA double helix including the models of simple tunneling [174, 190], semiconducting energy gap [191–193], polaron hopping [194] and fluctuation limited transport [195]. None of these models is good enough and the problem of theoretical modeling of the process still remains unsolved.

2.8.8
Single Molecule Experiments

Single molecule are now becoming almost routine thanks to the remarkable progress of experimental tools. Investigators are now able to unfold a protein by pulling, to denaturate DNA by torsion, to measure the elasticity of a single molecule or the torque of a molecular motor, to investigate the microscopic mechanics of protein–DNA interactions or the disruption of the double-helix [66]. Micromanipulation experiments on proteins and on nucleic acids are based on magnetic beads, optical tweezers, micro-needles, biomembrane force probes and atomic force spectroscopy. They allow measurements of forces in the range from the "thermal" (fN) up to the rupture of covalent bonds (nN), and are based on the control of subnanometer displacements.

Recent single DNA molecule experiments have permitted the detailed study of the mechanical separation (unzipping) of the two strands of sequences [196, 175–178]. Experimental results obtained are very impressive, however, their interpretation is not trivial and their analysis requires some confrontation with microscopic modeling [197–199].

Thus, even from this brief excursion into the world of experimental study of DNA dynamics we can draw a conclusion about the importance of the correct choice of model of the internal DNA dynamics for interpretation of the experimental results. In Chapters 4–7 we shall discuss possible DNA models in detail.

3
DNA Function

DNA function is usually considered as a field of molecular biology. For many years the main aim of investigators dealing with this field was only to explain the functional properties of DNA in terms of its primary structure. But in recent years they have paid attention to the physical aspects of DNA function.

In this chapter we describe briefly the main elements of the DNA function, which are necessary to understand the following chapters. We stress the elements where physical properties, and especially the dynamical properties, play a crucial role.

3.1
Physical Aspects of DNA Function

In Section 1.6 we described some of the physical properties of the DNA molecule. We mentioned that the DNA molecule is a quasi-one-dimensional and quasi-periodical system, and that this property makes it very similar to a model of a one-dimensional crystal, which has been well studied in physics. We stressed also that the DNA molecule is very flexible and has many internal degrees of freedom. We noted that the DNA molecule is essentially an inhomogeneous system.

Now, however, when considering physical aspects of DNA function, we need to add some more details to this description. The first addition concerns the character of the DNA inhomogeneity. We should stress here that DNA inhomogeneity differs essentially from that traditionally considered in simple physical models, where point inhomogeneities or the boundary between two homogeneous regions are usually suggested.

DNA inhomogeneity is characterized by the presence of different local regions (named 'sites' or 'blocks'), each having a very specific sequence of bases and a very specific function. So, any DNA molecule or its fragment can be represented as divided into different functional regions. As an example, we present in Figure 3.1 a simple scheme of the DNA fragment containing several functional regions necessary for RNA synthesis and regulation. The fragment contains a promoter region, P, a coding region, C, several regulatory regions, R_1, R_2, R_3 and a terminator region, T, which separates two genes, the *i*th and the (i+1)th. The terminator region is shown as a cruciform region. Each of the regions plays its own specific role at a definite stage of the transcription process.

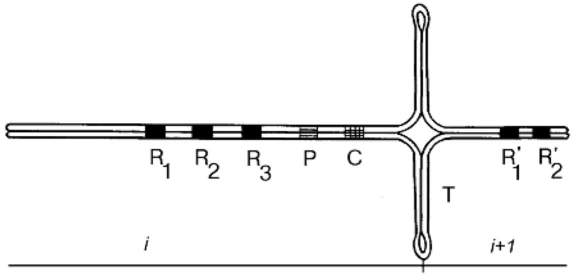

Figure 3.1 A DNA fragment scheme. P, C, T are the promoter, coding region and terminator respectively; R_1, R_2, R_3 are the regulatory regions of the *i*th gene; R_1', R2′, etc., are the corresponding regions of the (*i*+1)th gene.

Another peculiarity is a strong dependence of the functional properties of the sites on the changes in the site structure. That is, any change in the structure of the local region considered (for example, change from the A- to the B-form) leads to change in the interactions of the fragment with proteins or with some other external molecules, and so leads to changes in the functional properties of the region. So, the dynamical properties of the local region, which determine its ability to change the internal structure, are directly connected to the functional properties of the region.

3.2 Intercalation

Interaction of DNA with external molecules occurs in all stages of DNA life. DNA interacts, in particular, with many drugs, cancerogens, mutants and dyes. Because the DNA molecule plays an important role in the replication process and protein biosynthesis, any modification of it caused by interactions with these compounds has a strong influence on the cell metabolism, decreasing or (in some special cases) terminating cell growth. These properties are widely applied in medicine.

There are different ways in which the DNA molecule interacts with the compounds. One of them is intercalation of the compound between neighboring base pairs without any distortion of the pairs.

The first suggestion of the possibility of intercalation was made by Lerman [200] in 1961. He proposed that the process of intercalation involves the sandwiching of a drug molecule between two adjacent DNA base pairs (Figure 3.2). According to his approach the base pairs remain perpendicular to the helix axis, but they are moved apart to accommodate the drug molecule (of approximately 3.4 Å thickness) which lies in Van der Waals contact with the base pairs above and below. The intimate contact between the π-orbitals of the drug molecule and the base pairs will help to stabilize the complex via hydrophobic and charge-transfer forces. Since the DNA sugar–phosphate chain is virtually fully extended in native DNA, the helix has to unwind in order to admit the drug. This leads to a local distortion of the helix and the distortion of the helix at intercalated sites will destroy the long-range regularity of the helix.

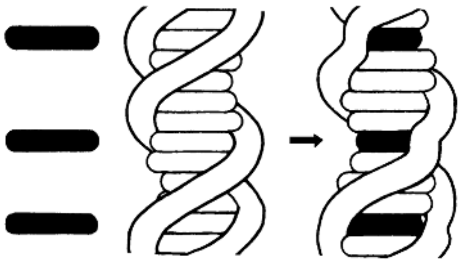

Figure 3.2 (a) DNA and three drug molecules; (b) DNA with three intercalated drug molecules.

The idea of intercalation has been further developed by Fuller and Waring [201] and by Neville and Davies [202]. Now this mechanism of interaction is widely accepted and applied not only in pharmacology when studying new drugs, but also, because dyes can be used, in investigations of DNA structure and function.

Investigations of thermodynamic and kinetic parameters of the intercalation process show that this process is not cooperative and that it consists of two stages: (1) bonding with the periphery of the double helix and (2) intercalation by itself. Investigations show also that the dynamical properties of DNA play a crucial role in understanding the mechanism of intercalation. So, for intercalation to occur we need to move adjacent base pairs apart. It can be suggested that two types of internal motions are required to achieve this moving apart: the local strengthening and simultaneous local unwinding of the double helix. These local distortions of the DNA structure are small but cumulatively they lead to an increase in the length and rigidity of the DNA.

3.3 DNA–Protein Recognition

Another way in which the DNA molecule interacts with compounds, and especially with proteins, is often named as recognition. In this case protein molecules interact very specifically with DNA, namely, they interact only with special DNA regions (sites) having a definite sequences of bases, which are recognized by them with a high degree of accuracy.

If we take into account the DNA structure, and the fact that the bases are placed inside the double helix (Figure 3.3), we naturally come to the following conclusion: to recognize the region with some special sequence of bases, the process of interaction should be accompanied by a preliminary stage where the double helix is locally unwound and the bases are open for recognition.

An example of such a specific interaction required at the stage of recognition is the interaction of the protein RNA-polymerase with the promoter region of DNA. This interaction is very specific, it occurs at the beginning of the process of transcription, and it is accompanied by local unwinding of the DNA double helix.

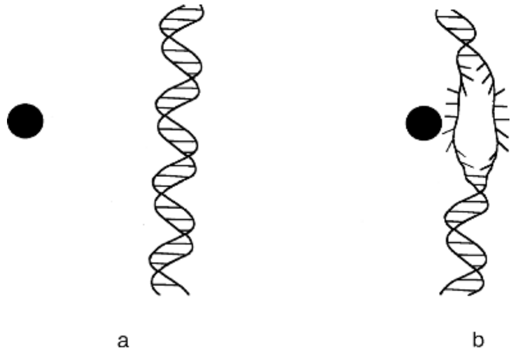

Figure 3.3 (a) DNA double helix and a protein molecule; (b) local unwinding of the double helix, which is assumed to be a preliminary stage required for recognition of the binding site.

3.4 Gene Expression

From the point of view of molecular biology, gene expression appears to be the primary and most fundamental event of life. Gene expression is the process whereby the information stored in DNA is transferred and materialized, most often in the production of proteins. The basic information needed to produce a given protein is deposited in a DNA gene, the size of the gene being from 150 to 6000 bases. A gene can be identified and localized genetically or biochemically.

Gene expression of a given gene occurs in two major steps: transcription and translation.

Transcription is the process whereby the (linear) genetic information is copied into an auxiliary nucleic acid, the messenger ribonucleic acid (mRNA). mRNA is produced by enzyme RNA polymerase which can be easily extracted from bacterial cells and purified in large quantities. In the following, we will refer to RNA polymerase from the bacterium *Escherichi coli (E. coli)*, which has a 'diameter' of about 150 Å. Purified RNA polymerase is able to perform transcription in the test tube with efficiency and fidelity comparable to those it has in vivo.

In general, transcription can be characterized as a complex multistage process which proceeds in a system of many components, including DNA, RNA polymerase, regulatory proteins, hormones, ions, and water. The simplest scheme of transcription includes three main stages: initiation, elongation and termination (Figure 3.4).

At the first stage RNA polymerase binds with the promoter region which can be defined as a point of initiation. When RNA polymerase takes a correct position and forms several phosphodietheric bonds, the second stage of the process begins. At this stage a small fragment (subunit σ) is released from the RNA polymerase and the rest of the molecule (core enzyme) moves along the DNA and elongates the RNA molecule step by step. In the third stage the process finishes and RNA polymerase is released from the DNA molecule. A special region of DNA, the terminator, gives a signal to stop the process.

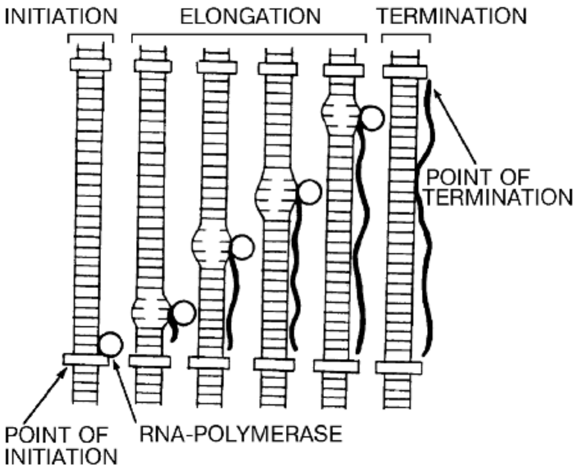

Figure 3.4 A generalized scheme of the main stages of transcription. At each stage the DNA molecule is shown by two long vertical lines imitating the DNA strands. Short horizontal lines between the long vertical lines imitate base pairs.

Translation is the process whereby information stored on mRNA is transferred into a linear sequence of amino acids. The mRNA produced in the first step (transcription) is functionally divided into three parts. Usually, the 15–30 first bases (5′-end) of the mRNA are not translated. They support the assembly of two ribosome units, each being made of about 50 different proteins, and set the assembly rate. The final (3′-end) tens to hundreds of bases are not translated either, and seem to be involved mainly in setting the life-time of the mRNA, usually of the order of 1–3 min. The middle part is the coding sequence, which bears the information needed to built the protein. This information is encoded as an ordered, linear array of the four bases. It is translated into a linear sequence of amino acids via the genetic code.

Transcription and translation processes are illustrated schematically in Figure 3.5. Here several RNA polymerase particles are attached to the central DNA strand, each in the process of synthesizing an mRNA. The picture looks like a Christmas tree, with DNA as the stem, and the mRNA as branches.

Figure 3.5 A sketch of the transcription–translation process.

From the physical point of view the most interesting elements of the processes considered are those associated with the formation of an open state (a 'bubble' in Figure 3.4), with the regulation of the processes at a given gene and with coordination of the work of many genes. We shall discuss these points in detail in Chapter 9.

3.5 Regulation of Gene Expression

Physical aspects of the regulation of gene expression are usually associated with the ability to transmit regulatory signals along the DNA molecule. The transmission of the signals permits one to explain in a very simple way the switching on and/or off of the work of different sites of a gene and coordination of the work of many genes.

The idea of transmission of regulatory signals came from the results of experimental study of the so-called long-range effects in DNA. To describe these effects, let us consider a simple system consisting of two protein molecules and one DNA molecule (Figure 3.6). It is assumed that the first protein molecule can bind (with good efficiency) to a special range (or site) of the DNA molecule. Let it be called site 1. It is also assumed that the other protein molecule can bind with another site, site 2. Numerous experimental data [203–208] show that the first protein bound at site 1 influences the interaction of the second protein molecule at site 2. The distance between the sites can reach hundreds or thousands of base pairs. This is the reason why the effect is named the long-range effect.

Figure 3.6 A schematic representation of the DNA molecule interacting with two protein molecules. The DNA molecule is represented by a black band; the sites interacting with proteins are shaded; protein molecules are represented by small circles.

To explain the effect many alternative models of the action at a long distance have been proposed [209–211]. Some of them are shown in Figure 3.7. According to the first model (Figure 3.7a), the DNA molecule forms a loop and, as a result, sites 1 and 2 become neighbors. In the second model (Figure 3.7b), the first protein binds to site 1 and then moves (or slides) along the DNA molecule to the vicinity of site 2. The third model (Figure 3.7c) suggests that binding of the first protein molecule to site 1 helps binding of another protein to the adjacent site, which in turn helps another protein to bind to the next site and so on. As a result, the protein molecules are sequentially bound and line up along the DNA double chain. In the fourth model (Figure 3.7d) it is assumed that binding of the first protein molecule to site 1 is accompanied by a local conformational distortion which then propagates along the double DNA chain. When reaching site 2 it changes the conformational structure of the site, which, in turn, changes the binding constants of the second protein with the site.

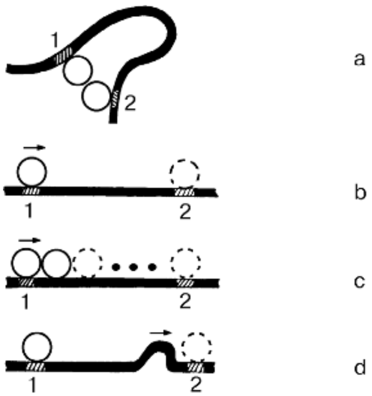

Figure 3.7 Models of the action at a long distance: (a) the model explaining the long-range effect by the formation of a loop, (b) the 'sliding' model, (c) the model of sequential binding, and (d) the model of propagation of conformational perturbation along the DNA molecule.

The fourth model correlates well with the idea of transmission of regulatory signals along the DNA molecule. Indeed, we can suggest that conformational perturbations moving along the DNA molecule can act as regulatory signals in some stages of gene expression. Experimental data obtained in Refs. [207, 212–216] provide further arguments in favor of the fourth model. The model looks very attractive because it enables one to relate the dynamical properties of the DNA molecule to its functional activity.

3.6 Replication

The ability to replicate is one of the most important functional properties of DNA. It usually starts at a special site of the DNA molecule, continues in both directions simultaneously with approximately the same velocity and makes copies with a very high accuracy (one mistake per 10^9–10^{10} base pairs).

A simple model of replication was proposed by Watson and Crick. They suggested that two complementary DNA chains serve as matrices to copy one another. In Figure 3.8 two DNA chains are shown as a pair of matrices for synthesis of new polynucleotide chains. So, a replication fork has a Y-like structure.

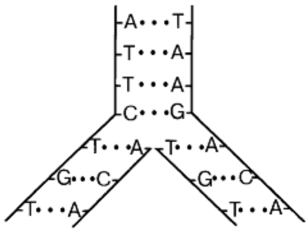

Figure 3.8 Replication fork.

In general, replication can be characterized as a many-component and many-stage process including complex biochemical reactions (the details can be found, for example, in the book of Straer [217]). From a physical point of view, the most interesting stage of the process is that preceding the synthesis of new polynucleotide chains. This stage is characterized by a very interesting dynamical behavior. So, it is suggested that in this stage hydrogen bonds between base pairs are broken, the chains unwind and separate. The energy required for unwinding and separation appears as a result of ATP hydrolysis.

4
Linear Theory of DNA

Before consideration of the nonlinear theory of DNA it would be useful to discuss briefly the linear theory of DNA, which can be considered as a first approximation of the general theoretical description of DNA, the nonlinear theory can be considered as the next (second) approximation. We begin this chapter with a description of the mathematical basis of the linear theory, which is formed mainly by mathematical models of the internal DNA dynamics. Then we illustrate how these models can be applied to the problem of statistics of linear excitations in DNA and to the scattering problem. At the end of the chapter we shall discuss briefly the relations between the linear theory and experiment.

4.1
The Main Mathematical Models

Before we start three small comments should be made. The first concerns the selection of the models. Mathematical models of internal DNA dynamics considered in this chapter have been selected in a special way. Namely, from a variety of the dynamical models we chose those which are the linear (first) approximations of the known nonlinear dynamical models. This makes it possible to compare the results obtained in the linear (first) and nonlinear (second) approximations.

Secondly a very important point is that the models considered in this chapter are arranged in order of increasing complexity. So, we begin here with the simplest model called the rod-like model of DNA. Then we proceed to the models of the second and higher levels of the hierarchy.

Thirdly, to simplify the calculations, we also restrict ourselves to ideal and homogeneous models, that is we neglect:

1. The interactions of DNA with the environment.
2. The processes of dissipation.
3. The differences between physical characteristics of nitrous bases such as mass, moment of inertia, interaction forces between them and other structural elements of DNA. Some elements of non-ideality, however, will be considered in Chapter 6.

4.1.1
Linear Rod-like Model

The uniform elastic rod with circular section is the simplest physical model of DNA. This model takes into account three types of internal motions: stretching, twisting and bending. So, we can write the Hamiltonian of the system in the following way:

$$H = H_{\mathrm{s}} + H_{\mathrm{t}} + \mathrm{H}_{\mathrm{b}} + \mathrm{H}_{\mathrm{s\text{-}t}} + H_{\mathrm{s\text{-}b}} + H_{\mathrm{t\text{-}b}}; \tag{4-1}$$

where the terms H_{s} , H_{t} and H_{b} describe longitudinal displacements (stretching), torsional motions (twisting) and bending, respectively; the terms $H_{\mathrm{s\text{-}t}}$, $H_{\mathrm{s\text{-}b}}$ and $H_{\mathrm{t\text{-}b}}$ describe interactions between these three types of motions.

To estimate the contribution of each of the terms, we can use the data gathered by McCommon and Harvey [13], which indicate that the amplitudes and characteristic times of bending motions differ from those of torsional and longitudinal motions by one or two orders, the ranges of their values being non-overlapping. So, we can neglect the terms $H_{\mathrm{s\text{-}b}}$ and $H_{\mathrm{t\text{-}b}}$ and divide the rest of the Hamiltonian H into two independent parts:

$$H = H^{(1)} + H^{(2)}; \tag{4-2}$$

where $H^{(1)} = H_{\mathrm{s}} + \mathrm{H}_{\mathrm{t}} + \mathrm{H}_{\mathrm{s\text{-}t}}$, and $H^{(2)} = H_{\mathrm{b}}$.

To derive the explicit form of the Hamiltonian $H^{(1)}$ it is convenient to consider first the discrete analog of the rod-like model [135, 218] and then pass to the continuous one.

4.1.1.1 Longitudinal and Torsional Dynamics: Discrete Case

Let the discrete analog consist of a chain of coupled disks (Figure 4.1), each disk having two degrees of freedom: longitudinal and angular (or torsional) displacements. This model is equivalent to the so-called bead–spring model widely used in polymer science. To apply it to DNA it is assumed that the DNA molecule can be modeled by an array of (N+1) beads strung out along an axis (3.4 Å apart for a Watson–Crick helix), indexed from 0 to N. It is assumed also that the (N+1) beads are linked by N identical torsional springs, each having an equilibrium rotation such that at equilibrium a helix results.

In the linear approximation, which is valid when the amplitudes of the internal motions are small, the terms H_{s} and H_{t} have the following standard form:

$$H_{\mathrm{s}} = \sum_n \left\{ M\dot{u}_n^2/2 + K(u_{n+1} - u_n)^2/2 \right\}$$

$$H_{\mathrm{t}} = \sum_n \left\{ I\dot{\varphi}_n^2/2 + k(\varphi_{n+1} - \varphi_n)^2/2 \right\}, \tag{4-3}$$

where u_n and φ_n are longitudinal and angular displacements of the nth disk; M and I are the mass and the moment of inertia of the disk; K and k are the coefficients of longitudinal and torsional rigidities.

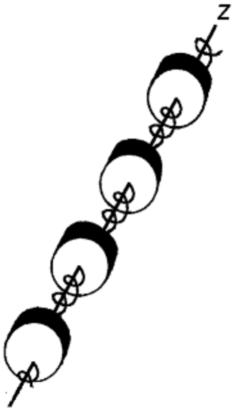

Figure 4.1 A chain of coupled disks.

It now remains only to derive the formula for $H_{\text{s-t}}$ which describes the interaction between longitudinal and torsional motions of the disks. To obtain $H_{\text{s-t}}$, we could use the following standard method, widely used in theoretical physics. Let us suggest that the coefficients K and k are not constant and depend now on the torsional and longitudinal displacements of the disks:

$$k \rightarrow k\{(u_{n+1} - u_n);\ (\varphi_{n+1} - \varphi_n)\};$$
$$K \rightarrow K\{(u_{n+1} - u_n);\ (\varphi_{n+1} - \varphi_n)\}. \tag{4-4}$$

Then we can expand functions (4-4) in a power series of $(u_{n+1} - u_n)$ and $(\varphi_{n+1} - \varphi_n)$:

$$k = k_0 + k_1(u_{n+1} - u_n) + k_2(\varphi_{n+1} - \varphi_n) + \ldots;$$
$$K = K_0 + K_1(u_{n+1} - u_n) + K_2(\varphi_{n+1} - \varphi_n) + \ldots. \tag{4-5}$$

and insert the expansions into the initial Hamiltonian H.

Restricting ourselves to terms of the second order (in this case, the corresponding equations are linear) we find that $H_{\text{s-t}}$ makes only a constant contribution to the total Hamiltonian H, and we can neglect it. Thus, in the framework of the approach we could suggest that longitudinal and torsional internal motions are independent. But it should be noted that sometimes another way of constructing the term $H_{s\text{-}t}$ is used. Namely, it is simply suggested that $H_{\text{s-t}}$ is a sum $(\sum_n)$ of terms each of them being proportional to the product $(u_{n+1} - u_n)\ (\varphi_{n+1} - \varphi_n)$. So, in the framework of this approach longitudinal and torsional motions are not independent. For simplicity in our further calculations we shall use the first of the approaches. In this case, the dynamical equations corresponding to Hamiltonian H take a very simple form:

$$M\ddot{u}_n = K_0\,(u_{n+1} - 2u_n + u_{n-1}), \tag{4-6}$$

$$I\ddot{\varphi} = k_0\,(\varphi_{n+1} - 2\varphi_n + \varphi_{n-1}). \tag{4-7}$$

In addition, we shall assume that periodical boundary conditions are fulfilled:

$$u_n = u_{n+N};\ \varphi_n = \varphi_{n+N}\,. \tag{4-8}$$

Equations (4-6) and (4-7) have simple solutions having the form of plane waves

$$\begin{aligned} u_n &= u_{n0}\exp\{i(qna\text{-}wt)\};\\ \varphi_n &= \varphi_{n0}\exp\{i(qna\text{-}wt)\}. \end{aligned} \tag{4-9}$$

And inserting Eqs. (4-9) into Eqs. (4-6) and (4-7) we find the frequencies of the linear waves in DNA

$$\begin{aligned} w_1 &= \{2K_0\,[1\text{-}\cos(qa)]/M\}\ ;\\ w_t &= \{2k_0\,[1\text{-}\cos(qa)]/I\}\ . \end{aligned} \tag{4-10}$$

4.1.1.2 Longitudinal and Torsional Dynamics: Continuous Case

Now let us pass from the discrete case to the continuous one, that is from the model of a chain of disks to that of an elastic rod. From the mathematical point of view this procedure is valid only if we assume that the solution we are determining consists of rather smooth functions and that they change slowly at a distance a between two neighboring disks. In this case, we can pass to the limit $a \to 0$ inEqs. (4-6) and (4-7).

To pass to the continuous case, it is convenient to rewrite Eqs. (4-6) and (4-7) in the form

$$\begin{aligned} (M/a)\ddot{u}_n &= K_0\,a(u_{n+1} - u_n)/a^2 - K_0\,a(u_n - u_{n-1})/a^2,\\ (I/a)\ddot{\varphi}_n &= k_0\,a(\varphi_{n+1} - \varphi_n)/a^2 - k_0\,a(\varphi_n - \varphi_{n-1})/a^2. \end{aligned} \tag{4-11}$$

If we assume now that $a \to 0$ the coefficients of the Eq. (4-11) will transform to

$$\begin{aligned} M/a &\to \rho; \qquad & K_0\,a &\to Y;\\ I/a &\to i; \qquad & k_0\,a &\to C; \end{aligned} \tag{4-12}$$

where i is a moment of inertia per unit of length, ρ is a linear density; Y is the Young's modulus, and C is the torsional rigidity of the rod.

In the continuous limit ($a \to 0$) the displacements u_n and φ_n are transformed in the following way:

$$\begin{aligned} &u_n(t) \to u(na,t) \to u(z,t), \\ &\varphi_n(t) \to \varphi(na,t) \to \varphi(z,t) \end{aligned} \tag{4-13}$$

and the differences

$$\begin{aligned} &(\varphi_{n+1} - \varphi_n)/a^2 - (\varphi_n - \varphi_{n-1})/a^2, \\ &(u_{n+1} - u_n)/a^2 - (u_n - u_{n-1})/a^2, \end{aligned} \tag{4-14}$$

transform to

$$u_{zz}, \quad \varphi_{zz} \tag{4-15}$$

respectively. As a result, instead of the discrete equations (4-11) we obtain two simple differential equations for longitudinal and torsional internal motions of the elastic rod

$$\begin{aligned} &\rho u_{tt} = Yu_{zz}, \\ &i\varphi_{tt} = C\varphi_{zz}. \end{aligned} \tag{4-16}$$

Assume that the solutions of equations (4-16) have the form of normal (linear) plane waves

$$\begin{aligned} &u = u_0 \exp\{i(qz - w_1 t)\}, \\ &\varphi = \varphi_0 \exp\{i(qz - w_t t)\}, \end{aligned} \tag{4-17}$$

where φ_0, u_0 and w_1, w_t are the amplitudes and frequencies of longitudinal and torsional waves, respectively. Inserting then Eq. (4-17) into Eq. (4-16) we obtain the frequencies of longitudinal and torsional oscillations in DNA

$$\begin{aligned} &w_1 = (Y/\rho)^{1/2}\, q, \\ &w_t = (C/i)^{1/2}\, q, \end{aligned} \tag{4-18}$$

where q is the wave vector, the values of which are in the interval

$$-\pi/a \le q \le \pi/a; \tag{4-19}$$

which coincides with the first zone of Brillouin for the case of a one-dimensional crystal. Because the number of disks is equal to N, we obtain N different solutions corresponding to N different values of q in the Brillouin zone.

These results indicate that there are two acoustic branches in the DNA spectrum. The first describes longitudinal acoustic oscillations and the second, torsional acoustic oscillations. The branches are shown schematically in Figure 4.2.

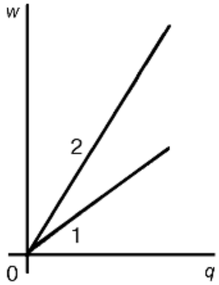

Figure 4.2 Schematic picture of two acoustic branches in the DNA spectrum. Branch 1 corresponds to the torsional oscillations with frequency w_t, and branch 2 corresponds to the longitudinal oscillations with frequency w_l.

After differentiation of Eq. (4-18) we find the velocities of the longitudinal and torsional acoustic waves

$$\begin{aligned} v_1 &= \partial w_1(q)/\partial q = (Y/\rho)^{1/2}, \\ v_t &= \partial w_t(q)/\partial q = (C/i)^{1/2}. \end{aligned} \tag{4-20}$$

Thus, in the linear approximation the velocities of the torsional and longitudinal waves are constant and do not depend on the wave vector q. Experimental data on the velocities of acoustic waves in DNA are gathered in Table 4.1. The data were used to find the mutual arrangement of the branches of the DNA spectrum in Figure 4.2.

Table 4.1 Velocities of the torsional (v_t) and longitudinal (v_l) waves in DNA.

v_t (cm s^{-1})	v_l (cm s^{-1})
1.3[a]	3.19 ÷ 3.60[b]
	2.11 ÷ 2.2[c]
	1.7 ÷ 4[d]

[a] Ref. [47]. [b] Ref. [219]. [c] Ref. [220]. [d] Ref. [221].

4.1.1.3 Bending Motions

To derive the equations for bending motions of an elastic rod, let us assume that the disks shown in Figure 4.1 can make transverse motions y_n in the planes which are perpendicular to the chain axis. In the continuous approximation ($a \to 0$) we have

$$y_n(t) \to y(na,t) \to y(z,t). \tag{4-21}$$

Here $y(z,t)$ is the transverse displacement of the elastic rod from an equilibrium position. The force which acts on the unit length of the elastic rod due to the displacement is equal to

$$F(z) = -\,By_{zzzz}; \tag{4-22}$$

where $B = IY$ is the bending rigidity of the rod. Here I is the moment of inertia of the cross section of the rod relative to the rod axis; Y is Young's modulus.

The dynamical equation describing the bending internal motions can then be written in the form

$$S\rho\ddot{y} = -Yiy_{zzzz}; \tag{4-23}$$

where S is the area of the rod section; ρ is the linear density (i.e. mass per rod length).

Assuming the solution of Eq. (4-23) in the form of a plane wave

$$y = y_0 \exp\{i(qz - w_b t)\}; \tag{4-24}$$

and inserting Eq. (4-24) into Eq. (4-23) we find the frequency of the bending oscillations in DNA

$$w_b = (B/\rho S)^{1/2}\, q^2\,. \tag{4-25}$$

The corresponding branch in the DNA spectrum is shown schematically in Figure 4.3, and for the velocity of propagation of bending waves we find

$$v_b = 2(B/\rho S)^{1/2}\, q. \tag{4-26}$$

In contrast to the results obtained in the previous section for longitudinal and transverse waves, the velocity of the bending waves depends on the wave vector q.

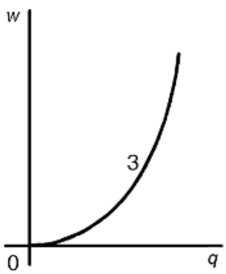

Figure 4.3 Schematic picture of the acoustic branch (3) corresponding to bending oscillations with frequency w_b.

4.1.2
Linear Double Rod-like Model

Let us consider now a more complex mathematical model of DNA which belongs to the second level of the hierarchy described in Sections 1.6.2 and 2.7.2. In the general case, the model consists of two elastic chains wound around each other to produce the double helix. However, in this chapter we restrict ourselves to consideration of a simpler version of the model where the helicity of the DNA structure is neglected. The effects of the helicity will be discussed in Chapter 6. As in the previous section, we consider first the discrete version of the model and then pass to the continuous one.

4.1.2.1 Discrete Case

A discrete analog of the model is shown in Figure 1.10b. It consists of two straight chains of disks connected by longitudinal and transverse springs. It is convenient to denote by i the number of the chain ($i = 1, 2$) and by n the number of the disk in the chain. Every disk in the chain (for example, the nth disk in the ith chain) has three degrees of freedom. It can move along the chain (longitudinal motion), it can move perpendicular to the chain (transverse motion), and it can rotate around the chain (torsional motion). So, in the general case we can write the Hamiltonian H of the system in the following way:

$$H = \sum_{i=1}^{2} \{H_{\mathrm{l}}^{(i)} + H_{\mathrm{t}}^{(i)} + H_{\mathrm{tr}}^{(i)} + H_{\mathrm{l-t}}^{(i)} + H_{\mathrm{l-tr}}^{(i)} + H_{\mathrm{t-tr}}^{(i)}\} \tag{4-27}$$

where the terms $H_{\mathrm{l}}^{(i)}$, $H_{\mathrm{t}}^{(i)}$ and $H_{\mathrm{tr}}^{(i)}$ describe the contribution of longitudinal, torsional and transverse motions of the disks in the ith chain ($i = 1, 2$); the terms $H_{\mathrm{l-t}}^{(i)}$, $H_{\mathrm{l-tr}}^{(i)}$ and $H_{\mathrm{t-tr}}^{(i)}$ describe interactions between the motions of the disks in the same (ith) chain; the term $H^{(1-2)}$ describes interaction between the chains through transverse springs

$$H^{(1-2)} = H_{\mathrm{l-l}}^{(1-2)} + H_{\mathrm{t-t}}^{(1-2)} + H_{\mathrm{tr-tr}}^{(1-2)} + H_{\mathrm{l-t}}^{(1-2)} + H_{\mathrm{l-tr}}^{(1-2)} + H_{\mathrm{t-tr}}^{(1-2)}. \tag{4-28}$$

If we suggest that in the first approximation the internal motions of different types are independent, the terms $H_{\mathrm{l-t}}^{(1-2)}$, $H_{\mathrm{l-tr}}^{(1-2)}$ and $H_{\mathrm{t-tr}}^{(1-2)}$ in the Hamiltonian H can be neglected.

As regards the terms $H_{\mathrm{l}}^{(i)}$, $H_{\mathrm{t}}^{(i)}$ and $H_{\mathrm{tr}}^{(i)}$, they have a rather standard form

$$\begin{aligned}
H_{\mathrm{l}}^{(i)} &= \sum_{n,i} \left\{ M\ddot{u}_{n,i}^{(i)^2}/2 + K(u_{n+1,i}^{(i)} - u_{n,i}^{(i)})^2/2 \right\}; \\
H_{\mathrm{t}}^{(i)} &= \sum_{n,i} \left\{ I\ddot{\varphi}_{n,i}^{(i)^2}/2 + k(\varphi_{n+1,i}^{(i)} - \varphi_{n,i}^{(i)})^2/2 \right\}; \\
H_{\mathrm{tr}}^{(i)} &= \sum_{n,i} \left\{ M\ddot{y}_{n,i}^{(i)^2}/2 + b(y_{n+1,i}^{(i)} - y_{n,i}^{(i)})^2/2 \right\}.
\end{aligned} \tag{4-29}$$

And the term $H^{(1\text{-}2)}$ reduces to the form

$$H^{(1-2)} = H_{\mathrm{l-l}}^{(1-2)} + H_{\mathrm{t-t}}^{(1-2)} + H_{\mathrm{tr-tr}}^{(1-2)} \tag{4-30}$$

where

$$\begin{aligned} H_{\mathrm{l-l}}^{(1-2)} &= \sum_n \alpha(u_{n,1} - u_{n,2})^2/2; \\ H_{\mathrm{t-t}}^{(1-2)} &= \sum_n \beta(\varphi_{n,1} - \varphi_{n,2})^2/2; \\ H_{\mathrm{tr-tr}}^{(1-2)} &= \sum_n \gamma(y_{n,1} - y_{n,2})^2/2. \end{aligned} \tag{4-31}$$

Here M and I are the masses and the moments of inertia of the disks; K, k and b are the coefficients of the longitudinal, torsional and transverse rigidities; α, β and γ are the coefficients of harmonic potentials describing interactions between the disks which belong to different chains, but have the same index n.

Thus, in the linear approximation, the initial complex Hamiltonian H is divided into three independent parts

$$H = H^{\mathrm{I}} + \mathrm{H}^{\mathrm{II}} + H^{\mathrm{III}}; \tag{4-32}$$

where

$$\begin{aligned} H^{\mathrm{I}} &= \sum_{n,i} H_{\mathrm{l}}^{(i)} + H_{\mathrm{l-l}}^{(1-2)}; \\ H^{\mathrm{II}} &= \sum_{n,i} H_{\mathrm{t}}^{(i)} + H_{\mathrm{t-t}}^{(1-2)}; \\ H^{\mathrm{III}} &= \sum_{n,i} H_{\mathrm{tr}}^{(i)} + H_{\mathrm{tr-tr}}^{(1-2)}. \end{aligned} \tag{4-33}$$

So, in the approximation considered we can study, independently, three different problems. The first concerns longitudinal internal motions in DNA, the second the torsional motions and the third the transverse motions.

Let us write the dynamical equations corresponding to these three problems. The equations imitating longitudinal motions will then have the form

$$\begin{aligned} M\ddot{u}_{n,1} &= K(u_{n+1,1} - 2u_{n,1} + \mathrm{u}_{n-1,1}) + \alpha\,(u_{n,2} - u_{n,1}); \\ M\ddot{u}_{n,2} &= \mathrm{K}(u_{n+1,2} - 2u_{n,2} + u_{n-1,2}) + \alpha\,(u_{n,1} - \mathrm{u}_{n,2}). \end{aligned} \tag{4-34}$$

The equations describing torsional motions are

$$I\ddot{\varphi}_{n,1} = k(\varphi_{n+1,1} - 2\varphi_{n,1} + \varphi_{n-1,1}) + \beta(\varphi_{n,2} - \varphi_{n,1});$$
$$I\ddot{\varphi}_{n,2} = k(\varphi_{n+1,2} - 2\varphi_{n,2} + \varphi_{n-1,2}) + \beta(\varphi_{n,1} - \varphi_{n,2}). \tag{4-35}$$

And those describing transverse motions are

$$M\ddot{y}_{n,1} = b(y_{n+1,1} - 2y_{n,1} + y_{n-1,1}) + \gamma(y_{n,2} - y_{n,1});$$
$$M\ddot{y}_{n,2} = b(y_{n+1,2} - 2y_{n,2} + y_{n-1,2}) + \gamma(y_{n,1} - y_{n,2}). \tag{4-36}$$

Assuming the solutions of the equations have the form

$$u_1 = u_{01} \exp\{i(qa\text{-}wt)\}; \qquad u_2 = u_{02} \exp\{i(qa\text{-}wt)\};$$
$$\varphi_1 = \varphi_{01} \exp\{i(qa\text{-}wt)\}; \qquad \varphi_2 = \varphi_{02} \exp\{i(qa\text{-}wt)\}; \tag{4-37}$$
$$y_1 = y_{01} \exp\{i(qa\text{-}wt)\}; \qquad y_2 = y_{02} \exp\{i(qa\text{-}wt)\};$$

and inserting Eq. (4-37) into Eqs. (4-34) and (4-36), we find the dispersion laws for all of the problems. Then for the frequencies of longitudinal oscillations in DNA we have

$$w_1^{l} = \{[4K\sin^2(qa/2)]/M\}^{½}; \qquad w_2^{l} = \{[4K\sin^2(qa/2) + 2\alpha]/M\}^{½}. \tag{4-38}$$

For the frequencies of torsional oscillations we have

$$w_1^{t} = \{[4k\sin^2(qa/2)]/I\}^{½}; \qquad w_2^{t} = \{[4k\sin^2(qa/2) + 2\beta]/I\}^{½}. \tag{4-39}$$

For the frequencies of transverse oscillations we have

$$w_1^{tr} = \{[4b\sin^2(qa/2)]/M\}^{½}; \qquad w_2^{tr} = \{[4b\sin^2(qa/2) + 2\gamma]/M\}^{½}. \tag{4-40}$$

4.1.2.2 Continuous Case

In the continuum approximation Eqs. (4-34) to(4-36) transform to

$$\rho\ddot{u}_1 = Yu_{1_{zz}} + \alpha(u_2 - u_1); \qquad \rho\ddot{u}_2 = Yu_{2_{zz}} + \alpha(u_1 - u_2); \tag{4-41}$$

$$i\ddot{\varphi}_1 = C\varphi_{1_{zz}} + \beta(\varphi_2 - \varphi); \qquad i\ddot{\varphi}_2 = C\varphi_{2_{zz}} + \beta(\varphi_1 - \varphi_2); \tag{4-42}$$

$$\rho\ddot{y}_1 = by_{1_{zz}} + \gamma(y_2 - y_1); \qquad \rho\ddot{y}_2 = by_{2_{zz}} + \gamma(y_1 - y_2); \tag{4-43}$$

where $\rho = M/a$, $i = I/a$.

Assuming the solutions of the equations have the form of plane waves

$$u_1 = u_{01} \exp\{i(qz\text{-}wt)\}; \qquad u_2 = u_{02} \exp\{i(qz\text{-}wt)\}; \tag{4-44}$$

$$\varphi_1 = \varphi_{01} \exp\{i(qz\text{-}wt)\}; \qquad \varphi_2 = \varphi_{02} \exp\{i(qz\text{-}wt)\}; \tag{4-45}$$

$$\gamma_1 = \gamma_{01} \exp\{i(qz\text{-}wt)\}; \qquad \gamma_2 = \gamma_{02} \exp\{i(qz\text{-}wt)\}; \tag{4-46}$$

and inserting Eqs. (4-44) to (4-46) into Eqs. (4-41) to (4-43), we find the frequencies of longitudinal

$$w_1^{\,l} = (Ka^2q^2/M)^{½}; \qquad w_2^{\,l} = \{(Ka^2q^2 + 2\alpha)/M\}^{½}; \tag{4-47}$$

torsional

$$w_1^{\,t} = (ka^2q^2/I)^{½}; \qquad w_2^{\,t} = \{(ka^2q^2 + 2\beta)/I\}^{½}; \tag{4-48}$$

and transverse oscillations

$$w_1^{\,tr} = (ba^2q^2/M)^{½}; \qquad w_2^{\,tr} = \{(ba^2q^2 + 2\gamma)/M\}^{½}. \tag{4-49}$$

So, the whole spectrum of DNA in this case consists of six branches: three acoustic and three optical ones.

There is a simple relation between formulas (4-47) to (4-49) and (4-38) to(4-41). Indeed, if we expand the function $\sin(qa/2)$ in formulas (4-38) to (4-41)

$$\sin(qa/2) = qa/2 - (qa/2)^3\,/3! + \ldots \tag{4-50}$$

and restrict ourselves to the first term, we easily obtain formulas (4-47) to (4-49).

4.1.3
Linear Models of Higher Levels

Many properties of the models described in the previous two sections are inherent in the models of higher levels, but mathematical description of them becomes rather cumbersome. Therefore we do not give here a detailed description of the models and restrict ourselves to consideration of only the main features of the dynamics of higher-level models, which differ from those of the first- and the second-level models.

4.1.3.1 The Third-Level Models

As we mentioned above, the most accurate approach (five-level model) requires a complete mathematical description of all motions of all atoms of DNA. But in practice investigators often use a reduced version of the description, which takes into account the motions of subunits consisting of mutually rigidly bound atomic groups with relatively weak, flexible joints connecting them. This approach corresponds to the third level of the hierarchy. In this approach the dynamical models take into account only solid-like motions of the main structural elements such as bases, sugar rings, nucleotides, nucleosides, phosphate–carbon pieces and so on.

The form of the dynamical equations describing the motions is very similar to that considered in the previous section, but the number of dynamical equations differs substantially. In general it depends on the method of selection of the dominant motions, which in turn depends on the problem considered.

One possible method of selection has been proposed by Saxena et al. [120]. The corresponding model is shown schematically in Figure 1.11. If we take into account all possible solid-like motions of the elements shown in the figure the number of corresponding dynamical equations will be rather large. Indeed every solid-like element has six degrees of freedom (three rotational and three translational). Because the number of elements is equal to $6N$, we find that the total number of dynamical equations can reach $36N$ for the discrete case and 36 for the continuous one.

Another method of selection appears in the work of Volkov and Kosevich [222], where, to describe the low-frequency DNA dynamics, the following subunits and motions were chosen: two types of transverse displacements of nucleotides ($y_{n,i}$; $x_{n,i}$), the torsional displacements of nucleosides ($\varphi_{n,i}$), and the intranucleoside displacements due to the changes in the conformation of the sugar ring ($\rho_{n,i}$) ($i = 1, 2$). So, they proposed the model consisting of $8N$ dynamical equations for the discrete case and eight dynamical equations for the continuous approximation.

One more example we find in the work of Krumhansl and Alexander [20] where, to describe the A–B conformational transition, the following subunits and motions were chosen: the longitudinal displacements of the nucleoside groups ($u_{n,i}$), the changes in the pseudorotational phase angle describing the changes in the conformational states of the sugar groups ($P_{n,i}$), and the angular displacements of the bases ($\varphi_{n,i}$) ($i = 1, 2$). So, in this case, the number of dynamical equations has been decreased from $8N$ to $6N$ for the discrete case and from 8 to 6 for the continuous case.

Two more examples we find in the works of Zang and Olson [52] and Peyrard and Bishop [34]. In the first work to describe the B–Z conformational transition only $4N$ and 4 (for the discrete and continuous approximations, respectively) were used, and in the second work to describe the process of DNA denaturation only $2N$ and 2 (for the discrete and continuous approximations, respectively) were found to be sufficient.

In the linear approximation the solutions of all equations discussed above are linear waves of type (4-44) to (4-46). The frequencies of the waves can be found by inserting the plane wave solutions into the corresponding dynamical equations. The DNA spectrum consisting of acoustic and optical branches can be calculated in the same way as in the previous subsections.

4.1.3.2 The Fourth-level (Lattice) Models

To describe the dynamics of the fourth-level models it is convenient to use the following approach. Let us consider the motions of atoms in DNA as a superposition of normal mode oscillations. In the linear approximation, which is valid only for small amplitudes of the displacements, the normal modes are all independent. This type of analysis within the harmonic approximation has been applied to DNA by Prohofsky and coauthors [223–229]. It has led to a successful theoretical explanation of the experimental data such as speed of longitudinal sound [230] and inelastic scattering neutron data [153–155].

In a normal mode analysis, the assumption is made that the potential energy surface explored by the DNA atoms is quadratic (harmonic approximation). Each individual atomic trajectory is then a superposition of contributions from $3N$-6 vibrational modes, where N is the number of atoms. If we restrict ourselves to the consideration of homopolymer chains, the dynamics of long lengths of DNA can be reduced to the motions of atoms within a single base pair [231]. For DNA, each base pair contains 41 atoms and every atom has 3 degrees of freedom. Therefore, the corresponding dynamical force constant matrix D is of rank 123. So, the diagonalization of D yields 123 eigenvalues, each being the square of the frequency of oscillation of a mode, and the eigenvectors describing the amplitudes of the individual atomic displacements during the oscillations. The resulting phonon dispersion spectrum has, in this case, 123 branches.

4.2 Statistics of Linear Excitations

In the previous sections we considered some problems of the dynamical theory of DNA. We described in detail the main dynamical models, corresponding Hamiltonians, dynamical equations and their solutions having the form of normal plane waves. It should be noted, however, that the general solutions of the equations have the form of a set of plane waves, so in the general case we need to consider an assembly of plane waves (or phonons). In this section we describe assemblies of phonons for different DNA models and discuss the problem of statistics.

4.2.1 Phonons in the Rod-like Model

In the previous section we showed that different types of internal DNA motions could be considered as independent in the first approximation and the general dynamical problem can be described as consisting of three independent problems: the dynamics of longitudinal motions, the dynamics of torsional motions and the dynamics of bending motions. The problems of statistics of the longitudinal, torsional and bending phonons could also be considered approximately as independent. For simplicity, we describe here in detail the main features of the statistics of assembly of torsional phonons. The statistics of the other two assemblies could be considered similarly.

So, let us return to the Hamiltonian H_t , to model Eq. (4-7) imitating DNA torsional dynamics, and to linear wave solutions Eq. (4-9) with frequencies determined by Eq. (4-10).

4.2.1.1 General Solution of the Model Equations

To find the general solution of Eq. (4-7) it is convenient to make a transformation from the variables $\varphi_n(t)$ to the variables $Q_q(t)$ which are usually named the normal coordinates. For the purpose, let us assume that the angular displacements $\varphi_n(t)$ have the time dependence

$$\varphi_n(t) = \overline{\varphi}_n \exp(-\mathrm{i}wt). \tag{4-51}$$

Then Eq. (4-14) becomes

$$Iw^2\, \overline{\varphi}_n = -k\{\overline{\varphi}_{n+1} - 2\overline{\varphi}_n + \overline{\varphi}_{n-1}\}. \tag{4-52}$$

The set of N linear equations (4-59) has a non-trivial solution if the determinant of the coefficients vanishes:

$$\det|Iw^2\, \delta_{n,n'} - A_{n,n'}| = 0. \tag{4-53}$$

Here the non-zero coefficients have the form

$$\begin{aligned} A_{n,n} &= 2k, \\ A_{n,n+1} &= A_{n,n-1} = -k, \end{aligned} \tag{4-54}$$

and the roots of Eq. (4-53) are the so-called normal mode frequencies.

Because of the translation symmetry, it is useful to make the substitution

$$\overline{\varphi}_n = \{\overline{\overline{\varphi}}/I^{½}\} \exp(\mathrm{i}qna); \tag{4-55}$$

where q is the wave vector, and its values lie within the first Brillouin zone.

The eigenvalue equation for the normal-mode frequencies can then be written

$$Iw^2\overline{\overline{\varphi}} = \sum_{n©} A_{n,n'} \exp[\mathrm{i}q(n' - n)a]. \tag{4-56}$$

Taking into account Eq. (4-54) we can rewrite Eq. (4-56) in the form

$$w^2\overline{\overline{\varphi}} = \{2k(1 - \cos qa)/I\}\overline{\overline{\varphi}}. \tag{4-57}$$

For each value of q we find one solution for w

$$w^2(q) = 2k(1 - \cos qa)/I; \tag{4-58}$$

and for each $w^2(q)$ there is a corresponding eigenvector $\overline{\overline{\varphi}}$. We shall henceforth write these as $\overline{\overline{\varphi}}(q)$. Thus the eigenvalue equation (4-56) now reads

$$w^2(q)\, \overline{\overline{\varphi}}\,(q) = A(q)\, \overline{\overline{\varphi}}\,(q); \tag{4-59}$$

where $A(q) = 2k(1 - \cos qa)/I$.

As a result we can write the solution of Eq. (4-52) for the angular displacement $\varphi_n(t)$ in the form of expansion

$$\varphi_n(t) = [1/(NI)^{1/2}] \sum_q \overline{\overline{\varphi}}(q) Q_q(t) \exp(iqna); \tag{4-60}$$

where $Q_q(t)$ are normal coordinates mentioned above.

4.2.1.2 Secondary Quantum Representation

Let us consider how the initial Hamiltonian H_t

$$H_t = T + V; \tag{4-61}$$

will change. Here T and V are the kinetic and potential energies having the form

$$T = \sum_n \{I\dot{\varphi}_n^2/2\}; \qquad V = \sum_n \{k(\varphi_{n+1} - \varphi_n)^2/2\}. \tag{4-62}$$

Inserting Eq. (4-60) into Eq. (4-61), we can reduce Hamiltonian H_t to the form

$$H_t = (1/2) \sum_q [\dot{Q}_q \dot{Q}_{-q} + w^2(q) Q_q Q_{-q}]. \tag{4-63}$$

Introducing then impulse $P_q = [\partial(T-V)/\partial Q_{-q}]$ we can rewrite Hamiltonian (4-63) in the form

$$H = (1/2) \sum_q [P_q P_{-q} + w_q^2(q)\, Q_q Q_{-q}]. \tag{4-64}$$

It is convenient to pass to the quantum case by substitution

$$\begin{aligned} Q_q(t) &\to \hat{Q}_q(t) = (\hbar/2w(q))^{1/2}\, (\hat{b}_q(t) + \hat{b}^+_{-q}(t)), \\ P_q(t) &\to \hat{P}_q(t) = i(\hbar w(q)/2)^{1/2}\, (\hat{b}^+_q(t) + \hat{b}_{-q}(t)), \end{aligned} \tag{4-65}$$

where operators of coordinates, $\hat{Q}_q$, and impulses, $\hat{P}_q$, satisfy commutative relations

$$[\hat{Q}_q(t), \hat{P}_{q'}(t)] = i\hbar\delta_{q,q'}, \tag{4-66}$$

and Bose operators $\hat{b}^+_q$, $\hat{b}_q$ satisfy commutative relations

$$\begin{aligned} [\hat{b}_q(t), \hat{b}^+_{q'}(t)] &= \delta_{q,q'}, \\ [\hat{b}_q(t), \hat{b}_{q'}(t)] &= 0. \end{aligned} \tag{4-67}$$

Then the Hamiltonian will take the form

$$\hat{H}_t = \sum_n \hbar w(q) \{\hat{b}_q^+(t)\ \hat{b}_q(t) + 1/2\} \tag{4-68}$$

and the operator of the angular displacement, $\hat{\varphi}_n(t)$, can be written as

$$\hat{\varphi}_n(t) = (\hbar/2NI)^{½} \sum_q \{\overline{\overline{\varphi}}(q)/[w(q)]^{½}\}\ (\hat{b}_q(t) + (\hat{b}^+_{-q}(t))\exp(iqna). \tag{4-69}$$

4.2.1.3 Correlation Functions

Usually correlation functions are determined as a product of operators written in the Heisenberg representation, which is averaged over a statistical ensemble:

$$<\hat{A}(t), \hat{B}(t')> = \mathrm{Sp}\{\hat{A}(t)\hat{B}(t')\ \exp(-\hat{H}/k_B T)\}/\mathrm{Sp}\{\exp(-\hat{H}/k_B T)\}. \tag{4-70}$$

Here $\hat{A}$ and $\hat{B}$ are the operators. In our case they are equal to $\hat{b}_q$ or $\hat{b}^+{}_q$. The symbol of spur (Sp) denotes summation over all diagonal elements of the matrix of the corresponding operator. The symbol <...> denotes statistical averaging over the grand canonical ensemble.

According to Eq. (4-68), in the linear approximation the internal DNA dynamics is described by a model of ideal Bose gas. This model has been well studied in physics and the correlation functions $<\hat{b}\ (t), \hat{b}\ (t')$, $<\hat{b}^+\ (t), \hat{b}\ (t')$, $<\hat{b}\ (t), \hat{b}^+\ (t')$, $<\hat{b}^+\ (t), \hat{b}^+\ (t')>$, are known to be equal to

$$\begin{aligned} &<\hat{b}_q\ (0), \hat{b}_{q'}\ (t)> = <\hat{b}^+{}_q\ (0), \hat{b}^+{}_{q'}(t)> = 0, \\ &<\hat{b}^+{}_q\ (0), \hat{b}_{q'}(t)> = n_q \exp\,[-iw(q)t]\ \delta_{q,q'}, \\ &<\hat{b}_q\ (0), \hat{b}^+{}_{q'}\ (t)> = (n_q + 1)\ \exp\,[iw(q)t]\ \delta_{q,q'}, \end{aligned} \tag{4-71}$$

where $n_q = \{\exp\,[hw(q)/k_B\ T] - 1\}^{-1}$; k_B is the Boltzmann constant and T is the absolute temperature. Using Eq. (4-71) we can easily calculate different macroscopic characteristics of DNA. For example, let us calculate the torsion energy of the DNA molecule

$$E_t = < \hat{H}_t > = \sum_q \hbar w(q)\{< \hat{b}^+{}_q(t)\hat{b}_q(t) > +1/2 = \sum_q \hbar w(q)\ \{n_q + 1/2\}. \tag{4-72}$$

4.2.2 Phonons in the Double Rod-like Model

According to the hierarchy described in Sections 1.6 and 2.7, the second level DNA model consists of two chains of disks interacting with one another by longitudinal and transverse springs. Each of the disks has three degrees of freedom: longitudinal, transverse and rotational displacements from its equilibrium position. As in the previous section, let us assume that in the first approximation these three types of motions can be considered as independent and consider as an example one type of motion, namely, the angular displacements of the disks. It is more convenient to describe rotations of DNA bases by the angular displacements of pendula instead of those of disks. This approach has been developed in the work of Englander and coauthors [15], where the analogy between rotational motions of bases in DNA and rotational motions of pendula in the mechanical model of Scott [232] was used. The latter consists of a horizontal chain of pendula placed in a uniform gravitational field with each pendulum being able to rotate in the *xy* plane (Figure 4.4). To apply this approach to the double rod-like model we should slightly modify the mechanical model. We can do this by 'removing' the gravitational field and considering two parallel chains of pendula interacting with one another by longitudinal and transverse springs (Figure 4.5). The pendula then play the role of bases in DNA chains, the longitudinal springs imitate the sugar-phosphate backbone and the transverse springs imitate the hydrogen interactions of bases in pairs.

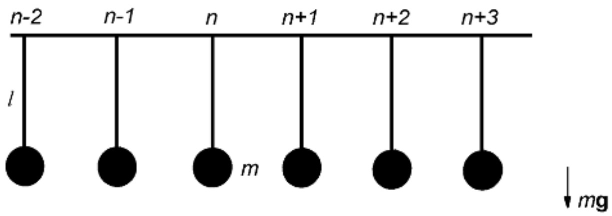

Figure 4.4 The mechanical model of Scott

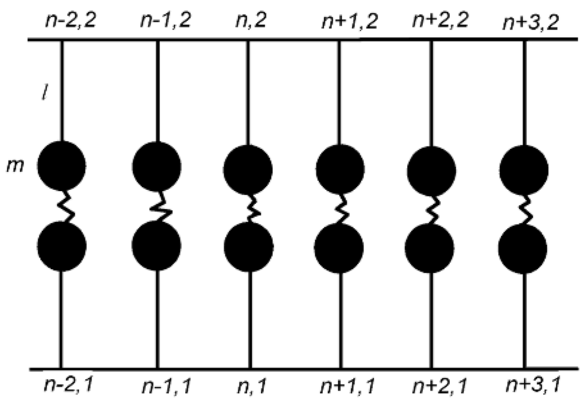

Figure 4.5 Modified mechanical analog: two chains of coupled pendula.

The model shown in Figure 4.5 looks like a one-dimensional lattice with two pendula per unit cell. If we introduce the basic vector $\boldsymbol{a}_z = \{0; 0; a\}$, then lattice vector $\boldsymbol{R}_n^0$ can be defined as

$$\boldsymbol{R}_n^0 = n\boldsymbol{a}_z\,; \tag{4-73}$$

where a is the distance between neighboring pendula and n is an integer (n = 1,2,...N). The equilibrium positions of the masses of pendula within a unit cell can be denoted by vectors

$$\boldsymbol{d}_1 = \{0\,; l; 0\}, \ \boldsymbol{d}_2 = \{0; b\text{-}l; 0\}, \tag{4-74}$$

where b is the distance between the chains and l is the length of pendula.

The position vector $\boldsymbol{R}^0_{n,j}$ of the jth pendulum mass (j = 1, 2) in the nth unit cell is now given by

$$\boldsymbol{R}^0_{n,j} = \boldsymbol{R}^0_n + \boldsymbol{d}_j\,. \tag{4-75}$$

Taking into account that every pendulum rotates only in the xy plane, we can write possible displacements of the masses as

$$\begin{aligned} \boldsymbol{R}_{n,1}(t) - \boldsymbol{R}^0_{n,1} &= \boldsymbol{u}_{\mathrm{n},1} = \{-l(1-\cos\varphi_{n,1});\, l\sin\varphi_{n,1};\, 0\}, \\ \boldsymbol{R}_{n,2}(t) - \boldsymbol{R}^0_{n,2} &= \boldsymbol{u}_{\mathrm{n},2} = \{l(1-\cos\varphi_{n,2});\, l\sin\varphi_{n,2};\, 0\}, \end{aligned} \tag{4-76}$$

where $\varphi_{n,j}$ is the angular displacement of the nth pendulum of the jth chain.

The kinetic and potential energies will have then the following forms:

$$T = \sum_n \{M\boldsymbol{u}^2_{n,1}/2 + M\boldsymbol{u}^2_{n,2}/2\}; \tag{4-77}$$

$$V = \sum_n K|\boldsymbol{u}_{n,1} - \boldsymbol{u}_{n-1,1}|^2/2 + \sum_n K|\boldsymbol{u}_{n,2} - \boldsymbol{u}_{n-1,2}|^2/2 + \sum_n k|\boldsymbol{u}_{n,1} - \boldsymbol{u}_{n,2}|^2/2; \tag{4-78}$$

where M is the mass of a pendulum, K is the rigidity of the longitudinal springs, and k is the rigidity of the transverse springs.

Inserting Eq. (4-76) into Eqs. (4-77) to (4-78), we obtain the model Hamiltonian H_{t} in the form

$$\begin{aligned} H_{\mathrm{t}} &= T + V = \\ &= \sum_n Ml^2\{\dot{\varphi}^2_{n,1} + \dot{\varphi}^2_{n,2}/2 + \sum_n\sum_j Kl^2(\varphi_{n,j} - \varphi_{n-1,j})^2/2 + \\ &+ \sum_n kl^2(\varphi_{n,1} - \varphi_{n,2})^2/2; \end{aligned} \tag{4-79}$$

where the variables $\varphi_{n,j}$ are independent.

We can now write the equations of motion corresponding to Eq. (4-79)

$$I\ddot{\varphi}_{n,1} = Kl^2(\varphi_{n+1,1} - 2\varphi_{n,1} + \varphi_{n-1,1}) - kl^2(\varphi_{n,1} - \varphi_{n,2}),$$
$$I\ddot{\varphi}_{n,2} = Kl^2(\varphi_{n+1,2} - 2\varphi_{n,2} + \varphi_{n-1,2}) - kl^2(\varphi_{n,2} - \varphi_{n,1}). \tag{4-80}$$

Here $I = Ml^2$.

4.2.2.1 General Solution of the Model Equations

To find the solutions of the model equations (4-80), let us make a transformation from the variables $\varphi_{n,j}$ (t) to the variables $Q_{q,g}$ (t) which are usually named the normal coordinates. For this purpose, let us assume that the angular displacements $\varphi_{n,j}(t)$ have the time dependence

$$\varphi_{n,j}\ (t) = \overline{\varphi}_{n,j} \exp(\text{-i}wt). \tag{4-81}$$

Then Eqs. (4-80) become

$$Iw^2\overline{\varphi}_{n,1} = -Kl^2(\overline{\varphi}_{n+1,1} - 2\overline{\varphi}_{n,1} + \overline{\varphi}_{n-1,1}) + kl^2\ (\overline{\varphi}_{n,1} - \overline{\varphi}_{n,2});$$
$$Iw^2\overline{\varphi}_{n,2} = -Kl^2(\overline{\varphi}_{n+1,2} - 2\overline{\varphi}_{n,2} + \overline{\varphi}_{n-1,2}) + kl^2(\overline{\varphi}_{n,2} - \overline{\varphi}_{n,1}). \tag{4-82}$$

The set of $2N$ linear equations (4-82) have a nontrivial solution if the determinant of the coefficients vanishes:

$$\det |Iw^2\delta_{n,n'}\delta_{j,j'} - \mathrm{A}_{n,n';j,j'}| = 0. \tag{4-83}$$

Here the non-zero coefficients have the forms

$$A_{n,n;1,1} = \mathrm{A}_{n,n;2,2} = 2Kl^2 + kl^2,$$
$$A_{n,n;1,2} = \mathrm{A}_{\ n,n;2,1} = -kl^2, \tag{4-84}$$
$$A_{n,n+1;j,j} = A_{n,n\text{-}1;j,j} = -Kl^2,$$

and the roots of Eq. (4-83) are the so-called normal mode frequencies.

Because of the translational symmetry of the lattice considered, it is useful to make the substitution

$$\overline{\varphi}_{n,j} = (\overline{\overline{\varphi}}_j/I^{1/2}) \exp(\mathrm{i}\boldsymbol{q}\boldsymbol{R}_n^0) = (\overline{\overline{\varphi}}_j/I^{1/2}) \exp(\mathrm{i}qna); \tag{4-85}$$

where $\boldsymbol{q} = \{q_x;\ q_y;\ q_z\} = \{0;\ 0;\ q\}$ is the wave vector, and its values lie within the first Brillouin zone.

The eigenvalue equation for the normal-mode frequencies can be written as

$$Iw^2\bar{\bar{\varphi}}_j = \sum_{n'}\sum_{j'} A_{n,n';j,j'} \exp[iq(n' - n)a]\bar{\bar{\varphi}}_{j'} . \tag{4-86}$$

Taking into account Eq. (4-84) we can rewrite Eq. (4-86) in the form

$$\begin{aligned} w^2\bar{\bar{\varphi}}_1 &= \{[2Kl^2(1\text{-}\cos qa) + kl^2]/I\}\bar{\bar{\varphi}}_1 - (kl^2/I)\bar{\bar{\varphi}}_2, \\ w^2\bar{\bar{\varphi}}_2 &= (kl^2/I)\bar{\bar{\varphi}}_1 + \{[2Kl^2(1\text{-}\cos qa) + \mathrm{kl}^2]/I\}\bar{\bar{\varphi}}_2. \end{aligned} \tag{4-87}$$

For each value of q we find two solutions for w^2

$$w_{1,2}^2(q) = [2Kl^2(1\text{-}\cos qa) + kl^2 \pm kl^2]/I, \tag{4-88}$$

and for each $w^2{}_g(q)$ (g=1,2) there is a corresponding eigenvector $\bar{\bar{\varphi}}_j$. We shall henceforth write these as $\bar{\bar{\varphi}}^g{}_j(q)$. Thus the eigenvalue equation (4-86) now reads

$$w_g^2(q)\bar{\bar{\varphi}}_j^g(q) = \sum_{j'} A_{j,j'}(q)\bar{\bar{\varphi}}_{j'}^g(q); \tag{4-89}$$

with non-zero coefficients $A_{j,j'}(q)$

$$\begin{aligned} A_{1,1}(q) &= A_{2,2}(q) = [2Kl^2(1\text{-}\cos qa) + \mathrm{kl}^2]/I, \\ A_{1,2}(q) &= A_{2,1}(q) = -kl^2/I. \end{aligned} \tag{4-90}$$

And the eigenvalues $\bar{\bar{\varphi}}^g{}_j(q)$ are usually constructed to satisfy

$$\begin{aligned} &\sum_g \bar{\bar{\varphi}}_j^{*g}(q)\bar{\bar{\varphi}}_{j'}^g(q) = \delta_{j,j'} ; \\ &\sum_j \bar{\bar{\varphi}}_j^{*g}(q)\bar{\bar{\varphi}}_j^{g'}(q) = \delta_{g,g'} . \end{aligned} \tag{4-91}$$

As a result, we can write the solution of Eq. (4-80) for the angular displacement $\varphi_{n,j}(t)$ in the form of the expansion

$$\varphi_{n,j}(t) = [1/(NI)^{½}]\sum_q\sum_g \bar{\bar{\varphi}}_j^g(q)Q_{q,g}(t)\exp(iqna); \tag{4-92}$$

where $Q_{q,g}(t)$ are the normal coordinates mentioned above.

4.2.2.2 Secondary Quantum Representation

Inserting Eq. (4-92) into Eqs. (4-79) and taking into account Eqs. (4-91) we can reduce the Hamiltonian (4-79) to the sum of independent harmonic oscillators

$$H_t = (1/2)\sum_q \sum_g [\dot{Q}_{q,g}\dot{Q}_{-q,g} + w_g^2(q)Q_{q,g}Q_{-q,g}] \tag{4-93}$$

Introducing then impulse $P_{q,g} = [\partial(\text{T-V})/\partial Q_{-q,g}]$, we can rewrite the Hamiltonian (4-93) in the form

$$H_t = (1/2)\sum_q \sum_g [P_{q,g}P_{-q,g} + w_g^2(q)Q_{q,g}Q_{-q,g}] \tag{4-94}$$

Let us pass now to the quantum case by substitution

$$\begin{aligned} &Q_{q,g}(t) \to \hat{Q}_{q,g}(t) = (\hbar/2w_g(q))^{½}\,(\hat{b}_{-q,g}(t) + \hat{b}^{+}_{-q,g}(t)),\\ &P_{q,g}(t) \to \hat{P}_{q,g}(t) = \mathrm{i}(\hbar w_g(q)/2)^{½}\,(\hat{b}^{+}_{-q,g}(t) - \hat{b}_{-q,g}(t)), \end{aligned} \tag{4-95}$$

where operators of coordinates, $\hat{Q}_{q,g}(\mathrm{t})$, and impulses, $\hat{P}_{q,g}(t)$, satisfy the commutative relations

$$[\hat{Q}_{q,g}(t),\ \hat{P}_{q',g'}(t)] = \mathrm{i}\hbar\ \delta_{q,q'}\delta_{g,g'}; \tag{4-96}$$

and Bose operators $\hat{b}^{+}_{-q,g}(\mathrm{t})$, $\hat{b}_{q,g}$ satisfy the commutative relations

$$\begin{aligned} &[\hat{b}_{q,g}(t),\ \hat{b}^{+}_{q',g'}(t)] = \delta_{q,q'}\,\delta_{g,g'},\\ &[\hat{b}_{q,g}(t),\ \hat{b}_{q',g'}(t)] = 0. \end{aligned} \tag{4-97}$$

Then the model Hamiltonian takes the form

$$\hat{H}_t = \sum_q \sum_g \hbar w_g(q)\{\hat{b}^{+}_{q,g}(t)\hat{b}_{q,g}(t) + 1/2\}; \tag{4-98}$$

and the operator of the angular displacement can be written as

$$\begin{aligned} \hat{\varphi}_{n,j}(t) &= (\hbar/2NI)^{½}\sum_q\sum_g \{\overline{\overline{\varphi}}{}^g_j(q)/[w_g(q)]^{½}\}(\hat{b}_{q,g}(t) + \hat{b}^{+}_{-q,g}(t))\exp(\mathrm{i}qna) =\\ &= (\hbar/2NI)^{½}\sum_q\sum_g (w_g(q))^{-½}\{\overline{\overline{\varphi}}{}^g_j(q)\hat{b}_{q,g}\exp(\mathrm{i}qna); + \overline{\overline{\varphi}}{}^{g*}_j(q)\hat{b}^{+}_{q,g}\exp(-\mathrm{i}qna)\}; \end{aligned} \tag{4-99}$$

where it was taken into account that $w^*_g(q) = w_g(-q)$ and $\overline{\overline{\varphi}}{}^{g*}_j(q) = \overline{\overline{\varphi}}{}^g_j(-q)$.

4.2.2.3 Correlation Functions

It follows from Eq. (4-98) that in the linear approximation the internal DNA dynamics is described by a model of ideal Bose gas. Correlation functions for this model are

$$<\hat{b}_{q,g}(0),\, \hat{b}_{q',g'}(t)> = <\hat{b}^{+}_{q,g}(0),\, \hat{b}^{+}_{q',g'}(t)> = 0,$$

$$<\hat{b}^{+}_{q,g}(0),\, \hat{b}_{q',g'}(t)> = n_{q,g}\exp[-\mathrm{i}w_g(q)t]\,\delta_{q,q'}\,\delta_{g,g'}, \tag{4-100}$$

$$<\hat{b}_{q,g}(0),\, \hat{b}^{+}_{q',g'}(t)> = (n_{q,g}+1)\exp[\mathrm{i}w_g(q)t]\,\delta_{q,q'}\,\delta_{g,g'},$$

where $n_{q,g} = \{\exp[\hbar w_g(q)/kT]-1\}^{-1}$. Using these formulas we can calculate different microscopic characteristics of the DNA. For example, the torsion energy will have the form

$$\begin{aligned} E_t =< \hat{H}_t > &= \sum_q \sum_g \hbar w_g(q)\{< \hat{b}^{+}_{q,g}(t)\hat{b}_{q,g}(t) > +1/2\} \\ &= \sum_q \sum_g \hbar w_g(q)\{n_{q,g} + 1/2\}. \end{aligned} \tag{4-101}$$

4.2.3
Phonons in the Higher-level Models

The approach described above can be easily expanded to a more complex model of DNA (the third- or the fourth-level models). If we restrict ourselves to the homogeneous case, we can consider the higher-level models as lattices containing several or several dozens of atoms in the cell. The general forms of the corresponding Hamiltonians and dynamical equations are very similar to Eq. (4-79) and Eqs. (4-80), respectively. But the index j takes the values

$$j = 1,2,\, \ldots\, m;$$

where m is the total number of atoms in the lattice cell.

Instead of $2N$ linear equations (4-82) we shall obtain mN equations, and the roots of the corresponding dispersion equation will determine the normal mode frequencies. As a result, for each value of the wave vector q we shall obtain m solutions for $w^2(q)$, and for each $w^2(q)$ there will be a corresponding eigenvector $\overline{\overline{\varphi}}_j$ ($j = 1.2, \ldots\, m$).

Following the algorithm described above we can obtain the Hamiltonian $\hat{H}_t$ in a form similar to Eq. (4-98), the operator of angular displacement $\hat{\varphi}_{n,j}$ in a form similar to Eq. (4-99), correlation functions of the type of Eqs. (4-100) and at least the average energy $<\hat{H}_t>$ in a form similar to Eq. (4-101).

4.3 Scattering Problem

Now let us apply the results obtained in the previous sections to the scattering problem. As an example let us consider the problem of scattering slow (thermal) neutrons by DNA. In Section 2.8 we described the main features of the method of neutron scattering. Here we shall present the algorithm for the calculation of the double differential cross-section.

As a model of the internal DNA dynamics let us take the double rod-like model described in detail in Section 4.1.2. According to the model, the DNA molecule can be considered as a lattice formed by two chains of pendula imitating DNA bases. First let us consider a perfect lattice, that is let us assume that each pendulum is at the equilibrium position. For simplicity we suggest also that the threads of the pendula are transparent for neutrons and only the masses take part in the scattering process. If we consider now the masses as 'nuclei', a standard theory of neutron scattering by a rigid array of nuclei can be applied.

Interaction of the incident neutron having mass m and coordinate $\boldsymbol{r}$ with a nucleus having mass M and coordinate $\boldsymbol{R}^0_{n,j}$ can be described by the Fermi pseudo-potential [233]:

$$V_{n,j} = (2\pi\hbar^2 B_{n,j}/m)\,\delta(\boldsymbol{r}-\boldsymbol{R}^0_{n,j}), \tag{4-102}$$

where $B_{n,j}$ is the scattering length. So, the interaction of the incident neutron with a rigid array of $2N$ nuclei is described by the potential

$$V = (2\pi\hbar^2/m)\sum_n\sum_j B_{n,j}\delta(\boldsymbol{r}-\boldsymbol{R}^0_{n,j}). \tag{4-103}$$

If we allow nuclei to undergo small displacements from their equilibrium positions, the coordinates of the nuclei will take the form

$$\boldsymbol{R}_{n,j}(t) = \boldsymbol{R}^0_{n,j} + \boldsymbol{u}_{n,j}(t), \tag{4-104}$$

where the displacements $\boldsymbol{u}_{n,j}(t)$ are determined by Eq. (4-76). Inserting Eq. (4-104) into Eq. (4-103) we obtain the generalized expression for the potential V

$$V = (2\pi\hbar^2/m)\sum_n\sum_j B_{n,j}\delta(\boldsymbol{r}-\boldsymbol{R}^0_{n,j}-\boldsymbol{u}_{n,j}). \tag{4-105}$$

Then the master formula for the partial differential cross-section takes the form [233]

$$\partial\sigma/\partial\Omega\partial E'' = 2N(k''/k')\,\overline{B}^2\,S^{\mathrm{coh}}(\boldsymbol{x},w') + 2N(k''/k')\,(\overline{B^2}-\overline{B}^2)\,S^{\mathrm{incoh}}(\boldsymbol{x},w'), \tag{4-106}$$

where $k'=|\boldsymbol{k}'|$, $k''=|\boldsymbol{k}''|$, and $\boldsymbol{k}'$ and $\boldsymbol{k}''$ are the wave-vectors of the incident and scattered neutrons, respectively; ... denotes averaging over all spins and isotopes; $S^{coh}(\boldsymbol{x},w')$ and $S^{incoh}(\boldsymbol{x},w')$ are the dynamical factors of coherent and incoherent scattering

$$S^{coh}(\boldsymbol{x},w') = (4\pi\hbar N)^{-1}\int_{-\infty}^{+\infty} dt \exp(-iw't)\sum_{n,n'}\sum_{j,j'} < \exp(-i\boldsymbol{x}\boldsymbol{R}^0_{n,j}(0)), \exp(i\boldsymbol{x}\boldsymbol{R}_{n',j'}(t)) >, \tag{4-107}$$

$$S^{incoh}(\boldsymbol{x},w') = (4\pi\hbar N)^{-1}\int_{-\infty}^{+\infty} dt \exp(-iw't)\sum_{n}\sum_{j} < \exp(-i\boldsymbol{x}\boldsymbol{R}^0_{n,j}(0)), \exp(i\boldsymbol{x}\boldsymbol{R}_{n,j}(t)) >,$$

Here $w' = (E' - E'')/\hbar$, and $E' = \hbar^2k'^2/2m$ and $E'' = \hbar^2k''^2/2m$ are the energies of the neutron before and after scattering; $\boldsymbol{x} = \boldsymbol{k}' - \boldsymbol{k}''$; <...> denotes averaging over the positions of the nuclei (or pendulum masses imitating nitrous bases).

4.3.1 Scattering by 'Frozen' DNA

If the temperature is rather low, we can assume

$$\boldsymbol{u}_{n,j}(t)=0. \tag{4-108}$$

Inserting Eqs. (4-108) and (4-107) into Eqn. (4-106) we find

$$\partial\sigma/\partial\Omega\partial E''=2N(k''/k')\,\overline{B}^2\,S^{coh}_{fr}(\boldsymbol{x},w') + 2N(k''/k')\,(\overline{B^2} - \overline{B}^2)\,S^{incoh}_{fr}(\boldsymbol{x},w'),$$

where

$$S^{coh}_{fr}(\boldsymbol{x},w') = (1/4\pi\hbar N)\sum_n\sum_{n'}\sum_j\sum_{j'}\exp[-i\boldsymbol{x}(\boldsymbol{R}^0_{n,j} - \boldsymbol{R}^0_{n',j'})]\int_{-\infty}^{+\infty} dt\exp(-iw't) =$$

$$= (1/2N)\{\sum_n\sum_{n'}\exp[-i\boldsymbol{x}(\boldsymbol{R}^0_{n,j} - \boldsymbol{R}^0_{n',j'})]\}\{\sum_j\sum_{j'}\exp[-i\boldsymbol{x}(\boldsymbol{d}_j - \boldsymbol{d}_{j'})]\}\delta(\hbar w') =$$

$$= [(1+\cos x_y h)/N]|\sum_n \exp(-i\boldsymbol{x}n\boldsymbol{a})|^2\delta(E' - E'') =$$

$$= [2(1+\cos x_y h)/a]\,\delta(E' - E'')\sum_{\tau_z}\delta(x_z - \tau_z), \tag{4-109}$$

$$S^{incoh}_{fr}(\boldsymbol{x},w') = (1/4\pi\hbar N)\sum_n\sum_j\int_{-\infty}^{+\infty} dt\exp(-iw't) = \delta(E' - E''), \tag{4-110}$$

where $h = b\text{-}2l$, and it is equivalent to the length of the H-bonds between the bases in pairs in DNA; x_y is the y-projection of the vector $\boldsymbol{x}$; $\tau = \{0;\,0;\,2\pi t'/a\}$ is a vector of the reciprocal lattice, and t' is an integer.

Then the cross-section takes the form

$$(\mathrm{d}\sigma/\mathrm{d}\Omega)_{\mathrm{fr}} = (\mathrm{d}\sigma/\mathrm{d}\Omega)_{\mathrm{fr}}^{\mathrm{coh}} + (\mathrm{d}\sigma/\mathrm{d}\Omega)_{\mathrm{fr}}^{\mathrm{incoh}}, \tag{4-111}$$

where the coherent cross-section is

$$(\mathrm{d}\sigma/\mathrm{d}\Omega)_{\mathrm{fr}}^{\mathrm{coh}} = (4\pi N\overline{B}^2/a)(1+\cos x_y h)\sum_{\tau_z}\delta(x_Z - \tau_z); \tag{4-112}$$

and the incoherent cross-section is

$$(\mathrm{d}\sigma/\mathrm{d}\Omega)_{\mathrm{fr}}^{\mathrm{incoh}} = 2N(\overline{B^2} - \overline{B}^2). \tag{4-113}$$

Equation (4-112) describes coherent scattering with sharp peaks of intensity of scattered neutrons as determined by the condition

$$x_z = \tau_z\,; \tag{4-114}$$

and Eq. (4-113) describes an incoherent scattering which does not depend on the angle of scattering and looks like a simple background.

4.3.2 Elastic Scattering

Let us allow nuclei to undergo small displacements from their equilibrium positions and consider the contribution of elastic scattering of neutrons by DNA. For the purpose, we can use Eq. (4-106) and extract there the terms which are independent of time t. This can be easily done if we rewrite the correlation functions in Eq. (4-107) in the following form

$$<\exp(-\mathrm{i}\boldsymbol{x}\boldsymbol{R}^0_{n,j}\ (0)),\ \exp(\mathrm{i}\boldsymbol{x}\boldsymbol{R}^0_{n',j'}(t)> =$$

$$= <\exp(-\mathrm{i}\boldsymbol{x}\boldsymbol{R}^0_{n,j}(0)),\ \exp(\mathrm{i}\boldsymbol{x}\boldsymbol{R}^0_{n',j'}(\infty)> + \{<\exp(-\mathrm{i}\boldsymbol{x}\boldsymbol{R}^0_{n,j}(0)),\ \exp(\mathrm{i}\boldsymbol{x}\boldsymbol{R}^0_{n',j'}(t)> -$$

$$- <\exp(-\mathrm{i}\boldsymbol{x}\boldsymbol{R}^0_{n,j}(0)),\ \exp(\mathrm{i}\boldsymbol{x}\boldsymbol{R}^0_{n',j'}(\infty)>\}. \tag{4-115}$$

and keep only the first term which is responsible for the elastic scattering. The term can be rewritten then in the following way

$$<\exp(-\mathrm{i}\boldsymbol{x}\boldsymbol{R}^0_{n,j}(0)),\ \exp(\mathrm{i}\boldsymbol{x}\boldsymbol{R}^0_{n',j'}(\infty)> = <\exp(-\mathrm{i}\boldsymbol{R}\boldsymbol{x}^0_{n,j}(0)> <\exp(\mathrm{i}\boldsymbol{x}\boldsymbol{R}^0_{n',j'}(\infty)> =$$

$$= \exp(-\mathrm{i}\boldsymbol{x}\boldsymbol{R}^0_{n,j})\exp(\mathrm{i}\boldsymbol{x}\boldsymbol{R}^0_{n',j'})\ <\exp(-\mathrm{i}\vec{\boldsymbol{x}}\boldsymbol{u}_{n,j})> <\exp(\mathrm{i}\vec{\boldsymbol{x}}\boldsymbol{u}_{n',j'})> =$$

$$= \exp(-2W_{x,j})|\exp(\mathrm{i}\boldsymbol{x}\boldsymbol{R}^0_{n,j})|^2 ; \tag{4-116}$$

where $\exp(-2W_{x,j}) = <\exp(-\mathrm{i}\boldsymbol{x}\boldsymbol{u}_{n,j})>$ is the well known Debye–Waller factor.

Inserting Eq. (4-116) into Eq. (4-107) and assuming for simplicity that $W_{x,1} = W_{x,2} = W_x$ we obtain

$$S^{coh}_{el}(\boldsymbol{x},w') = \exp(-2W_x)[2\pi(1+\cos x_y h)/a]\sum_{\tau_z}\delta(E' - E'')\delta(x_z - \tau_z),$$
$$S^{incoh}_{el}(\boldsymbol{x},w') = \exp(-2W_x)\delta(E'\text{-}E''). \tag{4-117}$$

So, the result is

$$(\mathrm{d}\sigma/\mathrm{d}\Omega)_{el} = (\mathrm{d}\sigma/\mathrm{d}\Omega)^{coh}_{el} + (\mathrm{d}\sigma/\mathrm{d}\Omega)^{incoh}_{el}, \tag{4-118}$$

where the coherent cross-section is

$$(\mathrm{d}\sigma/\mathrm{d}\Omega)^{coh}_{el} = \exp(-2W_x)\,(4\pi N\overline{B}^2/a)(1+\cos x_y h)\sum_{\tau_z}\delta(x_z - \tau_z); \tag{4-119}$$

and the incoherent cross-section is

$$(\mathrm{d}\sigma/\mathrm{d}\Omega)^{incoh}_{el} = \exp(-2W_x)2N\,(\overline{B^2} - \overline{B}^2). \tag{4-120}$$

Equationss (4-118) – (4-120) are very similar to Eqs. (4-111) – (4-113) and differ from them only by the factor $\exp(-2W_x)$. The presence of the factor means that the general diffraction picture (sharp peaks against a slight background) will be changed a little due to the weak angular dependence of the Debye–Waller factor.

4.3.3 Inelastic Scattering

In the calculations of the inelastic scattering let us restrict ourselves to the so-called one-phonon approximation [233]. According to the approximation the dynamical factors of the coherent and incoherent inelastic scattering Eq. (4-107) take the form

$$S^{coh}_{inel}(\boldsymbol{x},w') = [\exp(-2W_x)/4\pi\hbar N]\sum_n\sum_{n'}\sum_j\sum_{j'}\exp[-\mathrm{i}x(\boldsymbol{R}_{n,j} - \boldsymbol{R}_{n'j'})]$$
$$\int_{-\infty}^{+\infty}\mathrm{d}t[\exp(-\mathrm{i}w' t)] < \boldsymbol{x}\boldsymbol{u}_{n,j}(0), \boldsymbol{x}\boldsymbol{u}_{n'j'}(t) > \tag{4-121}$$

$$S^{incoh}_{inel}(\boldsymbol{x},w') = [\exp(-2W_x)/4\pi\hbar N]\sum_n\sum_j\int_{-\infty}^{+\infty}\mathrm{d}[\exp(-\mathrm{i}w' t)] < \boldsymbol{x}\boldsymbol{u}_{n,j}(0), \boldsymbol{x}\boldsymbol{u}_{n,j}(t) > .$$

We need now to calculate the correlation functions $<\boldsymbol{xu}_{n,j}(0),\ \boldsymbol{xu}_{n'j'}(t)>$. After inserting Eq. (4-76) into Eq. (4-11) we have

$$<\boldsymbol{xu}_{n,j}(0),\ \boldsymbol{xu}_{n',j'}(t)>=$$

$$=<x_x[-l(1-\cos\varphi_{n,j}(0))]+x_y l\sin\varphi_{n,j}(0),\ x_x[-l(1-\cos\varphi_{n',j'}(t))]+x_y l\sin\varphi_{n',j'}(t)>=$$

$$=x_x{}^2l^2<(1-\cos\varphi_{n,j}(0),\ (1-\cos\varphi_{n',j'}(t))>-x_yx_xl^2<\sin\varphi_{n,j}(0),\ (1-\cos\varphi_{n',j'}(t))>-$$

$$-x_xx_yl^2<(1-\cos\varphi_{n,j}(0)),\ \sin\varphi_{n',j}(t)>+x_y{}^2l^2<\sin\varphi_{n,j}(0),\ \sin\varphi_{n',j'}(t)>. \tag{4-122}$$

In the harmonic approximation Eq. (4-122) can be rewritten in the form

$$<\boldsymbol{xu}_{n,j}(0),\ \boldsymbol{xu}_{n',j'}(t)>=x_y{}^2l^2<\varphi_{n,j}(0),\ \varphi_{n',j'}(t)>. \tag{4-123}$$

Inserting then Eq. (4-99) into Eq.(4-123) we obtain

$$<\boldsymbol{xu}_{n,j}(0),\ \boldsymbol{xu}_{n',j'}(t)>=$$

$$=(x_y^2l^2\hbar/2NI)\sum_q\sum_{q'}\sum_g\sum_{g'}\{\overline{\overline{\varphi}}{}_j^g(q)\overline{\overline{\varphi}}{}_{j'}^{g'}(q')/[w_g(q)w_{g'}(q'\overset{\wp}{\mathrm{A}})]^{1/2}<(\hat{b}_{q,g}(0))+$$

$$+\hat{b}_{-q,g}(0)),\ (\hat{b}_{q',g'}(t)+\hat{b}^+{}_{-q',g'}(t))>\exp(iqna)\exp(iq'n'a). \tag{4-124}$$

Let us take into account that the model Hamiltonian (4-98) describes the ideal Bose gas and that the correlation functions in this case are

$$<\hat{b}_{q,g}(0),\ \hat{b}_{q',g'}(t)>=<\hat{b}^+{}_{q,g}(0),\ \hat{b}^+_{q',g'}(t)>=0,$$

$$<\hat{b}^+{}_{q,g}(0),\ \hat{b}_{q',g'}(t)>=n_{q,g}\exp[-iw_g(q)t]\,\delta_{q,q'}\,\delta_{g,g'}, \tag{4-125}$$

$$<\hat{b}_{q,g}(0),\ \hat{b}^+_{q',g'}(t)>=(n_{q,g}+1)\exp[iw_g(q)t]\,\delta_{q,q'}\,\delta_{g,g'},$$

where $n_{q,g}=\{\exp[\hbar w_g(q)/k_BT]-1\}^{-1}$; k_B is the Boltzmann constant and T is the absolute temperature. Inserting then Eq. (4-125) into Eq. (4-124) we obtain the correlation functions

$$<\boldsymbol{xu}_{n,j}(0),\ \boldsymbol{xu}_{n',j'}(t)>=$$

$$=(x_y^2l^2\hbar 2NI)\{\sum_q\sum_g[\overline{\overline{\varphi}}{}_j^g(q)\overline{\overline{\varphi}}{}_{j'}^{g*}(q)/w_g(q)](n_{q,g}+1)\exp[iw_g(q)t]\exp[iq(n-n')a]+$$

$$\sum_q\sum_g[\overline{\overline{\varphi}}{}_j^{g*}(q)\overline{\overline{\varphi}}{}_{j'}^g(q)/w(q)]n_{q,g}\exp[-iw_g(q)t][\exp[-iq(n-n')a]\}. \tag{4-126}$$

And finally, for $S_{\text{inel}}^{\text{coh}}(\boldsymbol{x},w')$,

$$S_{\text{inel}}^{\text{coh}}(x,w') = [\exp(-2W_x)x_y^2 l^2/8\pi IN^2]\sum_n\sum_{n'}\sum_j\sum_{j'}\exp[-\mathrm{i}\boldsymbol{x}(\boldsymbol{R}_n^0 - \boldsymbol{R}_{n'}^0)]$$

$$\exp[-\mathrm{i}\boldsymbol{x}(\boldsymbol{d}_j - \boldsymbol{d}_{j'})]\int_{-\infty}^{+\infty} \mathrm{d}t\,\exp(-\mathrm{i}w't)\{\sum_q\sum_g[\overline{\overline{\varphi}}_j^g(q)\overline{\overline{\varphi}}_{j'}^{g*}(q)/w_g(q)](1+n_{q,g})$$

$$\exp[\mathrm{i}w_g(q)t]\exp[\mathrm{i}q(n-n')a] + \sum_q\sum_g[\overline{\overline{\varphi}}_j^{g*}(q)\overline{\overline{\varphi}}_{j'}^g(q)/w(q)]n_{q,g}$$

$$\exp[-\mathrm{i}w_g(q)t]\,\exp[-\mathrm{i}q(n\text{-}n')a]\}. \tag{4-127}$$

If we take into account the relations

$$(1/2\pi)\int_{-\infty}^{+\infty}\mathrm{d}t\,\exp(\mathrm{i}xt) = \delta(x),$$

$$\delta(x)/a = \delta(ax),\ (a>0), \tag{4-128}$$

$$\delta(-x) = \delta(x),$$

Eq. (4-127) can be rewritten in the form

$$S_{\text{inel}}^{\text{coh}}(\boldsymbol{x},w') = [\exp(-2W_x)x_y^2 l^2\hbar 4IN^2]\sum_n\sum_{n'}\sum_j\sum_{j'}\sum_q\sum_g\ \exp[-x_z(n-n')a]$$

$$\exp[-\mathrm{i}\boldsymbol{x}(\boldsymbol{d}_j - \boldsymbol{d}_j)][1/w_g(q)]\{\overline{\overline{\varphi}}_j^g(q)\overline{\overline{\varphi}}_{j'}^{g*}(q)(1+n_{q,g})\exp[\mathrm{i}q(n-n')a]$$

$$\delta(w_g(q) - \mathrm{w}') + \overline{\overline{\varphi}}_j^{g*}(\mathrm{q})\overline{\overline{\varphi}}_{j'}^{g*}(\mathrm{q})\ \mathrm{n}_{q,g}\exp[-\mathrm{i}q(n-n')a]\ \delta(w_g(q)+w')\}. \tag{4-129}$$

If we take then into account that

$$(1/N)\sum_n\sum_{n'}\ \exp[-\mathrm{i}(x_z \mp q)(n-n')a] = (2\pi/a)\delta(x_z \mp q - \tau_z); \tag{4-130}$$

we can reduce Eq. (4-129) to

$$S_{\text{inel}}^{\text{coh}}(\boldsymbol{x},w') = [\exp(-2W_x)x_y^2 l^2\pi\hbar/2INa]\sum_q\sum_q\sum_{\tau_z}(1/w_q(q))|\sum_j\overline{\overline{\varphi}}_j^g(x_z)$$

$$\exp(-\mathrm{i}x\boldsymbol{d}_j)|^2\{(1+\mathrm{n}_{q,g})\ \delta(x_z - q - \tau_z)\ \delta(\hbar w_g(q) - hw') + n_{q,g}\ \delta(x_z + q - \tau_z)\ \delta(\hbar w_g(q) +$$

$$+\ \hbar w')\}. \tag{4-131}$$

So, the dynamical factor (4-131) is the sum of two terms. The first, which contains $\delta(x_z - q - \tau_z)\ \delta(\hbar w_g(q) - \hbar w')$ represents a scattering process in which one phonon is created and the second term containing $\delta(x_z + q - \tau_z)\ \delta\ (\hbar w_g(q) + \hbar w')$ represents a process in which one phonon is annihilated. The delta functions associated with the scattering process represent conservation of energy and momentum

$$\hbar w' = (\hbar^2 k'^2 - \hbar^2 k''^2)/2m = \pm\, \hbar w_g(q), \tag{4-132}$$

$$x_z = k'_z - k''_z = 2\, t'/a \pm q. \tag{4-133}$$

The upper symbol (plus) in Eqs. (4-132) and (4-133) corresponds to the process of scattering accompanied by creation of one phonon, and the lower symbol (minus) corresponds to the process of scattering accompanied by the annihilation of one phonon. Due to conditions (4-132) and(4-133) for a given scattering angle only phonons of a particular q and $w_g(q)$ can give scattering. This makes it possible to determine the DNA phonon spectrum, $w_g(q)$, as a function of q.

The dynamical factor of the incoherent inelastic scattering can be calculated from Eq. (4-127) if we take there $n = n'$ and $j = j'$

$$S_{\text{inel}}^{\text{incoh}}(\boldsymbol{x}, w') = [\exp(-2W_x) x_\gamma^2 l^2/8\pi I N^2] \sum_n \sum_j \sum_q \sum_g \int_{-\infty}^{+\infty}$$

$$dt \exp(iw' t)(|\overline{\overline{\varphi}}{}_j^g(q)|^2/w_g(q))\{(1+n_{q,g})\exp(iw_g(q)t) + n_{n,g}\exp(-iw_g(q)t)\} =$$

$$= [\exp(-2W_x) x_\gamma^2 l^2 \hbar/4IN] \sum_q \sum_g \{[(\sum_j |\overline{\overline{\varphi}}{}_j^g(q)|)/w_g(q)][(1+n_{q,g})\delta(\hbar w_g(q) -$$

$$- \hbar w') + n_{q,g}\, \delta(\hbar w_g(q) + \hbar w')]\}. \tag{4-134}$$

Notice, that Eq. (4-134) contains delta functions to ensure energy conservation, but there are no momentum conservation conditions.

If we use now Eq. (4-106) and (4-131) – (4-133), we obtain the final result for the inelastic cross-section

$$(\partial^2\sigma/\partial\Omega\partial E'')_{\text{inel}} = (2\overline{B}k''/k')[\exp(-2W_x) x_\gamma^2 l^2 \pi\hbar/Ia] \sum_q \sum_g \sum_{\tau_z}$$

$$(1/w_g(q))|\sum_j \overline{\overline{\varphi}}{}_j^g(x_z)\exp(-\boldsymbol{x}\boldsymbol{d}_j)|\{(1+n_{q,g})\delta(x_z - q - \tau_z)$$

$$\delta(\hbar w_g(q) - \hbar w') + n_{q,g}\, \delta(x_z + q - \tau_z)\, \delta(\hbar w_g(q) + \hbar w')\} + (k''/k')\,(\overline{B^2} - \overline{B})$$

$$[\exp(-2W_x) x_\gamma^2 l^2 \hbar/2I] \sum_q \sum_g \{[(\sum_j |\overline{\overline{\varphi}}{}_j^g(q)|^2)/w_g(q)][(1+n_{q,g})\delta(\hbar w_g(q) - \hbar w')$$

$$+ n_{q,g}\delta(\hbar w_g(q) + \hbar w')]. \tag{4-135}$$

4.4
Linear Theory and Experiment

Modeling DNA as an assembly of linear waves (phonons) is a widely used approach in DNA science. Below we illustrate applications of the approach to interpretation of experimental data. Some of the data admit, however, alternative interpretation based on the representation of DNA as an assembly of nonlinear waves (solitons). This possibility will be discussed in detail in Chapter 8.

4.4.1
Fluorescence Depolarization

In fluorescence depolarization measurements, the incident light pulse preferentially excites molecules whose absorption dipoles are parallel to the electric field of the light, causing an initial polarization of fluorescence. The polarization of emitted light decays with time as the excited molecules undergo rotatory Brownian motions. This decay process is usually represented by the emission anisotropy.

Dyes such as ethidium bind to DNA by intercalation between two base pairs. The transition dipole moments of ethidium lie in the plane of the dye. It is the reorientation of the fluorescent dye, embedded in DNA with its transition dipoles parallel to the bases, that is monitored in the fluorescence depolarization experiments. Assuming that the dye is closely attached to DNA, Barkley and Zimm [119] suggested that the dye reports rotatory Brownian motions of the helix. Assuming also that the rotations are rapid compared to the reorientations of the axis, they suggested that torsional motions in DNA account for most of the rotational diffusion observed on the nanosecond time-scale of the experiment.

To derive the rotational diffusion equation in normal coordinates Barkley and Zimm [119] used the linear dynamical equations for torsional internal motions of type (4-7) and their solutions. As a result they obtained the time distribution function of the angular orientation of a fluorescent probe, embedded in the DNA double chain, and calculated the emission anisotropy.

The predicted decay law was compared with experimental data [234]. It was found that the decay of the anisotropy arises primarily from twisting of the DNA helix, with a small contribution from bending.

4.4.2
Low-frequency Spectra: Neutron Scattering, Infrared scattering, Raman Scattering, Speed of Sound

As we mentioned above, the motions of atoms in DNA can be analyzed as a superposition of normal-mode oscillations. In the linear approximation, which is valid only for small amplitudes of the displacements, the behavior of the superimposed normal modes is all independent. This type of analysis within the harmonic approximation has been applied to DNA by Prohofsky and coauthors [223–230]. This application has led to a successful theoretical explanation of the experimental data such as the speed of longitudinal sound [231] and inelastic neutron scattering data [153–155]. The results of calculations performed in the linear approximation reproduce very well the Raman peak and the improved shifts observed upon the conformational transitions [235–237], and explain the low-frequency DNA spectrum [238–241], microwave absorption [159–161], infrared absorption [156–157] and NMR experimental data [242–248].

5
Nonlinear Theory of DNA: Ideal Dynamical Models

In the previous chapter we considered the linear (or harmonic) approximation of the DNA theory. This is valid when the amplitudes of the internal motions in DNA are small. If the amplitudes are large the nonlinear (or anharmonic) effects should be taken into account. In Chapter 2 we described several examples of large-amplitude internal motions. Conformational transitions, denaturation processes, the formation of opening states in DNA–protein recognition processes and the formation of opening states in the first stage of the process of transcription are only some of the best-known examples of large-amplitude motions.

In this chapter we present several nonlinear models which form the basis of the nonlinear theory of DNA and describe the main principles of constructing the models.

5.1
Nonlinear Mathematical Modeling: General Principles and Restrictions

In Chapter 2 we discussed the main principles of constructing DNA dynamical models. They are rather general and valid for both linear and nonlinear cases. So, we can state that the algorithm for constructing nonlinear models of DNA dynamics should include the following elements:

1. Selection of the main (dominant) motions.
2. Construction of the nonlinear differential equations imitating the motions.
3. Finding solutions to the equations.
4. Interpretation of the solutions.

In practice, however, after selection of dominant motions investigators often use an additional stage: they find a mechanical analog with the same types of internal motions and interactions. This additional stage permits simplification of the procedure of constructing the equations.

Let us illustrate the approach by two simple examples. But first we should note that, as in the previous chapter, we shall restrict ourselves to consideration of ideal models which are elements of the hierarchy described in Sections 1.6 and 2.7. In other words, we shall not take into account the influence of the environment, dissipative effects, inhomogeneity of the DNA structure and others. Conditions under which this approach becomes incorrect will be discussed in the next chapter.

Example 1

This example concerns the modeling of the DNA open states dynamics. The main stages of the algorithm of constructing the nonlinear models are the following:

1. *Selection*. Because the main contribution to the opening process is made by rotational motions of bases it is natural to suggest that just these motions can be selected as dominant ones. For simplicity, we can limit ourselves by consideration of rotational motions of bases in one of the two DNA strands and consider the other strand only as a source of some stabilizing potential field.

2. *Mechanical analog and equations*. The mechanical analog for rotational motions of DNA bases was found by Englander et al. [15]: they proposed the use of a simple mechanical system consisting of a chain of coupled pendula, each of the pendula being able to rotate in the plane perpendicular to the chain axis (Figure 4.4). Such a system was constructed earlier by Scott [232] to demonstrate the propagation of nonlinear waves.

Rotational motion of the nth pendulum is described by the equation

$$ml^2\ddot{\varphi}_n = Kl^2(\varphi_{n+1} - 2\varphi_n + \varphi_{n-1}) - mgl\sin\varphi_n, \tag{5-1}$$

where $\varphi_n(t)$ is the angular displacement of the nth pendulum; K is the rigidity of the horizontal thread; l and m are the length and mass of the pendulum, respectively; g is the gravitational field constant. If we assume that the solutions we are interested in are fairly smooth functions, Eq. (5-1) can be rewritten in the continuous approximation

$$I\varphi_{tt} = Kl^2a^2\varphi_{zz} - mgl\sin\varphi, \tag{5-2}$$

where $I = ml^2$. After renormalization Eq. (5-2) takes the form

$$\varphi_{ZZ} - \varphi_{TT} = \sin\varphi; \tag{5-3}$$

where $Z = (mg/Kl^2)^{1/2}z$; $T = (g/l)^{1/2}t$. Thus, the rotational motions of pendula in the model of Scott are described by the well-known sine-Gordon equation.

3. *Solutions and their interpretation*. Taking into account the analogy between (i) the rotational motions of bases in one of the DNA strands and rotational motions of pendula, (ii) the field formed by the second DNA strand and the gravitational field, (iii) the elasticity of the sugar–phosphate chain of the first strand and that of the horizontal thread of the mechanical model, Englander et al. [15] suggested that, in the first approximation, the dynamics of rotational motions of bases in DNA can also be described by the sine-Gordon equation and that the soliton-like solutions of the equation, having the form of kinks and antikinks,

$$\varphi_{\text{kink, antikink}}(Z,T) = 4\arctan\{\exp\pm\ [(1-v^2)^{-1/2}(Z-vT-Z_0)]\} \tag{5-4}$$

describe the DNA opening states (Figure 5.1). Here v is the soliton velocity and Z_0 is a constant.

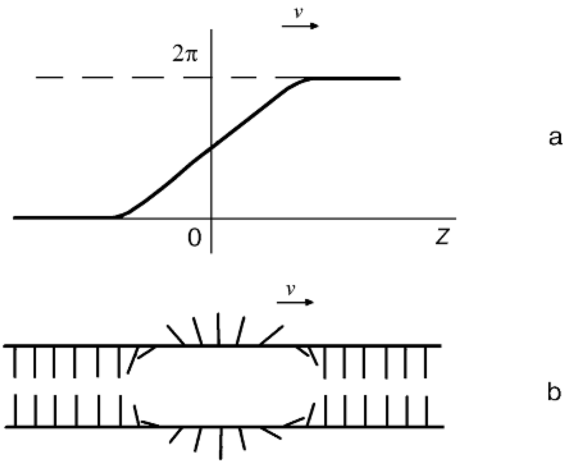

Figure 5.1 (a) Schematic picture of kink-solution of the sine-Gordon equation; (b) DNA open state corresponding to the solution.

We should add that besides kink- (antikink-) solutions the sine-Gordon equation has the phonon solutions

$$\varphi_{\mathrm{ph}}(Z,T) = A_q \exp[i(qZ - w_q T)], \quad w_q = (1 + q^2)^{1/2} \tag{5-5}$$

and the breather solutions

$$\varphi_{\mathrm{B}}(Z,T) = 4 \arctan\{\alpha \sin\theta / ch[\gamma\alpha(Z - vT - Z_0)]\}, \tag{5-6}$$

where $\theta = \gamma\Omega(T - vZ) + \theta_0$; $\gamma = (1 - v^2)^{-1}$; $\alpha^2 = (1 - \Omega^2)/\Omega^2$; $0 < \Omega < 1$; Ω is the intrinsic frequency of a breather; v is the velocity; Z_0, θ_0 are free parameters (the initial location and the phase). But the role of these two types of solutions in DNA dynamics and functioning is not clear at present.

Example 2

In this example, we again consider the DNA open states dynamics but in a more accurate way. In this case, the main stages of the algorithm are the following.

1. *Selection*. To make the model more accurate, we take into account the rotational motions of bases in both DNA strands.
2. *Mechanical analog and equations*. To find the 'mechanical' analog we can modify the model of Scott by removing 'gravitational' field and by adding the second chain

of coupled pendula interacting with the first one by additional transverse springs (Figure 4.5).

The differential equation imitating rotational motions of the nth pendulum in the first chain then takes the form [26]

$$I\ddot{\varphi}_{n,1} = Kl^2(\varphi_{n+1,1} - 2\varphi_{n,1} + \varphi_{n-1,1}) - kl^2[2\sin\varphi_{n,1} - \sin(\varphi_{n,1} + \varphi_{n,2})] \tag{5-7}$$

and the form of the equation imitating rotational motions of the nth pendulum in the second chain is

$$I\ddot{\varphi}_{n,2} = Kl^2(\varphi_{n+1,2} - 2\varphi_{n,2} + \varphi_{n-1,2}) - kl^2[2\sin\varphi_{n,2} - \sin(\varphi_{n,2} + \varphi_{n,1})]. \tag{5-8}$$

In the continuum limit Eqs. (5-7) and (5-8) reduce to

$$I\varphi_{1_{tt}} = Kl^2a^2\varphi_{1_{zz}} - kl^2\{2\sin\varphi_1 - \sin(\varphi_1 + \varphi_2)\}, \tag{5-9}$$

$$I\varphi_{2_{tt}} = \mathrm{K}l^2a^2\varphi_{2_{zz}} - kl^2\{2\sin\varphi_2 - \sin(\varphi_2 + \varphi_1)\}. \tag{5-10}$$

3. *Solutions*. Equations (5-9) and (5-10) have at least two groups of particular soliton-like solutions. The first one satisfies the condition $\varphi_1 = \varphi_2$, and the second the condition $\varphi_1 = -\varphi_2$. In the first case we have two pair solutions: kink–kink, and antikink–antikink solutions formed by kink and antikink solutions of the double sine-Gordon equation [249]

$$I\varphi_{tt} = Kl^2a^2\varphi_{zz} - kl^2\{2\sin\varphi - \sin2\varphi\}. \tag{5-11}$$

In the second case we have analogous pairs formed, however, by kink and antikink solutions of the sine-Gordon equation

$$I\varphi_{tt} = Kl^2a^2\varphi_{zz} - kl^2 2\sin\varphi. \tag{5-12}$$

4. *Interpretation*. Solutions of Eq. (5-12) describe the dynamics of DNA open states but more accurately.

The two nonlinear models presented above as examples could be considered as the elements of the hierarchy of nonlinear models [250]. Such a hierarchy can be easily constructed in the same way as was done in the previous chapter. In the following sections of this chapter we shall describe the main nonlinear models of different levels of the hierarchy.

5.2 Nonlinear Rod-like Models

Let us consider again the uniform elastic rod with circular section. This model takes into account three types of internal DNA motions: stretching, twisting and bending ones. As was shown in Chapter 4 the Hamiltonian of the model system has the form

$$H = H_{\mathrm{s}} + H_{\mathrm{t}} + H_{\mathrm{b}} + H_{\mathrm{s\text{-}t}} + H_{\mathrm{s\text{-}b}} + H_{\mathrm{t\text{-}b}}, \tag{5-13}$$

where the terms H_{s}, H_{t} and H_{b} describe longitudinal displacements (stretching), torsional motions (twisting) and bending motions in the elastic rod; the terms $H_{\mathrm{s\text{-}t}}$, $H_{\mathrm{s\text{-}b}}$ and $H_{\mathrm{t\text{-}b}}$ describe interactions between these motions. Taking into account the linear dynamical equations which we obtained in Section 4.2, the expected general form of the nonlinear equations corresponding to this Hamiltonian is

$$\rho u_{tt} = Yu_{zz} + \text{nonlinear term} + U_{\mathrm{s\text{-}t}} + \mathrm{U}_{\mathrm{s\text{-}b}}; \tag{5-14}$$

$$i\varphi_{tt} = C\varphi_{zz} + \text{nonlinear term} + \Phi_{\mathrm{t\text{-}s}} + \Phi_{\mathrm{t\text{-}b}}; \tag{5-15}$$

$$S\rho\gamma_{tt} = -YI\gamma_{zz} + \text{nonlinear term} + Y_{\mathrm{b\text{-}s}} + Y_{\mathrm{b\text{-}t}}; \tag{5-16}$$

where $U_{\mathrm{s\text{-}t}}$, $U_{\mathrm{s\text{-}b}}$, $\Phi_{\mathrm{t\text{-}s}}$, $\Phi_{\mathrm{t\text{-}b}}$, $Y_{\mathrm{b\text{-}s}}$ and $Y_{\mathrm{b\text{-}t}}$ are the terms describing interactions between internal motions in DNA.

The problem of deriving the form of all terms of Eqs. (5-14) – (5-16) has not been solved yet. Only a few simple models which could be considered as particular cases of the general problem have been investigated. Muto et al. [251], Christiansen et al. [252] and Ichikawa et al. [253] each developed such a model.

5.2.1 The Rod-like Model of Muto

To describe the model of Muto let us return again to the discrete version of the model of the elastic rod, and consider a one-dimensional lattice with lattice constant a and N lattice points (disks) (Figure 1.8b). Let us suggest that the longitudinal displacements of disks from their equilibrium positions are given by u_1, u_2, ... u_n, and the potential of the springs connecting the disks is described by the formula of Toda

$$V(u_{n+1} - u_n) = (A/B)\exp[-B(u_{n+1} - u_n)] + A(u_{n+1} - u_n), \tag{5-17}$$

where A and B are arbitrary parameters, $n = 1,2, \ldots N$.

Then the corresponding dynamical equations take the form

$$m\ddot{u}_n = V'(u_{n+1} - u_n) + V'(u_n - u_{n-1}), \quad n = 1,2, \ldots N. \tag{5-18}$$

To pass then to the continuum approximation, let us use the formula

$$\lim_{a\to 0} \{T(f_{n+1}) - 2T(f_n) + T(f_{n-1})\} = [1 - (a^2/12)(\partial^2/\partial z^2)]^{-1}\, a^2(\partial^2/\partial z^2)T(f); \tag{5-19}$$

obtained by Collins [254], Rosenau [255] and Hyman [256]. Here T is the nonlinear function of $f_n(t)$. In the continuum approximation $na \to z$; $f_n(t) \to f(z,t)$, and Eq. (5-18) reduces to

$$(\rho/A)u_{tt} = \beta u_{zz} - (\beta^2/2)(u^2)_{zz} + (\rho\alpha^2/12A)u_{zztt}; \tag{5-20}$$

where $\rho = m/a$, $\beta = aB$. Equation (5-20), obtained by Muto and coauthors, can be considered as a particular case of the more general Eq. (5-14) where only longitudinal motions are taken into account. Equation (5-20) has the form of the improved Boussinesq equation [257, 258], and in the soliton limit it has the compressional solitary-wave solution [252]

$$u(z,t) = -(3/\beta)(v^2-1)\ \mathrm{sech}^2\ \{[3/(v^2-1)]^{1/2}/va\}\{z\text{-}v(\beta A/\rho)^{1/2}t\text{-}z_0] \tag{5-21}$$

which travels with velocity $v(\beta A/\rho)^{1/2}(|v| > 1)$. The maximum amplitude is $3(v^2-1)/\beta$ and the width of the solitary wave is inversely proportional to $[3/(v^2-1)]^{1/2}/va$ (z_0 is the position of the solitary wave at time $t = 0$).

5.2.2
The Model of Christiansen

In 1990 Christiansen and coauthors suggested an improved model where the disks are permitted to move not only longitudinally but also transversely [252].

In the improved model it is assumed that longitudinal and transverse displacements of disks from their equilibrium positions are given by $u_1, u_2, \ldots, u_N$ and $y_1, y_2, \ldots, y_N$, respectively. The elongation (or compression) of the spring connecting the nth and the $(n+1)$th disks is given by

$$r_n = [(a + u_{n+1} - u_n)^2 + (y_{n+1} - y_n)^2]^{1/2} - l. \tag{5-22}$$

And the Toda potential imitating interactions between disks has the form

$$V(r_n) = (A/B)[\exp(-Br_n) - 1] + Ar_n;$$

where A and B are constants.

The Hamiltonian of the model can now be written in the form

$$H = \sum_{n=1}^{N} [m(\dot{u}_n^2 + \dot{y}_n^2) + V(r_n)]; \tag{5-23}$$

and the dynamical equations corresponding to the Hamiltonian are

$$m\ddot{u}_n = -V'(r_n)\,\partial r_n/\partial u_n - V'(r_{n-1})\,\partial r_{n-1}/\partial u_n;$$
$$m\ddot{y}_n = -V'(r_n)\,\partial r_n/\partial y_n - V'(r_{n-1})\,\partial r_{n-1}/\partial y_n. \qquad (5\text{-}24)$$

In the continuum limit and in the first approximation the dynamical equations reduce to two decoupled equations

$$(\rho/A)u_{tt} = \beta u_{zz} - (\beta^2/2)(u^2)_{zz} + (\rho\alpha^2/12A)u_{zztt}, \qquad (5\text{-}25)$$

$$(\rho/A)y_{tt} = (\rho/A)(a^2/12)y_{zztt}; \qquad (5\text{-}26)$$

where $\rho = m/a$, $\beta = aB$. The solitary wave solution of Eq. (5-25) has a form similar to Eq. (5-21).

5.2.3
The Rod-like Model of Ichikawa

The model of Ichikawa et al. [253] was developed to study anharmonic effects in the bending dynamics of a beam. If we use the approach based on the hierarchy, we can consider this model as the first-level model of DNA. So, we can apply the results obtained by Ichikawa and coauthors to DNA.

According to Ichikawa the equations of motion of the small element AB illustrated in Figure 5.2 can be written as

$$\rho S\partial^2 y/\partial t^2 = \partial\overline{S}/\partial x,$$
$$\partial M/\partial x + P\partial y/\partial x + \overline{S} = 0, \qquad (5\text{-}27)$$

where ρ is the density of the material, S is the cross-sectional area, $\overline{S}$ is the stress resultant parallel to the y axis, and P is the end-thrust parallel to the x axis. $\overline{S}$ and P are assumed to be constant. For bending moment M we have the following relation [259]

$$M = EI/R = EI(\partial^2 y/\partial x^2)/\{1 + (\partial y/\partial x)^2\}^{3/2}, \qquad (5\text{-}28)$$

where E is the Young's modulus, I the moment of inertia and R represents the radius of curvature of bending beam. Combining Eqs. (5-27) and (5-28) we obtain the nonlinear partial differential equation

$$\rho S\partial^2 y/t^2 + P(2y/x^2)y + EI2\{[2y/x^2]/[1 + (y/x)^2]^{3/2}\}/x^2 = 0, \qquad (5\text{-}29)$$

which describes the bending dynamics of the beam.

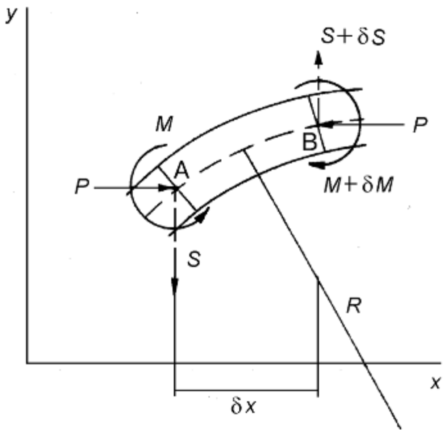

Figure 5.2 Transverse displacement of elastic rod.

Dynamical Eq. (5-29) can be considered as a particular case of the more general Eq. (5-16) describing the bending dynamics of DNA. It can be reduced to the form

$$\partial^2 Y/\partial T^2 - \partial^2 Y/\partial X^2 + 2\varepsilon d^2\{[1 + (\partial Y/\partial X)^2]^{3/2}\, \partial^2 Y/\partial X^2\}/X^2 = 0, \tag{5-30}$$

where the dimensionless variables X, Y and T are defined as $x = A^{½}X$, $y = A^{½}Y$, $t = (A^{½}/\lambda)T$, and the parameters are defined *as* $\lambda = (\sigma/\rho A)^{½}$, $\varepsilon = EI/2\sigma A$, $\sigma = -P$. Restricting our interests to propagation of the nonlinear deformation wave along DNA, we can introduce the stretched coordinates

$$\begin{aligned} \xi &= X + T, \\ \tau &= T. \end{aligned} \tag{5-31}$$

Retaining up to the first order of ε, which measures the relative size of bending stiffness over tensile along DNA, we can reduce Eq. (5-30) to

$$\partial(\partial Y/\partial\xi)/\partial\tau + \partial^2/\{[\partial^2 Y/\partial\xi^2]/[1+(\partial Y/\partial\xi)^2]^{3/2}\}/\partial\xi = 0. \tag{5-32}$$

Equation (5-32) has been shown to be integrable by the inverse scattering transformation [260]. Indeed, introducing the variable η defined as

$$\eta = \xi \pm \nu, \;\; \nu > 0 \tag{5-33}$$

and carrying out the integration twice, we obtain

$$\nu Y \pm \{1 + (\partial Y/\partial\eta)^2\}^{3/2}\, \partial^2 Y/\partial\eta^2 = 0. \tag{5-34}$$

This equation is known to be the equation which determines the shape of the surface of a fluid in a gravitational field and bounded on one side by a vertical wall [261]. The localized solitary solution of the equation is determined by the expression

$$\pm v^{1/2}(\eta - \eta_0) = -\operatorname{sech}^{-1}|\nu^{1/2}Y/2| + 2(1 - \nu Y^2/4)^{1/2}. \tag{5-35}$$

The solution is illustrated in Figure 5.3. We can interpret it as a local deformation moving along the DNA.

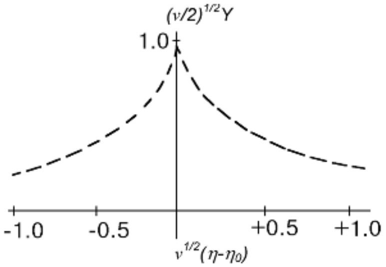

Figure 5.3 The solution of Ichikawa's model. Reproduced with permission from Ref. [253].

5.3 Nonlinear Double Rod-like Models

Let us consider now the model consisting of two elastic chains weakly interacting with one another (Figure 1.9a). A discrete analog of the model is shown in Figure 1.9b. It consists of two straight chains of disks connected by longitudinal and transverse springs. We assume that every disk in a chain can (i) move along the chain (longitudinal motions), (ii) move perpendicular to the chain (transverse motions), and (iii) rotate around the chain (torsional motions).

5.3.1 General Case: Hamiltonian

As we could expect the general form of the Hamiltonian, consisting of several terms

$$H = \sum_{i=1}^{2} \{H_{\mathrm{l}}^{(i)} + H_{\mathrm{t}}^{(i)} + H_{\mathrm{tr}}^{(i)} + H_{\mathrm{l\text{-}t}}^{(i)} + H_{\mathrm{l\text{-}tr}}^{(i)} + H_{\mathrm{t\text{-}tr}}^{(i)}\} \quad + H^{(1\text{-}2)}, \tag{5-36}$$

coincides with Eq. (4-27) except that each of the terms contains, besides harmonic (quadratic) terms, terms of higher order (anharmonic terms). The terms $H_{\mathrm{l}}^{(i)}$, $H_{\mathrm{t}}^{(i)}$ and $H_{\mathrm{tr}}^{(i)}$ of Eq. (5-36) describe the contribution of longitudinal, torsional and transverse motions of the disks in the ith chain ($i = 1, 2$); the terms $H_{\mathrm{l\text{-}t}}^{(i)}$, $H_{\mathrm{l\text{-}tr}}^{(i)}$ and $H_{\mathrm{t\text{-}tr}}^{(i)}$ describe interactions between the motions of the disks in the same (ith) chain; the term $H^{(1\text{-}2)}$ describes the interaction between the chains through transverse springs, and it has a form very similar to Eq. (4-28):

$$H^{(1\text{-}2)} = H^{(1\text{-}2)}_{\text{l-l}} + H^{(1\text{-}2)}_{\text{t-t}} + H^{(1\text{-}2)}_{\text{tr-tr}} + H^{(1\text{-}2)}_{\text{l-t}} + H^{(1\text{-}2)}_{\text{l-tr}} + H^{(1\text{-}2)}_{\text{t-tr}}. \tag{5-37}$$

5.3.2
General Case: Dynamical Equations

Let us write the dynamical equations corresponding to the Hamiltonian (5-36). We can do this easily if we take into account the form of the equations written in the first (linear) approximation. So, the general form of the equations imitating longitudinal motions is

$$\begin{aligned} M\ddot{u}_{n,1} &= K_1^l\ (u_{n+1,1} - 2u_{n,1} - u_{n-1,1}) + \text{nonlinear terms} + \text{coupling terms}, \\ M\ddot{u}_{n,2} &= K_2^l\ (u_{n+1,2} - 2u_{n,2} - u_{n-1,2}) + \text{nonlinear terms} + \text{coupling terms}. \end{aligned} \tag{5-38}$$

The equations describing torsional motions are

$$\begin{aligned} I\ddot{\varphi}_{n,1} &= K_1^t\ l^2(\varphi_{n+1,1} - 2\varphi_{n,1} - \varphi_{n\text{-}1,1}) + \text{nonlinear terms} + \text{coupling terms}, \\ I\ddot{\varphi}_{n,2} &= K_2^t\ l^2(\varphi_{n+1,2} - 2\varphi_{n,2} - \varphi_{n\text{-}1,2}) + \text{nonlinear terms} + \text{coupling terms}. \end{aligned} \tag{5-39}$$

And those describing transverse motions are

$$\begin{aligned} M\ddot{y}_{n,1} &= K^{\text{b}}(y_{n+1,1} - 2y_{n,1} - y_{n-1,1}) + \text{nonlinear terms} + \text{coupling terms}, \\ M\ddot{y}_{n,2} &= K^{\text{b}}(y_{n+1,2} - 2y_{n,2} - y_{n-1,2}) + \text{nonlinear terms} + \text{coupling terms}. \end{aligned} \tag{5-40}$$

Here $u_{n,i}$, $\varphi_{\text{n,i}}$ and $y_{\text{n,i}}$ are longitudinal, angular and transverse displacements, respectively; M and I are the masses and the moments of inertia of the disks; K_i^{l} and K_i^{t} are the longitudinal and torsional rigidities of the ith chain ($i = 1, 2$) and K^{b} is the rigidity of the transverse springs between the chains.

The explicit form of the nonlinear terms and coupling terms of Eqs. (5-38) – (5-40) has not been found yet, and nobody has tried to construct them and to consider the problem in the general case. Only a few simplified approaches to the problem have been proposed. One was presented in the works of Yomosa [16, 17], Takeno and Homma [18, 19], Fedyanin and coauthors [23, 24], Zhang [28] and Yakushevich [26]. We shall call the corresponding approximate model the Y-model. Another version was developed by Peyrard and Bishop [34, 262]. One more interesting version was proposed by Muto and coauthors [32]. And other versions were proposed by Christiansen and coauthors [258], by Zhang [47], by Xiao and coauthors [263], by Zhang and Collins [264], by Barbi and coauthors [265, 266], and Campa [267]. Below we describe the main models in detail.

5.3.3
The Y-model

The Y-model can be considered on the one hand as an improved version of Englander's model described in Section 5.1, and on the other hand as a particular case of the general problem Eq. (5-38) – (5-40). The improvement consists in taking into account the rotational motions of the bases in both polynucleotide chains of the DNA molecule, while in Englander's model the rotational motions of the bases of only one of two polynucleotide chains were taken into account, and the other chain played the role of the source of some potential field which was an analog of the gravitational field in the mechanical model of Scott. This improvement leads to the appearance of two coupled nonlinear equations [26]

$$I\ddot{\varphi}_1 = K_1^t a^2 l^2 \varphi_{1\,zz} + K^b l^2[2\sin\varphi_1 - \sin(\varphi_1 + \varphi_2)],$$
$$I\ddot{\varphi}_2 = K_2^t a^2 l^2 \varphi_{2\,zz} + K^b l^2[2\sin\varphi_2 - \sin(\varphi_2 + \varphi_1)] \tag{5-41}$$

instead of one equation of type (5-2). Let us illustrate how Eq. (5-41) can be obtained. It is convenient to begin with a discrete version of the double rod-like model shown in Figure 1.9b and then pass to the continuous approximation.

5.3.3.1 Discrete Case

The discrete analog of the Y-model consists of two chains of disks connected by longitudinal and transverse springs. The Hamiltonian of such a model has the form

$$H = T + V^{(1)} + V^{(2)}, \tag{5-42}$$

where T is the kinetic energy of torsional vibrations of the disks, and $V^{(1)}$ is the potential energy of the longitudinal springs and $V^{(2)}$ is the potential energy of the transverse ones. For T we have

$$T = \sum_{i,n} I_i \dot{\varphi}_{i,n}^2/2. \tag{5-43}$$

Here i and n are the numbers of the chains and disks, respectively, ($i = 1, 2$; $n = 1, 2,\ldots N$), $\varphi_{i,n}$ is the angle of rotation of the nth disk of the ith chain; and I_i is the moment of inertia of the disks of the ith chain. For $V^{(1)}$ we have

$$V^{(1)} = \sum_{i,n} K_i^1 \Delta \bar{\bar{l}}^{\,2}_{i;n,n+1}/2, \tag{5-44}$$

where K_i^1 is the rigidity of the longitudinal springs of the ith chain, and $\Delta\bar{\bar{l}}_{i;n,n+1}$ is the stretching of the longitudinal spring between the nth and (n+1)th disks in the *ith chain*

$$\Delta\bar{\bar{l}}_{i;n,n+1} = l\,[1\text{-}\cos(\varphi_{i,n} - \varphi_{i,n+1})]. \tag{5-45}$$

Here l is the radius of the disks.

In Section 1.3, when describing the main interactions in DNA, we showed that hydrogen interactions between bases in pairs are much weaker than the usual chemical interactions. So, we can assume that in our model longitudinal springs imitating chemical bonds in sugar–phosphate chains are more rigid than transverse springs imitating hydrogen bonds. As a result, we can conclude that the linear approximation is quite correct when modeling $V^{(1)}$, but the nonlinear approximation should be used when modeling $V^{(2)}$.

In the linear approximation the potential energy of the longitudinal springs $V^{(1)}$ then transforms to

$$V^{(1)} = \sum_{i,n} K_i^{\mathrm{t}} l^2 (\varphi_{i,n+1} - \varphi_{i,n})^2/2. \tag{5-46}$$

For $V^{(2)}$ we assume the form

$$V^{(2)} = \sum_{n} K^{\mathrm{b}} (\Delta \bar{l})^2/2; \tag{5-47}$$

where K^{b} is the rigidity of the transverse springs, and $\Delta \bar{l}_n$ is the stretching of the nth transverse spring due to rotations of the disks (see Figure 5.4)

$$\Delta \bar{l}_n = [(2l + \bar{l}_0 - l\cos\varphi_{1,n} - l\cos\varphi_{2,n})^2 + (l\sin\varphi_{1,n} - l\sin\varphi_{2,n})^2]^{½} - \bar{l}_0. \tag{5-48}$$

Here $\bar{l}_0$ is the length of the transverse spring in the equilibrium state.

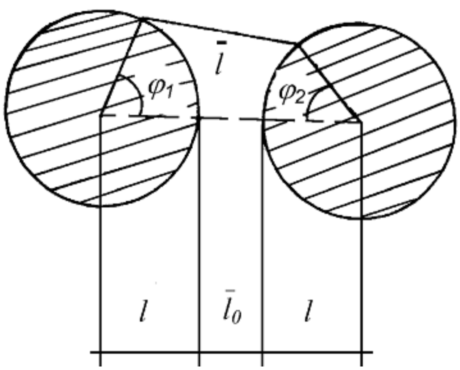

Figure 5.4 Cross-section of a pair of disks.

The dynamical equations associated with the Hamiltonian H are

$$I_1\ddot{\varphi}_{1,n} = K_1^t l^2(\varphi_{1,n+1} + \varphi_{1,n-1} - 2\varphi_{1,n}) - K^{\mathrm{b}}(\Delta\bar{l}_n/\bar{l}_n)[(2l^2 + l\bar{l}_0)\sin\varphi_{1,n} -$$

$$- l^2\sin(\varphi_{1,n} + \varphi_{2,n})], \tag{5-49}$$

$$I_2\ddot{\varphi}_{2,n} = K_2^t l^2(\varphi_{2,n+1} + \varphi_{2,n-1} - 2\varphi_{2,n}) - K^b(\Delta\bar{l}_n/\bar{l}_n)[(2l^2 + l\bar{l})\sin\varphi_{2,n} -$$

$$- l^2\sin(\varphi_{2,n} + \varphi_{1,n})]; \tag{5-50}$$

where $\bar{l}_n = \bar{l}_0 + \Delta\bar{l}_n$.

5.3.3.2 Continuous Case

Now we can pass to the continuous limit by (1) substituting $\varphi_i(z,t)$ for $\varphi_{i,n}(t)$ and (2) expanding $\varphi_{i,n\pm1}(t)$ by the Taylor series up to $\varphi_{i_{zz}}$,

$$\varphi_{i,n\pm1}(t) \cong \varphi_i(z,t) \pm \varphi_{iz}(z,t) + (1/2)\varphi_{i_{zz}}(z,t)\, a^2 \pm \ldots \tag{5-51}$$

As a result, Eqs. (5-47) –(5-50) take the form

$$\begin{aligned} I_1\ddot{\varphi}_1 &= K_1^t\, l^2a^2\varphi_{1zz} - K^b(\Delta\bar{l}/\bar{l})[(2l^2 + l\bar{l}_0)\sin\varphi_1 - l^2\sin(\varphi_1 + \varphi_2)], \\ I_2\ddot{\varphi}_2 &= K_2^t\, l^2a^2\varphi_{2zz} - K^b(\Delta\bar{l}/\bar{l})[(2l^2 + l\bar{l}_0)\sin\varphi_2 - l^2\sin(\varphi_2 + \varphi_1)], \end{aligned} \tag{5-52}$$

where a is the distance between the nearest disks in the chains. For DNA in the B-conformation a is approximately equal to 3.4 Å.

The nonlinear Eq. (5-52) is rather complex because the coefficient $\Delta\bar{l}/\bar{l}$ is a function of variables φ_1 and φ_2

$$\Delta\bar{l}/\bar{l} = 1 - \bar{l}_0[(2l + \bar{l}_0 - l\cos\varphi_1 - l\cos\varphi_2)^2 + (l\sin\varphi_1 - l\sin\varphi_2)^2]^{½} \tag{5-53}$$

The equations can however be simplified if we assume that the distance between the disks in pairs is negligibly small ($\bar{l}_0$<< l). Putting $\bar{l}_0 = 0$, we finally obtain Eq. (5-41). The approximate Hamiltonian associated with Eq. (5-41) has the form

$$H = \int dz\{I_1\dot{\varphi}_1^2/2 + I_2\dot{\varphi}_2^2/2 + K_1^t a^2l^2\varphi_{1zz}^2/2 + K_2^t a^2l^2\varphi_{2zz}^2/2 - K^bl^2[2\cos\varphi_1 +$$

$$+ 2\cos\varphi_2 - \cos(\varphi_1+\varphi_2)]\} + \text{const.} \tag{5-54}$$

5.3.3.3 Linear Approximation

The solutions of Eqs. (5-41) can be easily obtained in the linear approximation. In this case, Eqs. (5-41) take the form

$$\begin{aligned} I_1\ddot{\varphi}_1 &= K_1^t l^2a^2\varphi_{1zz} - K^bl^2(\varphi_1 - \varphi_2) = 0, \\ I_2\ddot{\varphi}_2 &= K_2^t l^2a^2\varphi_{1zz} - K^bl^2(\varphi_2 - \varphi_1) = 0. \end{aligned} \tag{5-55}$$

Assuming that the solutions have the form of plane waves,

$$\varphi_1 = \varphi_{01} \exp[i(qz - wt)],$$
$$\varphi_2 = \varphi_{02} \exp[i(qz - wt)], \tag{5-56}$$

and inserting Eq. (5-56) into Eq. (5-55), we find the dispersion law

$$(Q_1 - I_1 w^2)(Q_2 - I_2 w^2) - K^{b2} l^4 = 0; \tag{5-57}$$

where $Q_i = K^{b2} a^2 l^2 q^2 + K^b l^2$, $(i = 1, 2)$, q is the wave vector, w is the frequency, and φ_{01}, φ_{02} are the amplitudes. Finally from Eq. (5-57) we find the values of the frequencies

$$w^2{}_{1,2}(q) = \{I_1 Q_2 + I_2 Q_1 + [(I_1 Q_2 - I_2 Q_1)^2 \pm 4 I_1 I_2 K^{b2} k^2 l^4]^{1/2}\}/2 I_1 I_2. \tag{5-58}$$

In the 'symmetrical' case, when $I_1 = I_2 = I$, $K_1^t = K_2^t = K^t$, the frequencies are

$$w_1^2 = K^t a^2 l^2 q^2 / I, \qquad w_2^2 = (K^t a^2 l^2 q^2 + 2K^b l^2)/I. \tag{5-59}$$

This result correlates well with Eqs. (4-48) obtained in the previous chapter. So, we can conclude that the torsional vibrations with frequency w_1 are of the acoustic type (i.e. $\lim_{q\to 0} w_1 = 0$) and those with frequency w_2 are of the optical type (i.e. $\lim_{q\to 0} w_2 = (2K^b l^2/I)^{1/2} = 0$) (Figure 5.5).

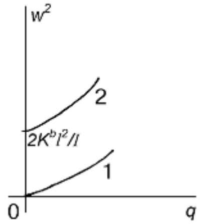

Figure 5.5 Two branches of the DNA torsional vibrations calculated in the framework of the linear approximation of the Yomosa model.

The same picture can be found in the general case. Indeed, if we insert $q = 0$ into Eqs. (5-58), we obtain

$$w_1^2(q = 0) = 0; \qquad w_2^2(q = 0) = K^b l^2 (I_1 + I_2)/I_1 I_2. \tag{5-60}$$

Eqs. (5-60) show that the vibrational spectrum of the model considered consists of two branches: acoustic and optical. Let us now compare this result with the result of calculations of the frequency of the torsional oscillations obtained in the framework of a rod-like model (see Section 4.2). In that case only the acoustic branch in the DNA spectrum was obtained. So, we can conclude that the appearance of the second (optical) branch in the DNA spectrum can be explained by the double-strand character of the Y-model.

5.3.3.4 The First Integral

The general solution of Eqs. (5-41) has not been found yet but the first integral can be easily obtained by the following algorithm:

1. Let us assume that the solution of Eqs. (5-41) has the form of running waves:

$$\varphi_1 = \varphi_1(z\text{-}vt), \qquad \varphi_2 = \varphi_2(z\text{-}vt), \tag{5-61}$$

where v is the velocity of the waves.

2. Insert Eq. (5-61) into Eq. (5-41):

$$\begin{aligned} &W_1^2\,\varphi_1'' - K^{\mathrm{b}}l^2[2\sin\varphi_1 - \sin(\varphi_1 + \varphi_2)] = 0,\\ &W_2^2\,\varphi_1'' - K^{\mathrm{b}}l^2[2\sin\varphi_2 - \sin(\varphi_1 + \varphi_2)] = 0. \end{aligned} \tag{5-62}$$

Here

$$W_1^2 = I_i v^2 - K_i^t a^2 l^2; \qquad \varphi_i'' = d^2\varphi_i/\mathrm{d}\xi^2;\ \xi = z\text{-}vt;\ i = 1, 2.$$

3. Multiply the first of Eqs. (5-62) by φ_1' and the second by φ_2'.
4. Sum the results.
5. Integrate the expression obtained.

   As a result we obtain the first integral in the form

$$W_1^2\,\varphi_1'^2/2 + W_2^2\,\varphi_2'^2/2 - K^{\mathrm{b}}l^2[2\cos\varphi_1 + 2\cos\varphi_2 - \cos(\varphi_1 + \varphi_2)] = \text{const.} \tag{5-63}$$

Expression (5-63) can be interpreted as an energy conservation law.

5.3.3.5 Kink-like Solutions Found by Newton's Method

To solve Eqs. (5-41) by Newton's method, let us assume that their solutions have the form of Eq.(5-61) and rewrite the corresponding Eqs. (5-63) in the following way:

$$\begin{aligned} &\mathrm{d}^2\varphi_1/\mathrm{d}\xi^2 + \alpha_1\{2\sin\varphi_1 - \sin(\varphi_1 + \varphi_2)\} = 0,\\ &\mathrm{d}^2\varphi_2/\mathrm{d}\xi^2 + \alpha_2\{2\sin\varphi_2 - \sin(\varphi_1 + \varphi_2)\} = 0, \end{aligned} \tag{5-64}$$

where $\alpha_1 = K^{\mathrm{b}}l^2/W_1^2$; $\alpha_2 = K^{\mathrm{b}}l^2/W_2^2$. For simplicity we shall assume below that $\alpha_1 \cong \alpha_2 = \alpha$.

Equations (5-64) can be interpreted as those describing torsional oscillations of two coupled nonlinear pendula. In the framework of this mechanical model the variable ξ plays the role of 'time' and the variables φ_1 and φ_2 the role of angular displacements of the pendula from their equilibrium positions.

One more interpretation of Eqs. (5-64) can be proposed. If we suggest that the variable ξ is the 'time' and the fields φ_1 and φ_2 are 'coordinates', then Eqs. (5-64) can be considered as an ordinary Newton's law which describes two-dimensional motion of a mechanical particle under the action of some potential $V(\varphi_1, \varphi_2)$.

Indeed, it is easy to rewrite Eqs. (5-64) in the form of Newton's law:

$$d^2\varphi_i/d\xi^2 = -dV(\varphi_1, \varphi_2)/d\varphi_i; \quad i = 1, 2; \tag{5-65}$$

with the potential function $V(\varphi_1, \varphi_2)$ determined by

$$V(\varphi_1, \varphi_2) = 2\alpha(\cos\varphi_1 + \cos\varphi_2) - \alpha\cos(\varphi_1 + \varphi_2) + C. \tag{5-66}$$

Here C is an arbitrary constant. It is convenient to choose the constant C so that the function V is nonpositive and equal to zero at the points of the absolute maximum. Then the potential V takes the form

$$V(\varphi_1, \varphi_2) = \alpha[1 - \cos(\varphi_1 + \varphi_2)] - 2\alpha(1 - \cos\varphi_1) - 2\alpha(1 - \cos\varphi_2). \tag{5-67}$$

For a correct statement of the 'mechanical' problem, Newton's equations (5-65) should be supplemented with boundary conditions. These conditions can be found from the requirement that the energy density of a solitary wave $\varepsilon(z,t)$ must be localized in space. Since we use variable ξ instead of z and t, the requirement can be formulated in the following way: $\varepsilon(\xi)$ must be a limited function at some interval on the axis and tend to zero when $\xi \to \pm\infty$. From this it follows that

$$d\varphi_1/d\xi \to 0, \quad d\varphi_2/d\xi \to 0, \tag{5-68}$$

$$V(\varphi_1,\varphi_2) \to 0, \tag{5-69}$$

when $\xi \to \pm\infty$.

Designating the points of the maximum of the potential function $V(\varphi_1,\varphi_2)$ by pairs of 'coordinates' $\{g_{1,n}; g_{2,m}\}$ and using condition (5-69), we find that

$$\varphi_1 \to g_{1,n}; \quad \varphi_2 \to g_{2,m}; \tag{5-70}$$

when $\xi \to \pm\infty$.

Expressions (5-68) and (5-70) completely determine the boundary conditions for the 'mechanical' problem.

Integration of Newton's equations (5-65) supplemented with potential (5-67) and boundary conditions (5-68), (5-70) is a rather difficult problem. Nobody has succeeded in finding the general solutions. However, some particular solutions can be found by using the method of trajectories [268]. Let us illustrate this method.

First, we should model the function $G(\varphi_1, \varphi_2)$ which determines the so-called equation of trajectories

$$G(\varphi_1, \varphi_2) = 0. \tag{5-71}$$

Taking into account the form of the potential (5-67), it is natural to assume that the function G is a linear combination of the functions $\cos\varphi_1$ and $\cos\varphi_2$. Then Eq. (5-71) transforms to

$$G(\varphi_1, \varphi_2) = A\cos\varphi_1 + B\cos\varphi_2 = 0; \tag{5-72}$$

where A and B are arbitrary constants.

Let us consider here a more simple variant of Eq. (5-71). Namely, let us assume that $A + B = 0$. Then, instead of Eq. (5-72) we have

$$\cos\varphi_1 = \cos\varphi_2, \tag{5-73}$$

whence we find two families of trajectories

$$\begin{aligned} \varphi_1^{(1)} &= \varphi_2 \pm 2n, \quad n = 0, 1, 2, \ldots, \\ \varphi_2^{(2)} &= \varphi_1 \pm 2m, \quad m = 0, 1, 2, \ldots . \end{aligned} \tag{5-74}$$

The mechanical trajectories obtained are shown in Figure 5.6. Filled circles designate the 'coordinates' of the maxima of the potential function V.

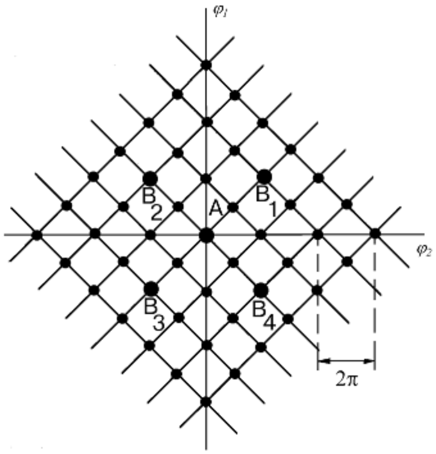

Figure 5.6 Mechanical trajectories.

Let us assume now that at $\xi = -\infty$ the mechanical particle analog is at point A. Then it can continue its movement along one of four trajectories (AB_1, AB_2, AB_3 or AB_4) to reach one of the nearest points of maxima at $\xi = +\infty$. At the same time the functions φ_1 and φ_2 will change from zero (when $\xi = -\infty$) to 2π or -2π (when $\xi = +\infty$). So, we can conclude that Eqs. (5-65) have at least four pairs of kink- (antikink-) like solutions. They are shown in Figure 5.7. The full lines show the asymptotic behavior of the solutions when $\xi \to \pm\infty$. The dashed lines show conventionally the behavior of the solutions in the vicinity of the point $\xi = 0$. The exact behavior near the zero point can be found from Eqs. (5-64) supplemented by additional requirements: $\varphi_1 = \varphi_2$ or $\varphi_1 = -\varphi_2$. In the first case, Eqs. (5-64) transform to the double sine-Gordon equation

$$d^2\varphi/d\xi^2 + 2\alpha\sin\varphi - \alpha\sin 2\varphi = 0, \qquad \varphi_1 = \varphi_2 = \varphi. \tag{5-75}$$

In the second case, Eqs. (5-64) transform to the ordinary sine-Gordon equation

$$d^2\varphi/d\xi^2 + 2\alpha\sin\varphi = 0, \quad \varphi_1 = -\varphi_2 = \varphi. \tag{5-76}$$

Both Eqs. (5-75) and (5-76) have kink- (antikink-) like solutions (see, for example, Refs. [8, 249]) of the type shown in Figure 5.7.

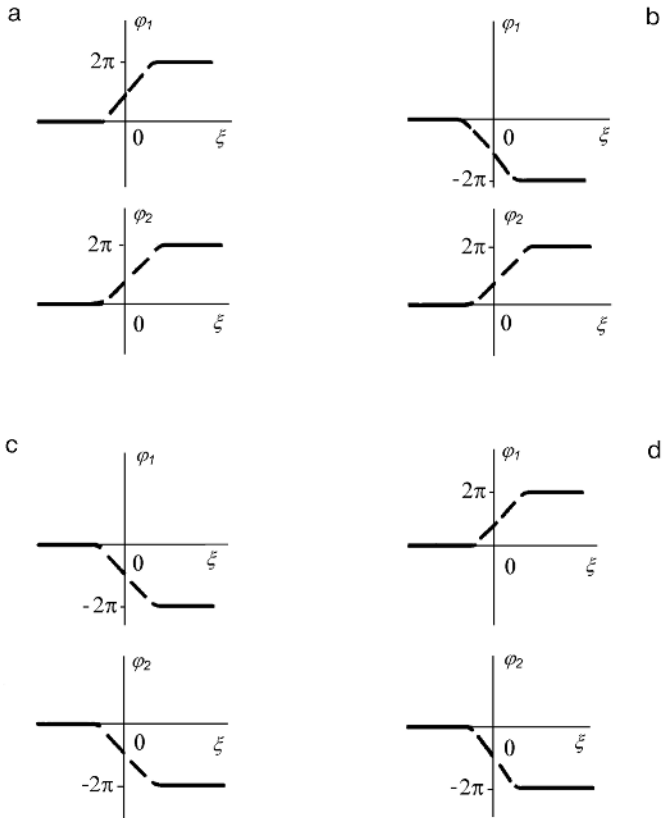

Figure 5.7 Soliton-like solutions corresponding to trajectories (a) AB_1, (b) AB_2, (c) AB_3 and (d) AB_4.

Let us now try to interpret these solutions. If we again use a simple schematic picture of the DNA molecule consisting of two long lines imitating sugar–phosphate chains and short transverse lines imitating bases, four types of local distortions corresponding to the four solutions shown in Figure 5.7 can be easily drawn (see Figure 5.8), and they do look like local open states moving along the DNA molecule.

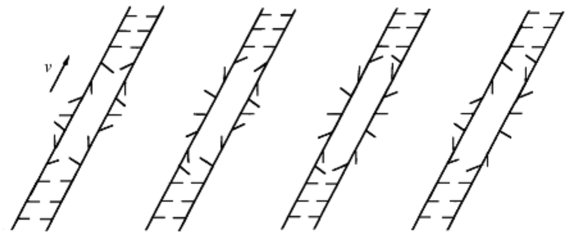

a b c d

Figure 5.8 Four types of conformational distortion in DNA, which correspond to trajectories (a) AB_1, (b) AB_2, (c) AB_3 and (d) AB_4.

These results have been obtained, however, only for a particular case when two assumptions (5-72) and (5-73) were made. In the general case application of the method of trajectories becomes rather complex and nobody has succeeded in finding new types of solutions by this method.

5.3.3.6 Kink-like Solutions Found by the Method of Hereman

Nonlinear Eqs. (5-41) can be solved by the direct algebraic method described in detail in the works of Hereman and coauthors [269–271]. This method is based on the search for solutions of nonlinear differential equations in the form of infinite series of exponential functions with real exponents. It is suggested that these exponents are the solutions of corresponding linearized differential equations. The coefficients in the expansions are found from recurrent relations and the infinite series obtained are summed to obtain solutions of the initial nonlinear differential equations in a closed form.

A significant limitation of this method is the requirement that the nonlinear equations should contain only strictly polynomial terms. Equations (5-41) do not meet this requirement: they contain three transcendent terms $\sin\varphi_1$, $\sin\varphi_2$ and $\sin(\varphi_1 + \varphi_2)$. We shall show below that this difficulty can be easily overcome.

First let us rewrite Eqs. (5-41) in a more convenient form

$$\begin{aligned} &\varphi_{1TT} - \varphi_{1ZZ} + 2\sin\varphi_1 - \sin(\varphi_1 + \varphi_2) = 0, \\ &\varphi_{2TT} - \varphi_{2ZZ} + 2\sin\varphi_2 - \sin(\varphi_1 + \varphi_2) = 0, \end{aligned} \tag{5-77}$$

where the new variables Z and T are determined by the formulas

$$Z = \alpha z; \quad T = \beta t; \tag{5-78}$$

where $\alpha = (K^b/K^t)^{1/2}/a$, $\beta = (K^b/I)^{1/2} l$. To overcome the limitation described above, let us expand the transcendental terms into the following series

$$\sin\varphi_1 = \varphi_1 - \varphi_1^3/3! + \varphi_1^5/5! - \ldots,$$

$$\sin\varphi_2 = \varphi_2 - \varphi_2^3/3! + \varphi_1^5/5! - \ldots, \tag{5-79}$$

$$\sin(\varphi_1 + \varphi_2) = (\varphi_1 + \varphi_2) - (\varphi_1 + \varphi_2)^3/3! + (\varphi_1 + \varphi_2)^5/5! - \ldots$$

Inserting expansions (5-79) into Eq. (5-77) yields

$$\varphi_{1TT} - \varphi_{1ZZ} + \sum_{n=0}^{\infty} (-1)^n [2\varphi_1^{2n+1} - (\varphi_1 + \varphi_2)^{2n+1}/(2n+1)!] = 0,$$

$$\varphi_{2TT} - \varphi_{2ZZ} + \sum_{n=0}^{\infty} (-1)^n [2\varphi_2^{2n+1} - (\varphi_1 + \varphi_2)^{2n+1}/(2n+1)!] = 0. \tag{5-80}$$

All terms in Eq. (5-80) are strictly polynomial, and, therefore, the Hereman method can be applied. The only difficulty which still remains is the presence of an infinitely large number of terms in the equations. However, we shall show below that this is not a serious difficulty because, at the final stage, all expansions can be easily summed, and the final results will be obtained in a closed form.

Following the procedure suggested by Hereman, let us transform the partial differential Eqs. (5-80) to ordinary differential equations by going over to the coordinate system

$$\xi = Z - vT; \tag{5-81}$$

which moves at some constant velocity v. Equations (5-80) then become

$$(v^2 - 1)\varphi_{1\xi\xi} + \sum_{n=0}^{\infty} (-1)^n [2\varphi_1^{2n+1} - (\varphi_1 + \varphi_2)^{2n+1}/(2n+1)!] = 0;$$

$$(v^2 - 1)\varphi_{2\xi\xi} + \sum_{n=0}^{\infty} (-1)^n [2\varphi_2^{2n+1} - (\varphi_1 + \varphi_2)^{2n+1}/(2n+1)!] = 0. \tag{5-82}$$

Then we assume that the solutions of Eqs. (5-82) can be represented as expansions in terms of exponential functions $g(\xi) = \exp(-q\xi)$

$$\varphi_1 = \sum_{n=1}^{\infty} a_n g^n, \qquad \varphi_2 = \sum_{n=1}^{\infty} b_n g^n, \tag{5-83}$$

where the value of q is an arbitrary constant. It is required that the exponential function $g(\xi)$ is the solution of the linear part of Eq. (5-82), which has the form

$$(\nu^2-1)\varphi_{1\xi\xi}+(\varphi_1-\varphi_2)=0;$$
$$(\nu^2-1)\varphi_{2\xi\xi}+(\varphi_1-\varphi_2)=0. \tag{5-84}$$

Inserting exponential function $g(\xi)$ into Eq. (5-84) yields the possible values of q

$$q^2(1-\nu^2)=\begin{cases}0\\2\end{cases} \tag{5-85}$$

In the general case we should consider all possible values of q. For simplicity, however, we consider here only one case when q is real and positive:

$$q=[2/(1-\nu^2)]^{1/2},\ \nu^2<1. \tag{5-86}$$

Inserting expansions (5-83) with the values of q determined by Eq. (5-86) into Eq. (5-82) we obtain the following recurrent relations:

$$\begin{aligned}
&2(1-n^2)a_n-(a_n+b_n)+(1/3!)\sum_{m=2}^{n-1}\sum_{l=1}^{m-1}[(a_l+b_l)(a_{m-l}+\\
&+b_{m-l})(a_{n-m}+b_{n-m})-2a_la_{m-l}a_{n-m}]-(1/5!)\sum_{p=4}^{n-1}\sum_{q=3}^{p-1}\sum_{m=2}^{q-1}\sum_{l=1}^{m-1}[(a_l+\\
&+b_l)(a_{m-l}+b_{m-l})(a_{q-m}+b_{q-m})(a_{p-q}+b_{p-q})(a_{n-p}+b_{n-p})-\\
&-2a_la_{m-l}a_{q-m}a_{p-q}a_{n-p}]+(1/7!)\sum_{r=6}^{n-1}\sum_{s=5}^{r-1}\sum_{p=4}^{s-1}\sum_{q=3}^{p-1}\sum_{m=2}^{q-1}\sum_{l=1}^{m-1}[(a_l+\\
&+b_l)(a_{m-l}+b_{m-l})(a_{q-m}+b_{q-m})(a_{p-q}+b_{p-q})(a_{s-p}+b_{s-p})(a_{r-s}+\\
&+b_{r-s})(a_{n-r}+b_{n-r})-2a_la_{m-l}a_{q-m}a_{p-q}a_{s-p}a_{r-s}a_{n-r}]=0;
\end{aligned} \tag{5-87}$$

$$\begin{aligned}
&2(1-n^2)b_n-(a_n+b_n)+(1/3!)\sum_{m=2}^{n-1}\sum_{l=1}^{m-1}[(a_l+b_l)(a_{m-l}+\\
&+b_{m-l})(a_{n-m}+b_{n-m})-2b_lb_{m-l}b_{n-m}]-(1/5!)\sum_{p=4}^{n-1}\sum_{q=3}^{p-1}\sum_{m=2}^{q-1}\sum_{l=1}^{m-1}[(a_l+\\
&+b_l)(a_{m-l}+b_{m-l})(a_{q-m}+b_{q-m})(a_{p-q}+b_{p-q})(a_{n-p}+b_{n-p})-
\end{aligned}$$

$$-2b_l b_{m-l} b_{q-m} b_{p-q} b_{n-p}] + (1/7!) \sum_{r=6}^{n-1} \sum_{s=5}^{r-1} \sum_{p=4}^{s-1} \sum_{q=3}^{p-1} \sum_{m=2}^{q-1} \sum_{l=1}^{m-1} [(a_l +$$

$$+b_l)(a_{m-l} + b_{m-l})(a_{q-m} + b_{q-m})(a_{p-q} + b_{p-q})(a_{s-p} + b_{s-p})(a_{r-s} +$$

$$+b_{r-s})(a_{n-r} + b_{n-r}) - 2b_l b_{m-l} b_{q-m} b_{p-q} b_{s-p} b_{r-s} b_{n-r}] = 0.$$

To solve Eqs (5-87) and to find the general structure of the coefficients a_n and b_n, let us compute step by step the first several coefficients. This yields

$$\begin{aligned}
&n = 1,\ a_1 + b_1 = 0, && \text{where } a_1 \text{ has an arbitrary value;}\\
&n = 2,\ a_2 = b_2 = 0; &&\\
&n = 3,\ a_3 + b_3 = 0, && \text{where } a_3 = -a_1^3/2^4 \times 3;\\
&n = 4,\ a_4 = b_4 = 0; &&\\
&n = 5,\ a_5 + b_5 = 0, && \text{where } a_5 = a_1^5/2^8 \times 5;\\
&n = 6,\ a_6 = b_6 = 0; &&\\
&n = 7,\ a_7 + b_7 = 0, && \text{where } a_7 = -a_1^7/2^{12} \times 7.
\end{aligned} \tag{5-88}$$

Formulas (5-88) allow us to recognize the general structures for the coefficients a_n and b_n

$$\begin{aligned}
&a_{2m+1} = -b_{2m+1} = (-1)^m a_1^{2m+1}/2^{4m}(2m+1).\\
&a_{2m} = b_{2m} = 0;\ m = 1, 2, \ldots
\end{aligned} \tag{5-89}$$

Inserting Eq. (5-89) into Eq. (5-83) yields

$$\varphi_1 = -\varphi_2 = \sum_{m=1}^{\infty} (-1)^m [a_1^{2m+1}/2^{4m}(2m+1)] \exp[-(2m+1)q]. \tag{5-90}$$

Sum (5-90) can be calculated by, first, differentiating Eq. (5-90):

$$\varphi_{1\xi} = -\varphi_{2\xi} = -4aqg \sum_{m=1} (-1)^m (a^2 g^2)^m = 4aqg/(1 + a^2 g^2), \tag{5-91}$$

where $a = a_1/4$, and, next, integrating the equation obtained. The integration of Eq. (5-91) gives the solutions of Eq. (5-82) in the form

$$\varphi_1(\xi) = -\varphi_2(\xi) = \int \varphi_{1\xi} d\xi = 4\arctan[a\exp(q\xi)] = 4\arctan[\exp q(\xi - \xi_0)]; \tag{5-92}$$

where $\xi_0 = -\ln a/q$.

Since the expansion (5-91) is convergent under the condition $ag < 1$, formulas (5-92) seem to be valid only in the region $\xi > \xi_0$. However, Hereman and coauthors noticed, that formulas (5-91) can be expanded in a convergent power series in $1/ag$ if $ag < 1$ (that is in the region $\xi < \xi_0$). Moreover, they proved that the left- and right-hand limits for $\xi \rightarrow \xi_0$ coincide. So, it can be concluded that formula (5-92) is valid over the whole region $-\infty < \xi < +\infty$.

Expression (5-92) transformed to the initial coordinates Z and T takes the form

$$\varphi_1(Z,T) = -\varphi_2(Z,T) = 4\arctan\{\exp[2/(1-v^2)]^{1/2}(Z-vT-Z_0)\}. \tag{5-93}$$

One of the functions in Eq. (5-93) coincides with the kink-like solution (5-4), the other is a reflection onto the negative plane. The only difference between Eq. (5-93) and Eq. (5-4) is the multiplier 2 in the square brackets, which in turn is explained by the multiplier 2 before $\sin\varphi$ and $\sin\varphi$ in the initial Eqs. (5-77). So, now we can easily draw a schematic picture of the functions (5-93) (see Figure 5.9), and the local distortion corresponding to the solution is shown in Figure 5.10. This solution coincides with one of the solutions found in the previous section by the method of Newton. It corresponds to the trajectory AB_4 and is shown schematically in Figure 5.7d.

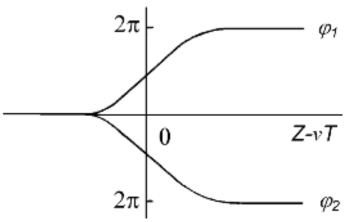

Figure 5.9 Solution of the equations (5-77) found by the method of Hereman.

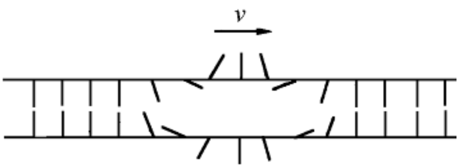

Figure 5.10 Conformational distortion corresponding to the solution (5-93).

5.3.4
The Model of Peyrard and Bishop

In contrast to the Y model, in the model of Bishop and Peyrard [34, 262] it is assumed that the main contribution to the process of local opening of base pairs (or local melting of the double helix) is made by the stretching of the hydrogen bonds. This is why, instead of rotation motions of bases, the model includes another two types of internal motions, namely, the displacements ($y_{1,n}$ and $y_{2,n}$) of the bases from their equilibrium positions along the direction of the hydrogen bonds that connect the two bases in a pair. The potential V for the hydrogen bonds is modeled by a Morse potential and a harmonic coupling due to the stacking is assumed between neighboring bases. So, the Hamiltonian for the model is

$$H = \sum_n \{m(\dot{y}_{1,n}^2 + \dot{y}_{2,n}^2)/2 + k[(y_{1,n} - y_{1,n-1})^2 + (y_{2,n} - y_{2,n-1})^2]/2 + V(y_{1,n} - y_{2,n})\} \tag{5-94}$$

with

$$V(y_{1,n} - y_{2,n}) = D\{\exp[-A(y_{1,n} - y_{2,n})] - 1\}^2.$$

As in the previous model the inhomogeneities due to the base sequence and the asymmetry of the two strands are neglected. Therefore, a common mass m is used for the bases and the same coupling constant k along each strand is assumed. The Morse potential $V(y_{1,n} - y_{2,n\text{-}1})$ is an average potential representing the two or three bonds which connect the two bases in a pair.

It is more convenient to describe the motion of two strands in terms of the variables

$$\begin{aligned} x_{1,n} &= (y_{1,n} + y_{2,n})/2^{½}; \\ x_{2,n} &= (y_{1,n} - y_{2,n})/2^{½}; \end{aligned} \tag{5-95}$$

which represent the in-phase and out-of-phase motions, respectively. The out-of-phase displacements $x_{2,}$n stretch the hydrogen bonds.

Hamiltonian (5-94) then takes the form

$$H = H(x_1) + H(x_2), \tag{5-96}$$

where

$$H(x_1) = \sum_n \{m\dot{x}_{1,n}^2/2 + k(x_{1,n} - x_{1,n-1})^2/2\}, \tag{5-97}$$

$$H(x_2) = \sum_n \{m\dot{x}_{2,n}^2/2 + k(x_{2,n} - x_{2,n-1})^2/2 + D[\exp(-A2^{½}x_{2,n}) - 1]^2\}. \tag{5-98}$$

The dynamical equations derived from the Hamiltonian are

$$m\partial^2 x_{1,n}/\partial t^2 - k(x_{1,n+1} + x_{1,n\text{-}1} - 2x_{1,n}) = 0; \tag{5-99}$$

$$m\partial^2 x_{2,n}/\partial t^2 - k(x_{2,n+1} + x_{2,n\text{-}1} - 2x_{2,n}) - 2^{3/2}DA\{\exp(-2^{½}Ax_{2,n})[\exp(-2^{½}Ax_{2,n}) - 1]\} = 0. \tag{5-100}$$

The first of the equations describes usual linear waves (phonons), the second describes the nonlinear waves (breathers). Equation (5-100) can be expanded in the continuum limit for small values of x as

$$m\partial^2 x/\partial t^2 - ka^2\partial^2 x/\partial z^2 + 2D\overline{A}^2 x - 3D\overline{A}^3 x^2 + (7/3)D\overline{A}^4 x^3 = 0; \tag{5-101}$$

where a is the distance between two base pairs; $\overline{A} = A(2)^{1/2}$. The solution of Eq. (5-101) was obtained in Ref. [271] via a multiple-scale expansion

$$x = \epsilon[F_1\,(Z,T)\exp(iwt) + c.c.] + \epsilon^2[F_0\,(Z,T) + F_2\,(Z,T)\exp(2iwt) + c.c.];$$

where $Z = \epsilon z$; $T = \epsilon t$; the functions F_0 and F_2 are expressed in terms of F_1 as $F_0 = 3\overline{\mathbf{A}}|F_1|^2$ and $F_2 = -\overline{\mathbf{A}}F_1{}^2/2$, and the function F_1 is a solution of the nonlinear Schrödinger equation

$$i\partial F_1/\partial s + (c_0{}^2/2w)\partial^2 F_1/\partial Z^2 + 2w\overline{A}^2|F_1|^2 F_1 = 0, \tag{5-102}$$

with $s = \epsilon T$; $c_0{}^2 = ka^2/m$ and $w = 2D\overline{A}^2/m$.

Equation (5-102) has soliton solutions which are interpreted as local distortions moving along the DNA molecule.

5.3.5
The Double Rod-like Model of Muto

To investigate the process of DNA denaturation, Muto et al. [32] suggested a simple model imitating two polynucleotide strands which are linked together through the hydrogen bonds. As in the previous two cases, to simplify the calculations the helical structure of DNA is neglected, and instead of the double helix, two parallel strands, each being a spring and mass system (Figure 5.11), are considered. Each mass represents a single base. The longitudinal springs connecting masses of the same strand represent the van der Waals potential between adjacent base pairs. The transverse springs represent the hydrogen bonds that connect bases in pairs. A homogeneous DNA is assumed, therefore each particle has mass m.

For each base pair, the model includes four degrees of freedom, $u_{1,n}$, $y_{1,n}$ and $u_{2,n}$, $y_{2,n}$, for the two strands, respectively. The $u_{1,n} = u_{1,n}(t)$ and $u_{2,n} = u_{2,n}(t)$, $n = 1, 2,...N$ denote the longitudinal displacements, i.e., the displacements of the bases from their equilibrium positions along the direction of the phosphodiester bridge that connects two bases of the same strand. The $y_{1,n} = y_{1,n}(t)$ and $y_{2,n} = y_{2,n}(t)$, $n = 1, 2,...N$ denote the transverse displacements, i.e., the displacements of the bases from their equilibrium positions along the direction of the hydrogen bonds that connect the two bases of the base pair.

The Toda potential which models the phosphodiester bridge has the form

$$V(r_n) = (A/B)\exp(-Br_n) + Ar_n; \tag{5-103}$$

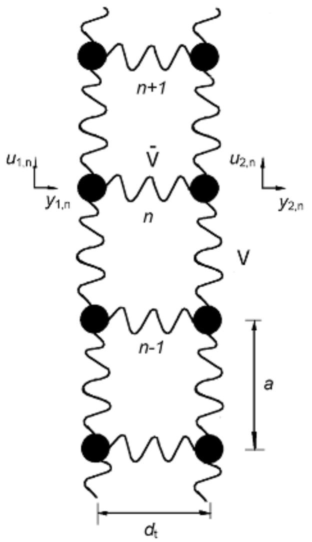

Figure 5.11 Schematic plot of the model of Muto. The two identical anharmonic Toda chains are connected by a Lennard-Jones potential representing the H-bonds between the two strands.

where r_n denotes the relative displacements, and A and B are positive parameters. So, the anharmonic potentials for the first and the second strands are given by

$$V_i(\lambda_{i,n} - a_i) = A/B \exp[-B(\lambda_{i,n} - a_i)] + A(\lambda_{i,n} - d_i),\ i = 1, 2. \tag{5-104}$$

Here $\lambda_{\mathrm{i,n}}$ denotes the distance between the nth and the $(n+1)$th base in the ith strand, and its expression is given by

$$\lambda_{i,n} = [(d_i + u_{i,n+1} - u_{i,n})^2 + (y_{i,n+1} - y_{i,n})^2]^{½}\,. \tag{5-105}$$

The Lennard-Jones potential which models hydrogen bonds is given by

$$\overline{V}(\tau_n - d_t + d_h) = 4\epsilon\{[\sigma/(\tau_n - d_t - d_h)]^{12} - [\sigma/(\tau_n - d_t - d_h)]^6\}; \tag{5-106}$$

where ε and σ are the parameters; $\tau_n - d_t - d_h$ is the length of the hydrogen bond between the two bases in the nth pair; and τ_n denotes the distance between two bases of the two strands

$$\tau_n = [(d_t + y_{2,n} - y_{1,n})^2 + (u_{2,n} - u_{1,n})^2]^{½}\,. \tag{5-107}$$

Moreover, d_t, is the equilibrium distance between the bases in a pair, namely the diameter of the helix (d_t = 20 Å), and d_h is the equilibrium length of the hydrogen bond.

The Hamiltonian of the model is given then by

$$H = \sum_{n=1}^{N} \sum_{i=1}^{2} \{M(\dot{u}_{i,n})^2/2 + M(\dot{y}_{i,n})^2/2\} + V_i(\lambda_{i,n} - a_i) + (\tau_n - d_t + d_h)\}. \quad (5\text{-}108)$$

Equations corresponding to the Hamiltonian were solved, however, only numerically and soliton-like solutions imitating open states were found [32].

5.3.6 The Model of Barbi

The model of Maria Barbi et al. [265, 266] takes into account the topological constraints related to the helicoidal structure of the molecule and provides an extension of the approach of Peyrard and Bishop [34, 262] towards a more realistic description of DNA dynamics.

The model consists of a sugar ring and its connected base which is treated simply as a point mass (without distinction between the different base types); the phosphate backbone between two base pairs is modeled as an elastic rod. The additional twist motion is introduced by allowing the two bases in each pair to move in the base pair plane instead of constraining them on a line. For convenience a polar coordinate system is chosen. The model does not attempt to describe the acoustic motions of the molecule since only the stretching of the base pair distance is considered. This amounts to fixing the center of mass of the base pair, i.e. the two bases in a pair are constrained to move symmetrically with respect to the axis of the molecule. Then, to describe the stretching of a base pair and the variation of the helicoidal twist, two degrees of freedom per base pair: the coordinates r_{n} and φ_{n} of one of the two bases with respect to a fixed reference frame, are used.

As in the model of Peyrard and Bishop [34, 262], a Morse potential describes the hydrogen bonds linking bases in a pair with an equilibrium distance R_0.

A proper choice of the coupling between radial and angular variables has to reproduce the equilibrium helicoidal structure. In DNA, the latter originates from the competition between the hydrophobic effect (that tends to eliminate water from the core of the molecule by bringing the neighboring base pair planes closer) and the rigidity of the two strands (that separates the external ends of the base pairs by essentially a fixed length related to the phosphate length).

The final Hamiltonian then takes the form

$$H = \sum_n \{m(\dot{r}_n^2 + r_n^2\dot{\varphi}_n^2)/2 - D\{\exp[-\alpha(r_n - R_0)] - 1\}^2 +$$

$$+ \sum_n K\{\sqrt{h^2 + r_{n-1}^2 + r_n^2 - 2r_{n-1}r_n\cos(\varphi_n - \varphi_{n-1})} - L\}^2 +$$

$$+ \sum_n G_0(\varphi_{n-1} + \varphi_{n+1} - 2\varphi_n)^2, \quad (5\text{-}109)$$

where m is the base mass, D and α are the depth and width of the Morse potential well, K is the backbone elastic constant, G_0 is the backbone curvature constant and L is determined by

$$L = \sum_n \sqrt{h^2 + 4R_0^2 \sin^2[(\varphi_n - \varphi_{n-1})/2]}. \tag{5-110}$$

Dynamical equations corresponding to Hamiltonian (5-109) have a small amplitude envelope solution made of a breather in radial variables combined with a kink in the angular variables. Just this solution was interpreted as that describing local opening of the hydrogen bonds and formation of denaturation bubbles.

5.3.7
The Model of Campa

Campa [267] extended the model of Barbi [265, 266] to include the case of heterogeneous chains, in order to get closer to a description of real DNA. He also suggested that (1) the bases can move only in planes perpendicular to the helix axis; (2) the center of the mass of the base pair is held fixed, and (3) the two complementary bases move symmetrically with respect to the axis of the molecule. So, for each base pair, there are only two degrees of freedom: r_n is the distance between each complementary base in the nth base pair and the helix axis; θ_n is the angle that the line joining the two complementary bases make with a given direction in the planes where the bases move.

The difference is that in the model of Campa the Morse potential representing the interaction between complementary bases has two possible depths, one for A-T base pairs and one for G-C base pairs. And the potential energy will have the following form

$$V = \sum_n \{D_n\{\exp[-\alpha(r_n - R_0)] - 1\}^2$$

$$+ \sum_n (1/2)\{C(r_{n+1} - r_n)^2 + K(L_{n+1,n} - L_0)_2\}, \tag{5-111}$$

where h is the fixed distance between neighboring base planes, R_0 is the equilibrium value of r_n, L_{n+1} is the distance between neighboring bases on the same strand

$$L_{n+1,n} = \sqrt{h^2 + r_{n+1}^2 + r_n^2 - 2r_{n+1}r_n\cos(\Delta\theta_n)}; \tag{5-112}$$

L_0 is the same function computed for $r_{n+1} = r_n = R_0$ and $\Delta\theta_n = \theta_0 = \pi/5$. So, the equilibrium configuration is that with $r_n = R_0$ and $\Delta\theta_n = \theta_0$ for each n, which gives the system its helicoidal structure.

The first two terms in Eq. (5-111) are the same as in the model of Peyrard and Bishop [34, 262], and there can be two different values for D_n: $D_{A\text{-}T}$ for A-T base pairs and $D_{G\text{-}C}$ for G-C base pairs. The last term in Eq. (5-111) describes a restoring force that acts when the distance L between neighboring bases on the same strand is different from L_0.

The model described above has been applied to study the process of local uncoupling of the double helix. It was shown analytically that, under some uncoiling, the system exhibits a stable equilibrium configuration in which there is a small region, of about 20 base pairs, where the hydrogen bond between complementary bases is completely disrupted, allowing access to the genetic code. Then, through MD simulations, it was found that these open regions can travel along the DNA chain, also when both thermal noise and heterogeneity are present.

5.4 Nonlinear Models of Higher Levels

To describe the nonlinear internal DNA dynamics more accurately we should use models of the third and higher levels. But, even models of the third levels are too complex to deal with. So, to investigate them we restrict ourselves to consideration of only a limited amount of dominant motions.

The form of the nonlinear dynamical equations describing the motions and the total amount of them depend substantially on the method of selection of the subunits and motions.

Here we describe briefly two examples of the model dynamical equations. The first was proposed by Krumhansl and Alexander [20], the other by Volkov [54].

5.4.1 The Model of Krumhansl and Alexander

To describe the A–B conformational transition in DNA, Krumhansl and Alexander selected the following subunits and motions: the longitudinal displacements of the nucleoside groups ($u_{i,n}$), the changes in pseudorotational phase angle describing the changes in the conformational states of the sugar groups ($P_{i,n}$), and the angular displacements of the bases ($\varphi_{\mathrm{i,n}}$) ($i = 1, 2$). So, the total Hamiltonian has the following form:

$$H = H_0 + H_{\mathrm{int}}. \tag{5-113}$$

The first term in Eq. (5-113) consists of three terms:

$$H_0 = H_{01} + H_{02} + H_{03}. \tag{5-114}$$

Let us discuss each of them. The term H_{01} takes the form

$$H_{01} = \sum_n \sum_{i=1}^{2} \{M\dot{P}^2_{i,n}/2 - AP^2_{i,n}/2 + BP^4_{i,n}/4 + (-1)^i CP_{i,n} + K(P_{i,n+1} - P_{i,n})^2/2\}. \tag{5-115}$$

It contains (i) the kinetic energy of the sugars with effective mass M; (ii) the local potential energy of the deoxyribose as a function of the pseudorotational phase angle (the parameters A and B are uncertain but a slightly asymmetric double-well is commonly accepted [273]) and a local field giving rise to asymmetry (this is characterized by the parameter C); (iii) interaction between adjacent sugars expressing the (energetic) favorability of uniform conformation of the sugars (this is characterized by the parameter K).

The term H_{02} takes the form

$$H_{02} = \sum_n \sum_{i=1}^{2} \{M_N \dot{u}_{i,n}^2/2 + k_N (u_{i,n+1} - u_{i,n})^2/2\}. \tag{5-116}$$

This contains the kinetic and potential energy associated with the motions of nucleotides parallel to the helix axis.

The term H_{03} takes the form

$$H_{03} = \sum_n \sum_{i=1}^{2} \{M_B \sum_n \sum_{i=1}^{2} a^2/2 + k_B a^2 (\varphi_{i,n+1} - \varphi_{i,n})^2/2 \tag{5-117}$$

This contains kinetic and potential energy associated with the angular motions of the bases

The second term in Eq. (5-113) H_{int} describes the coupling between different types of motions

$$H_{\text{int}} = \sum_n \sum_{i=1}^{2} \{X_0 (P_{i,n+1} - P_{i,n})(u_{i,n+1} - u_{i,n}) + X_2 (\varphi_{i,n+1} - \varphi_{i,n})(P_{i,n+1} - P_{i.n})\} +$$
$$+ \sum_n X_1 \{P_{n+1,1}(u_{n+1,1} - u_{n,1}) + P_{n+1,2}(u_{n+1,2} - u_{n+2,2})\}. \tag{5-118}$$

Dynamical equations corresponding to the Hamiltonian (5-113) are

$$-M\partial^2 P_{1,n}/\partial t^2 = -C - AP_{1,n} + BP_{1,n}^3 + K(2P_{1,n} - P_{1,n-1} - P_{1,n+1}) + X_0(2u_{1,n} - u_{1,n-1} -$$

$$- u_{1,n+1}) + X_1(u_{1,n} - u_{1,n-1}) + X_2(2\varphi_{1,n} - \varphi_{1,n-1} - \varphi_{1,n+1}),$$

$$-M\partial^2 P_{2,n}/\partial t^2 = C - AP_{2,n} + BP_{2,n}^3 + K(2P_{2,n} - P_{2,n-1} - P_{2,n+1}) + X_0(2u_{2,n} - u_{2,n-1} -$$

$$- u_{2,n+1}) + X_1(u_{2,n} - u_{2,n-1}) + X_2(2\varphi_{2,n} - \varphi_{2,n-1} - \varphi_{2,n+1}),$$

$$-M_N\partial^2 u_{1,n}/\partial t^2 = k_N(2u_{1,n} - u_{1,n-1} - u_{1,n+1}) + X_0(2P_{1,n} - P_{1,n-1} - P_{1,n+1}) +$$

$$+ X_1(P_{1,n} - P_{1,n+1}),$$

$$-M_N\partial^2 u_{2,n}/\partial t^2 = k_B(2u_{2,n} - u_{2,n-1} - u_{2,n+1}) + X_0(2P_{2,n} - P_{2,n-1} - P_{2,n+1}) +$$

$$+ X_1(P_{2,n} - P_{2,n-1}),$$

$$- M_B a^2 \partial^2 \varphi_{1,n}/\partial t^2 = k_B a^2 (2\varphi_{1,n} - \varphi_{1,n-1} - \varphi_{1,n+1}) + X_2(2P_{1,n} - P_{1,n-1} - P_{1,n+1}),$$

$$- M_B a^2 \partial^2 \varphi_{2,n}/\partial t^2 = k_B a^2 (2\varphi_{2,n} - \varphi_{2,n-1} - \varphi_{2,n+1}) + X_2(2P_{2,n} - P_{2,n-1} - P_{2,n+1}).$$

(5-119)

For the nonlinear wave solutions with length, d >> the spacing of the base pairs and for which P, u and φ are smoothly varying, we can go to the continuum limit:

$$- M\partial^2 P_i/\partial t^2 = (-1)^i C - AP_i^3 - K\partial^2 P_i/\partial z^2 - X_0\partial^2 u_i/\partial z^2 + X_1 \partial u_i/\partial z - X_2 \partial^2 \varphi_i/\partial z^2,$$

$$- M_N \partial^2 u_i/\partial t^2 = - k_N \partial^2 u_i/\partial z^2 - X_0 \partial^2 P_i/\partial z^2 + X_1 \partial \mathrm{P}_i/\partial z, \qquad (5\text{-}120)$$

$$- M_B a^2 \partial^2 \varphi_i/\partial t^2 = - k_B a^2 \partial^2 \varphi_i/\partial z^2 - X_2 \partial^2 P_i/\partial z^2, \qquad i = 1, 2.$$

Suggesting solutions in the form of travelling waves

$$P_i = P_i(z - vt), \quad u_i = u_i(z - vt), \quad \varphi_i = \varphi_i(z - vt); \quad i = 1, 2; \qquad (5\text{-}121)$$

we obtain

$$\overline{K}^2 \partial P_i/\partial z^2 = (-1)^i C - \overline{A} P_i + BP_i^3 - X_1 u_i^0/(k_N - M_N v^2),$$

$$(k_N - M_N v^2)\partial u_i/\partial z = - X_0 \partial P_i/\partial z + (-1)^i [X_1 P_i + u_i^0], \qquad (5\text{-}122)$$

$$a^2(k_B - M_B v^2)\partial \varphi_i/\partial z = - X_2 \partial \varphi_i/\partial z,$$

where $\overline{K} = [K - Mv^2 - X_0^2/(k_N - M_N v^2) - X_2^2/a^2(k_B - M_B v^2)]$; $u_i^0 (i = 1,2)$ are constants; $\overline{A} = [A + X_1^2/(k_N - M_N v^2)]$.

The first of the three Eqs. (5-121) has the form of the well known Schrödinger equation which has, among others, the soliton-like solution of the type

$$P_i = \overline{P}_\mathrm{i} \tanh[(z - vt)/d], \qquad (5\text{-}123)$$

where $\overline{P}_\mathrm{i} = \pm (\overline{A}/\mathrm{B})^{1/2}$, $d^2 = 2\overline{K}/\overline{A}$.

The solutions of the other two equations are then

$$\partial u_i/\partial z = - [X_0 \overline{P}_\mathrm{i}/d(k_N - M_N v^2)] \operatorname{sech}^2[(z - vt)/d] +$$

$$+ (-1)^i/(k_N - M_N v^2)\{X_1 \overline{P}_\mathrm{i} \tanh[(z - vt)/d] + u_i^0\}, \qquad (5\text{-}124)$$

$$\partial \varphi_i/\partial z = - [X_2 \overline{P}_\mathrm{i}/da^2(k_B - M_B v^2)] \operatorname{sech}^2[(z - vt)/d], \quad i = 1, 2. \qquad (5\text{-}125)$$

Solutions (5-123) –(5-125) are shown schematically in Figure 5.12. They can be interpreted as follows: (1) the pucker P goes from say a C2′ endo to a C3′ endo as one traverses the kink; (2) in the same region the two chains are strained, particularly in the vicinity of the center of the kink; (3) the inter-base-pair angles are decreased within the kink.

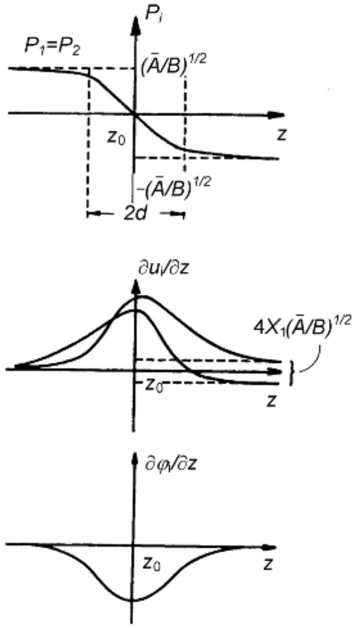

Figure 5.12 Sketch of soliton like solutions of the model of Krumhansl and Alexander. Reproduced with permission from Ref. [20].

5.4.2 The Model of Volkov

To describe conformational transitions in DNA, Volkov [54] suggested a model including two groups of internal motions. The first consists of the motions associated with the conformational changes inside the monomer link of the double-stranded chain. The second involves changes in position of the nucleotide link as a whole. It is suggested that the intralink changes are related to the transition of a monomer link into another conformational state through a potential barrier, and the conformational changes of the second type are simple deviations from equilibrium positions.

The simplest model which takes into account these specific features of conformational transitions in DNA is the two-component model, where one component describes displacements inside the monomer link (r), and the other describes the monomer as a whole (τ). As a definition, it is suggested that r describes the relative transverse displacements of the base pairs in the direction of the double helix grooves, and τ describes the torsion of a polynucleotide chain.

The Hamiltonian of this two-component system is

$$H = \sum_n [I\dot{\tau}_n^2 + m\dot{r}_n^2 + g_0(\tau_n - \tau_{n-1})^2 + f_0(r_n - r_{n-1})^2 + \Phi(r_n) + kF(r_n)(\tau_{n+1} - \tau_{n-1})]/2; \tag{5-126}$$

Here the summation is over all the monomers in the chain (index n); m is the reduced mass of a nucleotide link

$$m = m_{bp}m_{bb}/(m_{bp} + m_{bb}); \tag{5-127}$$

where m_{bp} is the mass of a base pair; m_{bb} is the mass of a backbone piece; $(m_{bp}+m_{bb})$ is the mass of a nucleotide link; I is the moment of inertia of a nucleotide link with respect to the double helix; g_0 and f_0 are the force constants of interactions along the chain (coordinate z); k is the force constant of interaction of the subsystems r and τ, Φ is the double well potential energy of a conformational transition in a monomer link (Figure 5.13)

$$\Phi(r) = \varepsilon_0 + \varepsilon_1(r/a) + \varepsilon(1 - r^2/a^2)^2, \tag{5-128}$$

and $F(r)$ characterizes the structural relations between the subsystems and the mutual alignment of motions in both components

$$F(r) = (r_0^2 - r^2)/a^2; \tag{5-129}$$

where r is defined by the condition

$$H(-r_0) = 0, \tag{5-130}$$

and ε, ε_0 and ε_1 are the parameters that define the form of the two-well potential shown in Figure 5.13.

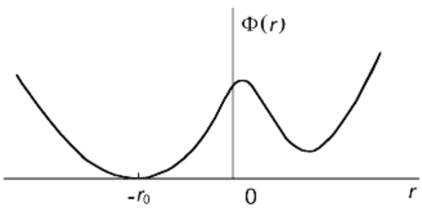

Figure 5.13 The form of the potential function of a conformational transition of a monomer link in the model of Volkov.

In the continuum approximation the Hamiltonian H takes the form

$$H = \int dz\{I[\dot{\tau}^2 + s_1^2(\partial\tau/\partial z^2] + ma^2[\dot{u}^2 + s_2^2(\partial u/\partial z)^2] + \Phi(u) + 2Ik_0F(u)\partial\tau/\partial z\}/2h; \tag{5-131}$$

where $u(z,t) = r(z,t)/a$; $s_1^2 = g_0h^2/I$; $s_2^2 = f_0h^2/m$; $k_0 = kh/I$; h is the distance between the monomers along the chain. The corresponding equations of motion then have the form

$$\ddot{\tau} = s_1^2(\partial\tau^2/\partial z^2) + k_0(\partial F/\partial u)(\partial u/\partial z);$$
$$\ddot{u} = s_2^2(\partial^2 u/\partial z^2) - (\partial\Phi/\delta u)/2ma^2 - k_0I(\partial F/\partial u)(\partial\tau/\partial z)/ma^2. \tag{5-132}$$

And the soliton solutions of the equations found by Volkov are

$$\tau = \tau_v\,\mathrm{cth}[q(z - vt - z_0)]/\{1 - R^2\mathrm{cth}^2[q(z - vt - z_0)]\}; \tag{5-133}$$

$$u = u_0 - b - 2b/\{R^2\,\mathrm{cth}^2[q(z - vt - z_0)] - 1\}; \tag{5-134}$$

where $\tau_v = k_0b(2\tau_0 + ab)/q(s_0^2 - v^2)$, $R^2 = (2u_0 + b)/(2\bar{\bar{u}}_0 - b)$; $b = [2(u_0^2 - 1)/(\bar{b} - 1)]^{½}$; $q = \pm\, \mathrm{p}^{½}\gamma^{-½}$; $p = u_0^2(2\bar{b} - 3) + 1$; $\gamma = ma^2(v^2 - s_2^2)/\varepsilon$; $\bar{b} = k_0^2\dot{I}/\varepsilon(s2_1 - v^2)$; u_0 is defined by the condition: $\partial\,\mathrm{u}/\partial(z\text{-}vt) = 0$ at $u = u_0$.

The solution of Eq. (5-133) has a kink-type form and the solution of Eq. (5-134) is a bell-shaped function of z–vt (Figure 5.14). Both solutions were obtained by Volkov and interpreted as those describing the transmission of local transitions of the A–B type along the DNA double chain.

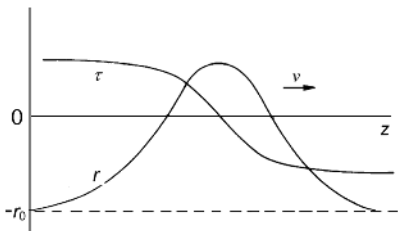

Figure 5.14 Soliton solutions of the model of Volkov. Reproduced with permission from Ref. [54].

6
Nonlinear Theory of DNA: Non-ideal Models

In the previous chapter we discussed in detail ideal nonlinear DNA models where the effects of the environment and inhomogeneity were not taken into account. In the ideal models considered we also did not take into account the helicity and asymmetry of the internal DNA structure. All these effects can be omitted in the first approximation of the theory, but they become important when we try to apply theoretical results to explain experimental data on the DNA dynamics and function.

In this chapter we describe the main approaches and results on studying the effects.

6.1
Effects of Environment

In the general case, the modeling of the DNA–environment interaction is a rather complex problem, but here we shall discuss only a simple case when the interaction of DNA with the environment can be reduced to two effects: the effect of dissipation and the effect of external fields [25]. We shall also assume that the DNA–environment interaction leads to small perturbations of the solutions of the ideal model dynamical equations. In this case a linear perturbation technique can be used. To simplify the calculations, we suggest that the unperturbed (or ideal) model equation is a simple sine-Gordon equation

$$I\varphi_{tt} = Kl^2a^2\varphi_{zz} - \nu_0 \sin\varphi, \tag{6-1}$$

as proposed by Englander et al. [15] and described in detail in Section 5.1. Here $\varphi(z,t)$ are the angular displacements of DNA bases from their equilibrium positions; I is the moment of inertia of the bases; K is the torsional rigidity; l is the distance from the centers of mass of the bases to the nearest sugar–phosphate chain; a is the distance between the neighboring base pairs; ν_0 is the parameter characterizing hydrogen interactions between the bases in the pairs.

6.1.1 General Approach

It is more convenient to rewrite Eq. (6-1) in the continuum approximation

$$\varphi_{tt} - C_0{}^2\varphi_{zz} + w_0{}^2 sin\varphi = 0; \qquad (6\text{-}2)$$

where $C_0{}^2 = Kl^2a^2/I$; $w_0{}^2 = v_0/I$. This procedure is correct if the solutions we are interested in change rather slowly and smoothly along the DNA. In particular, this can be achieved if $2d = 2al(K/v_0)^{1/2} >> a$, where d is the parameter specifying the size of the sine-Gordon soliton.

Let us assume now that the interaction with the environment leads to the appearance of two additional terms in Eq. (6-2). The first term describing the effect of dissipation has the form

$$\beta\varphi_t. \qquad (6\text{-}3)$$

Here β = damping parameter/I. The second additional term has the form

$$f_0(z,t). \qquad (6\text{-}4)$$

Here f_0 = external 'force'/I. The first term is called the damping or viscous term, the second, the external driving term.

The problem considered then takes the form

$$\varphi_{tt} - C_0{}^2\varphi_{zz} + \beta\varphi_t + w_0{}^2 sin\ \varphi = f_0(z,t). \qquad (6\text{-}5)$$

It is assumed here that the additional terms are small

$$\beta\varphi_t \sim \varepsilon, \quad f_0 \sim \varepsilon, \quad \varepsilon << 1. \qquad (6\text{-}6)$$

According to the linear perturbation theory, Eq. (6-5) can be treated by assuming a solution of the form

$$\varphi(z,t) = \varphi^0(z,t) + \psi(z,t), \qquad (6\text{-}7)$$

where $\varphi^0(z,t)$ is the solution of the unperturbed Eq. (6-2), and $\psi \sim \varepsilon$. For the definition, let us suggest that $\varphi^0(z,t)$ has the form of the kink solution

$$\varphi^0(z,t) = 4\ \arctan\{\exp[(z\text{-}vt)\gamma/d]\}, \qquad (6\text{-}8)$$

where $\gamma = (1 - v^2/C_0{}^2)^{-1/2}$, $d = C_0/w_0$.

Inserting Eq. (6-7) into Eq. (6-5) and linearizing the result in a small quantity ε we find the following equation for $\psi(z,t)$

$$\psi_{tt} - C_0^2\psi_{zz} + \beta\varphi_t^0 + [w_0^2 \cos\varphi^0] = f_0(z,t). \tag{6-9}$$

Taking into account that the ‘potential’ $[w_0^2\ cos\varphi^0]$ in Eq. (6-9) is the function of the variable $\gamma(z\text{-}vt)/d$, we can introduce new variables

$$\bar{z} = \gamma(z\text{-}vt);\ \bar{t} = \gamma(t - vz/C_0^2). \tag{6-10}$$

Eqs. (6-10) describe a transformation, called the Lorentz transformation, to a new moving system of coordinates. In this system the functions occurred in Eq. (6-9) and their derivatives take the form

$$\psi(z, t) \to \overline{\psi}(\bar{z}, \bar{t}), \qquad f_0(z, t) \to \overline{f}_0(\bar{z}, \bar{t}),$$

$$\varphi^0(z, t) \to \overline{\varphi}^0(\bar{z}),$$

$$\psi_t \to \overline{\psi}_{\bar{z}}\ \bar{z}_t + \overline{\psi}_{\bar{t}}\ \bar{t}_t = \gamma(\overline{\psi}_{\bar{t}} - v\overline{\psi}_{\bar{z}}), \qquad \varphi_t^0 \to -\gamma v\overline{\varphi}_z^0, \tag{6-11}$$

$$\psi_z \to \gamma(\overline{\psi}_{\bar{z}} - v\overline{\psi}_{\bar{t}}/C_0^2), \qquad \psi_{tt} \to \gamma^2(\overline{\psi}_{\bar{t}\bar{t}} - 2v\overline{\psi}_{\bar{t}\bar{z}} + v^2\overline{\psi}_{\bar{z}\bar{z}}),$$

$$\psi_{zz} \to \gamma^2(\overline{\psi}_{\bar{z}\bar{z}} - 2v\overline{\psi}_{\bar{z}\bar{t}}/C_0^2 + v^2\overline{\psi}_{\bar{t}\bar{t}}/C_0^4).$$

Inserting Eq. (6-11) into Eq. (6-9), we obtain the equation for $\overline{\psi}(\bar{z}, \bar{t})$:

$$\overline{\psi}_{\bar{t}\bar{t}} - C_0^2\overline{\psi}_{\bar{z}\bar{z}} + [w_0^2 \cos\overline{\varphi}^0(\bar{z})]\overline{\psi} = \overline{f}_0(\bar{z}, \bar{t}) + \beta\gamma v\overline{\varphi}_z^0. \tag{6-12}$$

The solution of Eq. (6-12) can be found by the following algorithm.

To begin with, let us consider the homogeneous equation

$$\overline{\psi}_{\bar{t}\bar{t}} - C_0^2\overline{\psi}_{\bar{z}\bar{z}} + [w_0^2 \cos\overline{\varphi}^0(\bar{z})]\overline{\psi} = 0; \tag{6-13}$$

and suggest that the solution of the equation has the form

$$\varphi_{\text{hom}}(\bar{z}, \bar{t}) = \exp(\mathrm{i}W\bar{t})\, f(\bar{z}). \tag{6-14}$$

Then by inserting Eq. (6-14) into Eq. (6-13) we obtain the linear Schrödinger equation

$$-C_0^2 f_{\bar{z}\bar{z}} + [w_0^2 \cos\overline{\varphi}^0(\bar{z})]f = W^2 f; \tag{6-15}$$

the solutions of which are ([274, 275]):

1. One bound state which is characterized by the eigenvalue W_b and the eigenfunction $f^b(\bar{z})$

$$W_b^2 = 0;\quad f^b(\bar{z}) = (2/d)sech(\bar{z}/d); \tag{6-16}$$

2. The continuum spectrum which is characterized by an ensemble of the eigenvalues W_k and the eigenfunctions $f^k(\overline{z})$

$$W_k^2 = C_0^2 k^2 + w_0^2; \quad f^k(\overline{z}) = (C_0/2\pi W_k)[k + (i/d)\,\mathrm{th}(\overline{z}/d)]\exp(ik\overline{z}). \tag{6-17}$$

Because the functions $f^b(\overline{z}), f^k(\overline{z})$ are the eigenfunctions of the self-adjoint operator $\hat{D}$

$$\hat{D} = -C_0^2(d^2/d\overline{z}^2) + [w_0^2 \cos\overline{\varphi}^0(\overline{z})], \tag{6-18}$$

we can state that they form the complete orthonormal basis in the space of functions of the variable $\overline{z}$. The condition of orthogonality is provided by the equations

$$\int_{-\infty}^{+\infty} f^b(\overline{z}) f^b(\overline{z})\,d\overline{z} = 8/d,$$

$$\int_{-\infty}^{+\infty} f^k(\overline{z}) f^b(\overline{z})\,d\overline{z} = 0, \tag{6-19}$$

$$\int_{-\infty}^{+\infty} f^{*k}(\overline{z}) f^{k'}(\overline{z})\,d\overline{z} = \delta(k - k'),$$

and the condition of the completeness is provided by the equation

$$\int_{-\infty}^{+\infty} f^{*k}(\overline{z}') f^k(\overline{z})\,dk + (d/8) f^b(\overline{z}') f^b(\overline{z}) = \delta(\overline{z}' - \overline{z}), \tag{6-20}$$

Let us return now to the initial inhomogeneous Eq. (6-12) and expand its solution ($\overline{\psi}(\overline{z}, \overline{t})$) in the basic functions f^b, f^k

$$\overline{\psi}(\overline{z}, \overline{t}) = (d/8)\varphi^b(\overline{t}) f^b(\overline{z}) + \int_{-\infty}^{+\infty} \varphi^k(\overline{t}) f^k(\overline{z})\,dk. \tag{6-21}$$

Let us expand also the function $\overline{f}_0(\overline{z}, \overline{t})$ in the same way:

$$\overline{f}_0(\overline{z}, \overline{t}) = (d/8) q^b(\overline{t}) f^b(\overline{z}) + \int_{-\infty}^{+\infty} q^k(\overline{t}) f^k(\overline{z})\,dk; \tag{6-22}$$

and suggest that

$$\overline{\varphi}^{0}_{\bar{z}} = f^{b}(\bar{z}). \tag{6-23}$$

Here the coefficients $q^{b}(\bar{t})$, $q^{k}(\bar{t})$ are determined by

$$q^{i}(\bar{t}) = P\int \overline{f}_{0}\,(\bar{z},\bar{t})\,f^{i}(\bar{z})\mathrm{d}\bar{z};\;\; i = \mathrm{b, k}. \tag{6-24}$$

The validity of Eq. (6-23) can be easily checked by differentiation of Eq. (6-2) and by comparison of the result obtained with Eq. (6-15). Equations determining the coefficients $\varphi^{i}(\bar{t})$ (i = b, k) can be found in the following way.

Let us (i) insert Eqs. (6-21) – (6-23) into Eq. (6-12), (ii) multiply the result by $f^{b}(\bar{z})$ and (iii) integrate over the variable $\bar{z}$. As a result we obtain the equation

$$\varphi^{b}_{\bar{t}\bar{t}} = q^{b}(\bar{t}) + 8v/d. \tag{6-25}$$

By the same method we can obtain the equation determining the coefficient $\varphi^{k}(\bar{t})$. Indeed, let us (i) insert Eq. (6-21) – (6-23) into Eq. (6-12), (ii) multiply the result by $f^{k}(\bar{z})$ and (iii) integrate over the variable $\bar{z}$. As a result we obtain the equation

$$\varphi^{k}_{\bar{t}\bar{t}} + W_{k}^{2}\varphi^{k} = q^{k}(\bar{t}). \tag{6-26}$$

Equations (6-25), (6-26) supplemented by Eq. (6-24) complete the solution of the problem. Inserting the solutions of Eqs. (6-25) and (6-26) into Eq. (6-21) one can find the unknown function $\overline{\psi}(\bar{z},\bar{t})$. And finally after returning to the old variables

$$z = \gamma(\bar{z} + v\bar{t}); \qquad t = \gamma(\bar{t} + v\bar{z}/C_{0}^{2}); \tag{6-27}$$

the function $\psi(z,t)$ can be found.

To understand the physical sense of the results obtained, let us look again at the resulting Eq. (6-21). It consists of two terms. The first term, $d/8\varphi^{b}(\bar{t})f^{b}(\bar{z})$, is called the soliton component. It can be shown that this term describes the movement of the center of soliton mass. Indeed, let us return to the beginning of the previous section and suggest that small perturbations caused by the DNA–environment interaction lead to two types of changes in the behavior of the sine-Gordon kink. The first is the change in the velocity of the soliton, and the second is the change in the form of the solitary wave. Let us assume that these changes have an additive character and consider separately the problem of changing the velocity of the soliton when the form remains unchanged. That is, let us consider the case when

$$\overline{\psi}(\bar{z},\bar{t}) = \overline{\varphi}^{0}\,(\bar{z} - [v_{0} + \Delta v(\bar{t})]\bar{t}); \tag{6-28}$$

where v_0 is the initial velocity of the soliton, and $\Delta v(\bar{t})$ is the change in the velocity. Initially the soliton is assumed to be at rest (in the system of coordinates $\{\bar{z},\ \bar{t}\}$, which is moving with velocity v). If we now expand the function $\overline{\psi}(\bar{z}, \bar{t})$ in a Taylor series and take into account Eq. (6-23) we obtain

$$\overline{\psi}(\bar{z}, \bar{t}) = \overline{\varphi}(\bar{z}) + (\partial\overline{\varphi}^0/\partial\bar{z})(-\Delta v\bar{t}) + \ldots =$$

$$= \overline{\varphi}^0(\bar{z}) + f^{\mathrm{b}}(\bar{z})(-\Delta v\bar{t}) + \ldots \tag{6-29}$$

Comparing Eqs. (6-29) and (6-21), we find that in the first approximation the change in the soliton velocity, Δv, is determined by the formula

$$\Delta v = -(d/8)\varphi_{\bar{t}}^{\mathrm{b}}(\bar{t}). \tag{6-30}$$

So, the soliton component of Eq. (6-21) does describe the movement of the center of mass of the soliton.

The second term in Eq. (6-21) is called the radiation component. It determines (in the main) the change in the form of the solitary wave due to perturbations. This term could be considered in the same way. For simplicity, however, we shall restrict ourselves to the first term associated with the change in the velocity of the soliton.

6.1.2
Particular Examples

To illustrate applications of the algorithm, let us consider briefly several simple models of the DNA–environment interactions. From the mathematical point of view the models are completely determined by the form of the function f_0.

Example 1

Let us consider the simplest case when the function f_0 is a constant. It is assumed also that this constant has a negative value, $-J_0$. In other words, it is assumed that there is a constant energy pumping. We can show that this pumping can be a good counterweight to the energy loss due to the effect of dissipation.

To calculate the change in the velocity of the soliton we should use Eq. (6-24) with $f_0 = -J_0$. Then we have

$$q_{\mathrm{b}}(\bar{t}) = \int_{-\infty}^{+\infty} f_0 f^{\mathrm{b}}(\bar{z})\mathrm{d}\bar{z} = -2\pi J_0. \tag{6-31}$$

Inserting Eq. (6-31) into Eq. (6-25) and integrating the result we obtain

$$\varphi_{\bar{t}}^{\mathrm{b}} = (8\beta\gamma v/d - 2\pi J_0)\bar{t} + C; \tag{6-32}$$

where C is a constant determined by the initial condition of the problem. If we assume the initial condition to be in the form

$$\varphi_{\bar{t}}^{\mathrm{b}}(\bar{t}=0)=0; \tag{6-33}$$

we obtain $C=0$. Inserting Eq. (6-32) into Eq. (6-30) we find

$$v=(J_0\pi d/4-\beta\gamma v)\bar{t}. \tag{6-34}$$

So, it follows from this that the movement of a soliton under the action of a small constant moment of force is uniformly accelerated, and the movement under the action of dissipation is uniformly decelerated. There is a critical value of J_0

$$J_0{}^{\mathrm{crit}}=4\beta\gamma v/\pi d, \tag{6-35}$$

when the action of dissipation and the action of the constant force are in balance. This result points to a similarity in the behavior of the soliton and of aclassical particle.

Example 2

Consider the case when the time period of the action of the external field is much less than the time period of propagation of the soliton (or the soliton lifetime). Let us assume also that the action of external force is localized in the region of the DNA, the size of the region being much less than the distance of propagation of the solitary wave. In this case the function f_0 can be modeled in the following way:

$$f_0=-J_0\,\delta(z-z_0)\delta(t-t_0). \tag{6-36}$$

To calculate the corresponding change in the soliton velocity, let us rewrite the function f_0 in the coordinates $\bar{z}$, $\bar{t}$

$$f_0\to\bar{f}_0=-J_0\,\delta(\gamma(\bar{z}+v\bar{t})-z_0)\,\delta(\gamma(\bar{t}+v\bar{z}/C_0{}^2)-t_0) \tag{6-37}$$

and insert Eq. (6-37) into Eq. (6-24). As a result, we obtain

$$q^{\mathrm{b}}(\bar{t})=-J_0\,\gamma f^{\mathrm{b}}((z_0-\gamma v\bar{t}_0)/\gamma)\delta(\bar{t}-\bar{t}_0). \tag{6-38}$$

Inserting Eq. (6-38) into Eq. (6-25) and integrating the result we find

$$\varphi_{\bar{t}}^{\mathrm{b}}=8\beta\gamma v\bar{t}/d+C, \tag{6-39}$$

where C is a constant. If we now take the initial conditions in the form of Eq. (6-33) the constant becomes equal to zero, and the final result obtained by using Eq. (6-30) takes the following form:

$$\Delta v \cong -\beta\gamma v\bar{t}. \tag{6-40}$$

This means that the soliton is decelerating.

Other Examples

There are many other possible ways of modeling the function f_0. For example, we could consider intermediate cases such as

$$f_0 = -J_0\,\delta(z - z_0) \quad \text{or} \quad f_0 = -J_0\,\delta(t - t_0). \tag{6-41}$$

We could consider a periodical (in time t or/and in the variable z) model of the external field as was done by Zhang [47] when studying the problem of microwave absorption in DNA. Finally, we could consider a random model function F

$$f_0 = F(z,t); \tag{6-42}$$

with the statistical averaging

$$\begin{aligned} &<F(z,t)> = 0; \\ &<F(z,t); F(z', t')> = \text{const}\,\delta(z - z')\delta(t - t'). \end{aligned} \tag{6-43}$$

This model is useful when we study random collisions of small molecules of the solution with the DNA molecule. A very similar model has been proposed by Muto et al. [32] to imitate the interaction of DNA with a thermal reservoir.

All these examples can be analyzed step by step in accordance with the algorithm described above.

6.1.3
DNA in a Thermal Bath

To model DNA in a thermal bath the random model function F described at the end of the previous section and the method of perturbation described can be used. Another interesting approach based on the methods of computer simulation has been recently proposed in Refs. [267, 276].

In the first work [267] published by Campa the traveling of a bubble (or open state) in the double chain consisting of 2500 base pairs, with fixed boundary conditions was studied. The bubble was formed by imposing a partial unwinding at one end of the chain. The chain was initially in a thermal bath at 300 K, and both homogeneous and heterogeneous chains were studied. As a result, it was shown that in both cases the bubble can travel further than 1000 base pairs.

In the second work [276] published by Yakushevich et al. kink-type solitons imitating bubbles moving along the double chain were simulated. To model a thermalized chain the authors used the Langevin equations with the Hamiltonian of the Y model. The results of the simulations showed a rather high stability of the solitons.

6.2 Effects of Inhomogeneity

As follows from Chapters 1 and 3 the DNA molecule has an inhomogeneous structure, and this property plays an important role in the function of the molecule. Let us discuss possible inhomogeneous models of the nonlinear DNA dynamics. It is convenient to begin with the ideal nonlinear models described in the previous chapter and to suggest that the parameters of the dynamical equations such as base masses, moments of inertia, coefficients characterizing interactions, are dependent on the base positions.

For example, if we take as a basis the discrete version of the model of Englander the new dynamical equations describing the inhomogeneous case will have the form

$$I_n\ddot{\varphi} = K_n\, l^2(\varphi_{n+1} - 2\varphi_n + \varphi_{n-1}) - v_{0n}\sin\varphi_n, \quad n = 1, 2, \ldots N; \tag{6-44}$$

which is very similar to the form of Eq. (5-1). The only difference is that the coefficients I, K, v_0 are now dependent on the index n. A very similar approach was used in the work of Hasakado and Wadati [277] to obtain the inhomogeneous version of the discrete model of Peyrard and Bishop. The same method can also be used to obtain continuous inhomogeneous equations. For this purpose, it is enough to substitute constant parameters of corresponding dynamical equations for functions depending on the variable z, z axis being parallel to the DNA axis.

So, there is not a problem in obtaining inhomogeneous nonlinear equations, but there is a problem in solving them. In the general case, nonlinear differential equations describing inhomogeneous DNA are too complex to be solved by analytical methods, and a computer technique should be used to solve them. But for a few simple models of the DNA inhomogeneity, such as the boundary between two different homogeneous regions (blocks) or the local homogeneous region inside another inhomogeneous region, the solution of the problem can be found analytically [25].

In this chapter we discuss both, simple and complex cases.

6.2.1 Boundary

Let us assume that inhomogeneity has the form of a boundary between two homogeneous regions as shown in Figure 6.1a. It may be, for example, the boundary between the region consisting of A-T base pairs and the region consisting of G-C base pairs

...AAAAAAAAAAAAAAAGGGGGGGGGGGGGG...

...TTTTTTTTTTTTTTTCCCCCCCCCCCCCC...

Such a sequence does not exist in living organisms but can be synthesized artificially. This sequence can also be considered as a first approximation to a real sequence of bases in the DNA fragments, one part of which contains mainly A-T base pairs and the other part mainly G-C base pairs.

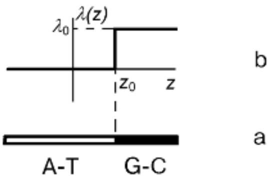

Figure 6.1 (a) Boundary between two blocks and (b) the model function $\lambda(z)$ describing this inhomogeneity.

Let us assume for simplicity that the basic ideal model of the internal DNA dynamics is described by Eq. (6-2). Now we should modify it to take into account the inhomogeneity having the form of a boundary. As we mentioned before, the most general method of taking into account any inhomogeneity consists in substitution of the constant parameters of Eq. (6-2) for functions depending on the variable z:

$$C_0 \to C_0(z);\ w_0 \to w_0(z). \tag{6-45}$$

To simplify the calculations, we shall consider here the case where only one of two parameters, namely w_0, is substituted for a function of z. This means that we neglect the differences in mass and moments of inertia of the bases and take into account only the difference in the interactions between the bases in the pairs. Then the perturbed problem takes the form

$$\varphi_{tt} - C_0^2\varphi_{zz} + w_0^2 \sin\varphi + \lambda(z) \sin\varphi = 0, \tag{6-46}$$

where $\lambda(z) = w_0^2(z) - w_0^2$. For the case considered, the function $\lambda(z)$ can be modeled in the following way

$$\lambda(z) = \lambda_0\, \Theta\, (z - z_0); \tag{6-47}$$

where λ_0 is a constant that can be positive or negative depending on the situation; $\Theta(z - z_0)$ is a step Heavyside function:

$$\Theta\, (z - z_0) = \begin{cases} 0, & z < z_0; \\ 1, & z \geq z_0. \end{cases} \tag{6-48}$$

The model function (6-47) describes the boundary between two regions, which is placed at the point z_0. A schematic picture of the function $\lambda(z)$ for the case $\lambda_0 > 0$ is shown in Figure 6.1b. The picture corresponds to the case where the region which is placed on the left of the boundary is saturated by A-T base pairs and the other region on the right is saturated by G-C base pairs.

To find the change in the velocity of solitary wave, let us use the method of perturbation described in the previous section. So, we suggest that the solution has a form analogous to Eq. (6-7). Applying step by step the algorithm described above we find that the solution can be presented in the form of an expansion of type (6-22) with the coefficients of the expansion determined by the equations

$$\varphi^{\mathrm{b}}_{\bar{t}\bar{t}} = \mathrm{g}^{\mathrm{b}}(\bar{t}); \tag{6-49}$$

$$\varphi^{\mathrm{k}}_{\bar{t}\bar{t}} + W_{\mathrm{k}}{}^2\varphi^{\mathrm{k}} = g^{\mathrm{k}}(\bar{t}); \tag{6-50}$$

where the functions $g^i(\bar{t})$ ($i = \mathrm{b, k}$) have the form

$$g^i(\bar{t}) = -P\int\lambda[\gamma(\bar{z} + v\bar{t})]\sin\varphi^0(\bar{z})f^i(\bar{z})\mathrm{d}\bar{z}. \tag{6-51}$$

Equations (6-49) – (6-51) together with Eq. (6-22) give a complete solution of the problem. Indeed, if we rewrite Eqs. (6-47) in coordinates $\bar{z}$, $\bar{t}$ and insert the resulting expression into Eq. (6-51) we find

$$\mathrm{g}^{\mathrm{b}}(\bar{t}) = 2\lambda_0/\{\mathrm{ch}^2[(v\bar{t} - z_0/\gamma)/d]\}. \tag{6-52}$$

Then from Eq. (6-49) and Eq. (6-52) we find the equation for the coefficient φ^{b}

$$\varphi^{\mathrm{b}}_{\bar{t}\bar{t}} = 2\lambda_0/\mathrm{ch}^2[(v\bar{t} - z_0/\gamma)/d]. \tag{6-53}$$

After integration of (6-53) we find

$$\varphi^{\mathrm{b}}_{\bar{t}} = (2\lambda_0 d/v)\,\mathrm{th}[(v\bar{t} - z_0/\gamma)/d] + C. \tag{6-54}$$

Assuming that

$$\varphi^{\mathrm{b}}_{\bar{t}}\ (\bar{t} = -\infty) = 0; \tag{6-55}$$

we obtain that $C = 2\lambda_0 d/v$. Then in accordance with Eq. (6-30) we finally obtain the change of the velocity of the soliton

$$\Delta v = -(\lambda_0 d^2/4v)\{1 + \mathrm{th}[(v\bar{t} - z_0/\gamma)/d]\}. \tag{6-56}$$

This result shows that when crossing the boundary of two homogeneous regions the velocity of the soliton wave increases or decreases depending on the sign (+ or –) of λ_0. For example, in the case shown in Figure 6.1 (λ_0>0), the velocity of the soliton moving from left to right, decreases. This dynamical behavior of the solitary wave has been recently confirmed by computer simulations [276]

6.2.2 Local Region

The results obtained can be easily extended to the case where we have some special region of finite length, for example, a G-C block against an A-T background

...AAAAAAAAAAGGGGGGGGGAAAAAAAAAA...

...TTTTTTTTTTCCCCCCCCCTTTTTTTTTT...

This problem differs from the previous one only in the existence of two boundaries (instead of one); the first is placed at point $z = -a$ and the second at point $z = a$ (Figure 6.2). Hence, the model function $\lambda(z)$ is equal to

$$\lambda(z) = \lambda_0[\Theta\,(z - a) - \Theta\,(z + a)]. \tag{6-57}$$

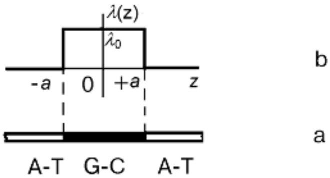

Figure 6.2 (a) A-T double chain containing the G-C block of finite length $L = 2a$ and (b) the model function $\lambda(z)$ describing this inhomogeneity.

To find the change in the velocity of the solitary wave due to inhomogeneity, having the form of the local region, let us suggest again that the solution of the corresponding perturbed equation

$$\varphi_{tt} - C_0{}^2\varphi_{zz} + w_0{}^2\sin\varphi + \lambda(z)\sin\varphi = 0, \tag{6-58}$$

is of a form analogous to Eq. (6-7). Now applying the perturbation technique step by step we find that the solution has the form of expansion of Eq. (6-21) and the equations determining the coefficients of the expansion are similar to Eqs. (6-49) and (6-50).

After integration of one of the equations, which determines the coefficient $\varphi^{\mathrm{b}}(\bar{t})$ we obtain

$$\varphi^{\mathrm{b}}_{\bar{t}} = (2\lambda_0 d/v)\,\{\mathrm{th}[(v\bar{t} - a/\gamma)/d] - \mathrm{th}[(v\bar{t} + a/\gamma)/d]\}. \tag{6-59}$$

In this equation the initial condition

$$\varphi^{\mathrm{b}}_{\bar{t}}\ (\bar{t} = -\infty) = 0 \tag{6-60}$$

has been taken into account.

Then in accordance with Eq. (6-30) we obtain the change in velocity of the soliton

$$\Delta v = -(\lambda_0 d^2/4v)\{\mathrm{th}[(vt - a/\gamma)/d] - \mathrm{th}[(vt + a/\gamma)/d]\}. \tag{6-61}$$

This result shows that when $\gamma_0 > 0$ the soliton decelerates when passing through the first (left) boundary and accelerates when passing through the second (right) one.

We can estimate the minimal value of the velocity of the solitary wave (v_{min}), which is necessary to surmount the energy barrier ($\lambda_0 > 0$) (Figure 6.2) or the trap potential well ($\lambda_0 < 0$) (Figure 6.3) and to continue the movement. For the purpose let us introduce the parameter ΔE which is equal to the barrier height (or to the well depth) and write the condition of passage in the form

$$E_{kin} \geq \Delta E; \tag{6-62}$$

where E_{kin} is the kinetic energy of the sine-Gordon soliton determined by the formula

$$E_{kin} = E_0(\gamma - 1). \tag{6-63}$$

Here E_0 is the rest energy of the soliton. From Eqs. (6-62) and (6-63) we find the unknown condition for the velocity

$$v^2 > v_{min}{}^2 = 2C_0{}^2\Delta E/E_0. \tag{6-64}$$

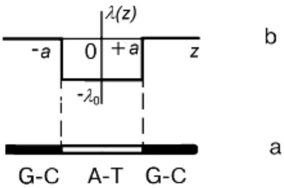

Figure 6.3 (a) G-C double chain containing the A-T block of finite length $L = 2a$ and (b) the model function $\lambda(z)$ describing this inhomogeneity.

6.2.3
Sequence of Bases

A more complex model of inhomogeneity having the form of a random sequence of bases has been considered recently in Refs. [267, 276], and the model imitating real (or natural) sequences of bases was studied in the series of works of Salerno [39, 278–280]. For computer calculations Salerno used the model equations

$$I\ddot{\psi} = Kl^2(\psi_{n+1} - 2\psi_n + \psi_{n-1}) - V_n \sin\psi_n = 0, \quad n = 1, 2, \ldots N, \tag{6-65}$$

which are very similar to Eq. (5-1) but have the coefficients V_n depending on the positions of the bases.

Equations (6-65) can be derived in the following way. First of all let us write the system of two discrete equations describing the torsional DNA dynamics in the frameworks of the second level of the hierarchy

$$I_{n,1}\ddot{\varphi}_{n,1} = K_{n,1}l^2(\varphi_{n+1,1} - 2\varphi_{n,1} + \varphi_{n-1,1}) - V_{n,1}\sin(\varphi_{n,1} + \varphi_{n,2}),$$
$$I_{n,2}\ddot{\varphi}_{n,2} = K_{n,2}l^2(\varphi_{n+1,2} - 2\varphi_{n,2} + \varphi_{n-1,2}) - V_{n,2}\sin(\varphi_{n,2} + \varphi_{n,1}). \tag{6-66}$$

Here $\varphi_{n,i}(t)$ is the rotational angle of the nth base of the ith chain ($i = 1, 2$). Suggesting (for simplicity) that the moments of inertia of the DNA bases are approximately equal and the coefficients of the rigidities are constant we can then easily obtain Eq. (6-65) for the angle sum $\psi_n = \varphi_{n,1} + \varphi_{n,2}$. Thus in the model of Salerno the sequence of bases is taken into account only due to the dependence of the coefficient V_n on the base positions. This coefficient characterizes hydrogen interactions between bases in pairs. Because there are only two possibilities: two hydrogen bonds are involved in the formation of an A-T base pair and three hydrogen bonds are involved in the formation of a G-C base pair, the coefficient V_n can be written in the form

$$V_n = \beta\lambda_n, \tag{6-67}$$

where $\lambda_n = 2$ for A-T base pairs, and $\lambda_n = 3$ for G-C base pairs.

In numerical calculations of Eq. (6-65) Salerno used an initial condition in the form of the ideal sine-Gordon equation. To model inhomogeneity, the specific base sequence which corresponds to T7A_1 DNA promoter was taken. As a result, it was found that the soliton passing through the inhomogeneous DNA fragment can (i) remain static or (ii) make small oscillations or (iii) move along the DNA.

The difference in the dynamical behavior of the initially static solitary wave can be used as a criterion for identification of dynamically active sites in the DNA molecule. The sites found in this way could be considered as biologically active regions. If this is so, the approach developed by Salerno could be used as a new method of testing and interpreting the DNA code.

6.3
Effects of Helicity

In all the nonlinear models considered above, the helicity of the DNA structure has not been taken into account. This approach was used in order to simplify the calculations but there are many problems where the helical geometry of DNA is important. Problems of scattering light and neutrons by DNA are the best known of these. In both problems the initial flow of particles (photons or neutrons) which are moving parallel to some line (for example, parallel to the z axis) is sensitive to the internal geometry of the sample. So, one can expect that the results of scattering will be different for nonhelical and helical DNA models. To find the difference we should know how to construct helical DNA models and how to use them for scattering problems.

In this section we discuss one method taking into account the helical structure of DNA. It was proposed and developed in the works of Gaeta [4, 37, 38] and Dauxois [281]. In the next chapter, when considering the problem of neutron scattering by DNA, we shall describe one more method developed in the work of Fedyanin and Yakushevich [22].

As an example, let us take the Y-model which is nonhelical and then let us show how it can be improved to take into account the effects of the helicity. The Hamiltonian of the Y-model, which has been discussed in detail in Section 5.3.3.2, has the form

$$H^{\mathrm{Y}} = \int dz\{I_1\dot{\varphi}_1^2/2 + I_2\dot{\varphi}_2^2/2 + K_1{}^t a^2 l^2 \varphi/2 + K_2 a^2 l^2 \varphi/2 - K^{\mathrm{b}}\, l^2[2\cos\varphi_1 + 2\cos\varphi_2 -$$

$$- \cos(\varphi_1 + \varphi_2)]\} + \text{const.} \tag{6-68}$$

Here φ_i is the angular displacement of bases in the ith chain; I is the moment of inertia; K^{t}, K^{b} are the coefficients of longitudinal and transverse rigidity, respectively.

It is more convenient for discussion to deal with the discrete version of the hamiltonian H^{Y}

$$\overline{H}^{\mathrm{Y}} = \sum_n \sum_{i=1}^{2} \{I\dot{\varphi}_{i,n}^2/2 + K^{\mathrm{t}} l^2 (\varphi_{i,n+1} - \varphi_{i,n})^2/2\} + \sum_n K^{\mathrm{b}} l^2 [2\cos\varphi_{1,n} +$$

$$+ 2\cos\varphi_{2,n} - \cos(\varphi_{1,n} + \varphi_{2,n})]. \tag{6-69}$$

One of the peculiarities of the DNA helical structure is that some of the nucleotides which are far apart in the polynucleotide chain can be close enough in space to be connected by hydrogen-bonded water filaments. To take into account these filaments, we must include an additional term describing coupling between the nth nucleotide on one strand and the $(n+h)$th nucleotide on the other ($h = 4$). Let us assume that the coupling term has the following simple form

$$H^{\mathrm{h}} = \sum_n K^{\mathrm{h}} d^2 [(\varphi_{1,n+h} - \varphi_{2,n})^2/2 + (\varphi_{2,n+h} - \varphi_{1,n})^2/2]; \tag{6-70}$$

where K^{h} is the elastic constant characterizing the coupling and d is the distance in space between the nth and $(n+h)$th nucleotides.

So, the total Hamiltonian of the helical Y-model is

$$H^{\mathrm{tot}} = \overline{H}^{\mathrm{Y}} + H^{\mathrm{h}}. \tag{6-71}$$

The corresponding dynamical equations written in the continuum approximation will then have the form [4]

$$\begin{aligned} I\ddot{\varphi}_1 &= K^{t}a^2l^2\varphi_{1zz} - K^{b}l^2[2\sin\varphi_1 - \sin(\varphi_1+\varphi_2)] + K^{h}d^2[2(\varphi_2-\varphi_1) + w^2\varphi_{1zz}], \\ I\ddot{\varphi}_2 &= K^{t}a^2l^2\varphi_{2zz} - K^{b}l^2[2\sin\varphi_2 - \sin(\varphi_2+\varphi_1)] + K^{h}d^2[2(\varphi_1-\varphi_2) + w^2\varphi_{2zz}], \end{aligned} \tag{6-72}$$

where w is the length of a half-wind of the helix in the z coordinate (that is along the double helix).

The solutions of the equations can be easily found in two particular cases: (1) when $\varphi_1(z,t) = -\varphi_2(z,t)$ and (2) when $\varphi_1(z,t) = \varphi_2(z,t)$. In the first case instead of Eq. (6-72) we obtain

$$I\ddot{\varphi} = (K^{t}a^2l^2 + K^{h}d^2w^2)\varphi_{zz} - 2K^{b}l^2\sin\varphi - 4K^{h}d^2\varphi; \tag{6-73}$$

where $\varphi \equiv \varphi_1 = -\varphi_2$. Equation (6-73) can be easily transformed to a simple sine-Gordon equation

$$(K^{t}a^2l^2 + K^{h}d^2w^2)\overline{\varphi}_{zz} - 2K^{b}l^2\sin\overline{\varphi} = 0; \tag{6-74}$$

by the following transformation

$$\varphi = \exp\{i2d(K^{h}/I^{1/2})\overline{\varphi}\}. \tag{6-75}$$

In the second case we obtain the double sine-Gordon equation:

$$I\ddot{\varphi} = (K^{t}a^2l^2 + K^{h}d^2w^2)\varphi_{zz} - K^{b}l^2(2\sin\varphi - \sin 2\varphi); \tag{6-76}$$

where $\varphi \equiv \varphi_1 = \varphi_2$.

Both the sine-Gordon equation and the double sine-Gordon equation have kink-like soliton solutions. But if we now compare Eqs. (6-73) and (6-76) with Eqs. (5-11) and (5-12) obtained for the nonhelical model we find two things which make them different: (1) the coefficients in the first terms of the right-hand sides of Eqs. (6-73) and (6-76) are renormalized and (2) in the first of the equations we obtained the additional term $4K^{b}d^2\varphi$.

6.4 Effects of Asymmetry

In the nonlinear models described above, the difference in mass of the bases in pairs has been neglected, and symmetry between two strands relative to the general DNA axis has been assumed. This assumption is widely used to simplify calculations. However, even in homogeneous DNA the difference in mass of adenine and thymine in A-T base pairs and of guanine and cytosine in G-C base pairs is rather substantial (see Appendix 2). The difference was first considered in Ref. [276]. It was shown that the absence of symmetry led to the appearance of new interesting soliton solutions which were obtained numerically with the help of the variation technique [282]. The model Hamiltonian used had the following form:

$$H^{\mathrm{h}} = T^{\mathrm{h}} + V^{\mathrm{h}}_{||} + V^{\mathrm{h}}_{\perp}; \tag{6-77}$$

where the kinetic energy (T^{h}), the energy of the interactions along the chains ($V^{\mathrm{h}}_{||}$) and the energy of the interactions between bases in pairs ($V^{\mathrm{h}}_{\perp}$) were determined by

$$T^{\mathrm{h}} = \sum_n \{(m_1 r_1^2/2)(d\varphi_{n,1}/\mathrm{d}t)^2 + (m_2 r_2^2/2)(\mathrm{d}\varphi_{n,2}/\mathrm{d}t)^2\}, \tag{6-78}$$

$$V^{\mathrm{h}}_{||} = \sum_n \{K_1 r_1^2[1 - \cos(\varphi_{n,1} - \varphi_{n-1,1})] + K_2 r_2^2[1 - \cos(\varphi_{n,2} - \varphi_{n-1,2})]\}, \tag{6-79}$$

$$V^{\mathrm{h}}_{\perp} = \sum_n k_{1-2}\{r_1(r_1 + r_2)(1 - \cos\varphi_{n,1}) + r_2(r_1 + r_2)(1 - \cos\varphi_{n,2}) -$$

$$- r_1 r_2[1 - \cos(\varphi_{n,1} - \varphi_{n,2})]\}. \tag{6-80}$$

Here $\varphi_{n,i}$ is the angular displacement of the nth base of the ith chain from its equilibrium position; r_{i} is the distance between the center of mass of the ith base and the nearest sugar–phosphate chain; a is the distance between neighboring bases along the chains; m_i is the mass of the bases of the ith chain; K_i is the coupling constant along the sugar–phosphate chain; k_{1-2} is the force constant that characterizes interactions between bases in pairs; $n = 1, 2, \ldots N$; $i = 1, 2$.

The Hamiltonian (6-77) can be considered as a generalized version of the Y-model (6-69), which takes into account the difference in mass of the bases in the pairs as well as the difference in the distance between the center of the base masses and the nearest sugar–phosphate chain. We can call it the asymmetrical Y-model.

Dynamical equations corresponding to the Hamiltonian (6-77) can then be written in the following form:

$$m_1 r_1^2(\mathrm{d}^2\varphi_{n,1}/\mathrm{d}t^2) = K_1 r_1^2[\sin(\varphi_{n-1,1} - \varphi_{n,1}) - \sin(\varphi_{n,1} - \varphi_{n+1,1})] -$$

$$- k_{1-2}[r_1(r_1 + r_2)\sin\varphi_{n,1} - r_2 r_1 \sin(\varphi_{n,1} - \varphi_{n,2})], \tag{6-81}$$

$$m_2 r_2^2(\mathrm{d}^2\varphi_{n,2}/\mathrm{d}t^2) = K_2 r_2^2[\sin(\varphi_{n-1,2} - \varphi_{n,2}) - \sin(\varphi_{n,2} - \varphi_{n+1,2})] -$$

$$- k_{1-2}[r_2(r_1 + r_2)\sin\varphi_{n,2} - r_2 r_1 \sin(\varphi_{n,2} - \varphi_{n,1})]. \tag{6-82}$$

Investigations of the problem (6-81) – (6-82) show that contrary to the case of the simple Y-model with the solution shown in Figure 5.9, the asymmetry Y-model has three types of soliton solutions with different topological charges (q) (Figure 6.4).

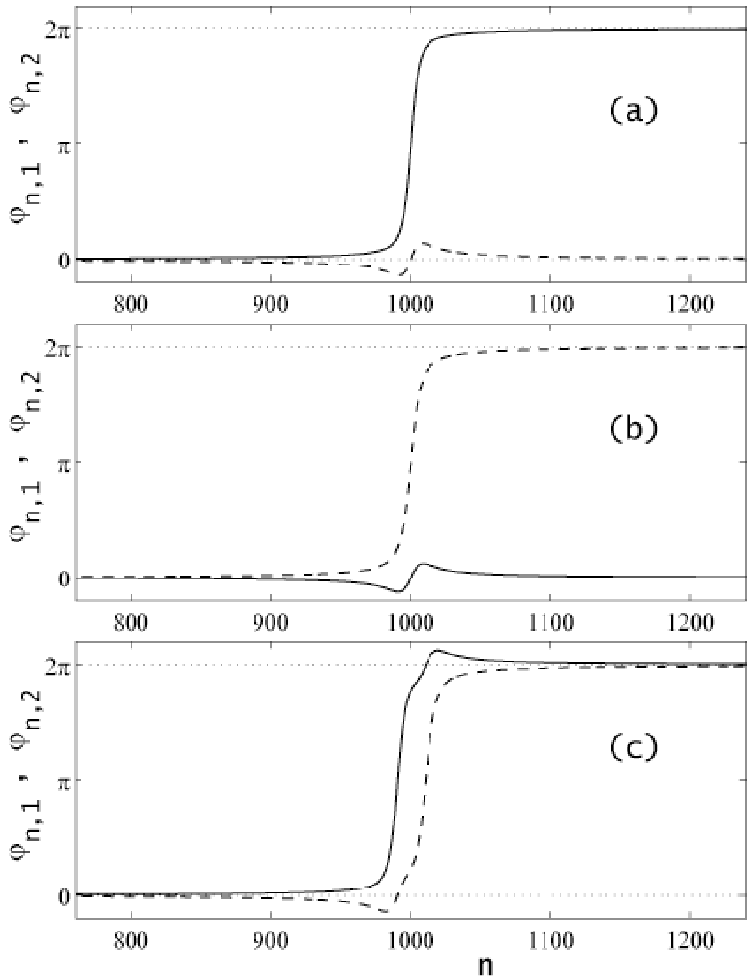

Figure 6-4 The view of three types of soliton solutions of the problem (6-81) – (6-82) with different topological charges (a) $q = (1,0)$, (b) $q = (0,1)$ and (c) $q = (1,1)$. Continuos lines correspond to angular displacements by the first component $\varphi_{n,1}$, dotted lines – to displacements by the second component $\varphi_{n,2}$.

7
Nonlinear Theory of DNA: Statistics of Nonlinear Excitations

In the dynamical models described in the previous chapter it was assumed that only one nonlinear excitation (soliton) was excited, the possibility of exciting two or more nonlinear excitations, their collisions and interactions were not considered. But DNA is a rather long molecule, and we can expect that several nonlinear excitations can be excited simultaneously. In this case, we should consider an ensemble of solitons and discuss their statistics. The latter becomes very important when we try to interpret experimental data on scattering (neutrons or light) by DNA or the data on DNA denaturation.

In this section we shall describe briefly two possible approaches to the problem of DNA soliton statistics. The first, based on the transfer operator method, was developed by Peyrard, Bishop and Dauxois [34, 283]. We shall call this approach the PBD approach. The second, based on the ideal gas approximation, was proposed by Fedyanin and Yakushevich [7, 22].

7.1
PBD Approach

The method of transfer operators was developed by Krumhansl and Schrieffer [284] for the statistical mechanics of the φ^4 field. Peyrard and coworkers [34, 283] applied it to describe the statistical mechanics of solitons in DNA.

To illustrate the method, let us take as a basis the model of Peyrard and Bishop which was described in detail in Section 5.3.4. The Hamiltonian of the model consists of two decoupled terms

$$H = H(x_1) + H(x_2). \tag{7-1}$$

The term $H(x_1)$ describes a harmonic lattice for the variable x_1

$$H(x_1) = \sum_n \{m\dot{x}_{1,n}^2/2 + k(x_{1,n} - x_{1,n-1})^2/2\}; \tag{7-2}$$

and the term $H(x_2)$ contains nonlinear terms for the variable x_2

$$H(x_2) = \sum_n \{m\dot{x}_{2,n}^2/2 + k(x_{2,n} - x_{2,n-1})^2/2\} + D[\exp(-A2^{1/2}x_{2,n}) - 1]^2\} \tag{7-3}$$

Let us consider now the statistical mechanics of the subsystem described by the Hamiltonian $H(x_2)$. This part of the total Hamiltonian H describes stretching internal motions, and is very important in the process of DNA denaturation. For simplicity, in further calculations we shall omit the index 2.

For a chain containing N units with nearest neighbor coupling and periodic boundary conditions, the classical partition function, given in terms of the Hamiltonian (7-3), can be expressed as

$$Z = \int_{-\infty}^{+\infty} \prod_{n=1}^{N} \mathrm{d}x\mathrm{d}p \exp\{H(x)/k_B T\} = Z_p Z_x, \tag{7-4}$$

where

$$Z = \int_{-\infty}^{+\infty} \prod_{n=1}^{N} \mathrm{d}p \exp\{-\sum_n [p^2/2m]/k_B T\}, \quad p = m\dot{x}, \tag{7-5}$$

$$Z = \int_{-\infty}^{+\infty} \prod_{n=1}^{N} \mathrm{d}p \exp\{-V(x_m; x_{n-1})k_B T\}, \tag{7-6}$$

$$V(x_n; x_{n-1}) = \sum_n \{k(x_n - x_{n-1})^2/2 + D[\exp(-A2^{1/2}x_n) - 1]^2\}. \tag{7-7}$$

The momentum part Z_p is readily integrated to give the usual kinetic factor for N particles

$$Z_p = (2\pi m k_B T)^{N/2}. \tag{7-8}$$

The potential part Z_x can be evaluated exactly in the thermodynamical limit of a large system ($N \to \infty$) using the eigenvalues and eigenfuctions of the transfer integral operator [284–286]

$$\int dx_{n-1}\{\exp[-V(x_n;x_{n-1})/k_B T]\}\Phi_i(x_{n-1}) = \{\exp[-\varepsilon_i/k_B T]\}\Phi_i(x_n). \tag{7-9}$$

Here Φ_i are the distribution functions for the field amplitude x, which are not only useful for computing Z_x, but also for computing expectation values of various quantities. The result of the calculations is

$$Z_x = \exp(-N\varepsilon_0/k_B T), \tag{7-10}$$

where ε_0 is the lowest eigenvalue of the operator.

The free energy of the model F can be computed then as

$$F = -k_B T \ln Z = -(Nk_B T/2)\ln(2\pi m k_B T) + N\varepsilon_0; \tag{7-11}$$

the specific heat C_v is equal to

$$C_v = -T(\partial^2 F/\partial T^2), \tag{7-12}$$

and finally the mean stretching $<x>$ of the hydrogen bonds, which gives the measure of the extent of the denaturation of the DNA molecule, can be calculated from

$$<x> = <x_n> = \frac{\sum_{i=1}^{N} \{<\Phi_i(x)|x|\Phi_i(x)>\Phi_i \exp[-N\varepsilon_i/k_B T]\}}{\sum_{i=1}^{N} \{<\Phi_i(x)|\Phi_i(x)> \exp[-N\varepsilon_i/k_B T]\}} = <\Phi_0(x)|x|\Phi_0(x)> = \int \Phi_0^2(x)x\,dx; \tag{7-13}$$

where it was taken into account that in the limit of large N the result will be dominated by the lowest eigenvalue ε_0 associated with the normalized eigenfunction $\Phi_0(x)$. A schematic picture of the temperature behavior of the calculated mean stretching of hydrogen bonds $<x>$ is shown in Figure 7.1.

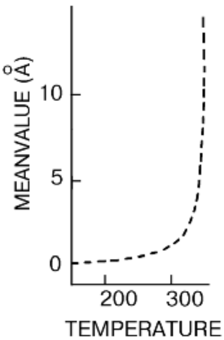

Figure 7.1 Schematic picture of the temperature behavior of the mean stretching of the hydrogen bonds in DNA. Reproduced with permission from Ref. [4].

This result has been successfully applied to the problem of DNA denaturation. We shall discuss this application in Chapter 9.

7.2 Ideal Gas Approximation

In this section we describe another approach to the problem of DNA soliton statistics, based on the similarity between the main dynamical properties of solitons and those of ordinary classical particles [7, 22].

For simplicity, let us assume, that internal DNA dynamics is modeled by the sine-Gordon equation:

$$\varphi_{ZZ} - \varphi_{TT} = \sin \varphi \tag{7-14}$$

having soliton solutions of kink type

$$\varphi(Z,T) = 4 \text{ arctg}\{\exp\pm[(1 - \nu^2)^{-1/2}(Z - \nu T - Z_0)]\}. \tag{7-15}$$

The corresponding Hamiltonian has the form

$$H = \int_{-\infty}^{+\infty} [(\varphi_T^2 + \varphi_Z^2)/2 + (1 - \cos\varphi)]dZ. \tag{7-16}$$

Inserting Eq. (7-15) into Eq. (7-16) we can calculate the energy of the DNA soliton

$$E_s = 8(1 - \nu^2)^{-1/2}. \tag{7-17}$$

In the 'nonrelativistic' limit when the velocity of the soliton ν is small, Eq. (7-17) takes the form

$$E_s = 8(1 + \nu^2/2). \tag{7-18}$$

This result can be interpreted as a sum of the kinetic energy

$$T = 8\nu^2/2; \tag{7-19}$$

and the potential energy

$$V = 8. \tag{7-20}$$

So, in this approximation we can ascribe mass $m_0 = 8$ and the velocity ν to the nonrelativistic DNA soliton and consider it as an ordinary classical material particle. In the relativistic case the soliton of the sine-Gordon equation can be characterized by mass $m = m_0\gamma$, impulse $p = 8\gamma\nu$ and energy $E_s = E_0\gamma$. Here m_0 is the mass of the soliton at rest ($m_0 = 8$), E_0 is the energy of the soliton at rest ($E_0 = 8$), $\gamma = (1 - \nu^2)^{-1/2}$.

All these data lead us towards a model of the ensemble of solitons in the form of ordinary classical systems consisting of N_s interacting material particles which have mass, impulses and energies of solitons. To simplify the problem we can make some more assumptions. We can suggest that the number of particles N_s is not large and the ensemble of solitons can be described as an 'ideal gas'. To obtain different macroscopic characteristics of the system, we can now use the results of classical statistical physics known for the model of an ideal gas of N_s material particles.

Taking into account that N_s is not a fixed number, let us write the large statistical sum in the form

$$\Xi(T,L,\mu) = \sum_{N_s=0}^{\infty} \exp(N_s/k_B T) Z_{Ns} = \sum_{N_s=0}^{\infty} (1/N_s!)[\exp(\mu/k_B T) z_0]^{N_s} =$$

$$= \exp\{\exp(\mu/k_B T) z_0\}; \tag{7-21}$$

where

$$z_0 = (1/2\pi) \int_0^L \mathrm{d}Z \int \mathrm{d}P \exp(-E_s/k_B T) = (L/2\pi) \int \mathrm{d}P \exp(-E_s/k_B T). \tag{7-22}$$

With the help of Ξ we can calculate various equilibrium characteristics of the model system, namely the thermodynamical potential G, the density of the solitons n_s, the capacity C_L and others. For illustration, let us give here a scheme for the calculation of the density of the solitons.

First, let us calculate the quantity z_0

$$z_0 = (L/2\pi) \int \mathrm{d}P \exp(-E_s/k_B T) = (8L/\pi)\ K_1(8/k_B T), \tag{7-23}$$

where $K_1(x)$ is McDonald's function. Inserting Eq. (7-18) into Eq. (7-21), we find the large statistical sum

$$\Xi = \exp[(\exp(\mu/k_B T)\ (8L/\pi)\ K_1(8/k_B T)]. \tag{7-24}$$

Let us then use the formulas of classical statistical physics, according to which the density of particles is determined by the equation

$$n_s = -L^{-1} \partial G/\partial \mu|_{\mu=0}; \tag{7-25}$$

where G is the thermodynamic potential. The latter is in turn determined by the equation

$$G = -k_B T \ln \Xi. \tag{7-26}$$

Inserting Eqs. (7-24) and (7-26) into Eq.(7-25) we finally obtain

$$n_s = (8/\pi)\ K_1(8/k_B T). \tag{7-27}$$

At 'low' temperature ($T << 8/k_B$) Eq. (7-27) simplifies to

$$n_s \cong 2(k_B T/\pi)^{1/2} \exp(-8/k_B T). \tag{7-28}$$

Finally, to calculate the correlation functions <...> we again should take into account that (i) the behavior of DNA solitons is very like that of normal material particles and (ii) the number of particles is small. In this case, we can use as a first approximation the model of an ideal gas and rewrite correlation functions <...> which are averaged over the ensemble of solitons in the following form:

$$<...> = \overline{N}_s <...>_1; \tag{7-29}$$

where $\overline{N}_s$ is the average number of particles, and the brackets $<...>_1$ denote averaging over the states of an individual soliton

$$<...>_1 = \{ \int_0^L dZ \int dP\,(...) \exp(-E_s/k_B T)\} / \{ \int_0^L dZ \int dP \exp(-E_s/k_B T)\}. \tag{7-30}$$

7.3
The Scattering Problem and Nonlinear Mathematical Models

Let us now discuss how the approach described in the previous section can be applied to the scattering problem. As an example, let us consider the scattering of neutrons, as we did in Section 4.3. It should be noted, however, that the resulting formula for the dynamical factor is rather general and can be applied to any scattering problem. As an example, we shall demonstrate how the resulting formula can be applied to the light scattering problem.

Let us begin with Eq. (4-106) and the expressions for the dynamical factors of coherent and incoherent scattering (4-107) which are rather general and valid for both the linear and nonlinear cases. To calculate inelastic coherent scattering , we shall use the one-phonon approximation, as we did in Section 4.3. So, the resulting formula for the dynamical factor has the form

$$S^{coh}(\boldsymbol{x}, w') = (2\pi\hbar N)^{-1} \exp(-2W_x) \sum_n \sum_{n'} \{\exp[-\boldsymbol{x}(\boldsymbol{R}_n^0 - \boldsymbol{R}_{n'}^0)$$
$$\int_{-\infty}^{+\infty} dt \;\; \exp(w't) < \boldsymbol{x u}_n(t), \boldsymbol{x u}_{n'}(0) >. \tag{7-31}$$

It is very similar to Eq. (4-121).

We can expect, however, that the results of calculations of the correlation functions $< \boldsymbol{x u}_n(t), \boldsymbol{x u}_{n'}(0) >$ obtained for the nonlinear case will differ from those obtained in Chapter 4 for the linear case. We can also expect that the results will be different for different dynamical models.

In this section we present the results of calculations of the dynamical factors of neutron scattering obtained for three models: the simple sine-Gordon model proposed by Englander, the helical version of the sine-Gordon model and the Y-model.

7.3.1
The Simple Sine-Gordon Model

The sine-Gordon model of the internal DNA dynamics has been described in detail in Section 5.1, and the corresponding dynamical equation written in dimensionless form has been discussed again in the previous section (see Eq. (7-14)).

To make the interpretation of the results easier let us return to the initial variables z, t. Then instead of Eq. (7-14) we shall deal with the equation of type (6-1) (or (6-2)) and the corresponding kink-like solution can be written in the following form

$$\varphi(z,t) = 4\tan^{-1}\{\exp[(\gamma/d)(z - vt - z_0)]\}, \tag{7-32}$$

where $\gamma = (1 - v_0{}^2/C)^{-1/2}$; $d = al(K/v_0)^{1/2}$.

Let us illustrate now how to calculate the inelastic component of coherent scattering which is of most interest in the study of nonlinear DNA dynamics. The general expression for the dynamical factor of inelastic coherent scattering is determined by Eq. (4-121) which can be transformed, however, to a simpler form Eq. (7-31) because, in the case of the sine-Gordon model, the index j can be omitted.

To calculate the dynamical factor we should know the expression for the vector $\boldsymbol{u}_n$ describing displacements of DNA bases from their equilibrium positions. This expression can be easily found if we take into account the analogy between DNA and the mechanical analog of the sine-Gordon system. In this case, the base displacements are equivalent to the displacements of pendula and have the form

$$\boldsymbol{u}_n = \{-l(1 - \cos\varphi_n);\ l\sin\varphi_n;\ 0\}, \tag{7-33}$$

where $\varphi_n(t)$ is the angular displacement of the nth pendulum and l is its length. Then the formula for the dynamical factor of inelastic coherent scattering takes the form

$$S^{\mathrm{coh}}(\boldsymbol{x}, w') = S_{\perp}(\boldsymbol{x}, w') + S_{\parallel}(\boldsymbol{x}, \boldsymbol{w}'), \tag{7-34}$$

where longitudinal and transverse components are determined by formulas

$$S_{\|}(\boldsymbol{x}, w') = (l^2 x_x{}^2/2\pi\hbar N)\exp(-2W_x) \sum_n \sum_{n'} \exp[-ix_z a(n-n')])$$

$$\int_{-\infty}^{+\infty} dt \ \exp(iw't) < (1-\cos\varphi_n(t)), (1-\cos\varphi_{n'}(0))>; \tag{7-35}$$

$$S_{\perp}(\boldsymbol{x}, w') = (l^2 x_y{}^2/2\pi\hbar N)\exp(-2W_x) \sum_n \sum_{n'} \exp[-ix_z a(n-n')])$$

$$\int_{-\infty}^{+\infty} dt \ \exp(iw't) < \sin\varphi_n(t), \sin\varphi_{n'}(0)>;$$

In the continuum limit Eq. (7-35) can be transformed to

$$S_{\|}(\boldsymbol{x}, w') = (l^2 x_x{}^2/2\pi\hbar N)\exp(-2W_x) \int_{-\infty}^{+\infty} dz \int_{-\infty}^{+\infty} dz' \int_{-\infty}^{+\infty} dt \ \{\exp[-ix_z(z-z')]$$

$$\exp(iw't) <(1 - \cos\varphi(z,t)), (1-\cos\varphi(z',0))>\}; \tag{7-36}$$

$$S_{\perp}(\boldsymbol{x}, w') = (l^2 x_y{}^2/2\pi\hbar N)\exp(-2W_x) \int_{-\infty}^{+\infty} dz \int_{-\infty}^{+\infty} dz' \int_{-\infty}^{+\infty} dt \ \{\exp[-ix_z(z-z')]$$

$$\exp(iw't) < \sin\varphi(z,t), \sin\varphi(z',0)>\};$$

Now let us use the ideal gas approximation where it is assumed that

$$<...>_1 \cong \overline{N}_s <...>. \tag{7-37}$$

Here $\overline{N}_s$ is the average number. For $\overline{N}_s$ we shall take the value estimated by Currie et al. [286]

$$\overline{N}_s = (2Na/d)(E_0/2\pi k_B T)\exp(-E_0/k_B T). \tag{7-38}$$

For $<...>_1$ we shall take the formula

$$< \dots >_1 = \{2M_0 C_0 K_1(E_0/k_B T)\}^{-1} \int_{-\infty}^{+\infty} dp_z(\dots)\exp(E_s/k_B T); \tag{7-39}$$

where K_1 is the McDonald function.

Inserting Eqs. (7-32) and (7-38) into Eq. (7-36) and taking into account Eqs. (7-39) and (7-34) we find the final expression for the dynamical factor of inelastic scattering

$$S^{coh}(\boldsymbol{x}, w') = \{2l^2 ad\gamma_0(E_0/2k_BT)^{1/2}/\hbar C_0 x_z K_1(E_0/k_BT)\} \exp(-2W_x)$$

$$\exp(-E_0/k_BT)\ \{x_x{}^2[(\pi x_z d/\gamma_0)/\mathrm{sh}(\pi x_z d/2\gamma_0)]^2 +$$

$$+ x_y{}^2[(\pi x_z d/\gamma_0)/\mathrm{ch}(\pi x_z d/2\gamma_0)]^2\} \exp(-E_0\gamma_0/k_BT); \tag{7-40}$$

where $\gamma_0 = (1-w'^2/x_z{}^2C_0{}^2)^{1/2}$.

The result (7-40) was obtained for the general (or 'relativistic') case. For low temperature ($T<<E_0/k_B$) and small velocities ($(w'/x_z) << C_0$) Eq. (7-40) can be reduced to a simpler form

$$S^{coh}\ (\boldsymbol{x}, w') = \{4l^2 adE_0/\hbar C_0 x_z k_BT\} \exp(-2W_x)$$

$$\exp(-E_0/k_BT)\ \{x_x{}^2[(\pi x_z d/\gamma_0)/\mathrm{sh}(\pi x_z\ d/2\gamma_0)]^2 +$$

$$+ x_y{}^2[(\pi x_z d/\gamma_0)/\mathrm{ch}(\pi x_z d/2\gamma_0)]^2\} \exp(-M_0 w'_0{}^2/2x_z{}^2 k_BT). \tag{7-41}$$

Note, that both the temperature corresponding to normal physiological conditions, and room temperature belong to the range of so-called 'low' temperatures, that is the condition $T<<(E_0/k_B)$ is valid. Indeed, if we use the values E_0 = 6 kcal $\cdot$ mol^{-1}, given in Ref. [15] and $k_B = 1.38 \times 10^{-23}$ J K^{-1} then $(E_0/k_B) = 3 \times 10^3$ K. The last value exceeds room temperature by an order of magnitude. The second condition, $(w'/x_z) << C_0$, means that Eq. (7-41) is valid for soliton waves moving in DNA with velocities which are much less than the velocity of an acoustic wave, C_0, ($C_0 = 2 \times 10^3$ m s^{-1} [231]).

In conclusion, let us show that Eq. (7-40) and (7-41) can be used in some other scattering problems. For example, let us consider the problem of scattering of infrared light by DNA. In the works of Komarov, Fisher and Pecora [287, 288] it was shown that the spectral density of scattering light I (x, w') is determined by

$$I\ (\boldsymbol{x}, w') = (I_0\alpha^2 w' \sin\overline{\gamma}/2\pi c^4\rho^2) \sum_n \sum_{n'} \{\exp[-\boldsymbol{x}(\boldsymbol{R}_n^0 - \boldsymbol{R}_{n'}^0)$$

$$\int_{-\infty}^{+\infty} \mathrm{d}t\ \ \exp(iw't) < \exp(\boldsymbol{x}\boldsymbol{u}_n(t), \exp(\boldsymbol{x}\boldsymbol{u}_{n'}(0)) > \tag{7-42}$$

where α is the polarizability of the bases; w' is the difference between the frequencies of the incident and scattered light; c is the velocity of light; ρ is the distance between the scattering system and the point of observation; the angle $\overline{\gamma}$ and the intensity of incident light I_0 are determined by

$$\cos\overline{\gamma} = (\boldsymbol{E}_0\boldsymbol{\rho}/E_0\rho),\ I_0 = c|\boldsymbol{E}_0|^2\ /\ 2\pi, \tag{7-43}$$

where $\boldsymbol{E}_0$ is the vector of the amplitude of the wave of the incident light; the rest of the notation has the same meaning as in Eqs. (4-106) and (4-107). Comparing Eqs. (7-43) and (4-107) we find

$$I(\boldsymbol{x}, w') = (I_0\,\alpha^2 w'^4 \hbar N \sin^2\overline{\gamma}/c^4\rho^2)\; S^{\mathrm{coh}}\,(\boldsymbol{x}, w'), \tag{7-44}$$

where S^{coh} $(\boldsymbol{x}, w')$ is determined in the general case by Eq. (4-107), in the one-phonon approximation by Eq. (4-121), and, finally, in the case of the sine-Gordon model by Eqs. (7-40) or (7-41).

7.3.2
Helical Sine-Gordon Model

Now let us see how the results obtained in the previous section will be changed if we take into account the helical character of the DNA structure. Instead of a simple sine-Gordon model consisting of a straight horizontal chain of pendula which oscillate in the gravitational field of the Earth (see Figure 7.2a) we should consider now something like a chain of pendula which is wound around an axis to form a helix (Figure 7.2b). In the helical model the hanging points are on the helix and the pivots of the pendula are directed towards the axis. So, the neighboring pendula are twisted relative to one another by the angle φ_0 = 36°, and the direction of the 'gravitational' field induced by the second chain changes from one pendulum to another by the angle φ_0 = 36°.

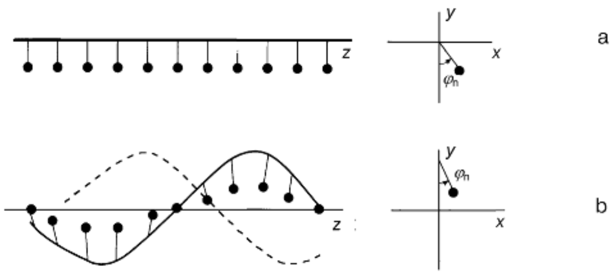

Figure 7.2 'Mechanical' models of DNA: (a) the linear model and (b) the helical model.

For simplicity let us neglect the changes in the Hamiltonian and those in the dynamical equations due to helicity. Then, in the calculations of the dynamical factor of neutron scattering we can use a kink-like solution of the type of Eq. (7-32). Let us take into account, however, that the vectors $\boldsymbol{R}_n$, $\boldsymbol{R}_n^0$, $\boldsymbol{u}_n$ in Eqs. (4-121) or (7-31) are substantially changed. Indeed, these vectors are now determined by:

$$\boldsymbol{R}_n^0 = \{(R - OO')\cos(2\pi n/10);\ -(R - OO')\sin(2\pi n/10);\ nl\},$$

$$\boldsymbol{R}_{\mathrm{n}} = \{(R\cos\varphi_n - OO')\cos(2\pi n/10) + R\sin\varphi_{\mathrm{n}}\sin(2\pi n/10);\ -(R\cos\varphi_n -$$

$$- OO')\sin(2\pi n/10) + R\sin\varphi_n\cos(2\pi n/10); nl\}, \quad (7\text{-}45)$$

$$\boldsymbol{u}_{\mathrm{n}} = \boldsymbol{R}_{\mathrm{n}} - \boldsymbol{R}_n^0 = \{R\cos(2\pi n/10)(\cos\varphi_n - 1) + R\sin(2\pi n/10)\sin\varphi_n;$$

$$- R\sin(2\pi n/10)(\cos\varphi_n - 1) + R\cos(2\pi n/10)\sin\varphi_n; 0\},$$

where OO' is the radius of the helix. Inserting the components of the vectors (7-45) into Eq. (7-31) and following step by step the scheme of calculation described in the previous section, we find the final formula for the dynamical factor:

$$S^{\mathrm{coh}}(\boldsymbol{x}, w') = \{l^2 ad(E_0/2k_{\mathrm{B}}T)^{1/2}/\hbar C_0 x_z K_1(E_0/k_{\mathrm{B}}T)\}\exp(-2W_{\mathrm{x}})$$

$$\exp(-E_0/k_{\mathrm{B}}T)(x_x^2 + x_y^2)\{F_+(x_z - 2\pi/10a) + F_-(x_z - 2\pi/10a)\}; \quad (7\text{-}46)$$

where the notations

$$F_\pm(\xi) = \{[\pi d\xi(1 - w'^2/C_0^2\xi^2)]/\mathrm{sh}[\pi d\xi(1 - w'^2/C_0^2\xi)/2] \pm$$

$$\pm [\pi d\xi(1 - w'^2/C_0^2\xi^2)]/\mathrm{ch}[\pi d\xi(1 - w'^2/C_0^2\xi^2)/2]\}(1/\xi)(1 - w'^2/C_0^2\xi^2)^{-1/2}$$

$$\exp[(-E_0/k_{\mathrm{B}}T)(1 - w'^2/C_0^2\xi^2)^{-1/2}] \quad (7\text{-}47)$$

are used.

For low temperatures and small velocities Eq. (7-46) transforms to

$$S^{\mathrm{coh}}(\boldsymbol{x}, w') = \{l^2 adE_0/\hbar C_0\,\pi k_{\mathrm{B}}T\}\exp(-2W_{\mathrm{x}})(x_x^2 + x_y^2)\{f_+(x_z + 2\pi/10a) +$$

$$+ f_-(x_z - 2\pi/10a)\}, \quad (7\text{-}48)$$

where

$$f_\pm(\xi) = [\pi d\xi/\mathrm{sh}(\pi d\xi/2) \pm \pi d\xi/\mathrm{ch}(\pi d\xi/2)](1/\xi)\exp(-E_0/k_{\mathrm{B}}T)\exp(-M_0 w'^2/2k_{\mathrm{B}}T\xi^2). \quad (7\text{-}49)$$

7.3.3 The Y-model

The Y-model was described in detail in Section 5.3. It consists of two parallel chains of pendula interacting with one another by longitudinal and transverse springs (Figure 4.5). The pendula play the role of bases in DNA chains, the longitudinal springs imitate the sugar–phosphate backbone and the transverse springs imitate the hydrogen interactions of bases in pairs.

The model shown in Figure 4.5 looks like a one-dimensional lattice with two pendula per unit cell. The lattice vector $\boldsymbol{R}_n^0$ is defined as

$$\boldsymbol{R}_n^0 = n\boldsymbol{a}; \tag{7-50}$$

where $\boldsymbol{a} = \{0;\ 0;\ a\}$. The equilibrium positions of the two pendula masses within a unit cell can be denoted by vectors

$$\boldsymbol{d}_1 = \{0;\ l;\ 0\},\quad \boldsymbol{d}_2 = \{0;\ b\text{-}l;\ 0\}, \tag{7-51}$$

where b is the distance between the chains and l is the length of the pendula.

The position vector $\boldsymbol{R}_{n,j}^0$ of the jth pendulum mass ($j = 1, 2$) in the nth unit cell is now given by

$$\boldsymbol{R}_{n,j}^0 = \boldsymbol{R}_n^0 + \boldsymbol{d}_j. \tag{7-52}$$

Taking into account that every pendulum rotates only in the xy plane, we can write possible displacements of the masses as

$$\begin{aligned} \boldsymbol{R}_{n,1}(t) - \boldsymbol{R}_{n,1}^0 &= \boldsymbol{u}_{n,1}(t) = \{-l(1\text{-}\cos\varphi_{n,1});\ l\sin\varphi_{n,1};\ 0\}, \\ \boldsymbol{R}_{n,2}(t) - \boldsymbol{R}_{n,2}^0 &= \boldsymbol{u}_{n,2}(t) = \{l(1\text{-}\cos\varphi_{n,2});\ l\sin\varphi_{n,2};\ 0\}, \end{aligned} \tag{7-53}$$

where $\varphi_{n,j}$ is the angular displacement of the nth pendulum of the jth chain.

To calculate the dynamical factor of inelastic neutron scattering we should insert Eq. (7-53) into Eq. (4-121). The correlation function which is a part of Eq. (4-121) then takes the form

$$\begin{aligned} &< \boldsymbol{x}\boldsymbol{u}_{n,j},\ \boldsymbol{x}\boldsymbol{u}_{n',j'} > = \\ &= x_x^{\,2} l^2 <(1-\cos\varphi_{n,j}(0),\ (1-\cos\varphi_{n',j'}(t))> - x_x x_y l^2 <(1-\cos\varphi_{n,j}(0)),\ \sin\varphi_{n',j'}(t) > - \\ &- x_y x_x l^2 <\sin\varphi_{n,j}(0),\ (1-\cos\varphi_{n',j'}(t))> + x_y^{\,2} l^2 <\sin\varphi_{n,j}(0),\ \sin\varphi_{n',j'}(t) >. \end{aligned} \tag{7-54}$$

Because of this we can rewrite the dynamical factor (4-121) in the following form:

$$S_{\text{inel}}^{\text{coh}}(\boldsymbol{x}, w') = S_{\text{xx}}^{\text{coh}}(\boldsymbol{x}, w') - S_{\text{xy}}^{\text{coh}}(\boldsymbol{x}, w') - S_{\text{yx}}^{\text{coh}}(\boldsymbol{x}, w') + S_{\text{yy}}^{\text{coh}}(\boldsymbol{x}, w'), \tag{7-55}$$

where

$$\begin{aligned} S_{\text{xx}}^{\text{coh}}(\boldsymbol{x}, w') &= [\exp(-2W_{\text{x}})/4\pi\hbar \text{N}] \sum_n \sum_{n'} \sum_j \sum_{j'} \exp[-i\boldsymbol{x}(\boldsymbol{R}_{n,j}^0 - \boldsymbol{R}_{\text{n}',\text{j}'}^0)] \\ &\int_{-\infty}^{+\infty} \text{d}t\ \ [\exp(-iw't)]\ x_{\text{x}}^{\,2} l^2 < (1-\cos\varphi_{n,j}(0)),\ (1-\cos\varphi_{n',j'}(t))>, \end{aligned} \tag{7-56}$$

$$S_{xy}^{coh}(\boldsymbol{x}, w') = [\exp(-2W_x)/4\pi\hbar N] \sum_n \sum_{n'} \sum_j \sum_{j'} \exp[-i\boldsymbol{x}(\boldsymbol{R}_{n,j}^0 - \boldsymbol{R}_{n',j'}^0)]$$

$$\int_{-\infty}^{+\infty} dt\ [\exp(-iw't)]\, x_x x_y l^2 < (1-\cos\varphi_{n,j}(0)), \sin\varphi_{n',j'}(t))>, \tag{7-57}$$

$$S_{yx}^{coh}(\boldsymbol{x}, w') = [\exp(-2W_x)/4\pi\hbar N] \sum_n \sum_{n'} \sum_j \sum_{j'} \exp[-i\boldsymbol{x}(\boldsymbol{R}_{n,j}^0 - \boldsymbol{R}_{n',j'}^0)]$$

$$\int_{-\infty}^{+\infty} dt\ [\exp(-iw't)]\, x_y x_x l^2 < \sin\varphi_{n,j}(0), (1-\cos\varphi_{n',j'}(t))>, \tag{7-58}$$

$$S_{yy}^{coh}(\boldsymbol{x}, w') = [\exp(-2W_x)/4\pi\hbar N] \sum_n \sum_{n'} \sum_j \sum_{j'} \exp[-i\boldsymbol{x}(\boldsymbol{R}_{n,j}^0 - \boldsymbol{R}_{n',j'}^0)]$$

$$\int_{-\infty}^{+\infty} dt\ [\exp(-iw't)]\, y_x{}^2 l^2 < \sin\varphi_{n,j}(0), \sin\varphi_{n',j'}(t))>, \tag{7-59}$$

Now let us pass to the continuum approximation

$$\begin{aligned} &a \to 0, \qquad N \to \infty \\ &na \to z, \\ &\varphi_{n,j}(t) = \varphi_j(na,t) \to \varphi_j(z,t), \\ &\sum_n \to (1/a) \int_{-\infty}^{+\infty} dz, \end{aligned} \tag{7-60}$$

and rewrite the components of the dynamical factor in this approximation

$$S_{xx}^{coh}(\boldsymbol{x}, w') = [\exp(-2W_x) x_x{}^2 l^2/4\pi\hbar N a^2]$$

$$\int_{-\infty}^{+\infty} dt \int_{-\infty}^{+\infty} dz \int_{-\infty}^{+\infty} dz' \sum_j \sum_{j'} \exp[-i\boldsymbol{x}(\boldsymbol{R}_j^0(z) - \boldsymbol{R}_{j'}^0(z'))][\exp(-iw't)]$$

$$<(1\text{-}\cos\varphi_j(z,0)), (1\text{-}\cos\varphi_{j'}(z',t))> = 2[\exp(-2W_x) x_x{}^2 l^2 (1+\cos x_y h)/\pi\hbar N a^2]$$

$$\int_{-\infty}^{+\infty} dt \int_{-\infty}^{+\infty} dz \int_{-\infty}^{+\infty} dz' \exp[-ix_z(z-z')]\exp(-iw't)$$

$$<\mathrm{sech}^2[(\gamma/d)(z-z_0)], \mathrm{sech}^2[(\gamma/d)(z'-z_0-vt)]>\}, \tag{7-61}$$

$$S_{xy}^{coh}(\boldsymbol{x}, w') = [\exp(-2W_x)x_x x_y l^2/4\pi\hbar \mathrm{Na}^2]$$

$$\int_{-\infty}^{+\infty} dt \int_{-\infty}^{+\infty} dz \int_{-\infty}^{+\infty} dz' \sum_j \sum_{j'} \exp[-i\boldsymbol{x}(\boldsymbol{R}_j^0(z) - \boldsymbol{R}_{j'}^0(z'))][\exp(-iw't)]$$

$$<(1\text{-}\cos\varphi_j(z,0)), (\sin\varphi_{j'}(z',t))> = -2i[\exp(-2W_x)x_x x_y l^2 \sin x_y h)/\pi\hbar Na^2]$$

$$\int_{-\infty}^{+\infty} dt \int_{-\infty}^{+\infty} dz \int_{-\infty}^{+\infty} dz' \{\exp[-ix_z(z-z')]\exp(-iw't) < \mathrm{sech}^2[(\gamma/d)(z-z_0)],$$

$$\mathrm{sh}[(\gamma/d)(z'-z_0) - vt]\,\mathrm{sech}^2[(\gamma/d)(z'-z_0-vt)]>\}, \tag{7-62}$$

$$S_{yx}^{coh}(\boldsymbol{x}, w') = [\exp(-2W_x)x_y x_x l^2/4\pi\hbar \mathrm{Na}^2]$$

$$\int_{-\infty}^{+\infty} dt \int_{-\infty}^{+\infty} dz \int_{-\infty}^{+\infty} dz' \sum_j \sum_{j'} \exp[-i\boldsymbol{x}(\boldsymbol{R}_j^0(z) - \boldsymbol{R}_{j'}^0(z'))][\exp(-iw't)]$$

$$<(\sin\varphi_j(z,0)), (1\text{-}\cos\varphi_{j'}(z',t))> = 2i[\exp(-2W_x)x_x x_y l^2(\sin x_y h)/\pi\hbar Na^2]$$

$$\int_{-\infty}^{+\infty} dt \int_{-\infty}^{+\infty} dz \int_{-\infty}^{+\infty} dz' \{\exp[-ix_z(z-z')]\exp(-iw't) < \mathrm{sh}[(\gamma/d)(z-z_0]\,\mathrm{sech}^2[\gamma/d)(z-z_0)],$$

$$\mathrm{sech}^2[(\gamma/d)(z'-z_0-vt)]>\}, \tag{7-63}$$

$$S_{yy}^{coh}(\boldsymbol{x}, w') = [\exp(-2W_x)x_y{}^2 l^2/4\pi\hbar Na^2]$$

$$\int_{-\infty}^{+\infty} dt \int_{-\infty}^{+\infty} dz \int_{-\infty}^{+\infty} dz' \sum_j \sum_{j'} \exp[-i\boldsymbol{x}(\boldsymbol{R}_j^0(z) - \boldsymbol{R}_{j'}^0(z'))][\exp(-iw't)]$$

$$<(\sin\varphi_j(z,0)), (\sin\varphi_{j'}(z',t))> = 2[\exp(-2W_x)x_y{}^2 l^2(1-\cos x_y h)/\pi\hbar Na^2]$$

$$\int_{-\infty}^{+\infty} dt \int_{-\infty}^{+\infty} dz \int_{-\infty}^{+\infty} dz' \{\exp[-ix_z(z-z')]\exp(-iw't) < \mathrm{sh}[(\gamma/d)(z-z_0)]\,\mathrm{sech}^2[(\gamma/d)(z-z_0)],$$

$$\mathrm{sh}[(\gamma/d)(z'-z_0-vt)]\,\mathrm{sech}^2[(\gamma/d)(z'-z_0-vt)]>\}. \tag{7-64}$$

To calculate the correlation functions <...>, let us again use the ideal gas approximation:

$$<...> = \overline{N}_s <...>_1. \tag{7-65}$$

Here $\overline{N}_s$ is the average number of solitons

$$\overline{N}_s = (2aN/d)(E_0/2\pi k_B T)^{1/2} \exp(-E_0/k_B T); \tag{7-66}$$

and $<...>_1$ is the averaging over the states of one isolated soliton

$$<...>_1 = \{\int_{-\infty}^{+\infty} \mathrm{d}p_z \int_{-L}^{+L} \mathrm{d}z_0\ (...)\exp[-E_0/k_B T]\}/\{\int_{-\infty}^{+\infty} \mathrm{d}p_z \int_{-L}^{+L} \mathrm{d}z_0\ \exp[-E_0\gamma/k_B T] =$$

$$= \{C_0/[2E_0 NaK_1(E_0/k_B T)]\} \int_{-\infty}^{+\infty} \mathrm{d}p_z \int_{-L}^{+L} \mathrm{d}z_0\ (...)\exp[-E_0/k_B T], \tag{7-67}$$

where $K_1(x)$ is a Macdonald function.

If we insert Eqs. (7-65) –(7-67) into Eqs. (7-61) –(7-64), we obtain

$$S_{xx}^{\mathrm{coh}}\ (\boldsymbol{x}, w') = \exp(-2W_x)[x_x{}^2 l^2(1 + \cos x_y h)C_0\overline{N}_s/\pi\hbar N^2 a^3 E_0 K_1(E_0/k_B T)]$$

$$\int_{-\infty}^{+\infty} \mathrm{d}t \int_{-\infty}^{+\infty} \mathrm{d}z \int_{-\infty}^{+\infty} \mathrm{d}z' \int_{-\infty}^{+\infty} \mathrm{d}p_z \int_{-L}^{+L} \mathrm{d}z_0\ \{\exp[-\mathrm{i}x_z(z-z')]\exp(-\mathrm{i}w' t)\exp(-E_0\gamma/k_B T)$$

$$\mathrm{sech}^2[(\gamma/d)(z-z_0)]\ \mathrm{sech}^2[(\gamma/d)(z'-z_0-vt)]\} =$$

$$= B\int_{-\infty}^{+\infty} \mathrm{d}t \int_{-\infty}^{+\infty} \mathrm{d}z \int_{-\infty}^{+\infty} \mathrm{d}z' \int_{-\infty}^{+\infty} \mathrm{d}p_z \int_{-L}^{+L} \mathrm{d}z_0\ \{\exp[-\mathrm{i}x_z(z-z')]\exp(-\mathrm{i}w' t)\exp(-\mathrm{E}_0\gamma/\mathrm{k_B T})$$

$$\mathrm{sech}^2[\gamma(z-z_0)/d]\ \mathrm{sech}^2[\gamma(z'-z_0-vt)]\} \equiv BI(x); \tag{7-68}$$

where

$$B = \exp(-2W_x)[2x_x{}^2 l^2 C_0(1 + \cos x_y h)/\pi\hbar Na^2 d(2\pi k_B T E_0)^{1/2}$$

$$K_1(E_0/k_B T)]\ \exp(-E_0/k_B T); \tag{7-69}$$

$$I(x_z) = \int_{-\infty}^{+\infty} \mathrm{d}t \int_{-\infty}^{+\infty} \mathrm{d}z \int_{-\infty}^{+\infty} \mathrm{d}z' \int_{-\infty}^{+\infty} \mathrm{d}p_z \int_{-L}^{+L} \mathrm{d}z_0 \, \exp[-\mathrm{i}x_z(z - z')]\exp(-\mathrm{i}w' t)$$

$$\exp(-E_0/k_\mathrm{B}T) \, \{\mathrm{sech}^2[\gamma(z - z_0)/d] \, \mathrm{sech}^2[\gamma(z' - z_0 - vt)]\}. \tag{7-70}$$

If we take into account that

$$\int_{-\infty}^{+\infty} \mathrm{d}z \, \exp(-\mathrm{i}x_z z) \, \mathrm{sech}[\gamma(z - z_0)/d] = (d/\gamma) \, \exp(-\mathrm{i}x_z z_0)(\pi d x_z/\gamma)/\mathrm{sh}(\pi d x_z/2\gamma) \tag{7-71}$$

and

$$\int_{-\infty}^{+\infty} \mathrm{d}z' \, \exp(\mathrm{i}x_z z') \, \mathrm{sech}^2[\gamma(z' - z_0 - vt)/d] = (d/\gamma) \, \exp(\mathrm{i}x_z(z_0 + vt)]$$

$$(\pi d x_z/\gamma)/\mathrm{sh}(\pi d x_z/2\gamma); \tag{7-72}$$

we obtain

$$I(x_z) = (d/\gamma)^2 \int_{-\infty}^{+\infty} \mathrm{d}t \int_{-\infty}^{+\infty} \mathrm{d}p_z \int_{-L}^{+L} \mathrm{d}z_0 \, \exp(-\mathrm{i}w' t) \, \exp(ix_z vt)\exp(-E_0\gamma/k_B T)$$

$$(\pi d x_z/\gamma)^2/\mathrm{sh}^2(\pi d x_z/2\gamma). \tag{7-73}$$

Let us take into account also that

$$\int_{-\infty}^{+\infty} \mathrm{d}t \, \exp[-\mathrm{i}(w' - x_z v)t] = (2\pi/x)\delta(v - w'/x_z) \tag{7-74}$$

and

$$\int_{-L}^{+L} \mathrm{d}z_0 = Na. \tag{7-75}$$

Then we obtain

$$I(x_z) = (2\pi Nad^2/x_z)\int_{-\infty}^{+\infty} \mathrm{d}p_z\,\delta(v - w'/x_z)\gamma^{-2}(\pi dx_z/\gamma)^2/sh^2(\pi dx/2\gamma)$$

$$\exp(-E_0/k_B T) = (2\pi Nad^2/x_z)\int_{-\infty}^{+\infty} \mathrm{d}v\; M\gamma^3\delta(v - w'/x_z)\gamma^{-2}$$

$$(\pi dx_z/\gamma)^2/\mathrm{sh}^2(\pi dx_z/2\gamma)\exp(-E_0/k_\mathrm{B}T) =$$

$$= (2\pi Nad^2 M\gamma_0/x_z)\,[(\pi dx_z/\gamma_0)/\mathrm{sh}^2(\pi dx_z/2\gamma_0)]\exp(-E_0\gamma/k_\mathrm{B}T), \tag{7-76}$$

where we used the following relations

$$p_z = Mv\gamma;\ \mathrm{d}p_z = \mathrm{d}(Mv\gamma) = M\gamma\,\mathrm{d}v + Mv\,\mathrm{d}\gamma = M\gamma^3\,\mathrm{d}v. \tag{7-77}$$

The final result for the component $\mathrm{S}^{\mathrm{coh}}_{xx}$ will have the form

$$\mathrm{S}^{\mathrm{coh}}_{xx}(\boldsymbol{x}, w') = Ax_x^{\,2}(1 + \cos x_y h)\,(\pi dx_z/\gamma_0)^2/\mathrm{sh}^2(\pi dx_z/2\gamma_0); \tag{7-78}$$

where

$$A = \{4l^2 d\gamma_0(E_0/2\pi k_\mathrm{B}T)/\hbar C_0 a x_z K_1(E_0/k_\mathrm{B}T)\}\exp(-2W_\mathrm{x})\exp(-E_0/k_\mathrm{B}T)$$

$$\exp(-E_0\gamma_0/k_\mathrm{B}T);\ \gamma_0 = (1 - v_0^{\,2}/C_0^{\,2})^{-1/2},\ v_0 = w'/x_z. \tag{7-79}$$

We can calculate the other three components $S^{\mathrm{coh}}_{xy}(\boldsymbol{x}, w')$, $S^{\mathrm{coh}}_{yx}(\boldsymbol{x}, w')$, in the same way. As a result, we obtain

$$S^{\mathrm{coh}}_{xy}(\boldsymbol{x}, w') = \exp(-2W_\mathrm{x})[x_x x_y l^2(-\mathrm{i})C_0\overline{N}_\mathrm{s}\sin(x_y h)/\pi\hbar N^2 a^3 E_0 K_1(E_0/k_\mathrm{B}T)]$$

$$\int_{-\infty}^{+\infty}\mathrm{d}t\int_{-\infty}^{+\infty}\mathrm{d}z\int_{-\infty}^{+\infty}\mathrm{d}z'\int_{-\infty}^{+\infty}\mathrm{d}p_z\int_{-L}^{+L}\mathrm{d}z_0\ \{\exp[-\mathrm{i}x_z(z - z')]\exp(-\mathrm{i}w't)\exp(-E_0\gamma/k_B T)$$

$$\mathrm{sech}^2[(\gamma/d)(z - z_0)]\,\mathrm{sh}[(\gamma/d)(z' - z_0 - vt)]\,\mathrm{sech}^2[(\gamma/d)(z' - z_0 - vt)]\} =$$

$$= Ax_x x_y(-\,\mathrm{i}\sin x_y h)\,(\pi dx_z/\gamma_0)^2/[\mathrm{sh}(\pi dx_z/2\gamma_0)\,\mathrm{ch}(\pi dx_z/2\gamma_0)], \tag{7-80}$$

$$S_{yx}^{\mathrm{coh}}(\boldsymbol{x}, w') = \exp(-2W_{\mathrm{x}})[x_y x_x l^2(+\,\mathrm{i})C_0\overline{N}_{\mathrm{s}}\sin(x_y h)/\pi\hbar N^2 a^3 E_0 K_1(E_0/k_{\mathrm{B}}T)]$$

$$\int_{-\infty}^{+\infty}\mathrm{d}t\int_{-\infty}^{+\infty}\mathrm{d}z\int_{-\infty}^{+\infty}\mathrm{d}z'\int_{-\infty}^{+\infty}\mathrm{d}p_z\int_{-L}^{+L}\mathrm{d}z_0\ \{\exp[-\mathrm{i}x_z(z-z')]\ \exp(-\mathrm{i}w' t)\ \exp(-E_0\gamma/k_B T)$$

$$\mathrm{sh}[(\gamma/d)(z-z_0)]\ \mathrm{sech}^2[(\gamma/d)(z'-z_0)]\ \mathrm{sech}^2[(\gamma/d)(z'-z_0-vt)]\} =$$

$$= A x_y x_x(-\,i\sin x_y h)\ (\pi d x_z/\gamma_0)^2/[\mathrm{sh}(\pi d x_z/2\gamma_0)\ \mathrm{ch}(\pi d x_z/2\gamma_0)], \tag{7-81}$$

$$S_{yy}^{\mathrm{coh}}(\boldsymbol{x}, w') = \exp(-2W_{\mathrm{x}})[x_y{}^2 l^2(1-\cos x_y h)C_0\overline{N}_{\mathrm{s}}/\pi\hbar N^2 a^3 E_0 K_1(E_0/k_{\mathrm{B}}T)]$$

$$\int_{-\infty}^{+\infty}\mathrm{d}t\int_{-\infty}^{+\infty}\mathrm{d}z\int_{-\infty}^{+\infty}\mathrm{d}z'\int_{-\infty}^{+\infty}\mathrm{d}p_z\int_{-L}^{+L}\mathrm{d}z_0\ \{\exp[-\mathrm{i}x_z(z-z')]\ \exp(-\mathrm{i}w' t)\ \exp(-E_0\gamma/k_B T)$$

$$\mathrm{sh}[(\gamma/d)(z-z_0)]\ \mathrm{sech}^2[(\gamma/d)(z-z_0)]\ \mathrm{sh}[(\gamma/d)(z'-z_0-vt)]$$

$$\mathrm{sech}^2\,[(\gamma/d)(z'-z_0-vt)]\} = A x_y{}^2\,(1-\cos x_y h)\ (\pi d x_z/\gamma_0)^2/\mathrm{ch}^2(\pi d x_z/2\gamma_0). \tag{7-82}$$

And the final formula for coherent inelastic scattering, which is determined by a sum of four components (see Eq. (7-55)) then has the form

$$S_{\mathrm{inel}}^{\mathrm{coh}}(\boldsymbol{x}, w\overset{\wp}{\mathrm{A}}) = \{[4l^2\gamma_0 d\,\exp(-\,2W_{\mathrm{x}})\ (E_0/2\pi k_{\mathrm{B}}T)^{1/2}]/[\hbar C_0 a x_z K_1(E_0/k_{\mathrm{B}}T)$$

$$\exp(-\,E_0/k_{\mathrm{B}}T)\ \exp(-\,E_0\gamma/k_{\mathrm{B}}T)\ \{X^2(1+\cos x_y h) - 2XY\sin x_y h +$$

$$+\ Y^2(1-\cos x_y h)\}; \tag{7-83}$$

where $X = x_x(\pi d x_z/\gamma_0)/\mathrm{sh}(\pi d x_z/2\gamma_0)$; $Y = x_y(\pi d x_z/\gamma_0)/\mathrm{ch}(\pi d x_z/2\gamma_0)$.

8
Experimental Tests of DNA Nonlinearity

In this chapter we describe experimental data which have been interpreted in terms of nonlinear theory. To be impartial, we present both the arguments in favor of interpretation of experimental data in the framework of the nonlinear concept and those against. In addition, we describe new approaches in the experimental study of nonlinear DNA properties, which may be able to resolve the contradiction between these two positions.

8.1
Hydrogen–Tritium (or Hydrogen–Deuterium) Exchange

Hydrogen–tritium (or hydrogen–deuterium) exchange is widely used to study internal DNA dynamics [145–147]. (A simple scheme for the exchange was described in detail in Section 2.8). The method is especially effective in studying the dynamics of open states. As we mentioned above, the formation of an open state (or base-pair opening) is a complex process which includes different types of simpler internal motions, and some of the motions can have large amplitudes. So, one can expect that opening of bases is one example where the nonlinear properties of the DNA molecule should be actively displayed.

Indeed, from analysis of the data on hydrogen–tritium exchange, Englander et al. [15] came to the conclusion that open states with low energies and slow opening and closing rates can be interpreted as structural deformations formed by several adjacent unpaired base pairs (Figure 8.1). They assumed a mobile character for the deformations, that is a capability to diffuse along the double helix. It was suggested also that the movement of the deformations can be modeled mathematically as a propagation of solitary waves which are the kink- and antikink-like solutions:

$$\varphi_{\substack{\text{kink}\\ \text{antikink}}}(Z,T) = 4\ \text{arctg}\{\exp\pm[(1-v^2)^{-1/2}(Z - vT - Z_0)]\}; \tag{8-1}$$

of the sine-Gordon equation

$$\varphi_{ZZ} - \varphi_{TT} = \sin\varphi; \tag{8-2}$$

described in Section 5.1.

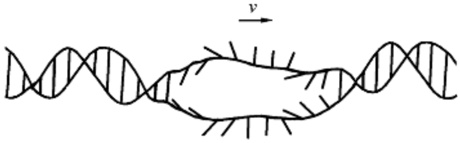

Figure 8.1 Diagram of a mobile defect within DNA.

These suggestions have been widely discussed and criticized by some theoreticians and experimenters. The criticism of theoreticians was directed towards the oversimplicity of model Eq. (8-2). As a result, many improvements of the initial model have been proposed [16–26], most of which were described in Chapter 5.

The criticism of experimenters, and especially, the arguments of Frank-Kamenetskii [289, 290], were based on the statement that the value of the probability of base-pair opening which was taken from the data of Mandal et al. [147] and used later by Englander et al. [15], is incorrect. Indeed, according to the data of Mandal et al. [147] the probability is rather high (about 10^{-2}), but according to the data of Frank-Kamenetskii [289, 290] (and also of Gueron et al. [291]) the probability of base opening is only about 10^{-5}. The latter result is considered by opponents as an argument in favor of another suggestion according to which only single unpaired base pairs can occur. To be impartial, we should state that the question still remains open, and some other additional experimental investigations are required to clarify it.

An idea very close to that of Englander and coauthors, was proposed independently by Fernandez [234] who considered the proton exchange activity of RNA. He suggested that RNA provides a better study case than its counterpart, DNA, and showed that the proton exchange catalytic activity of RNA may serve as a probe for solitons.

8.2 Resonant Microwave Absorption

One more useful tool in research on the nonlinear properties of biomolecules is the study of the interaction of the molecule with microwaves. A simple scheme of the microwave experiment is shown in Figure 8.2.

The most impressive example of the application of this method is the investigation of resonant microwave absorption (in the range of several gigahertz) by aqueous solutions containing DNA.

Experimental evidence of resonant microwave absorption in DNA was first reported by Webb and Booth [43] and later by Swicord and Davis [44, 45]. Although their results are still controversial [160, 293–295], they stimulated theoreticians to study the problem. As a result, many different approaches have been proposed. Some were based on the linear (harmonic) model of the internal DNA dynamics [161, 186,187], and others were based on the nonlinear concept [30, 47, 251].

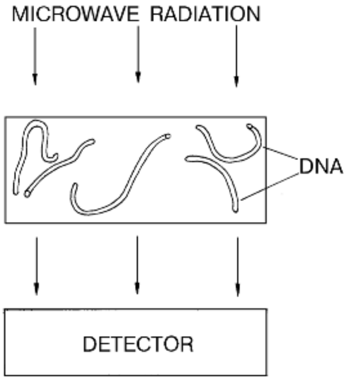

Figure 8.2 A simple scheme of the experiment on microwave absorption by an aqueous solution containing DNA.

The first nonlinear mathematical model of the interaction of DNA with an external microwave field was proposed by Muto et al. [30, 251]. As the basis they used the ideal rod-like model of internal DNA dynamics

$$u_{tt} = C^2 u_{zz} - (\varepsilon/C^2) u_{zztt} + \delta(u_z{}^2)_z, \tag{8-3}$$

which describes longitudinal displacements ($u(z,t)$) in DNA. An equation of the type of Eq. (8-3) was considered in Section 5.2. To imitate the conditions of the microwave experiment, Muto et al. added two additional terms imitating the effects of dissipation:

$$-A_t u \tag{8-4}$$

and the effects of interaction with the external (microwave) field

$$F(z) \cos\Omega t. \tag{8-5}$$

The resulting equation, which is known as the Ostrovskii–Sutin equation, has the following form:

$$u_{tt} = C^2 u_{zz} - (\varepsilon/C^2) u_{zztt} + \delta(u_z{}^2)_z - A u_t + F(z) \cos\Omega t. \tag{8-6}$$

Here $u(z,t)$ is the longitudinal displacement, C is the sound wave velocity, and ε, δ are the dispersive and anharmonic parameters, respectively.

Using a special numerical procedure Muto et al. [30] calculated the absorption spectrum and compared it with the spectrum calculated earlier by Van Zandt [186] in the framework of the linear approximation. The results obtained were in close agreement only for the fourth peak (the third overtone). The most marked differences were observed for the first (fundamental) peak, namely, in the nonlinear approximation, the resonance peak exhibited a multicomponent character (fine structure) and the linewidth of the peak was not simply related to the damping constant as in the case of the linear approximation. The difference between the spectra can be explained by the presence of the nonlinear term $\delta(u_z{}^2)_z$ in Eq. (8-6).

The approach of Muto et al. was improved by Zhang [47]. He considered a rod-like model of DNA (as did Muto et al.), but he took into account both longitudinal and torsional degrees of freedom. As a result, instead of an equation of the type of Eq. (8-3) he proposed two coupled equations:

$$\begin{aligned} u_{tt} &= C^2 u_{zz} - (\varepsilon/C^2)u_{zztt} + \delta(u_z{}^2)_z + \chi_1(\varphi_z{}^2)_z + \chi_2(\varphi_z u_z)_z, \\ \varphi_{tt} &= v^2\varphi_{zz} - w_0{}^2\varphi + s\chi_2(u_z{}^2)_z + 4s\chi_1(\varphi_z u_z)_z, \end{aligned} \tag{8-7}$$

where $u(z,t)$, $\varphi(z,t)$ are the longitudinal and rotational displacements, respectively; C and v are the torsional and longitudinal acoustic velocities; ε and δ are the dispersive and anharmonic parameters; w_0 and s are the frequency parameter and the parameter for dimensional transform; χ_1 and χ_2 are the coupling parameters.

To consider the microwave absorption by aqueous solutions containing DNA, Zhang added four terms to Eq. (7-8) (two damping terms and two driving terms) and solved the resulting system of two nonlinear coupled equations by the method of perturbation.

As a result, he obtained that (i) the resonant absorption of microwave energy is possible for both longitudinal and torsional modes, (ii) the resonance frequencies are in the region of gigahertz and subterahertz, (iii) for both modes so-called subharmonic resonances are possible.

However, these theoretical predictions have not yet been checked by experimenters.

8.3 Scattering of Neutrons and Light

There have been a few attempts to explain the neutron scattering by DNA in terms of solitons. We describe here two of them by Fedyanin and Yakushevich [3, 7, 22] and Baverstock and Cundall [48, 296, 297].

8.3.1 Interpretation of Fedyanin and Yakushevich

Fedyanin and Yakushevich [3, 7, 22] made some predictions of the results of the scattering of thermal neutrons by DNA solitons. To describe them, let us return again to Section 2.8, where the general characteristics of the neutron scattering method and basic conservation equations governing the interaction between incident radiation and scattering centers (DNA bases) were presented.

As we mentioned there, most of the spectrometers in current use work with unpolarized neutrons and produce data in the form of a partial differential cross-section $d^2\sigma/d\Omega dE'$ which gives the intensity of neutrons with energies between E'

and $E'+dE'$ scattered into a solid angle element $d\Omega$. Below we shall use the results of the calculations of the partial differential cross-section, and especially the contribution of inelastic coherent scattering obtained in Section 7.3.

First let us consider a simple sine-Gordon model of the internal DNA dynamics (Figure 7.2a). Let us write the formula for the dynamical factor of inelastic coherent scattering obtained in Section 7.3

$$S^{\mathrm{coh}}\,(\boldsymbol{x}, w') = \{2l^2 ad\gamma_0(E_0/2\pi k_B T)^{1/2}/\hbar C_0 x_z K_1(E_0/k_B T)\}\exp(-2W_x)$$
$$\exp(-E_0/k_B T)\{x_x{}^2[(\pi x_z d/\gamma_0)/\mathrm{sh}(\pi x_z d/2\gamma_0)]^2 +$$
$$+ x_y{}^2[(\pi x_z d/\gamma_0)/\mathrm{ch}(\pi x_z d/2\gamma_0)]^2\}\exp(-E_0\gamma_0/k_B T), \tag{8-8}$$

where $\gamma_0 = (1-w'^2/x_z{}^2C_0{}^2)^{-1/2}$.

In the case of low temperature $(T<<E_0/k_B)$ and small velocities $((w'/x_z) << C_0)$ instead of Eq. (8-8) we have

$$S^{\mathrm{coh}}\,(\boldsymbol{x}, w') = \{4l^2 adE_0/\hbar C_0 x_z \pi k_B T\}\exp(-2W_x)$$
$$\exp(-E_0/k_B T)\,\{x_x{}^2[(\pi x_z d/\gamma_0)/\mathrm{sh}(\pi x_z d/2\gamma_0)]^2 +$$
$$+ x_y{}^2[(\pi x_z d/\gamma_0)/\mathrm{ch}(\pi x_z d/2\gamma_0)]^2\}\exp(-M_0 w'_0{}^2/2x_z{}^2 k_B T). \tag{8-9}$$

From Eq.(8-9) we can predict the existence of the central peak in the scattering spectrum, and that the parameters of the peak such as the integral intensity I

$$I = \int S^{\mathrm{coh}}\,(\boldsymbol{x}, w')\,dw' = A(\boldsymbol{x})\{k_B T\}^{-1/2}\exp(E_0/k_B T); \tag{8-10}$$

and the width Δw

$$\Delta w = B(\boldsymbol{x})\{k_B T\}^{1/2}; \tag{8-11}$$

depend on the temperature T and the wave vector $\boldsymbol{x}$. Note that the coefficients $A(\boldsymbol{x})$ and $B(\boldsymbol{x})$ do not depend on the temperature. They are determined by

$$A(\boldsymbol{x}) = \{4(2)^{1/2}R^2 ad/\hbar(\pi E_0)^{1/2}\}\exp(-2W_x)\,\{x_x{}^2[(\pi x_z d)/\mathrm{sh}(\pi x_z d/2)]^2 +$$
$$+ x_y{}^2[(\pi x_z d)/\mathrm{ch}(\pi x_z d/2)]^2\}, \tag{8-12}$$
$$B(\boldsymbol{x}) = x_z/M_0{}^{1/2}. \tag{8-13}$$

The dependence of the parameters I and Δw on temperature is shown schematically in Figure 8.3. With increasing temperature, the intensity of the central peak increases exponentially and the width increases in proportion to the root of T. The behavior of the parameters of the central peak predicted by theory could be checked experimentally.

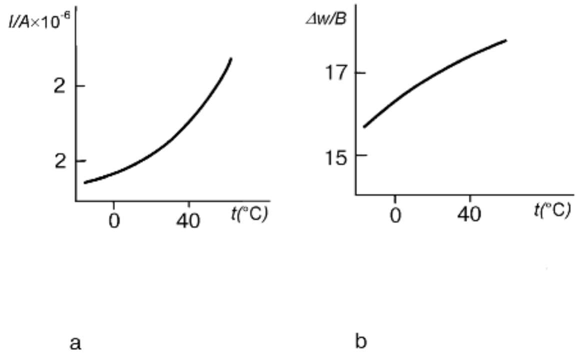

Figure 8.3 Temperature dependence of (a) the integral intensity I and (b) the line width Δw of the central peak.

Now let us consider how these results change if, instead of a simple sine-Gordon model, we take the helical sine-Gordon model described in Section 6.3 and shown in Figure 7.2b.

According to the calculations in Section 7.3, the dynamical factor of neutron scattering by the helical sine-Gordon model has the form

$$S^{\mathrm{coh}}(\boldsymbol{x}, w') = \{l^2 ad(E_0/2\pi k_B T)^{1/2}/\hbar C_0 x_z K_1(E_0/k_B T)\}\exp(-2W_x)$$

$$\exp(-E_0/k_B T)\,(x_z + x_y)\{F_+(x_z - 2\pi/10a) + F_-(x_z - 2\pi/10a)\}, \tag{8-14}$$

where the notations

$$F_\pm(\xi) = \{[\pi d\xi(1 - w'^2/C_0{}^2\xi^2)]/\mathrm{sh}[\pi d\xi((1 - w'^2/C_0{}^2\xi^2)/2] \pm$$

$$\pm[\pi d\xi(1 - w'^2/C_0{}^2\xi^2)]/\mathrm{ch}[\pi d\xi(1 - w'^2/C_0{}^2\xi^2)/2]\}\,(1/\xi)\,(1 - w'^2/C_0{}^2\xi^2)^{-1/2}$$

$$\exp[(-E_0/k_B T)\,(1 - w'^2/C_0{}^2\xi^2)^{-1/2}] \tag{8-15}$$

are used.

For low temperatures and small velocities we have

$$S^{\mathrm{coh}}(\boldsymbol{x}, w') = (l^2 adE_0/\hbar C_0\,\pi k_B T)\ \exp(-2W_x)\,(x_x{}^2 + x_y{}^2)\{f_+(x_z + 2\pi/10a) +$$

$$+ f_-(x_z - 2\pi/10a)\}, \tag{8-16}$$

where

$$f_\pm(\xi) = [\pi d\xi/\mathrm{sh}(\pi d\xi/2) \pm \pi d\xi/\mathrm{ch}(\pi d\xi/2)]^2\,(1/\xi)$$

$$\exp(-E_0/k_B T)\exp(-M_0 w'^2/2k_B T\xi^2). \tag{8-17}$$

From Eq. (8-17) we can predict the splitting of the central peak (according to the variable x_z) into two components, shifted towards each other by $4\pi/10a \cong 1$ Å^{-1} (Figure 8.4). This prediction could also be checked experimentally.

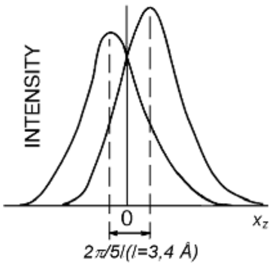

Figure 8.4 A scheme of splitting of the central peak due to the helicity of the DNA structure.

To improve the calculations presented here, we should use a more accurate model of the internal DNA dynamics. In this way new interesting predictions on the behavior of the central peak of the neutron scattering spectrum of DNA could be obtained.

8.3.2
Interpretation of Cundall and Baverstock

Baverstock and Cundall [48, 296, 297] used the soliton concept to interpret the experimental data on the scattering of fast neutrons by DNA. We should note that the interaction of the fast (high-energy) neutrons with DNA differs substantially from the interaction of thermal (low-energy) neutrons described in Section 2.8. The main difference is that the fast neutron scattering is accompanied by the formation of radical anions. Studying the yield of the radicals is one of the powerful methods of obtaining information about DNA internal dynamics.

In 1986 Arroyo et al. [298] investigated the radical yield dependence on the direction of irradiation of oriented fibers of DNA. Their results showed that the radical anions of thymine were formed in roughly equal amounts to the guanine anions when the neutron flux was perpendicular to the axes of the DNA molecules. When the flux was parallel to the DNA axes a protonated form of thymine anions dominated, and overall radical yields were lower by a factor of three in the parallel sample.

These results were interpreted by Miller et al. [299]. They assumed that there is a large asymmetry in the thermal conductivity of oriented films. With the help of the track structure model for protons it was shown that irradiation by the protons parallel to the axes of the DNA molecule results both in the formation of the thymine anion and, from the same particle, further energy deposits of the vibrational excitations. Some of these may migrate to the sites of thymine anions and result in sufficient thermal stimulation of the thymine to promote protonation. Where the proton direction is perpendicular to the axes of the DNA molecules such migration will be impeded by the low intra-molecular thermal conductivity.

This idea was developed by Baverstock and Cundal [296,297]. Taking into account that the deposition of ionizing energy into condensed media is a highly nonlinear process they suggested that it can give rise to soliton-like species and that this enables energy to be transferred without loss over long distances (Miller et al. predicted transfer distances of up to 0.2 μm). This interpretation cannot, however, be checked experimentally.

8.4 Fluorescence Depolarization

Fluorescence depolarization is widely used for measurements of the torsional constants of biopolymers. In 1992 Selvin et al. [49] used this method for measurements of the torsional rigidity of positively, relaxed and negatively supercoiled DNA. For the purpose they used time correlated single photon counting (TCSPC) of intercalated ethidium bromide. The measurements were made over a wide range of superhelical density with a time-resolution of 75 ps extending from 0.75 ns, the range in which DNA twisting motions dominate the fluorescence depolarization signal.

The main result of the measurements was rather unusual: the torsional rigidity of the DNA molecule was not a constant, as had usually been suggested in good agreement with the linear mathematical models of DNA. Selvin and coauthors found that at physiological ionic strength (175 mM), the torsional rigidity increases monotonically from 1.76×10^{-19} erg cm for the most positively supercoiled DNA, to 2.28×10^{-19} erg cm for the most negatively supercoiled DNA. At low ionic strength (7.5 mM) the torsional constant rapidly increases from positively supercoiled (1.91×10^{-19} erg cm) to relaxed DNA (2.42×10^{-19} erg cm), and then levels off at negative superhelical densities ($\cong 2.3 \times 10^{-19}$ erg cm).

From these data Selvin and coauthors concluded that the DNA molecule is not a linear system, and that a more accurate mathematical model of the internal DNA dynamics should consist of coupled nonlinear torsional springs. According to their estimations the anharmonic term in the model Hamiltonian should be approximately 15% for twist fluctuations at room temperature.

These results appear to be quite reliable evidence for the nonlinear nature of internal DNA dynamics.

9 Nonlinearity and Function

An important and traditional problem of DNA science is to relate the DNA functional properties to its structural and dynamical properties.

In this chapter we try to consider the relation between DNA function and nonlinear dynamics, by describing several examples where the mechanisms of conformational transitions, of long-range effects, of regulation of transcription process and of DNA denaturation are explained in terms of the nonlinear concept.

9.1 Nonlinear Mechanism of Conformational Transitions

An interesting application of the nonlinear theory is associated with the interpretation of the mechanism of transitions between different conformational forms of the DNA molecule. The relation between the phenomenon and nonlinear theory was first noticed and reported in 1982 at the workshop in Gysinge [300]. Then this approach was developed by many other authors [20, 21, 28, 50, 52, 54, 142, 301].

To describe the approach, let us return to Figure 1.6, where three of the main DNA forms: A-DNA, B-DNA and Z-DNA, are shown. Each of the forms is characterized by a group of parameters including the helix sense (right-handed or left-handed), the number of residues per turn, the diameter, the helix pitch, the tilting of the base pairs relative to the helix axis, the displacement of the base pairs away from the helix axis, the pucker of the furanose rings and others.

As an example, let us consider the transition between the A- and B-forms of the DNA molecule, which can occur due to the change in temperature, of pH, hydration or some other parameters. The transition is easily visualized by X-ray diffraction studies of DNA fibers: if the fibers, for example, are allowed to dry, they produce an A-type diffraction pattern, and if the fibers remain hydrated, the pattern is a B-type. A schematic picture of A–B transition is shown in Figure 9.1a where one region of the DNA molecule is shown in the A-form, and the other in the B-form. The process of transition is shown there as a movement (from the left to the right) of the boundary between two regions. So, this process is very similar to that of phase transition in physical systems. It is well known, however, that, in physics, the transition processes of this type are successfully described by kink and antikink solutions of corresponding nonlinear dynamical equations. So, we can expect that the movement of the boundary between two DNA regions is also described by soliton-like solutions of kink (or antikink) type.

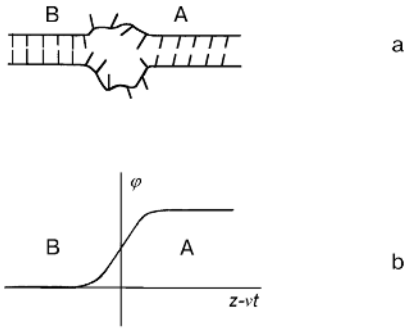

Figure 9.1 A schematic picture of (a) A → B transition; (b) kink-like solution describing the movement of the boundary between two regions: A and B.

This suggestion is confirmed by theoretical results. Indeed, let us return to the Section 5.4 where the model of Volkov [54] consisting of two nonlinear differential equations

$$u_{tt} = s^2 u_{zz} - A\Phi_u + BF_u \tau_z,$$
$$\tau_{tt} = s_1^2 \tau_{zz} + CF_u u_z. \tag{9-1}$$

was discussed. The first of the equations describes displacements inside the monomer link (the variable u) and the other describes the displacement of the monomer as a whole (the variable τ). Here $\Phi(u)$ is the potential energy of the conformational transition in a monomer link, and has the form of a double well (Figure 5.13); $F(u)$ is the function which characterizes the structural relations between subsystems: $F(u) = (u_0^2 - u^2)$; A, B, s, s_1, C and u_0 are constant parameters of the system.

One of the exact solutions of Eq. (9-1) having the form of a kink is shown schematically in Figure 9.1b. This solution can be interpreted as a moving boundary between two regions, one of them having the A-form and the other having the B-form.

9.2 Nonlinear Conformational Waves and Long-range Effects

During the 1970s and 1980s a great deal of experimental work was done on long-range effects [249, 206–208, 302]. The most impressive results came from the experiments where special regions of DNA molecule (enhancers) were discovered.

A simple scheme illustrating these effects has been described in Section 3.5. The scheme consists of two protein molecules and one DNA molecule (Figure 3.6). It is assumed that these proteins interact specifically with DNA sites, namely, the first protein molecule can bind to site 1 and the other protein molecule can bind to site 2. The effect is that the binding of the first protein with site 1 influences the binding of the second protein molecule with site 2, although the distance between the sites can reach hundreds or thousands (as in the case of enhancers) of base pairs.

Among different explanations of the effect there is one which is of most interest. According to it the effect of the binding of the first protein molecule to site 1 is accompanied by a local distortion of the DNA conformation, which can propagate along the double DNA chain. When reaching site 2 it changes the conformational structure of the site which, in turn, changes the binding constants of the second protein with the site. This mechanism can be easily interpreted in terms of nonlinear dynamics. Indeed, formation of the local distortion can be interpreted as an excitation of the nonlinear wave (or soliton) and propagation of the distortion along the double helix, as transmission of the nonlinear wave along the DNA.

To describe this phenomenon mathematically, we need to have some information about the distortion. For example, if we know that the binding of some protein molecule with site 1 is accompanied by a substantial change in the DNA twist in the vicinity of site 1, we can use (as a first approximation) the model of Englander:

$$I\varphi_{tt} = Kl^2a^2\varphi_{zz} - v_0\sin\varphi; \tag{9-2}$$

or (as a second approximation) the Y-model

$$\begin{aligned} I\varphi_{1tt} &= Kl^2a^2\varphi_{1zz} - kl^2\{2\sin\varphi_1 - \sin(\varphi_1 + \varphi_2)\}, \\ I\varphi_{2tt} &= Kl^2a^2\varphi_{2zz} - kl^2\{2\sin\varphi_2 - \sin(\varphi_2 + \varphi_1)\}. \end{aligned} \tag{9-3}$$

If we know that the binding of some other protein molecule with site 1 is accompanied by the separation of the DNA strands. we can use the model of Peyrard and Bishop:

$$\begin{aligned} &mx_{1tt} - ka^2{}_{1zz} = 0; \\ &mx_{2tt} - ka^2x_{2zz} + 2D\overline{A}^2\,x - 3D\overline{A}^3\,x^2 + (7/3)D\overline{A}^4\,x^3 = 0. \end{aligned} \tag{9-4}$$

Parameters of Eqs. (9-3), (9-4) are described in Sections 5.1 and 5.3.

To model the long-range effect more correctly we need to know much more details about the DNA–protein interaction and to try to construct mathematically a model which takes them all into account. Such ideas were developed in the works of Ladik and coauthors [58, 303]. To explain the long-range effects of carcinogens, they assumed that the binding of carcinogen to DNA leads to strong distortion of the DNA structure (Figure 9.2), and that after the removal of carcinogen, the system will not relax immediately and conformational distortion caused by the binding can travel through large distances along the DNA double helix. Mathematically a distortion of such a type is described by a solitary wave. It was suggested that the propagating soliton along the DNA molecule causes long-range interference with the DNA–protein interaction, and in this way possibly it can initiate the activation of oncogene.

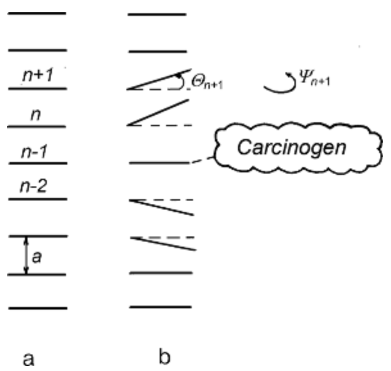

Figure 9.2 A scheme of (a) undisturbed and (b) disturbed DNA. The distortion angle θ_{n+1} measures the deviation of the $(n+1)$th nucleotide base from its original position; Ψ_{n+1} is the deviation of the base from the equilibrium value of rotation around the helix axis (36° in B-DNA).

We discussed one more example of the explanation of the long-range effects in terms of the nonlinear conception in Section 8.3 when describing the interpretation of the results on neutron scattering by DNA proposed by Baverstock and Cundall.

9.3 Nonlinear Mechanism of Regulation of Transcription

The general characteristics of the transcription have been described in Section 3.4. A scheme shown in Figure 3.4 illustrates the main stages of the process.

In this section we interpret the stages in terms of the nonlinear concept, as proposed by Polozov and Yakushevich [55, 56].

According to their approach let us consider an essentially heterogeneous model of a fragment of the DNA molecule, which contains the main functional regions necessary for RNA synthesis and regulation: a promoter, P, a coding region, C, several regulatory regions, R_1, R_2, R_3 and a terminator, T. A scheme of the fragment is shown in Figure 3.1.

Usually the transcription process starts with the binding of RNA-polymerase to a promoter, P. Experimental data indicate that the binding of RNA-polymerase to a promoter is accompanied by a considerable local distortion of the DNA conformation which can propagate along the DNA double helix [304–308]. These events can be interpreted in terms of nonlinear dynamics as excitation and propagation of a nonlinear conformational wave or soliton.

When passing through the coding region, C, the distortion will change the conformation of the region. Support for this comes from the experiments [309–311] which indicate that the interaction of RNA-polymerase with promoter P causes structural alterations in the coding region C. These alterations may give rise to changes in the matrix properties of DNA, which, in turn, will change the rate of RNA synthesis at the stage of elongation. In the framework of the nonlinear dynamics the distortion can be considered as a soliton and the movement of the distortion can be considered as a propagation of a soliton of kink-type. A simple example of this is where the solitary wave imitates the moving boundary between two regions (A and B) having different conformations.

Having passed through the C-region, the distortion reaches the terminator, T, which separates two genes, the ith and $(i+1)$th. Experimental data indicate that the T-region has often has a rather heterogeneous structure [312–314]. For example, the terminator is shown in Figure 3.1 as a cruciform region. If we interpret the distortion as a soliton we lead to the problem of passing the soliton through the local inhomogeneity region. A simple case of the problem was considered in Section 6.2. Applying the results obtained there we can conclude that the passage of the soliton through this region may result in a complete absorption of the soliton, or the soliton will surmount the T-region, with the velocity and profile being substantially changed. The first case corresponds to a termination and the second to a preparation for switching on the next gene transcription.

The propagation of local distortion (or soliton in terms of nonlinear dynamics) through the regulatory regions R_1', R_2' (or R_1, R_2, R_3) is accompanied by changes in the conformation of the regions, and hence in the binding constants of regulatory proteins within these regions. As a consequence, the distribution of ligands throughout the regions will change, which is known to be of crucial importance to the regulation of DNA activity.

In addition, we should add that in all cases described above, when considering the possible role of solitons in the different stages of the transcription process we restricted ourselves to the case where then transcription process occurs in the vicinity of only one gene. However, we could make a more general assumption and suggest that the nonlinear solitary waves moving along the DNA molecule are also a suitable model for the regulation and coordination of simultaneous transcription of many genes.

9.4 Direction of Transcription Process

From numerous biological experiments it is well known that the directions of transcription processes are different not only for DNA molecules of different living organisms but also for different promoter regions of the same DNA molecule. For some promoters the transcription process preferably develops in the upstream direction, for others in the downstream direction. There are also promoters which do not have a preferred direction of transcription.

Explanation of these phenomena has been given by Salerno [39, 278–280]. Let us return to Section 6.3. The nonlinear model proposed by Salerno consists of a set of nonlinear discrete equations

$$I\psi_n = Kl^2(\psi_{n+1} - 2\psi_n + \psi_{n-1}) - V_n \sin\psi_n = 0, \quad n = 1, 2,\ldots, N; \tag{9-5}$$

where $\psi_n = \varphi_{n,1} - \varphi_{n,2}$; and $\varphi_{n,1}$, $\varphi_{n,2}$ are the rotational angles of the nth bases of the first and second polynucleotide chains, respectively; I is the moment of inertia of the individual bases; K is the backbone spring constant; V_n is a parameter modeling the strength of hydrogen bonds between complementary bases. Through the coefficient V_n the specific base sequence information is included: V_n is double ($V_n = 2\beta$) for the adenine-thymine (A-T) base pair and triple ($V_n = 3\beta$) for the guanine-cytosine (G-C) base pair.

In the particular case where the parameter V_n is uniform, that is $V_n = \nu_0$, and in the continuum limit Eq. (9-2) reduces to the well-known sine-Gordon equation

$$I\psi_{tt} = Kl^2a^2\psi_{zz} - \nu_0 \ \sin\psi, \tag{9-6}$$

having an exact kink-like solution

$$\psi(z,t) = 4\tan^{-1}\{\exp[(z - \nu t - z_0)(\gamma/d]\}; \tag{9-7}$$

where $d = la(K/\nu_0)^{1/2}$.

Equations (9-5) have been studied numerically, and a kink-like solution Eq. (9-7) was used as an initial condition. As a result, it was found that an initially static soliton can (i) remain static (ii) oscillate, or (iii) move along the DNA molecule in one of two possible directions: upstream or downstream. Which of these three events happens depends on the sequence of bases in the DNA fragment. In case (iii) when the soliton moves, the problem of the direction of the movement (or the problem of direction of transcription) arises. Salerno suggested that the direction depends on the sequence of bases near the starting point. To check the suggestion, he took the sequence (S) of 168 bases corresponding to T7A$_1$ DNA promoter:

TTGTCTTTATTAATACAACTCACTATAAGGAGAGACAACTTAAAGA

↓50 ⇒

GACTTAAAAGATTAATTTAAAATTTATCAAAAAGAGTATTGACTTA

(−1)↓↓(+1)

AACTCTAACCTATAGGATACTTACAGCCATCGAGAGGGACACGGC

⇐ ↓ 140

GAATAGCCATCCCAATCGACAACCGGGGTCAA (9-8)

and constructed with its help a longer sequence of 1000 base pairs according to the rule

$$S(1,5) + 9S(1,50) + S(51,140) + 16S(140,168) + S(162,168), \tag{9-9}$$

where the symbol $kS(i,j)$ denotes the subsequence of S going from the ith base pair to the jth base pair k times. The longer chain permitted the use of safe reflexive boundary conditions in the numerical simulation.

As a result, it was found that when the soliton was initially placed outside the promoter the soliton remained static. When the soliton was placed inside the promoter region the solitary wave began to move to the left end of the chain. This result is in good agreement with the known data on the functional properties of the $T7A_1$ promoter. Moreover, this result shows the existence of a dynamically 'active' region inside the promoter region.

So, the approach of Salerno gives us a new effective tool for indication of dynamically active regions in DNA. Moreover, we could expect that these regions correspond to functionally active regions. If our suggestion is confirmed, scientists will obtain one more new method of analyzing and interpreting the DNA code.

9.5
Nonlinear Model of DNA Denaturation

The nonlinear model for thermal denaturation of the DNA molecule was been proposed by Peyrard and Bishop [34, 262]. It was based on the assumption that local DNA denaturation is due to the breaking of the hydrogen bond and the separation of DNA strands (Figure 9.3). To model hydrogen bonds Peyrard and Bishop used the Morse potential V_n. And to model the internal DNA dynamics they assumed that each base pair has only two degrees of freedom (u_n and v_n) which correspond to the displacements of bases from their equilibrium positions along the direction of the hydrogen bonds (Figure 9.4). So, the Hamiltonian of the model has the form

$$H = \sum_n \left\{ m(\dot{u}_n^2 + \dot{v}_n^2)/2 + k[(u_n - u_{n-1})^2 + (v_n - v_{n-1})^2]/2 + V_n \right\} \tag{9-10}$$

with

$$V_n = D\{\exp[-A(u_n - v_n)] - 1\}^2, \tag{9-11}$$

where m is a common mass for the bases; k is a coupling constant; D and A are parameters of the system. Strand separation is described then by the variable x_n

$$x_n = (u_n - v_n)/2^{1/2}. \tag{9-12}$$

This variable represents the out-of-phase displacement which stretches the hydrogen bonds. The dynamical equation for the variable x_n (see Eq. (5-99) and its soliton-like solutions has been discussed in Section 5.3.

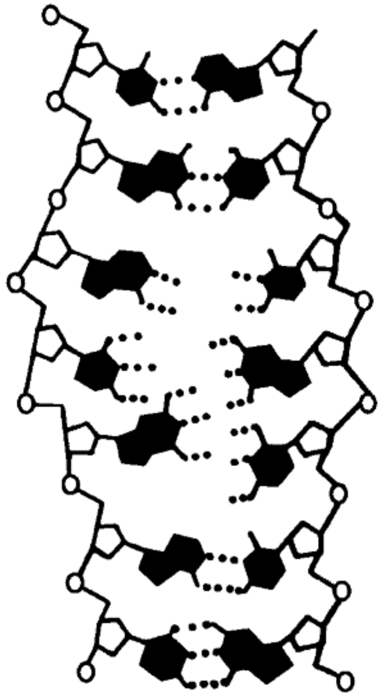

Figure 9.3 Schematic picture of DNA denaturation due to local strand separation. Hydrogen bonds are shown by dotted lines.

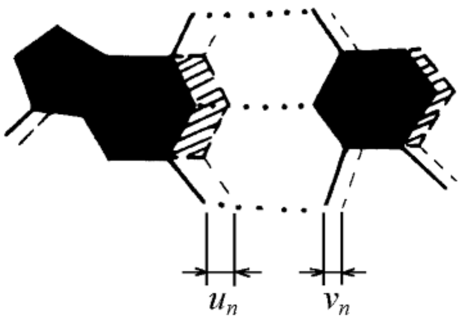

Figure 9.4 Displacements (u_n, v_n) of the bases in the model of Peyrard and Bishop.

To apply these solutions to the problem of DNA denaturation we should admit, however, the possibility of excitation of more than one soliton imitating local denaturation and suggest that the amount of solitons will increase with the increasing of temperature. So, the study of the denaturation process is closely connected with the problem of the statistics of solitons in DNA. We can now use the results on soliton statistics described in Section 7.1 where the method of calculation of the average value $<x>$ was given. These calculations were made by Peyrard and Bishop and their results showed that $<x>$ rapidly increased in the vicinity of a particular temperature which was a characteristic of DNA denaturation, as observed for instance by measuring its absorbance of ultraviolet light at 260 nm [315].

Note, however, that calculations of $<x>$ indicate at which temperature the denaturation occurs, but do not indicate how it occurs. To answer this question let us return again to the model Hamiltonian (9-10) and write the corresponding dynamical equation

$$m\, x_{n_{tt}} - k(x_{n+1} + x_{n-1} - 2x_n) - 2^{3/2} DA \exp(-2^{1/2} A x_n)[\exp(-2^{1/2} A x_n - 1] = 0. \qquad (9\text{-}13)$$

To simplify the problem let us expand Eq. (9-13) for small x_n as

$$m\, x_{n_{tt}} - k(x_{n+1} + x_{n-1} - 2x_n) - 4DA^2 x_n - 6D2^{1/2} A^3 x_n^2 + 28DA^4 x_n^3/3 = 0. \qquad (9\text{-}14)$$

The solution of this equation can be found by a multiple-scale expansion [272] as was done in Section 5.3. Indeed, the multiple-scale expansion of this type yields a nonlinear Schrödinger equation for F_1 similar to Eq. (5-102)

$$\mathrm{i}F_{1s} + PF_{1ZZ} + Q|\mathrm{F}_1|^2 F_1 = 0. \qquad (9\text{-}15)$$

The solitary waves resulting from this equation are breathing modes. Their statistics were studied by Lebowitz, et al. [316], who showed that the nonlinear system described by Eq. (9-15) could develop singularities in a finite time, and these singularities might be responsible for the nucleation of DNA denaturation.

Appendix

Appendix 1: Mathematical Description of Torsional and Bending Motions

The torsional motions are associated with the changes in the twist angle φ. In the general case this angle is determined in the following way. Let $\boldsymbol{r}(s)$ $(0 \le s \le L)$ be a smooth and simple (i.e. without intersection) curve of length L. We associate at each point on this curve a smoothly varying unit vector $\boldsymbol{u}(s)$ perpendicular to $\boldsymbol{r}(s)$ (Figure A.1). The set $\{\boldsymbol{r}(s),\ \boldsymbol{u}(s)\}$ is called a strip or 'ribbon'. On each point of a ribbon we have a naturally moving frame $\{\boldsymbol{t},\ \boldsymbol{u},\ \boldsymbol{v}\}$, where $\boldsymbol{t}(s) = \boldsymbol{r}'(s)$ is the tangential vector and $\boldsymbol{v}$ is defined by $\boldsymbol{v} = \boldsymbol{t} \times \boldsymbol{u}$.

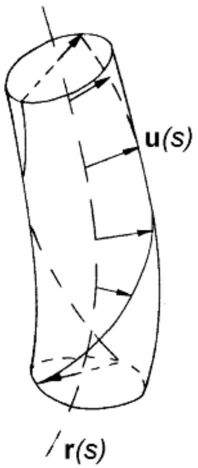

Figure A.1 Elastic rod. The axis curve $\boldsymbol{r}(s)$ and normal unit vector $\boldsymbol{u}(s)$ in the direction to one strand form a ribbon.

Let us introduce a rotational vector $\Omega = \varphi_1\boldsymbol{t} + \varphi_2\boldsymbol{u} + \varphi_3\boldsymbol{v}$ by differentiating this moving frame, i.e., $\boldsymbol{u}(s)$

$$\boldsymbol{t}' = \Omega \times \boldsymbol{t},\ \boldsymbol{u}' = \Omega \times \boldsymbol{u} \text{ and } \boldsymbol{v}' = \Omega \times \boldsymbol{v}. \tag{A1-1}$$

Then φ_1 is called the 'twist' of the ribbon. The total twist number is defined by

$$Tw\{\boldsymbol{r}, \boldsymbol{u}\} = (1/2\pi) \int_0^L \varphi_1(s)\, \mathrm{d}s. \tag{A1-2}$$

In a particular case where $\boldsymbol{u}(s)$ is taken to be the principal normal, φ_1 is the torsion τ of the curve. So, twisting motions are those which lead to changes in the twist angle φ_1 from some equilibrium (stable) value. The energy associated with these motions takes the form

$$E^{\mathrm{tw}}(\boldsymbol{r}, \boldsymbol{u}) = (1/2\pi) \int_0^L [C(\varphi_1 - \varphi_1^{(0)})^2]\, \mathrm{d}s, \tag{A1-3}$$

where C is the torsional elastic constant of the rod and $(\varphi_1 - \varphi_1^{(0)})$ is the amount by which the local twist density deviates from its unstressed value.

Now let us assume that $\boldsymbol{r}(s)$ is the center axis of the complementary double strands of a DNA molecule. We regard $\boldsymbol{u}$ as a directional vector perpendicular to $\boldsymbol{r}$ which indicates the position of one strand. For B-DNA the equilibrium value of the twist is known to be $\varphi_1^{(0)} = 2\pi/3.4$ nm. A typical values of C is estimated to be

$$C = 2.04 \times 10^{-28}\ \mathrm{J\ m}; \tag{A1-4}$$

in a dilute solution of NaCl with concentration less than 5 mM [119].

The bending of the rod can be described by the curvature of the axis. Bending motions lead to changes in the curvature. Let $k(s) = |\mathrm{F}''(s)|$ be the amount by which the local curvature of the DNA axis deviates from its unstressed value. Then the energy associated with the motions is given by

$$E^{\mathrm{b}}(\boldsymbol{r}, \boldsymbol{u}) = (1/2) \int_0^L [Bk^2]\, ds, \tag{A1-5}$$

where a typical value of the bending elastic constant, B, is estimated to be

$$B = 2.7 \times 10^{-28}\ \mathrm{J\ m}, \tag{A1-6}$$

in dilute salt solution of NaCl concentration less than 5mM [119].

If we describe the double strand by a homogeneous elastic rod of radius d, the constants C and B may be related to the Young's modulus E and the rigidity μ of the imaginary elastic body through the relations $B = \pi d^4 E/4$ and $C = \pi d^4 \mu/2$, where d is the radius of the covering rod (d ~ 1 nm for DNA in the natural state).

Appendix 2: Structural and Dynamical Properties of DNA

Radius (*l*) of DNA Helix

(Å)	Ref.
10	22
12.5	119, 317

Distance (*a*) between Base Pairs

(Å)
3.4

Mass of a Base Pair (g/*N*, where N is the Avogadro constant)

		Ref.
A-T base pair	614	238
G-C base pair	615	238

Moment of Inertia of a Base Pair

(10^{-37} g cm)	Ref.
5	318
34	54

Velocity of Sound in DNA (for propagation perpendicular to the fiber axis)

	(km s^{-1})	Ref.
dry DNA	3.38	321
A-DNA	2.22	231
A-DNA	3.25	221
B-DNA	3.50	221
B-DNA	1.89	231
wet DNA	1.69	231

Velocity of Sound in DNA (for propagation along the fiber axis)

	(km s^{-1})	Ref.
A-DNA	3.19	219
B-DNA	3.50	219

Velocity of Torsional Waves

(km s^{-1})	Ref.
1.3	47
1.85	153, 154

Force Constant (*K*) for Torsion Motions (discrete case)

(10^{-11} erg)	Ref.
0.2–2	22
5.2	319
0.42	318
1.43–3.4	320, 321

Force constant ($C = Ka$) for torsion motions (continuous case)

(10^{-19} erg cm)	Ref.
0.4 – 4.0	119, 320, 322, 323
0.4 – 14.0	324
0.4 – 1.4	326
0.6 – 1.4	319
0.6 – 4.4	318, 326 – 329
0.6 – 1.1	325
0.64 – 4.14	119
1.29	320
1.3	142, 317
1.43	321
2.4	330
3.1	331
5.9	325, 332
13	333

Force Constant for Roll Motions

(10^{-12} erg rad^{-2})	Ref.
7.554	334

Force Constant for Tilt Motions

(10^{-12} erg rad^{-2})	Ref.
7.554	334

Force Constant for Rise Motions

(10^{-14} erg Å^{-2})	Ref.
8.284	334

Force Constant for Bending Motions

(10^{-19} erg cm)	Ref.
2.63	119

Force Constant (*k*) for Hydrogen Bond Stretching

	(mdyn Å^{-1})	Ref.
single bond	0.13	335 – 337

Parameters of Homogeneous Dynamical Model of DNA	**Ref. [338]**
m_A (mass of adenine)	226.13×10^{-27} kg
m_T (mass of thymine)	211.04×10^{-27} kg
m_G (mass of guanine)	252.92×10^{-27} kg
m_C (mass of cytosine)	18592×10^{-27} kg
r_A (distance between the center of mass of adenine and sugar –phosphate chain)	5.8 Å
r_T (distance between the center of mass of thymine and sugar –phosphate chain)	4.8 Å
r_G (distance between the center of mass of guanine and sugar –phosphate chain)	5.7 Å
r_C (distance between the center of mass of cytosine and sugar –phosphate chain)	4.7 Å
I_A (moment of inertia of adenine)	$7607.03 \cdot 10^{-47}$ m^2 kg
I_T (moment of inertia of thymine)	$4862.28 \cdot 10^{-47}$ m^2 kg
I_G (moment of inertia of guanine)	$8217.44 \cdot 10^{-47}$ m^2 kg
I_C (moment of inertia of cytosine)	$4106.93 \cdot 10^{-47}$ m^2 kg
ε_H (energy required to break one hydrogen bond)	5 kcal mol^{-1}
ε_{AT} (energy required to break hydrogen bonds in AT base pair)	10 kcal mol^{-1} $\cong$ 41.868 kJ mol^{-1}
ε_{GC} (energy required to break hydrogen bonds in GC base pair)	15 kcal mol^{-1} $\cong$ 62.802 kJ mol^{-1}
$k_{A\text{-}T}$ (force constant that characterizes interactions between bases in AT base pairs)	0.062 N m^{-1}
$k_{G\text{-}C}$ (force constant that characterizes interactions between bases in GC base pairs)	0.096 N m^{-1}
w^{AT} (frequency of torsional oscillations of bases in homogeneous AT chain)	0.75×10^{12} s^{-1}
w^{GC} (frequency of torsional oscillations of bases in homogeneous GC chain)	0.94×10^{12} s^{-1}

References

1 Scott A.C. 'Solitons in biological molecules'. *Comments Mol.Cell. Biol.* **3**, 5–57 (1985).

2 Zhou G.-F. and Zhang Ch.-T. 'A short review on the nonlinear motion in DNA'. *Phys. Scr.* **43**, 347–352 (1991).

3 Yakushevich L.V. 'Nonlinear dynamics of biopolymers: theoretical models, experimental data'. *Q. Rev. Biophys.* **26**, 201–223 (1993).

4 Gaeta G., Reiss C., Peyrard M. and Dauxois T. 'Simple models of nonlinear DNA dynamics'. *Rev. Nuovo Cimento* **17**, 1–48 (1994).

5 *Nonlinear Excitations in Biomolecules.* M. Peyrard (ed.) Springer, Berlin (1995).

6 Davydov A.S. *Solitons in Bioenergetics.* Naukova Dumka, Kiev (1986).

7 Yakushevich L.V. *Methods of Theoretical Physics and Their Applications to Biopolymer Sciences.* Nova Science Publishers, New York (1996).

8 Scott A.C., Chu F.Y. and McLaughlin D.W. 'The soliton: a new concept in applied science'. *Proc. IEEE* **61**, N10, 1443–1483 (1973).

9 *Solitons in Action.* K. Lonngren and A. Scott (eds), Academic Press, New York (1978).

10 *Solitons.* R.K. Bullough and P.J. Caudrey (eds), Springer-Verlag, Berlin (1980.)

11 *Structure and Dynamics: Nucleic Acids and Proteins.* E. Clementi and R.H. Sarma (eds), Adenine Press, New York (1993).

12 *Structure and Motion: Membranes, Nucleic Acids and Proteins.* E. Clementi, G. Corongiu, M.H. Sarma and R.H. Sarma (eds), Adenine Press, New York (1985).

13 McCommon J.A., Harvey S.C. *Dynamics of Proteins and Nucleic Acids.* Cambridge University Press, Cambridge (1987).

14 Davydov A.S. 'Solitons in molecular systems'. *Physica Scr.* **20**, 387–394 (1979).

15 Englander S.W., Kallenbach N.R., Heeger A.J., Krumhansl J.A. and Litwin A. 'Nature of the open state in long polynucleotide double helices: possibility of soliton excitations'. *Proc. Natl. Acad. Sci. USA* **77**, 7222–7226 (1980).

16 Yomosa S. 'Soliton excitations in deoxyribonucleic acid (DNA) double helices'. *Phys. Rev. A* **27**, *2120–2125 (1983)*.

17 Yomosa S. 'Solitary excitations in deoxyribonucleic acid (DNA) double helices'. *Phys. Rev.* A **30**, 474–480 (1984.)

18 Takeno S. and Homma S. 'Topological solitons and modulated structure of bases in DNA double helices'. *Prog. Theor. Phys.* **70**, 308–311 (1983).

19 Homma S. and Takeno S. 'A coupled baserotator model for structure and dynamics of DNA'. *Prog. Theor. Phys.* **72**, 679–693 (1984).

20 Krumhansl J.A. and Alexander D.M. 'Nonlinear dynamics and conformational excitations in biomolecular materials'. In: *Structure and Dynamics: Nucleic Acids and Proteins.* E. Clementi and R.H. Sarma (eds), Adenine Press, New York (1983), pp. 61–80.

21 Krumhansl J.A., Wysin G.M., Alexander D.M., Garcia A., Lomdahl P.S. and Layne S.P. 'Further theoretical studies of nonlinear conformational motions in double-helix DNA'. In: *Structure and Motion: Membranes, Nucleic Acids and Proteins.* E. Clementi, G. Corongiu, M.H. Sarma and R.H. Sarma (eds), Adenine Press, New York (1985), pp. 407–415.

22 Fedyanin V.K. and Yakushevich L.V. 'Scattering of neutrons and light by DNA solitons'. *Stud. Biophys.* **103**, 171–178 (1984).

23 Fedyanin V.K., Gochev I. and Lisy V. 'Nonlinear dynamics of bases in continual model of DNA double helices'. *Stud. Biophys.* **116**, 59–64 (1986).

24 Fedyanin V.K. and Lisy V. 'Soliton conformational excitations in DNA'. *Stud. Biophys.* **116**, 65–71 (1986).

25 Yakushevich L.V. 'The effects of damping, external fields and inhomogeneity on the nonlinear dynamics of biopolymers'. *Stud. Biophys.* **121**, 201–207 (1987).

26 Yakushevich L.V. 'Nonlinear DNA dynamics: a new model'. *Phys. Lett. A* **136**, 413–417 (1989).

27 Yakushevich L.V. 'Investigation of a system of nonlinear equations simulating DNA torsional dynamics'. *Stud. Biophys.* **140**, 163–170 (1991).

28 Zhang Ch.-T. 'Soliton excitations in deoxyribonucleic acid (DNA) double helices'. *Phys. Rev. A* **35**, 886–891 (1987).

29 Prohofsky E.W. 'Solitons hiding in DNA and their possible significance in RNA transcription'. *Phys. Rev. A* **38**, 1538–1541 (1988).

30 Muto V., Holding J., Christiansen P.L. and Scott A.C. 'Solitons in DNA'. *J. Biomol. Struct. Dyn.* **5**, 873–894 (1988).

31 Muto V., Scott A.S. and Christiansen P.L. 'Thermally generated solitons in a Toda lattice model of DNA'. *Phys. Lett. A* **136**, 33–36 (1989).

32 Muto V., Lomdahl P.S. and Christiansen P.L. 'Two-dimensional discrete model for DNA dynamics: longitudinal wave propagation and denaturation'. *Phys. Rev. A* **42**, 7452- 7458 (1990).

33 Van Zandt L.L. 'DNA soliton realistic parameters'. *Phys. Rev. A* **40**, 6134–6137 (1989).

34 Peyrard M. and Bishop A.R. 'Statistical mechanics of a nonlinear model for DNA denaturation'. *Phys. Rev. Lett.* **62**, 2755–2758 (1989).

35 Dauxois T., Peyrard M. and Willis C.R. 'Localized breather-like solutions in a discrete Klein-Gordon model and application to DNA'. *Physica D* **57**, ,267–282 (1992).

36 Dauxois T. 'Dynamics of breather modes in a nonlinear 'helicoidal' model of DNA'. *Phys. Lett. A* **159**, 390–395 (1991).

37 Gaeta G. 'On a model of DNA torsion dynamics'. *Phys. Lett. A* **143**, 227–232 (1990).

38 Gaeta G. 'Solitons in planar and helicoidal Yakushevich model of DNA dynamics'. *Phys. Lett. A* **168**, 383–389 (1992).

39 Salerno M. 'Discrete model for DNA-promotor dynamics'. *Phys. Rev. A* **44**, 5292–5297 (1991).

40 Bogolubskaya A.A. and Bogolubsky I.L. 'Two-component localized solutions in a nonlinear DNA model'. *Phys. Lett. A* **192**, 239–246 (1994).

41 Hai W. 'Kink couples in deoxyribonucleic acid (DNA) double helices'. *Phys. Lett. A* **186**, 309–316 (1994).

42 Gonzalez J.A. and Martin-Landrove M. 'Solitons in a nonlinear DNA model'. *Phys. Lett. A* **191**, 409–415 (1994).

43 Webb S.J. and Booth A.D. 'Absorption of microwaves by microorganisms'. *Nature* **222**, 1199–1200 (1969).

44 Swicord M.L. and Davis C.C. 'Microwave absorption of DNA between 8 and 12 GHz'. *Biopolymers* **21**, 2453–2460 (1982).

45 Swicord M.L. and Davis C.C. 'An optical method of investigating the microwave absorption characteristics of DNA and other biomolecules in solution'. *Bioelectromagnetics* **4**, 21–42 (1983).

46 Edwards G.S., Davis C.C., Saffer J.D. and Swicord M.L. 'Resonant absorption of selected DNA molecules'. *Phys. Rev. Lett.* **53**, 1284–1287 (1984).

47 Zhang Ch.T. 'Harmonic and subharmonic resonances of microwave absorption in DNA'. *Phys. Rev. A* **40**, 2148–2153 (1989).

48 Baverstock K.F. and Cundal R.D. 'Are solitons responsible for energy transfer in oriented DNA?'. *Int. J. Radiat. Biol.* **55**, 152–153 (1989).

49 Selvin P.R., Cook D.N., Pon N.G., Bauer W.R., Klein M.P. and Hearst J.E. 'Torsional rigidity of positively and negatively supercoiled DNA'. *Science* **255**, 82–85 (1992).

50 Khan A., Bhaumic D. and Dutta-Roy B. 'The possible role of solitonic process during A to B conformational changes in DNA'. *Bull. Math. Biol.* **47**, 783–789 (1985).

51 Zhang Z. and Olson W. 'A model of the B-Z transition of DNA involving solitary excitations'. In: *Proceedings, 6th Annual Conference on Nonlinearity of Condensing Matter, Los Alamos, New Maxico, 5–9 May 1986.* A.R. Bishop, D.K. Campbell, P. Kumar and S.E. Trullinger (eds), Springer, Berlin (1987), pp. 265–270.

52 Sobell H.M. 'Kink-antikink bound states in DNA structure'. In*: Biological Macromolecules and Assemblies.* F.A. Jurnak and A. McPherson (eds), John Wiley and Sons, New York (1984), pp. 172–234.

53 Yakushevich L.V. ‘DNA dynamics’. *Mol. Biol.* (Russian J.) **23**, 652–662 (1989).

54 Volkov S.N. ‘Conformational transition. Dynamics and mechanism of long-range effects in DNA’. *J. Theor. Biol.* **143**, 485–496 (1990).

55 Yakushevich L.V. ‘Non-linear DNA dynamics and problems of gene regulation’. *Nanobiology* **1**, 343–350 (1992).

56 Polozov R.V. and Yakushevich L.V. ‘Nonlinear waves in DNA and regulation of transcription’. *J. Theor. Biol.* **130**, 423- 430 (1988).

57 Balanovski E. and Beaconsfield P. ‘Solitonlike excitations in biological systems’. *Phys. Rev.* **32**, 3059–3064 (1985).

58 Ladik J.J., Suhai S. and Seel M. ‘Electronic structure of biopolymers and possible mechanisms of chemical carcinogenesis’. *Int. J. Quantum Chem. Quantum Biol. Symp. Suppl.* **5**, 35–49 (1978).

59 *Nonlinear Cooperative Phenomena in Biological Systems*. L. Matsson (ed.) World Scientific, Singapore (1997).

60 *Nonlinear Dynamics in Polymer Science*. A.R. Khokhlov, Q. Tran-Cong-Miyata, V.A. Davydov, T. Yamaguchi and S.I. Kuchanov (eds) Wiley-VCH, Weinheim (2000).

61 *Nonlinear Science at the Dawn of the 21st Century*. P.L. Christiansen, M.P. Sorensen and A.C. Scott (eds) Heidelberg, Springer (2000).

62 *Nonlinear Dynamics in the Life and Social Sciences*. W. Sulis and I. Trofimova (eds) (NATO Science Series, Series A: Life Sciences – Vol. 320) IOS Press, Amsterdam (2000).

63 *Biological Physics 2000*. V. Sa-yakanit, L. Matsson and H. Frauenfelder (eds) World Scientific, New Jersey (2000).

64 *Computers and Supercomputers in Biology* V.D. Lakhno and M.N. Ustinin (eds) Institute Of Computer Education, Moscow (2002).

65 *Encyclopedia of Nonlinear Science*. A.C. Scott (ed.), Fitzroy Dearborn, in press.

66 *Single molecule studies: from the experiments to their analysis*. M. Peyrard (ed.) Abstracts of CECAM Workshop, 24–26 September 2001, Lyon, France (2001).

67 Zameroff S., Brawermann F., and Chargaff E. ‘On the deoxypentose nucleic acids from several microorganisms’. *Biochem. Biophys. Acta* **9**, 402–405 (1952).

68 Watson J.D. and Crick F.N.C. ‘Molecular structure of nucleic acids. A structure of deoxyribose nucleic acid’. *Nature* **171**, 737–738 (1953).

69 Crick F.H.C. and Watson J.D. ‘The complementary structure of deoxyribonucleic acid’. *Proc. R. Soc. London, Ser. A*-**223**, 80–96 (1954).

70 Franklin R.E. and Gosling R.G. ‘Molecular structure of nucleic acids. Molecular configuration in sodium thymonucleate’. *Nature* **171**, 740–741 (1953).

71 Wilkins M.H.F., Seeds W.E., Stokes A.R. and Wilson H.R. ‘Helical structure of crystalline deoxypentose nucleic acid’. *Nature* **172**, 759–762 (1953).

72 Saenger W. *Principles of Nucleic Acid Structure*. Springer-Verlag, Berlin (1984).

73 Sasisekharan V., Pattabiraman N. and Gupta Goutam. ‘Some implications of an alternative structure for DNA’. *Proc. Natl. Acad. Sci. USA* **75**, 4092–4096 (1978).

74 Rodley G.A., Bates R.H.T. and Arnott S. ‘Is DNA really a double helix?’ *Trends Biochem. Sci.* **5**, 231–234 (1980).

75 Crick F.H.C., Wang J.C. and Bauer W.R. ‘Is DNA really a double helix?’ *J. Mol. Biol.* **129**, 449–457 (1979).

76 Crick F.H.C. and Klug A. ‘Kinky helix’. *Nature* **255**, 530–553 (1975).

77 Vinogradov S.V. and Linnell R.H. *Hydrogen Bonding*. Van Nostrand Reinhold, New York (1971).

78 Kudritskaya Z.G. and Danilov V.I. ‘Quantum mechanical study of bases interactions in various associates in atomic dipole approximation’. *J. Theor. Biol.* **59**, 303–318 (1976).

79 Pauling L. *The Nature of the Chemical Bonds*. Cornell Univ. Press, Ithaca, New York (1978).

80 Staab H.A., *Einführung in die theoretische organische Chemie*. Verlag Chemie, Weinheim (1962).

81 Hanlon S. ‘The importance of London dispersion forces in the maintenance of the deoxyribonucleic acid double helix’. *Biochem. Biophys. Res. Commun.* **23**, 861–867 (1966).

82 DeVoe H. and Tinoco I., Jr. ‘The Stability of helical polynicleotides: Base contribution’. *J. Mol. Biol.* **4**, 500–517 (1962).

83 Gratzer W. ‘Association of nucleic-acid bases in aqueous solution: A solvent partition study’. *Eur. J. Biochem.* **10**, 184–187 (1969).

84 Solie T.N. and Schellman J.A. ‘The interaction of nucleosides in aqueous solution’. *J. Mol. Biol.* **33**, 61–77 (1968).

85 Mitchell P.R. and Sigel H. 'A proton nucleic magnetic resonance study of self-stacking in purine and pyrimidine nucleosides'. *Eur. J. Biochem.* **88**, 149–154 (1978).

86 Topal M.D., Warshaw M.M. 'Dinucleoside monophosphates. II. Nearest neighbor interactions'. *Biopolymers* **15**, 1775–1793 (1976).

87 Davies D.B. 'Co-operative conformational properties of nucleosides, nucleotides and nucleotidyl units in solution'. *Jerusalem Symposium On Quantum Chemistry And Biochemistry Vol.11. 'Nuclear Magnetic Resonance Spectroscopy in Molecular Biology.* B. Pullman (ed.), D. Reidel, Dordrecht (1978), pp. 71–85.

88 Ornstein R.L., Rein R., Breen D.L. and MacElroy R.D. 'An optimized potential function for calculation of nucleic acid interaction energies. I. Base stacking'. *Biopolymers* **17**, 2341–2360 (1978).

89 Manning G.S. 'The molecular theory of polyelectrolyte solutions with applications to the electrostatic properties of polynucleotides'. *Q. Rev. Biophys.* **2**, 179–246 (1978).

90 Mills P., Anderson C.F. and Record M.T. Jr. 'Monte Carlo studies of counterion-DNA interactions. Comparison of the radial distribution of counterions with predictions of other theories'. *J.Phys. Chem.* **89**, 3984–3994 (1985).

91 Fenley M.O., Manning G.S. and Olson W.K. 'Approach to the limit of counterion condensation'. *Biopolymers* **30**, 1191–1203 (1990).

92 Klementi R.D., Soumpasis D.M. and Jovin T.M. 'Computation of ionic distributions around charged biomolecular structures: results for right-handed and left-handed DNA'. *Proc. Natl. Acad. Sci. USA* **88**, 4631–4635 (1991).

93 Stigter D. 'Evaluation of the counterion condensation theory of polyelectrolytes'. *Biophys. J.* **68**, 380–388 (1995).

94 Vologodskii A. and Gozzarelli N. 'Modeling of long-range electrostatic interactions in DNA'. *Biopolymers* **35**, 289–296 (1994).

95 Duguid J.G. and Bloomfield V.A. 'Electrostatic effects on the stability of condensed DNA in the presence of divalent cations'. *Biophys. J.* **70**, 2838–2846 (1996).

96 Mistra V.K., Sharp K.A., Friedman R.A. and Honig B. 'Salt effects on ligand-DNA binding. Minor groove binding antibiotics'. *J. Mol. Biol.* **238**, 245–263 (1994).

97 Mistra V.K., Heitch J.L., Sharp K.A., Friedman R.A. and Honig B. 'Salt effects on ligand-DNA binding. The λcI repressor and endonuclease'. *J. Mol. Biol.* **238**, 264–280 (1994).

98 Polozov R.V., Dzhelyadin T.R., Sorokin A.A., Ivanova N.N. and Kamzolova S.G. 'Electrostatic potentials of DNA. Comparative analysis of promoter and nonpromoter nucleotide sequences'. *J. Biomol. Struct. Dyn.* **16** , 1135–1143 (1999).

99 Kamzolova S.G., Sivozhelezov V.S., Sorokin A.A., Dzhelyadin T.R., Ivanova N.N. and Polozov R.V. 'RNA polymerase – promoter recognition. Specific features of electrostatic potential of "early" T4 Phage DNA promoters' *J. Biomol. Struct.Dyn.* **18**, 325–334 (2000).

100 Sorokin A.A., Dzhelyadin T.R., Ivanova N.N., Polozov R.V. and Kamzolova S.G. 'The quest for new forms of promoter determinants. Relationship of promoter nucleotide sequence to their electrostatic potential distribution'. *J. Biomol. Struct. Dyn.* **18**, 1020 (2001).

101 Wilkins M.H.F. 'Molecular configuration of nucleic acids'. *Science* **140**, 941–950 (1963).

102 Leslie A.G.W., Arnott S., Chandrasekaran R. and Ratliff R.L. 'Polymorphism of DNA double helices'. *J. Mol. Biol.* **143**, 49–72 (1980).

103 Kornberg A. *DNA Replication.* Freeman, San Francisco (1980).

104 Gragerov A.I. and Mirkin S.M. 'Influence of DNA superhelicity on the major genetical processes in prokaryotes'. *Mol. Biol.* (Russian J.) **14**, 8–34 (1980).

105 Champoux J.J. 'Proteins that affect DNA conformation'. *Annu. Rev. Biochem.* **47**, 449–479 (1978).

106 Bauer W.R. 'Structure and reactions of closed duplex DNA'. *Annu. Rev. Biophys. Bioeng.* **7**, 287–313 (1978).

107 Bauer W.R. and Vinograd J. 'Circular DNA'. In: *Basic Principles of Nucleic Acid Chemistry.* P.O.P. Ts'o, (ed.) Vol.II, Academic Press, New York, (1974), pp. 265–303.

108 Cozalelly N.R. 'DNA gyrase and the supercoiling of DNA'. *Science,* **207**, 953–960 (1980).

109 Frank-Kamenetskii M.D. and Vologodskii A.V. 'Thermodynamics of the B-Z transition in superhelical DNA'. *Nature* **307**, 481–482 (1984).

110 Vologodskii A.V. and Frank-Kamenetskii M.D. 'Left-handed Z form in superhelical DNA: a theoretical study'. *J. Biomol. Struct. Dyn.* **1**, 1325–1333 (1984).

111 Vologodskii A.V. and Frank-Kamenetskii M.D. 'Theoretical study of cruciform states in superhelical DNA'. *FEBS Lett.* **143**, 257–260 (1982).

112 Vologodskii A.V. and Frank-Kamenetskii M.D. 'Premelting of superhelical DNA: an expression for superhelix energy'. *FEBS Lett.* **131**, 178–180 (1981).

113 Vologodskii A.V., Lukashin A.V., Anshelevich V.V. and Frank-Kamenetskii M.D. 'Fluctuations in superhelical DNA'. *Nucleic Acids Res.* **6**, 967–982 (1979).

114 Schlick T. 'Modeling superhelical DNA - recent analytical and dynamical approaches'. *Curr. Opin. Struct. Biol.* **5**, 245–262 (1995).

115 Benham C.J. 'Theoretical analysis of conformational equilibria in superhelical DNA'. *Annu. Rev. Biophys. Biophys. Chem.* **14**, 23–45 (1985).

116 Benham C.J. 'Energetics of the Strand. Separation Transition in Superhelical DNA'. *J. Mol. Biol.* **225**, 835–847 (1992).

117 Benham C.J., 'Duplex destabilization in superhelical DNA is predicted to occur preferentially at regulatory regions'. *J. Mol. Biol.* **255**, 425–434 (1996).

118 Bunn Ch. *Crystals. Their Role in Nature and in Science.* Academic Press, New York and London (1964).

119 Barkley M.D. and Zimm B.H. 'Theory of twisting and bending of chain macromolecules; analysis of the fluorescence depolarization of DNA'. *J. Chem. Phys.* **70**, 2991–3007 (1979).

120 Saxena V.K., Van Zandt L.L. and Schroll W.K. 'Atomic motions and high frequency cutoff in biological macromolecules'. *Chem. Phys. Lett.* **164**, 82–86 (1989).

121 Girirajan K.S., Young L. and Prohofsky E.W. 'Vibrational free energy, entropy, and temperature factors of DNA calculated by helix lattice approach'. *Biopolymers* **28**, 1841–1860 (1989).

122 Jordan D.O. 'Physicochemical properties of the nucleic acids'. In: *Progress in Biophysics and Biophysical Chemistry.* Vol.2, J.A. Butler and J.T. Randall (eds), Pergamon Press, London (1951), pp. 51–89.

123 Sardon C. 'Methods of determining the form and dimensions of particles in solution: A critical survey'. In: *Progress in Biophysics and Biophysical Chemistry.* Vol.3, J.A. Butler and J.T. Randall (eds), Pergamon Press, London (1953), pp. 237–304.

124 Willams R.C. 'Electron microscopy of sodium desoxyribonucleate by use of new freeze-drying method'. *Biochem. Biophys. Acta*, **9**, 237–239 (1952).

125 Kahler H. and Lloyd B.J. 'The electron microscopy of sodium desoxyribonucleate'. *Biochem. Biophys. Acta* **10**, 355–366 (1953).

126 Furberg S. 'The crystal structure of cytidine'. *Acta Crystallogr.* **3**, 325–331 (1951).

127 Dekker C.R., Michelson A.M. and Todd A.R. 'Nucleotides.Part XIX. Pyrimidine deoxyribonucleoside diphosphates'. *J. Chem. Soc.*, March, 947–951 (1953).

128 Austbury W.T. 'X-ray studies of nucleic acids'. *Symp. Soc. Exp. Biol. 'Nucleic Acids.* Vol.1. Cambridge: University Press, Cambridge (1947), pp. 66–76.

129 Gulland J.M. 'The structures of nucleic acids'. *Cold Spring Harbor Symp. Quantum Biol.* **12**, 95–103 (1947).

130 Watson J.D. *The Double Helix.* Weidenfeld and Nicholson, London (1968).

131 *Nucleic Acids Res.* **28**, N1 (2000).

132 Fritzsche H. 'New structural and dynamic aspects of DNA as revealed by nuclear magnetic resonance'. *Comments Mol. Biophys.* **1**, 325–336 (1982).

133 Keepers J.W. and James Th. L. 'Models for DNA backbone motions: an interpretation of NMR relaxation experiments'. *J. Am. Chem. Soc.* **104**, 929–939 (1982).

134 McClure W.R. 'Mechanism and control of transcription in procaryotes'. *Annu. Rev. Biochem.* **54**, 171–204 (1985).

135 Allison A. and Shurr J.M. 'Torsion dynamics and depolarization of fluorescence of linear macromolecules. I. Theory and application to DNA'. *Chem. Phys.* **41**, 35–59 (1979).

136 Benham C.J. 'Theoretical analysis of conformational equilibria in superhelical DNA'. *Annu. Rev. Biophys. Biophys. Chem.* **14**, 23–45 (1985).

137 Tanaka F. and Takahashi H. 'Theory of supercoiled DNA'. *J. Chem. Phys.* **83**, 6017–6026 (1985).

138 Landau L.D. and Lifshitz E.M. *Theory of Elasticity.* Addison-Wesley, Reading, MA (1959).

139 Calladine C.R. 'Mechanics of sequence-dependent stacking of bases in DNA'. *J. Mol. Biol.* **161**, 343–351 (1982).

140 Pilet J. and Brahms J. 'Dependence of A-B conformational change in DNA on base composition'. *Nature. New Biol.*, **236**, 99–100 (1972).

141 Harvey S.C. 'DNA structural dynamics: longitudinal breathing as a possible mechanism for the B-Z transition'. *Nucleic Acids Res.* **11**, 4867–4873 (1983).

142 Jensen P., Jaric M.V. and Bannemann K.H. 'Soliton-like processes during right-left transition in DNA'. *Phys. Lett. A* **95**, 204–208 (1983).

143 Early T.A., Kearns D.R., Hillen W. and Wells R.D. 'A 300- and 600- MHz proton nuclear magnetic resonance investigation of a 12 base pair deoxyribonucleic acid restriction fragment: Relaxation behavior of the low-field resonances in water'. *Biochemistry* **20**, 3756–3764 (1981).

144 Early T.A., Kearns D.R., Hillen W. and Wells R.D. 'A 300-MHz proton nuclear magnetic resonance investigation of deoxyribonucleic acid restriction fragments: Relaxation behavior of the low-field resonances in water'. *Biochemistry* **20**, 3764–3769 (1981).

145 Nakanishi M., Tsuboi M., Saijo Y. and Nagamure T. 'Stopped-flow ultraviolet spectroscopy for hydrogen-exchange studies of nucleic acids'. *FEBS Lett.* **81**, 61–64 (1977).

146 Nakanishi M. and Tsuboi M. 'Two channels of hydrogen exchange in a double-helical nucleic acid'. *J. Mol. Biol.* **124**, 61–77 (1978).

147 Mandal C., Kallenbach N.R. and Englander S.W. 'Base-pair opening and closing reactions in the double helix'. *J. Mol. Biol.* **135**, 391–411 (1979).

148 Yakushevich L.V. 'Modeling the nonlinear dynamics of DNA'. *Izvestiya VUZ. Applied Nonlinear Dynamics* (Russian J.) **4**, 107–111 (1997).

149 Peticolas W.L. and Tsuboi M. 'Raman spectroscopy of nucleic acids'. In: *Infrared and Raman Spectroscopy of Biological Macromolecules.* T.M. Theophanides (ed.), Reidel, London (1978), pp. 153–165.

150 Webb S.J. 'Laser-Raman spectroscopy of living cells'. *Phys. Rep.* **60**, 202–224 (1980).

151 Lomdahl P.C., MacNeil L., Scott A.C., Soneham M.E. and Webb S.J. 'An assignment to internal soliton vibrations of laser-Raman lines from living cells'. *Phys. Lett. A* **92**, 207–210 (1982).

152 Urabe H., Tominaga Y. and Kubota K. 'Experimental evidence of collective vibrations in DNA double helix (Raman spectroscopy)'. *J. Chem. Phys.* **78**, 5937–5939 (1983).

153 Grimm H., Stiller H, Maikrzak C.F., Rupprecht A. and Dahlborg U. 'Observation of acoustic umklapp phonons in water-stabilized DNA by neutron scattering'. *Phys. Rev. Lett.* **59**, 1780–1783 (1987).

154 Prabhu V.V., Schroll W.K., Van Zandt L.L. and Prohofsky E.W. 'Helical lattice vibrational modes in DNA'. *Phys. Rev. Lett.* **60**, 1587 (1988); Grimm H., Stiller H. 'Grimm and Stiller reply' *Phys. Rev. Lett.* **60**, 1588 (1988).

155 Schroll W.K., Prabhu V.V., Prohofsky E.W. and Van Zandt L.L. 'Phonon interpretation of inelastic neutron scattering in DNA crystals'. *Biopolymers* **28**, 1189–1193 (1989).

156 Powell J.W., Edwards G.S., Genzel L., Kremer F., Wittlin A., Kubasek W., and Peticolas W. 'Investigation of far-infrared vibrational modes in polynucleotides'. *Phys. Rev. A***35**, 3929–3939 (1987).

157 Van Zandt L.L. and Saxena V.K. 'Millimeter-microwave spectrum of DNA: six predictions for spectroscopy'. *Phys. Rev. A***39**, 2672–2674 (1989).

158 Englander S.W. and Kallenbach N.R. 'Hydrogen exchange and structural dynamics of proteins and nucleic acids'. *Q. Rev. Biophys.* **16**, 521–555 (1982).

159 Swicord M.L., Edwards G.S. and Davis C.C. 'Strong interactions of radiofrequency fields with nucleic acid'. In: *Nonlinear Electrodynamics in Biological Systems.* W. Ross Adey (ed.), Plenum Press, New York (1984), pp. 35–58.

160 Gabriel G., Grant E.H., Tata R., Brown P.R., Gestblom B. and Noreland E. 'Microwave absorption in aqueous solutions of DNA'. *Nature* **328**, 145–146 (1987).

161 Davis M.E. and Van Zandt L.L. 'Microwave response of DNA in solution. Theory'. *Phys. Rev. A* **37**, 888–899 (1988).

162 Lipari G. and Szabo A. 'Nucleic magnetic resonance relaxation in nucleic acid fragments: models for internal motion'. *Biochemistry* **20**, 6250–6256 (1981).

163 Keepers J.M. and James Th.L. 'Models for DNA backbone motions: an interpretation of NMR relaxation experiments'. *J. Am. Chem. Soc.* **104**, 929–939 (1982).

164 Mirau P.A., Behling R.E. and Kearns D.R. 'Internal motions in B- and Z-forms poly(dG-dC) (poly(dG-dC): ^{1}H NMR relaxation studies'. *Biochemistry* **24**, 6200–6211 (1985).

165 Leroy J.L., Broseta D., Bolo N. and Gueron M. 'NMR studies of base-pair kinetic of nucleic acids'. In: *Structure and Dynamics of RNA*. P.H. Knippenberg and C.W. Hilbers (eds), Plenum Press, New York (1986), pp. 31–34.

166 Barton J.K. 'Metals and DNA: Molecular Left-Handed Complements'. *Science* **233**, 727 –734 (1986).

167 Murphy C.J., Arkin M.R., Jenkins Y., Ghatlia N.D., Bossmann S., Turro N.J. and Barton J.K. 'Long Range Photoinduced Electron Transfer through a DNA Helix'. *Science* **262**, 1025 –1029 (1993).

168 Dandliker P.J., Holmlin R.E., and Barton J.K. 'Oxidative Thymine Dimer Repair in the DNA Helix'. *Science* **275**, 1465 –1468 (1997).

169 Tran P., Alavi B. and Gruner G. 'Charge transport along the λ-DNA double helix'. *Phys. Rev. Lett.* **85**, 1564–1567 (2000).

170 Jerome D. and Schulz H.J. 'Organic conductors and superconductors'. *Adv. Phys.* **31**, 299–400, (1982).

171 Devreux F., Nechtschein M. and Grüner G. 'Charge Transport in the Organic Conductor Qn (TCNQ)2'. *Phys. Rev. Lett.* **45**, 53 (1980).

172 Mihaly, G., Said, G., Gruner, G. and Kertesz, M. '2–3 Benzacridinium (TCNQ)2: A Small Band Gap Semiconductor'. *Solid State Commun.* **21**, 1115–1118 (1977).

173 Ye Y.J., Chen R.S., Martinez A., Otto P. and Ladik J., 'Calculation of Hopping Conductivity in Aperiodic Nucleotide Base Stacks'. *Solid State Commun.* **112**, 139–144 (1999).

174 Jortner J., Bixon M., Langenbacher Th. and Michel-Beyerle M.E. 'Charge transfer and transport in DNA'. *Proc. Natl. Acad. Sci. USA* **95**, 12759–12765 (1998).

175 Essevaz-Roulet B., Bockelmann U. and Heslot F. 'Mechanical separation of the complementary strands of DNA'. *Proc. Natl. Acad. Sci. USA* **94**, 11935–11940 (1997).

176 Bockelmann U., Essevaz-Roulet B. and Heslot F, 'DNA strand separation studied by single molecule force measurements'. *Phys. Rev.* E **58**, 2386–2394 (1998).

177 Bockelmann U., Thomen Ph., Essevaz-Roulet B., Viasnoff V. and Heslot F. 'Unzipping DNA with Optical Tweezers: High Sequence Sensitivity and Force Flips'. *Biophys. J.* **82**, 1537–1553 (2002).

178 Bockelmann U., Essevaz-Roulet B., Thomen Ph. and Heslot F., 'Mechanical opening of DNA by micromanipulation and force measurement'. *C. R. Phys.* **3**, 585–594 (2002).

179 Urabe H.and Tominaga Y. 'Low-lying collective modes of DNA double helix by Raman spectroscopy'. *Biopolymers* **21**, 2477–2481 (1982).

180 DeMarco C., Linsay S.M., Pokorny M., Powell J. and Rupprecht A. 'Interhelical effects on the low-frequency modes and phase transitions of Li- and Na-DNA'. *Biopolymers* **24**, 2035–2040 (1985).

181 Grimm H. and Rupprecht A. 'Statics and dynamics of oriented DNA as seen by neutrons'. *Physica B* **174**, 291–299 (1994).

182 Grimm H. and Rupprecht A. 'Inelastic neutron scattering studies of oriented DNA'. In: *Nonlinear Excitations in Biomolecules*. Springer, Berlin (1995), pp. 101–115.

183 Rupprecht A. 'Preparation of oriented DNA by wet spinning'. *Acta Chem. Scand.* **20**, 494–504 (1966).

184 Beetz C.P. and Ascarelli G. 'Far-infrared absorption of nucleotides and poly(I) • poly(C) RNA'. *Biopolymers* **21**, 1569–1586 (1982).

185 Wittlin A., Genzel L., Kremer F., Häseler S., Pogliysch A. and Rupprecht A. 'Far-infrared spectroscopy of oriented films of dry and hydrated DNA'. *Phys. Rev. A* **34**, 493–500 (1986).

186 Van Zandt L.L. 'Resonant microwave absorption by dissolved DNA'. *Phys. Rev. Lett.* **57**, 2085–2087 (1986).

187 Van Zandt L.L. and Davis M.E. 'Theory of anomalous resonant absorption of DNA at microwave frequencies'. *J. Biomol. Struct. Dyn.* **3**, 1045–1053, 1986.

188 McConnel B. 'Exchange mechanisms for hydrogen bonding protons of cytidylic and ganylic acids'. *Biochemistry* **17**, 3168–3176 (1978).

189 Eley D.D. and Leslie R.B., *Nature* (London) **197**, 898–899 (1963).

190 Hopfield J.J. 'Electron transfer between biological molecules by thermally activated tunneling'. *Proc. Natl. Acad. Sci. USA* **71**, 3640–3644 (1974).

191 Giamarchi T. 'Mott transition in one dimension'. *Physica* (Amsterdam) **230** B, 975–980 (1997).

192 Gruner G. *Density Waves in Solids*. Addison-Wesley Publishing Co., Reading (1994).

193 Bixon M. and Jortner J. 'Energetic Control and Kinetics of Hole Migration in DNA'. *J. Phys. Chem.* **104**, 3906–3913 (2000).

194 Henderson, P.T., Jones, D.M., Kan, Y., Hampikian, Schuster G.B. 'Long-Distance Charge Transport in Duplex DNA: The Phonon Assisted Polaron-Like Hopping Mechanism'. *Proc. Natl. Acad. Sci. USA* **96**, 8353–8358 (1999).

195 Bruinsma R., Gruner G., D'Orsogna M.R., Rudnik J. 'Fluctuation-facilitated charge migration along DNA'. *Phys. Rev. Lett.* **85**, 4393–4396 (2000).

196 Bockelmann U., Essevaz-Roulet B. and Heslot F. 'Molecular Stick-Slip Motion Revealed by Opening DNA with Piconewton Forces'. *Phys. Rev. Lett.* **79**, 4489–4492 (1997).

197 Cocco S., Monasson R. and. Marko J. 'Force and kinetic barriers in unzipping of DNA'. *Proc. Natl. Acad. Sci. USA* **98**, 8608–8613 (2001).

198 Cocco S., Monasson R. and Marko J. 'Force and kinetic barriers to initiation of DNA unzipping'. *Phys. Rev.* E **65**, 041907 (2002).

199 Cocco S., Monasson R. and Marko J. 'Unzipping dynamics of long DNAs'. *Phys. Rev.* E **66**, 051914 (2002).

200 Lerman L.S. 'Structural considerations in the interaction of DNA and acridines'. *J. Mol. Biol.* **3**, 18–30 (1961).

201 Fuller W. and Waring M.A. 'A molecular model for the interaction of ethidium bromide with deoxyribonucleic acid'. *Ber. Bunsen-Ges. Phys. Chem.*, **68**, 805–809 (1964).

202 Neville D.M. and Davies D.R. 'The interaction of acridine dyes with DNA: An X-ray diffraction and optical investigation'. *J. Mol. Biol.* **17**, 57–74 (1966).

203 Pohl F.M., Jovin T.M., Baehr W. and Holbrook J.J. 'Ethidium bromide as a cooperative effector of a DNA structure'. *Proc. Natl. Acad. Sci. USA* **69**, 3805–3809 (1972).

204 Kamzolova S.G., Kolontarov A.I., Elfimova L.I. and Sukhorukov B.I. 'Investigation of structural transformations of the complex of RNA-polymerase with Escherichia Coli in C T2-DNA'. *DAN USSR* **208**, 245–247 (1973).

205 Well R.D., Blachesley R.W., Hardies S.C., Horn G.T., Larso J.E., Sesling E., Burd J.F., Chan H.W., Dodgson J.B., Jensen K.F., Nes I.F. and Wartell R.M. 'The role of DNA structure in genetic regulation'. *CRC Crit. Rev. Biochem.* **4**, 305–340 (1977).

206 Kolata G.B. 'Bacterial genetics: action at a distance on DNA'. *Science* **198**, 41–42 (1977).

207 Hogan M., Dattagupta N. and Crothers D.M. 'Transmission of allosteric effects in DNA'. *Nature* **278**, 521–524 (1979).

208 Crothers D.M. and Fried M. 'Transmission of long-range effects in DNA'. *Cold Spring Harbor Symposia on Quantitative Biology* **47**, 263–269 (1983).

209 Ptashne M. 'Gene regulation by proteins acting nearby and at a distance'. *Nature* **322**, 697–701 (1986).

210 Wang J.C. and Giaever G.N. 'Action at a distance along a DNA'. *Science* **240**, 300–304 (1988).

211 Adzuma K. and Mizuuchi K. 'Interaction of proteins located at a distance along DNA: Mechanism of target immunity in the Mu DNA strand-transfer reaction'. *Cell* **57**, 41–47 (1989).

212 Burd J.F., Wartell R.M., Dodgson J.B. and Wells R.D. 'Transition of Stability (telestability) in deoxyribonucleic acid'. *J. Biol. Chem.* **250**, 5109–5113 (1975).

213 Washman W. and Anthony D.A. 'Conformational changes in deoxyribonucleic acid during transcription'. *Biochemistry* **19**, 5981–5986 (1980).

214 Sadler J.R., Teclenburg M. and Betz J.L. 'Plasmids containing many tandem copies of a synthetic lactose operator'. *Gene* **8**, 279–300 (1980).

215 Kamzolova S.G. and Postnikova G.B. 'Spin-labelled nucleic acids'. *Q. Rev. Biophys.* **14**, 223–288 (1981).

216 Wartell R.M., Klysic J., Hillen W. and Wells R.D. 'Junction between Z and B conformations in a DNA restriction fragment: evolution by Raman spectroscopy'. *Proc. Natl. Acad. Sci. USA* **79**, 2549–2553 (1982).

217 Strayer L. *Biochemistry*. Freeman, San Francisco, CA (1981).

218 Robinson B.H., Forgaes G., Dalton L.R. and Frish H.L. 'A simple model for internal motion of DNA based upon EPR studies in the slow motion region'. *J. Chem. Phys.* **73**, 4688–4692 (1980).

219 Lindsay S.M. and Powell J. 'Light scattering of lattice vibrations of DNA'. In: *Structure and Dynamics: Nucleic Acids and Proteins.* E. Clementi and R.H. Sarma (eds), Adenine Press, New York (1983), pp. 241–259.

220 Weidlich T., Lindsay S.M., Lee S.A., Tao N.-J., Lewen G.D., Peticolas W.L., Thomas G.A. and Rupprecht A. 'Low-frequency Raman spectra of DNA: a comparison between two oligonucleotide crystals and highly crystalline films of Calf Thymus DNA'. *J. Phys. Chem.* **92**, 3315–3317 (1988).

221 Lindsay S.M., Powell J., Prohofsky E.W. and Devi-Prasad K.V. 'Lattice modes, soft modes and local modes in double helical DNA'. In: *Structure and Motion: Nucleic Acids, Proteins.* E. Clementi E., G. Corongiu, M.H. Sarma and R.H. Sarma (eds), Adenine Press, New York (1985), pp. 531–551.

222 Volkov S.N. and Kosevich A.M. 'Theory of low-frequency vibrations in DNA macromolecules'. *J. Biomol. Struct. Dyn.* **8**, 1069–1083 (1991).

223 Devi-Prasad K.V. and Prohofsky E.W. 'Low-frequency lattice mode predictions in A-DNA compared to experimental observations and significance for A-to-B conformation change'. *Biopolymers* **23**, 1795–1798 (1984).

224 Kim Y. and Prohofsky E.W. 'Vibrational modes of a DNA polymer at low temperature'. *Phys. Rev. B* **36**, 3449–3451 (1987).

225 Prohofsky E.W. 'Quasi-momentum conservation and motion along the DNA double helix'. *Comments Mol. Cell. Biophys.* **2**, 65–86 (1983).

226 Eyster J.M. and Prohofsky W. 'Lattice vibrational modes of poly(rU) and poly(rA)'. *Biopolymers* **13**, 2505–2526 (1974).

227 Eyster J.M. and Prohofsky W. 'On the B to A conformation change of the double helix'. *Biopolymers* **16**, 965–982 (1977).

228 Van Zandt L.L., Lu K.-C. and Prohofsky E.W. 'A new procedure for refining force constants in normal coordinate calculations on large molecules'. *Biopolymers* **16**, 2481–2490 (1977).

229 Mei W.N., Kohli M., Prohofsky E.W. and Van Zandt L.L. 'Acoustic modes and nonbonded interactions of the double helix'. *Biopolymers* **20**, 833–852 (1981).

230 Maret G., Oldenbourg R., Winterling G., Dransfeld K. and Rupprecht A. 'Velocity of high frequency sound waves in oriented DNA fibres and films determined by Brillouin scattering'. *Colloid Polymer Sci.* **257**, 1017–1020 (1979).

231 Hakim M.B., Lindsay S.M. and Powell J. 'The speed of sound in DNA'. *Biopolymers* **23**, 1185–1192 (1984).

232 Scott A.C. 'A nonlinear Klein-Gordon equation'. *Am. J. Phys.* **37**, 52–61 (1969).

233 Marshall W. and Lovasev S.W. *Theory of Thermal Neutron Scattering.* Oxford University Press, Oxford (1971).

234 Wahl Ph., Paoletti J. and LePecq J.-B. 'Decay of fluorescence emission anisotropy of the ethidium bromide-DNA complex evidence for internal motion in DNA'. *Proc. Natl. Acad. Sci. USA* **65**, N2, 417–421, 1970.

235 Letellier A., Ghomi M. and Taillandier E. 'Interpretation of DNA vibration modes: I-the guanosine and cytidine residues involved in poly(dG-dC) • poly(dG-dC) and $d(CG)_3$ • $d(CG)_3$'. *J. Biomol. Struct. Dyn.* **3**, 671–687 (1986).

236 Letellier A., Ghomi M. and Taillandier E. 'Interpretation of DNA vibration modes II-the adenosine and thymidine residues involved in oligonucleotides and polynucleotides'. *J. Biomol. Struct. Dyn* **4**, 663–683 (1987).

237 Letellier R., Ghomi M. and Taillandier E. 'Interpretationof DNA vibration modes: IV. A single-helical approach to assign the phosphate-backbone contribution to the vibrational spectra in A and B conformations'. *J. Biomol. Struct. Dyn.* **6**, 755–768 (1989).

238 Chou K.-C. 'Low-frequency vibrations of DNA molecules'. *Biochem. J.* **221**, 27–31 (1984).

239 Chou K.C. 'Origins of low-frequency motions in biological macromolecules'. *Biophys. Chem.* **25**, 105–116 (1986).

240 Chou C-C., Chen N.Y. and Forsen S. 'The biological functions of low-frequency phonons'. *Chem. Scr.* **18**, 126–132 (1981).

241 Sobell H.M., Banerjee A., Lozansky E.D., Zhou G.P. and Chou K.-C. 'The role of low frequency (acoustic) phonons in determining the premelting and melting behavior of DNA'. In: *Structure and Dynamics in Nucleic Acids and Proteins.* E. Clementi, and R.H. Sarma (eds), Adenine Press, New York (1983), pp. 181–195.

242 Bolton P.H. and James T.L. 'Molecular motions in RNA and DNA investigated by Phosphorus-31 and carbon-13 NMR relaxation'. *J. Phys. Chem.* **83**, 3359–3366 (1979).

243 Bolton P.H. and James T.L. 'Fast and slow conformational fluctuations of RNA and DNA. Subnanosecond internal motion correlation times determined by ^{31}P NMR'. *J. Am. Chem. Soc.* **102**, 25–31, (1980).

244 Early T.H. and Kearns D.R. '^{1}H nuclear magnetic resonance investigation of flexibility in DNA'. *Proc. Natl. Acad. Sci. USA* **76**, 4165–4169 (1979).

245 Hogan M.E. and Jardetzky O. 'Internal motions in DNA'. *Proc. Natl. Acad. Sci. USA* **76**, 6341–6345 (1979).

246 Hogan M.E. and Jardetzky O. 'Internal motions in deoxyribonucleic acid II'. *Biochemistry* **19**, 3460–3468 (1980).

247 Klevan L., Avmitage I.M. and Crothers D.M. '^{31}P NMR studies of the solution structure and dynamics of nucleosomes and DNA'. *Nucl. Acids Res.* **6**, 1607–1616 (1979).

248 Shindo H. 'NMR relaxation processes of ^{31}P in macromolecules'. *Biopolymers* **19**, 509–522 (1980).

249 Condat C.A., Guyer R.A. and Miller M.D. 'Double sine-Gordon chain'. *Phys. Rev. B* **27**, 474–494 (1983).

250 Yakushevich L.V. 'Nonlinear DNA dynamics: hierarchy of the models'. *Physica D* **79**, 77–86 (1994).

251 Muto V., Scott A.C. and Christiansen P.L. 'Microwave and thermal generation of solitons in DNA'. *J. Phys.* **50** (C3, suppl. N3), 217–222 (1989).

252 Christiansen P.L., Lomdahl P.C. and Muto V. 'On a Toda lattice model with a transversal degree of freedom'. *Nonlinearity* **4**, 477–501 (1990).

253 Ichikawa Y.H., Konno K. and Wadati M. 'Nonlinear transverse oscillation of elastic beam under tension'. *J. Phys. Soc.* **50**, 1799–1802 (1981).

254 Collins M.A. 'A quasicontinuum approximation for solitons in atomic chain'. *Chem. Phys. Lett.* **77**, 342–347 (1981).

255 Rosenau P. 'Dynamics of nonlinear mass-spring chains near continuum limit'. *Phys. Lett. A* **118**, 222–227 (1986).

256 Hyman J.M. and Rosenau O. 'On the quasi-continuous approximation of the Toda lattice'. *Phys. Lett. A* **124**, 287–389 (1987).

257 Soerensen M.P., Christiansen P.L. and Lomdahl P.S. 'Solitary waves on nonlinear elastic rods. I'. *J. Acoust. Soc. Am.* **76**, 871–879 (1984).

258 Soerensen M.P., Christiansen P.L., Lomdahl P.S. and Scovgaard O. 'Solitary waves on nonlinear elastic rods. II'. *J. Acoust. Soc. Am.* **81**, 1718–1722 (1987).

259 Sokolnikoff I.S. *Mathematical Theory of Elasticity.* McGraw-Hill, New York (1956).

260 Wadati M., Konno K. and Ichikawa Y.H. 'A generalization of inverse scattering method'. *J. Phys. Soc. Jpn.* **46**, 1965–1966 (1979).

261 Landau L.D. and Lifshitz E.M. *Fluid Mechanics.* Perganon Press, Oxford (1959), Ch. 7.

262 Peyrard M. and Bishop A.R. 'Dynamics of nonlinear excitations in DNA'. In: *Nonlinear Coherent Structures.* M. Barthes and J. Leon (eds), Springer, Berlin (1990), pp. 29–41.

263 Xiao J.-X., Lin J.-T. and Zhang G.-X. 'The influence of longitudinal vibration on soliton excitation in DNA double helices'. *J.Phys. A: Math. Gen.* **20**, 2425–2432 (1987).

264 Zhang F. and Collins M.A. 'Model simulations of DNA dynamics'. *Phys.Rev. E* **52**, 4217–4224 (1995).

265 Barbi M., Cocco S. and Peyrard M. 'Helicoidal model of DNA opening'. *Phys. Lett. A* **253**, 358–369 (1999).

266 Barbi M., Cocco S., Peyrard M. and Ruffo S. 'A twist opening model for DNA'. *J. Biol. Phys.* **24**, 97–114 (1999).

267 Campa A. 'Bubble propagation in a helicoidal molecular chain'. *Phys. Rev. E* **63**, 021901–10 (1999).

268 Rajaraman R. *Solitons and Instatons.* North-Holland., Amsterdam, New York and Oxford (1982).

269 Hereman W., Korpel A. and Banerjee P.P. 'A general physical approach to solitary wave construction from linear solutions'. *Wave Motion* **7**, 283–289 (1985).

270 Hereman W., Banerjee P.P., Korpel A., Assanto G., Van Immerzeele A. and Meerpoel A. 'Exact solitary wave solutions of non-linear evolution and wave equations using a direct algebraic method'. *J. Phys. A: Math. Gen.* **19**, 607–628 (1986).

271 Hereman W. and Takaoka M. 'Solitary wave solutions of nonlinear evolution and wave equations using a direct method and MACSYMA'. *J. Phys. A.: Math. Gen.* **23**, 4805–4822 (1990).

272 Remoissenet M. 'Low-amplitude breather and envelope solitons in quasi-one-demensional physical models'. *Phys. Rev. B* **33**, 2386–2392 (1986).

273 Zhurkin V.B., Lysov Y.P., Florentiev V.L. and Ivanov V.I. 'Torsional flexibility of B-DNA as revealed by conformational analysis'. *Nucleic Acid Res.* **10**, 1811–1830 (1982).

274 Landau L.D. and Lifshitz E.M. *Quantum Mechanics*. Physmatgiz, Moscow 1963 (in Russian).

275 Rubinstein J. 'Sine-Gordon equation'. *J. Math. Phys.* **11**, 258–266 (1970).

276 Yakushevich L.V., Savin A.V. and Manevitch L.I. 'On the internal dynamics of topological solitons in DNA'. *Phys. Rev. E* **66**, 016614–29 (2002).

277 Hasakado M. and Wadati M. 'Inhomogeneous model for DNA dynamics'. *J. Phys. Soc. Jpn.* **64**, 1098–1103 (1995).

278 Salerno M. 'Dynamical properties of DNA promoters'. *Phys. Lett. A* **167**, 49–53 (1992).

279 Salerno M. and Kivshar Yu. S. 'DNA promoters and nonlinear dynamics'. *Phys. Lett. A* **193**, 263–266 (1994).

280 Salerno M. 'Nonlinear dynamics of plasmid pB R322 promoters'. In: *Nonlinear Excitations in Biomolecules*. M. Peyrard (ed.), Springer, Berlin (1995), pp. 147–153.

281 Dauxois T. 'Dynamics of breather modes in a nonlinear 'helicoidal' model of DNA'. *Phys. Lett. A* **159**, 390–395 (1991).

282 Christiansen P.L., Zolotaryuk A.V. and Savin A.V. 'Solitons in an isolated helix chain'. *Phys. Rev. E* **56**, 877–889 (1997).

283 Dauxois M., Peyrard M. and Bishop A.R. 'Entropy-driven DNA denaturation'. *Phys. Rev. E* **47**, R44-R47 (1993).

284 Krumhansl J.A. and Schrieffer J.R. 'Dynamics and statistical mechanics of a one-dimensional model hamiltonian for structural phase transitions'. *Phys. Rev. B* **11**, 3535–3545 (1975).

285 Scalapino D.J., Sears M. and Ferel R.A. 'Statistical mechanics of one-dimensional Ginzburg-Landau fields'. *Phys. Rev. B* **6**, 3409–3416 (1972).

286 Currie J.F., Krumhansl J.A., Bishop A.R. and Trullinger E.E. 'Statistical mechanics of one-dimensional solitary-wave-bearing scalar fields: exact results and ideal gas phenomenology'. *Phys. Rev. B* **22**, 477–496 (1980).

287 Komarov L.I. and Fisher I.Z. 'On the theory of Rayleigh scattering of light by liquids'. *JETP* **43**, 1927–1933 (1962).

288 Pecora R. 'Doppler shifts in light scattering. II. Flexible polymer molecule'. *J. Chem. Phys.* **43**, 1562–1564 (1965).

289 Frank-Kamenetskii M.D. 'Fluctuational motility of DNA'. *Mol. Biol.* (Russian J.) **17**, 639–652 (1983).

290 Frank-Kamenetskii M.D. 'How the double helix breathers'. *Nature* **328**, 17–18 (1987).

291 Gueron M., Kochoyan M. and Leroy J.-L, 'A single mode of DNA base-pair opening drives imino proton exchange'. *Nature* **328**, 89–92 (1987).

292 Fernandez A. 'Proton exchange activity as a probe for solitons in RNA'. *Physica A* **167**, 338–346 (1990).

293 Maleev V.Ya., Kashpur V.A., Glibitsky G.M., Krasnitskaya A.A. and Veretelnik Ye.V. 'Absorption of DNA solutions in the 9–12 GHz frequency range'. *Biopolim. Kletka* **2**, 35–38 (1986).

294 Foster K.R., Epstein B.R. and Galt M.A. 'Resonances' in the dielectric absorption of DNA ?' *Biophys. J.* **52**, 421–425 (1987).

295 Garibov R.A. and Ostrovskii A.V. 'Does the microwave radiation change the dynamical behaviour of macromolecules?' *Uspekhi Sovrem. Biol.* (Russian J.) **110**, 306–320 (1990).

296 Baverstock K.F. and Cundall R.B. 'Solitons and energy transfer in DNA'. *Nature* **332**, 312–313 (1988).

297 Baverstock K.F. and Cundall R.B. 'Long-range energy transfer in DNA'. *Radiat. Phys. Chem.*, **32**, 553–556 (1988).

298 Arroyo C.M., Carmichael A.J., Swenberg C.E., and Myers L.S. 'Neutron induced free radicals in oriented DNA'. *Int. J. Radiat. Biol.* **50**, 789–793 (1986).

299 Miller J.H., Wilson W.E., Swenberg C.E., Myers L.S. and Charlton D.E. 'Stochastic model for free radical yields in oriented DNA exposed to density ionising radiation at 77 K'. *Int.J. Radiat. Biol.* **53**, 901–907 (1988).

300 Edholm O., Nilsson L., Berg O., Ehrenberg M., Claesens F., Grässlund A., Jönsson B. and Taleman O. 'Biomolecular dynamics'. A report from a workshop in Gysinge, Sweden, October 4–7, 1982. *Q. Rev. Biophys.* **17**, 125–151 (1984).

301 Volkov S.N. 'Nonlinear waves and conformational mobility of DNA'. Preprint ITP-84-52P, Institute Of Theor. Phys., Kiev (1984).

302 Wells R.D., Goodman T.C., Hillen W., Horn G.T., Klein R.D., Larson J.E., Müller U.R., Nevendorf S.R., Panayatatos N. and Stirdivant S.M. 'DNA structure and gene regulation'. In: *Progress in Nucleic Acid Research and Molecular Biology*. Academic Press, New York Vol.24 (1980), pp. 167–267.

303 Ladik J.J. 'Some new results on the electronic structure of DNA and a new possible long range mechanism of chemical carcinogenesis'. In*: Structure and Motion: Membranes, Nucleic Acids and Proteins.* E. Clementi, G. Corongiu, M.H. Sarma and R.H. Sarma (eds), Adenine Press, New York (1985), pp. 553–568.

304 Pribnow D. 'Genetic control signals in DNA'. In: *Biological Regulation and Development. I. Gene Expression.* R.F. Golgberger (ed.), Plenum, New York (1979), pp. 219–277.

305 von Hippel P.H. 'On the molecular bases of the specificity of interaction of transcriptional proteins with genome DNA'. In: *Biological Regulation and Development. I. Gene Expression.* R.F. Golgberger (ed.), Plenum, New York (1979), pp. 279–347.

306 Siebenlist U. 'RNA polymerase unwinds an 11-base pair segment of a phage T7 promoter'. *Nature* **279**, 651–652 (1979).

307 Siebenlist U., Simpson R.B and Gilbert W. 'E.coli RNA polymerase interacts homologously with two different promoters'. *Cell* **20**, 269–281 (1980).

308 Sluyser M. 'Interaction of steroid hormone receptors with DNA'. *Trends Biochem. Sci.* **8**, 236–238 (1983).

309 Saucier J.W. and Wang J.C. 'Angular alteration of the DNA helix by E. coli RNA polymerase'. *Nature. New Biol.* **239**, 167–170 (1972).

310 Kamzolova S.G. 'Electron spin resonance melting of chemically spin-labeled DNA and its complex with RNA polymerase'. *Stud. Biophys.* **87**, 175–176 (1982).

311 Kamzolova S.G., Kalantarov A.I., Elfimova L.I., Petrov A.I. and Sukhorukov B.I. 'Studying conformational transformations of the complex of RNA-polymerase of E. coli with T2-DNA with the help of spin labels'. In: *Proceedings of the 4th International Biophysics Congress*, Vol.2, Moscow (1982), p. 264.

312 Benoist C., O'Hare K., Breathnach R. and Chambon P. 'The ovalbumin gene-sequence of putative control regions'. *Nucleic Acids Res.* **8**, 127–142 (1980).

313 Nosikov V.V. and Braga A.A. 'Genes of ribosome RNA'. In*: Genes of Eukaryotes.* Vol. 18, VINITI, Moscow (1982), pp.110–216.

314 Sinden R.R., Broyles S.S. and Pettijohn D.E. 'Perfect palindromic lac operator DNA sequence exists as a stable cruciform structure in supercoiled DNA in vitro but not in vivo'. *Proc. Natl. Acad. Sci. USA* **80**, 1797–1801 (1983).

315 Freifelder D. *Molecular Biology.* Jones and Bartlett, Boston (1987).

316 Lebowitz J.L., Rose H.A. and Speer E.R. 'Statistical mechanics of the nonlinear Schrödinger equation'. *J. Stat. Phys.* **50**, 657–687 (1988).

317 Barkley M.D., Kowalczyk A.A. and Brand L. 'Fluorescence decay studies of anizotropic rotations: Internal motions in DNA'. In *Biomolecular Stereodynamics*, R.H. Sarma (ed.), V.1, Adenine Press, New York (1981), pp. 392–403.

318 Tsuboi M., Tominaga Y. and Urabe H. 'Raman-active torsional vibrations in DNA molecule'. *J. Chem. Phys.* **78**, 991–992 (1983).

319 Schurr J.M., FujimotoB.S., Wu P. and Song L. 'Fluorescence studies of nucleic acids. Dynamics, rigidities, and structures'. Preprint Department of Chemistry University of Washington, Seattle (1991).

320 Thomas J.C., Allison S.A., Appellof C.J. and Schurr J.M. 'Torsion dynamics and depolarization of fluorescence of linear macromolecules. II. Fluorescence polarization anisotropy measurements on a clean viral 029 DNA'. *Biophys. Chem.* **12**, 177–188 (1980).

321 Millar D.R., Robbins R.J. and Zewail A.H. 'Torsion and bending of nucleic acids studied by subnanosecond time-resolved fluorescence depolarization of intercalated dyes'. *J. Chem. Phys.* **76**, 2080–2094 (1982).

322 Millar D.P., Robbins R.J. and Zewail A.H. 'Time-resolved spectroscopy of macromolecules: effect of helical structure on the torsional dynamics of DNA and RNA'. *J. Chem. Phys.* **74**, 4200–4201 (1981).

323 Le Bret M. 'Relationship between the energy of superhelix formation, the shear modulus, and the torsional Brownian motion of DNA'. *Biopolymers* **17**, 1939–1955 (1978).

324 Hogan M., Legrange J. And Austin B. 'Dependence of DNA helix flexibility on base composition'. *Nature* **304**, 752–754 (1983).

325 Tung C.-T. and Harvey S.C. 'A molecular mechanical model to predict the helix angles of DNA'. *Nucleic Acids Res.* **12**, 3343–3356 (1984).

326 Depew R.E. and Wang J.C. 'Conformational fluctuations of DNA helix'. *Proc. Natl. Acad. Sci. USA* **72**, 4275–4279 (1975).

327 Pulleyblank D.E., Shure M., Tang D., Vinograd J. and Vosberg H.P. 'Action of nicking-closing enzyme on supercoiled and nonsupercoiled closed circular DNA: formation of a Boltzmann distribution of topological isomers'. *Proc. Natl. Acad. Sci.* **72**, 4280–4284 (1975).

328 Vologodskii A.V., Anshelevich V.V., Lukashin A.V. and Frank-Kamenetskii M.D. 'Statistical mechanics of supercoils and the torsional stiffness of the DNA double helix'. *Nature* **280**, 294–298 (1979).

329 Strogatz S. 'Estimating the torsional rigidity of DNA from supercoiling data'. *J. Chem. Phys.* **77**, 580–581 (1982).

330 Shore D. and Baldwin R.L. 'Energetics of DNA twisting. I. Relation between twist and cyclization probability'. *J. Mol. Biol.* **170**, 957–981 (1983).

331 Robinson B.H., Lerman L.S., Beth A.H., Frisch H.L., Dalton L.R. and Auer C. 'Analysis of double-helix motions with spin-labeled probes: binding geometry and the limit of torsional elasticity'. *J. Mol.Biol.* **139**, 19–44 (1980).

332 Tung C.-S. and Harvey S.C. 'Base sequence, local structure, and macroscopic curvature of A-DNA and B-DNA'. *J. Biol. Chem.* **261**, 3700–3709 (1986).

333 Tidor B., Irikura K.K., Brooks B.R. and Karplus M. 'Dynamics of DNA oligomers'. *J. Biomol. Struct. Dyn.* **1**, 231–262 (1983).

334 Tan K.Z. and Harvey S.C. 'Molecular mechanics model of supercoiled DNA'. *J. Mol. Biol.* **205**, 573–591 (1989).

335 Itoh K. and Shimanouchi T. 'Vibrational frequencies and modes of alpha-helix'. *Biopolymers* **9**, 383–389 (1970).

336 Chou K.-C. 'Low-frequency vibrations of helical structures in protein molecules'. *Biochem. J.* **209**, 573–580 (1983).

337 Chou K.-C. 'Identification of low-frequency modes in protein molecules'. *Biochem. J.* **215**, 465–469 (1983).

338 Yakushevich L.V. 'On the parameters of the dynamical models of DNA'. *Mathematics & Computer & Education* **10**, 195–203 (2003).

Index